This is to certify that the
dissertation entitled

INVESTIGATION OF THE EFFICACY OF VARIOUS NEUROPROTECTION AGENTS FOR THEIR POTENTIAL USE IN THE TREATMENT OF PARKINSON'S DISEASE

presented by

Kelly Lynn Janis

has been accepted towards fulfillment
of the requirements for the

Doctoral Degree in Neuroscience

Ruth Luskingland
Major Professor's Signature

10-20-08
Date

INVESTIGATION OF THE EFFICACY OF VARIOUS NEUROPROTECTION AGENTS FOR THEIR POTENTIAL USE IN THE TREATMENT OF PARKINSON'S DISEASE

BY

Kelly Lynn Janis

A DISSERTATION

Submitted to
Michigan State University
in partial fulfillment of the requirements
for the degree of

DOCTOR OF PHILOSOPHY

Neuroscience

2008

ABSTRACT

INVESTIGATION OF THE EFFICACY OF VARIOUS NEUROPROTECTION AGENTS FOR THEIR POTENTIAL USE IN THE TREATMENT OF PARKINSON'S DISEASE

BY

Kelly Lynn Janis

Parkinson's disease (PD) is a neurodegenerative disorder characterized by the progressive loss of the nigrostriatal dopamine (NSDA) neurons. The loss of these neurons leads to several debilitating symptoms including slowness of movement, rigidity, postural instability, and resting tremor. Current therapies for PD are aimed at replacing DA deficits for symptomatic relief, but treatments to slow or halt the progressive loss of NSDA neurons are not yet available. Therefore, the primary goal of this dissertation was to examine potential neuroprotective therapies using rodent models of PD.

Several potential etiologies of PD have been proposed including environmental exposure to neurotoxins, oxidative stress, inflammation, mitochondrial dysfunction, and protein aggregation. The neuroprotective strategies explored in this dissertation were targeted to reduce one or more of these causes of PD, induce the development of new NSDA neurons, or explore the effects of a lack of specific functional proteins in either a neurotoxin or inflammatory model of PD. The potential neuroprotective effect of the drug sildenafil in the neurotoxin MPTP (1-methyl-2-phenyl-1,2,3,6-tetrahydropyridine) model of PD was examined. However, sildenafil failed to demonstrate neurogenesis or a neuroprotective effect as indicated by a lack of attenuation of the loss of NSDA cell bodies and axon terminals following MPTP treatment.

Increased inflammation and oxidative stress observed in models of PD are primarily mediated by microglial cells within the brain. These two processes contribute to the progression of PD and partially result from activation of the microglial enzyme nicotinamide adenine dinucleotide phosphate (NADPH) oxidase. Inhibition of NADPH oxidase using the inhibitor apocynin was tested as a potential neuroprotective drug in the MPTP model of PD but was found to be ineffective in attenuating MPTP induced activation of NADPH oxidase and loss of NSDA axon terminals.

Endogenous cannabinoids (ECB) are involved in the regulation of NSDA neurons and microglial inflammation. NSDA neuronal integrity, activity, and regulation were initially characterized in mice lacking functional cannabinoid (CB) 1 and CB2 receptors, to determine if these mice were comparable to wildtype (WT) control mice. Mice lacking CB1 and CB2 receptors were determined to have typical integrity, activity and regulation of NSDA neurons. Next, CB1/CB2 knockout (KO) mice were used to determine if absence of CB1 and CB2 receptors alters NSDA neuronal susceptibility to MPTP neurotoxicity or lipopolysaccharide (LPS) induced acute inflammation. The loss of axon terminal DA concentrations was found to be attenuated in a MPTP model of PD suggesting inhibition of one or more of these receptors could be neuroprotective in PD. However, pharmacologic inhibition of these receptors (either individually or together) failed to replicate the neuroprotective results seen in CB1/CB2 KO mice. In addition, acute inflammation induced by LPS did not alter the integrity or activity of NSDA neurons. These findings suggest that neither sildenafil or apocynin are viable neuroprotective agents in the treatment of PD, and that CB1 and CB2 receptors may play a role in MPTP induced loss of NSDA neurons.

This dissertation is dedicated to my Mom and Dad,

thank you for all of your support and encouragement through out the years,

and Mom for all of the times you listened to me,

and to Dr. Susan Aronica, my long time mentor for encouraging me to pursue this degree

after I discovered my love of scientific research when I worked in your lab

ACKNOWLEDGEMENTS

I would like to thank first my Mom and Dad who helped me get to this point in my life, Steve and Sarah for your love and encouragement, Matthew, Noah, and Anne who always remind me of the simple joys in life, and my many other family members who are to many to name for their support, and Lauren and Margaret for always being there for me you will always be my best friends.

I would like to thank my advisors Drs. Keith Lookingland and John Goudreau for their guidance and dedication to my scientific training over the past few years. I will always be thankful to have had the opportunity to be trained by you and be a member of your lab.

I would also like to thank my committee members Drs. Patricia Ganey, Barbara Kaplan, and David Kreulen for their help and advisement on my dissertation.

I would like to thank the Neuroscience and College of Osteopathic Medicine Dual Degree Programs' faculty for your support and mentorship you provided in my training, and also all my fellow students and especially my friends who were always there for me during the many steps it took to reach this point.

Lastly I would like to thank my fellow lab members who made my experience in the lab one I will never forget. The collaborative and fun environment you created both past and present, and thoughtful scientific input during my training made this journey one I will always be thankful for.

TABLE OF CONTENTS

List of Tables.....x

List of Figures.....viii-xv

List of Abbreviations.....xvi-xix

Chapter 1. Introduction.....1

A. Statement of Purpose.....1
B. Causes of PD.....3
C. The Basal Ganglia.....6
D. DA Synthesis, Release, and Metabolism.....9
E. DA Neuronal Populations.....15
F. DA Receptors.....18
G. Regulation of DA Synthesis in Central Dopaminergic Neurons.....21
H. Indices of DA Neuronal Integrity and Activity.....24
I. Serotonin Synthesis and Neuronal Function.....26
J. Neurotoxic Models of PD.....28
K. Inflammation in the Brain.....34
L. Neurogenesis and Sildenafil.....38
M. The Role of Nicotinamide Adenine Dinucleotide Phosphate (NADPH) Oxidase in Microglial Mediated Death of NSDA Neurons.....39
N. Cannabinoids and Endocannabinoids.....42
O. Dissertation Objectives.....51

Chapter 2. Materials and Methods.....53

A. Animals.....53
B. Drugs.....61
C. Brain Tissue Preparation.....68
D. Assay of Amines, Amine Metabolites, and Apocynin in Brain Tissue.....70
E. cGMP Assay.....79
F. Plasma Sildenafil Determination.....81
G. Western Blot Analysis.....82
H. Immunohistochemistry and Stereology Cell Counts.....90
I. NADPH Oxidase Activity Assay.....92
J. Mitochondrial Complex I Assay.....94
K. MPP+ Assay.....98
L. Statistical Analysis.....102

Chapter 3. Effects of Sildenafil on Nigrostriatal Dopamine Neurons in a Murine Model of Parkinson's Disease.....103

A. Introduction.....103
B. Materials and Methods.....107
C. Results.....109
D. Discussion.....118

Chapter 4. Apocynin as a Neuroprotective Agent in the MPTP Model of PD.....123

A. Introduction.....123
B. Materials and Methods.....128
C. Results.....130
D. Discussion.....153

Chapter 5. The Characterization of the Neurochemical Properties and Neuromodulation of Dopaminergic Neurons in Wildtype and Cannabinoid 1 and 2 Receptor Knockout Mice.....160

A. Introduction.....160
B. Materials and Methods.....166
C. Results.....168
D. Discussion.....191

Chapter 6. The Effects of a Lack of Cannabinoid Receptors in the MPTP Model of PD.....203

A. Introduction.....203
B. Materials and Methods.....208
C. Results.....210
D. Discussion.....252

Chapter 7. Lipopolysaccharide Activation of Microglia as an Inflammatory Model of PD in Wildtype and CB1/CB2 Receptor KO Mice.....262

A. Introduction.....262
B. Materials and Methods.....268
C. Results.....270
D. Discussion.....281

Chapter 8. Concluding Remarks.....286

References.....294

LIST OF TABLES

Table #	Title	Page #
2-1	PCR primers for CB1 and CB2 receptors and CB2 KO neomycin cassette	56
2-2	MPTP treatment paradigms	62
2-3	Primary and secondary antibodies used for Western blotting	89
3-1	Numbers of TH immunoreactive cells in the unilateral substantia nigra pars compacta of sildenafil and/or MPTP treated mice	117
4-1	Neurochemical concentrations in the nucleus accumbens following sub-chronic MPTP and apocynin treatment	143
4-2	Neurochemical concentrations in the median eminence following sub-chronic MPTP and apocynin treatment	144
4-3	Neurochemical concentrations in the nucleus accumbens following repeated acute MPTP and apocynin treatment	146
6-1	Parkin and DARPP-32 protein in the striatum following acute MPTP treatment	218
6-2	Effects of sub-chronic MPTP on DA, DOPAC and the DOPAC ratio in the nucleus accumbens and median eminence of rimonabant or SR144528 treated mice	246
6-3	Effects of sub-chronic MPTP on DA, DOPAC and the DOPAC ratio in the nucleus accumbens and median eminence of rimonabant and SR144528 treated mice	247

LIST OF FIGURES

Figure #	Title	Page #
1-1	Anatomy of the basal ganglia	7
1-2	TH synthesis of DOPA from dietary tyrosine	12
1-3	DA synthesis, release, reuptake, and metabolism at the NSDA axon terminal	13
1-4	DA is metabolized by one of two pathways to HVA	14
1-5	Catecholaminergic neuronal populations in the rodent brain	17
1-6	Feedback regulation of NSDA neuronal activity	23
1-7	Metabolism of MPTP to MPP+ and transport of MPP+ into DA neurons	30
1-8	Effects of MPP+ at the dopaminergic neuronal terminal	31
1-9	Direct and indirect activation of microglia induces microgliosis in models of PD	36
1-10	NADPH oxidase activation and production of superoxide in microglial cells	40
1-11	Depolarization induced suppression of neurotransmission by cannabinoids	46
1-12	CB1 receptor expression within the basal ganglia	48
2-1	CB1 receptor product in WT mice, but not CB1/CB2 KO mice	58
2-2	CB2 receptor product in WT mice, but not CB1/CB2 KO mice	59
2-3	Apocynin voltamogram	71
2-4	Diagram showing striatum and nucleus accumbens sampling sites	73

2-4	Chromatograms show peak height and retention time for the respective neurochemicals or apocynin	77
2-5	Chromatograms showing peak height and retention times for DA, DOPAC and apocynin in striatum samples	78
2-7	cGMP standard curve	80
2-8	Pictorial diagram of striatum and ventral midbrain tissue sites taken by tissue punch or dissection	83
2-9	Pictorial diagram of sucrose gradient fractionation of membrane and cytosolic fractions	85
2-10	Pictorial diagram of isolation of membrane and cytosolic fractions using ultracentrifugation	86
2-11	Plot of striatum brain tissue protein content verses the difference in absorbance decay before and after Complex I inhibition	97
2-12	Standard curve of MPP+ concentrations measured using liquid chromatography mass spectrometry	101
3-1	Plasma free sildenafil and brain cGMP levels after sildenafil administration	111
3-2	Effects of chronic MPTP administration on DA and DOPAC concentrations, and the DOPAC/DA in the striatum of mice pre-treated with sildenafil	112
3-3	Effects of chronic MPTP administration on DA and DOPAC concentrations, and the DOPAC/DA in the striatum of concurrent sildenafil treated mice	113
3-4	Effects of chronic MPTP administration on DA and DOPAC concentrations, and the DOPAC/DA in the striatum of post-treatment sildenafil treated mice	114
3-5	Effect of chronic MPTP administration on TH protein content in the striatum of mice pre-treated with sildenafil	115
3-6	Effects of chronic MPTP administration on TH immunoreactive cells in the substantia nigra	116
4-1	Measurement of apocynin in the brain using HPLC-EC	133

4-2 Apocynin decreases the concentrations of DOPAC and the DOPAC/DA ratio in the striatum.....134

4-3 Apocynin dose dependently decreases DOPAC concentrations and reduces the DOPAC/DA ratio in the striatum.....135

4-4 Apocynin does not inhibit MAO B *in vitro*.....136

4-5 Apocynin does not alter MPTP induced DA depletion in the striatum.....140

4-6 Apocynin does not alter MPTP induced HVA depletion in the striatum.....141

4-7 Membrane bound p67Phox protein in the striatum.....142

4-8 NADPH oxidase activation following repeated acute MPTP treatment.....146

4-9 Apocynin does not alter repeated acute MPTP induced DA depletion in the striatum.....149

4-10 Loss of TH protein content in the striatum with repeated acute MPTP treatment is not attenuated with apocynin.....150

4-11 Apocynin does not reduce p67Phox translocation to the membrane or an increase in gp91Phox subunit membrane expression in the striatum observed with repeated acute MPTP treatment.....151

5-1 CB1 receptor expression within the basal ganglia.....161

5-2 WT and CB1/CB2 KO mouse body weight.....167

5-3 Concentrations of DA and DOPAC and the DOPAC/DA ratio in the striatum of male WT and CB1/CB2 KO mice.....170

5-4 Concentrations of HVA and the HVA/DA ratio in the striatum of WT and CB1/CB2 receptor KO mice.....171

5-5 Expression of TH, phosphorylated serine 40 TH, and DAT in the striatum of WT and CB1/CB2 KO mice as determined by Western blot.....172

5-6 TH immunoreactive neurons within the substantia nigra of WT and CB1/CB2 KO mice.....173

5-7 Bilateral TH cell body stereological counts in the substantia nigra and TH protein expression in the ventral midbrain of WT and CB1/CB2 KO mice.....174

5-8 Concentrations of DA and DOPAC and the DOPAC/DA ratio in the nucleus accumbens of WT and CB1/CB2 KO mice.....176

5-9 Concentrations of HVA and the HVA/DA ratio in the nucleus accumbens of WT and CB1/CB2 KO mice.....177

5-10 Concentrations of DA and DOPAC and the DOPAC/DA ratio in median eminence of WT and CB1/CB2 KO mice.....178

5-11 D2 autoreceptor regulation in the striatum of WT and CB1/CB2 KO mice.....181

5-12 D2 autoreceptor regulation in the nucleus accumbens of WT and CB1/CB2 KO mice.....182

5-13 D2 autoreceptor regulation in the median eminence of WT and CB1/CB2 KO mice.....183

5-14 DA receptor regulation in the striatum of WT and CB1/CB2 KO mice.....185

5-15 DA receptor regulation in the nucleus accumbens of WT and CB1/CB2 KO mice.....186

5-16 DA receptor regulation in the median eminence of WT and CB1/CB2 KO mice.....187

5-17 Concentrations of 5HT, 5HIAA, and the 5HIAA/5HT ratio in the striatum of WT and CB1/CB2 KO mice.....189

5-18 Concentrations of 5HT, 5HIAA, and the 5HIAA/5HT ratio in the nucleus accumbens of WT and CB1/CB2 KO mice.....190

6-1 Schematic depicting the location of CB1 receptors within the basal ganglia.....204

6-2 Time course effects of acute MPTP treatment on DA, DOPAC and the DOPAC/DA ratio in the striatum of WT and CB1/CB2 KO mice.....212

6-3 Time course effects of acute MPTP treatment on HVA and the HVA/DA ratio in the striatum of WT and CB1/CB2 KO mice.....213

6-4 Lack of an effect of acute MPTP treatment on TH and DAT protein content in the striatum of WT and CB1/CB2 KO.....216

6-5 Alpha-synuclein and p67Phox cytosolic protein content in the striatum of WT and CB1/CB2 KO mice over time following saline or MPTP treatment.....217

6-6 DARPP-32 and Parkin protein expression in the striatum in WT and CB1/CB2 KO mice following saline or MPTP Treatment.....219

6-7 Time course effects of acute MPTP treatment on DA, DOPAC and the ratio of DOPAC/DA in the nucleus accumbens of WT and CB1/CB2 KO mice.....221

6-8 Time course effects of acute MPTP treatment on HVA and the ratio of HVA/DA in the nucleus accumbens of WT and CB1/CB2 KO mice.....222

6-9 Time course effects of acute MPTP treatment on DA, DOPAC and the ratio of DOPAC/DA in the median eminence of WT and CB1/CB2 KO mice.....224

6-10 Time course effects of acute MPTP treatment in the striatum of WT and CB1/CB2 KO mice.....226

6-11 Time course effects of acute MPTP treatment in the nucleus accumbens of WT and CB1/CB2 KO mice.....227

6-12 Effects of sub-chronic MPTP treatment on DA, DOPAC and the ratio of DOPAC/DA in the striatum of WT and CB1/CB2 KO mice.....231

6-13 The effect of sub-chronic MPTP treatment on TH and phosphorylated serine 40 TH protein in the striatum of WT and CB1/CB2 KO mice.....232

6-14 TH immunoreactive cells within the substantia nigra of WT and CB1/CB2 KO mice following sub-chronic MPTP treatment.....233

6-15 Bilateral TH cell counts in the substantia nigra and ventral midbrain TH protein content in WT and CB1/CB2 treated with MPTP using the sub-chronic treatment paradigm.....234

6-16 Effects of sub-chronic MPTP treatment on DA, DOPAC and the ratio of DOPAC/DA in the nucleus accumbens of WT and CB1/CB2 KO mice.....237

6-17 Effects of sub-chronic MPTP treatment on DA, DOPAC and the ratio of DOPAC/DA in the median eminence of WT and CB1/CB2 KO mice.....238

6-18 Lack of an effect of blockade of either CB1 or CB2 receptors on MPTP induced changes in DA, DOPAC and the ratio of DOPAC/DA in the striatum of WT mice.....242

6-19 Lack of an effect of blockade of both CB1 and CB2 receptors on MPTP induced changes in DA, DOPAC and the ratio of DOPAC/DA in the striatum of WT mice.....243

6-20 Mitochondrial complex I activity in the striatum of MPTP treated WT and CB1/CB2 KO mice.....250

6-21 Time course effects of a single injection of MPTP on the concentrations of MPP+ and DA and the DOPAC/DA ratio in the striatum of WT and CB1/CB2 KO mice.....251

7-1 Ipsilateral and contralateral concentrations of DA and DOPAC and the DOPAC/DA ratio in the striatum of mice injected unilaterally with PBS or LPS into the substantia nigra.....272

7-2 TH cell numbers in the contralateral and ipsilateral substantia nigra of mice injected unilaterally with either PBS or LPS into the substantia nigra.....273

7-3 TH protein content in the contralateral and ipsilateral substantia nigra of mice injected with either PBS or LPS.....274

7-4 Cytosolic p67Phox protein content in the contralateral and ipsilateral substantia nigra of mice injected with either PBS or LPS.....275

7-5 Concentrations of DA, DOPAC, and the DOPAC/DA ratio in the striatum of WT and CB1/CB2 KO mice following peripheral LPS administration.....278

7-6 Concentrations of DA, DOPAC, and the DOPAC/DA ratio in the nucleus accumbens of WT and CB1/CB2 KO mice following peripheral LPS administration.....279

7-7 Concentrations of DA, DOPAC, and the DOPAC/DA ratio in the median eminence of WT and CB1/CB2 KO mice following peripheral LPS administration.....280

LIST OF ABBREVIATIONS

2-AG	2-arachidonoylglycerol
3-MT	3-methoxytyramine
5HIAA	5-hydroxyindoleacetic acid
5HT	serotonin (5-hydroxytryptamine)
6-OHDA	6-hydroxydopamine
AD	aldehyde dehydrogenase
AMT	anandamide membrane transporter
ATP	adenine triphoshphate
BDNF	brain derived neurotrophic factor
BH_2	dihydrobiopterin
BH_4	tetrahydrobiopterin
cAMP	3',5'-cyclic adenosine monophosphate
CB	cannabinoid
CB1	cannabinoid 1 receptor
CB2	cannabinoid 2 receptor
COMT	catechol-O-methyltransferase
cGMP	3',5'-cyclic guanosine monophosphate
DA	dopamine
DARPP-32	DA and cAMP regulated phosphoprotein
DAT	dopamine transporter
DDC	DOPA decarboxylase

DOPA	3,4-dihydroxyphenylalanine
DOPAC	3,4-dihydroxyphenylacetic acid
DOPAL	dihydroxyphenylacetaldehyde
ECB	endocannabinoid
ED	erectile dysfunction
FAAH	fatty acid amide hydrolase
GABA	gamma-aminobutyric acid
GAPDH	glyceraldehyde-3-phosphate dehydrogenase
GBL	gamma-butyrolactone
GPe	globus pallidus external segment
GPi	globus pallidus internal segment
HPLC-EC	high performance liquid chromatography with electrochemical detection
HVA	homovanillic acid
HVAA	homovanillic acid aldehyde
IL-1β	interleukin-1 beta
IL-6	interleukin-6
iNOS	inducible nitric oxide synthase
KO	knockout
L-DOPA	3,4-dihydroxy-L-phenylalanine
LC-MS	liquid chromatography coupled to mass spectrometry
LPS	lipopolysaccharide
MAO B	monoamine oxidase B
MPDP+	1-methyl-4-phenyl-2,3-dihydropyridine

MLDA	mesolimbic dopamine
MPP+	1-methyl-4-phenylpyridinium
MPTP	1-methyl-phenyl-1,2,3,6-tetrahydropyridine
NADPH	nicotinamide adenine dinucleotide phosphate
NFκβ	nuclear factor kappa beta
NSDA	nigrostriatal dopamine
PBS	phosphate buffered saline
O_2	oxygen
PCR	polymerase chain reaction
PD	Parkinson's Disease
PDE5	phosphodiesterase 5
ROS	reactive oxygen species
SNpc	substantia nigra pars compacta
SNpr	substantia nigra pars reticulate
SNAP-25	synaptosomal-associated protein 25
STN	subthalamic nucleus
SVZ	subventricular zone
TH	tyrosine hydroxylase
TIDA	tuberoinfindibular
TLR-4	toll like receptor-4
TNF-α	tumor necrosis factor alpha
WT	wildtype
VTA	ventral tegmental area

VMAT2	vesicular monoamine transporter-2

Chapter 1: General Introduction

A. Statement of Purpose

Parkinson's disease (PD) is a neurodegenerative disorder resulting from the loss of the nigrostriatal dopamine (NSDA) neurons. NSDA neuronal cell bodies are present in the substantia nigra pars compacta (SNpc) of the ventral midbrain and their axonal processes terminate in the striatum. NSDA neurons are important in motor control, and the loss of these neurons is associated with the development of the classic symptoms of PD, which include resting tremor, rigidity, slowness of movement, and postural instability. The compensatory increase in activity that occurs in the remaining NSDA neurons likely prevents the symptoms of PD from being detected until 50-60% of the neurons have been lost.

Currently there is no neuroprotective treatment available to slow or halt the progression of PD upon diagnosis, rather only symptomatic treatments exist. Symptomatic treatments consist of administration of the DA precursor 3,4-dihydroxy-L-phenylalanine (L-DOPA) which is converted to DA, DA agonists, or monoamine oxidase B (MAO B) inhibitors which block the metabolism of DA to the metabolite 3,4-dihydroxyphenylacetic acid (DOPAC). Therefore, the elusive goal of a neuroprotective treatment for PD is still sought after.

The purpose of this dissertation is to test certain potential neuroprotective strategies for PD using neurotoxic and inflammatory models of the disease. The therapeutic potential of pharmacological agents or genetic deletion of specific genes was evaluated by measuring DA neuronal cell body and axon integrity, activity of

dopaminergic neurons, and microglial activation following neurotoxic or inflammatory insult. If a potential drug or genetic knockout of a gene is considered neuroprotective, NSDA neuronal integrity will be either partially or completely maintained.

B. Causes of PD

Several possible causes of idiopathic PD have been proposed including exposure to environmental toxins, mitochondrial dysfunction, oxidative stress, protein misfolding and aggregation, and inflammation related damage to NSDA neurons (Dauer and Przedborski, 2003). These potential causes of PD usually are interconnected with one or more of the others.

The environmental toxin hypothesis is associated with studies that have shown humans in rural areas exposed to pesticides have a higher incidence of PD (Gorell et al., 1998; Priyadarshi et al., 2001). Direct dopaminergic neurotoxins are also implicated in the progressive loss of NSDA neurons following a brief exposure to the relatively selective neurotoxin 1-methyl-4-phenyl-1,2,3,6-tetrahydropyridine (MPTP) (Langston et al., 1983). Although MPTP may initiate death of NSDA neurons acutely, the progressive loss of NSDA neurons long after MPTP is cleared from the system is attributed to inflammation and subsequent oxidative stress within the substantia nigra (Langston et al., 1999).

Mitochondrial dysfunction can be incredibly detrimental to NSDA neurons and leads to oxidative stress. The discovery of the mitochondrial Complex I inhibitors MPTP and rotenone (which induce the death of NSDA neurons) fielded the investigation of this cause of PD (Langston et al., 1983; Betarbet et al., 2000). Inhibition of the mitochondrial respiratory chain prevents the formation of adenosine triphosphate (ATP) by blocking the transfer of electrons down the chain to molecular oxygen. Reduced ATP production leads to energy depletion within the cell and reactive oxygen species (ROS) formation (Dauer and Przedborski, 2003). ROS species such as superoxide, hydroxyl radical, and

hydrogen peroxide can react with the reactive nitrogen species nitric oxide and produce the product peroxynitrite which inhibits the mitochondrial respiratory chain (Tieu et al., 2003; Tretter et al., 2004). ROS react with cellular proteins, DNA and lipids inducing cellular dysfunction. ROS also react with cytosolic DA forming DA-quinones which react with cellular proteins inducing further cellular damage (Asanuma et al., 2004). A reduced ability of NSDA neurons to combat oxidative stress can also contribute to the selective loss of NSDA neurons compared to other dopaminergic neuronal populations (Drechsel and Patel, 2008).

Protein misfolding and inclusion formation such as cytoplasmic Lewy bodies in NSDA neurons which contribute to the progression of PD could result from one of many causes. Age leads to a reduced ability to catabolize misfolded proteins which may contribute to an increase in inclusion formation seen with increasing age (Sherman and Goldberg, 2001). Damage of cellular proteins by ROS can contribute to an increase in damaged or misfolded proteins (Giasson et al., 2000). Altered proteosome function (the cellular unit which degrades proteins) or the pathway that leads to final degradation of proteins also contributes to build up of cytoplasmic inclusions (Tanaka et al., 2001; Petrucelli et al., 2002). Mutations in genes comprising part of the protein degradation pathway have been associated with genetic causes of PD, indicating the importance of appropriate handling of misfolded proteins (Dauer and Przedborski, 2003).

Inflammation is also implicated in the death of NSDA neurons and may contribute to the progressive nature of the disease. Activation of microglial cells, the resident immune cells in the brain, either directly through the death of NSDA neurons or indirectly through inflammatory activation of microglia can lead to the production of

ROS and reactive nitrogen species, and release of pro-inflammatory cytokines (Block and Hong, 2005). These factors lead to direct inflammatory mediated death of NSDA neurons and/or contribute to the recruitment of more microglial cells that perpetuate the inflammatory process. The greater number of microglia found in the ventral midbrain containing the substantia nigra, and the reduced ability of NSDA neurons to deal with oxidative stress likely contributes to a more selective inflammatory mediated loss of these neurons (Kim et al., 2000; Block and Hong, 2005; Drechsel and Patel, 2008).

C. The Basal Ganglia

The NSDA neurons are part of the basal ganglia network which controls motor output by the thalamus. The basal ganglia consists of two separate pathways; direct and indirect (Figure 1-1). Cortical neurons originating in the motor segment of the cerebral cortex project to the striatum and release the excitatory neurotransmitter glutamate onto medium spiny neurons (Squire, 2003). Medium spiny neurons are components of the striatonigral and striatalpallidal segments and the direct and indirect pathways, respectively.

As shown in Figure 1-1, the direct pathway begins with the projection of the striatonigral neurons from the striatum to the substantia nigra pars reticulata (SNpr) and internal segment of the globus pallidus (GPi) and release the inhibitory neurotransmitter gamma-aminobutyric acid (GABA) and the opioid peptides dynorphin and substance P (Steiner and Gerfen, 1998). GABAergic neurons project from the SNpr and GPi to the thalamus. The thalamus projects glutamatergic neurons onto the motor cortex facilitating movement (Squire, 2003). The direct pathway leads to the facilitation of movement since its activation causes inhibition of GABAergic neurons firing onto the thalamus (Benarroch, 2007).

As shown in Figure 1-1, the indirect pathway begins with the projections of the striatalpallidal medium spiny neurons onto the external segment of the globus pallidus (GPe) that releases GABA and the opioid peptide enkephalin (Steiner et al., 1999) and project onto the subthalamic nucleus (STN). The STN neurons project to the GPi/SNpr and release glutamate in these brains regions thereby exciting neurons in the Gpi/SNpr (Squire, 2003). Excitation of the GPi/SNpr neurons that release GABA in the thalamus

The Basal Ganglia

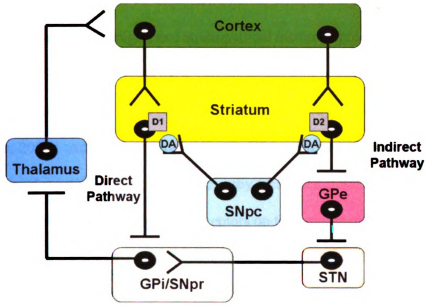

Figure 1-1. Anatomy of the basal ganglia. Neuronal axon terminals are represented as glutamatergic (^) and GABAergic (⊥). The basal ganglia can alter the activity of the thalamus output to the motor cortex using the direct (excitatory) pathway or the indirect (inhibitory) pathway on the thalamus. NSDA neurons originating in the substantia nigra pars compacta (SNpc) terminate in the striatum and regulate the activity of the direct and indirect pathways. Cell bodies of the different neuronal populations making up the basal ganglia originate or axonal terminals terminate in the cortex, striatum, internal segment of the globus pallidus (GPi), external segment of the globus pallidus (GPe), subthalamic nucleus (STN), substantia nigral pars reticulata (SNpr), or thalamus. D1 and D2 dopamine receptors are located on cell bodies of the medium spiny neurons originating in the striatum and terminating in the GPi/SNpr or the GPe.

causes inhibition of motor output thereby counteracting the excitatory effects of the direct pathway in the thalamus (Benarroch, 2007).

The ultimate regulatory mechanism of these two pathways is the NSDA neurons that synapse on both striatonigral and striatopallidal medium spiny neurons in the striatum. The release of DA onto these two populations of medium spiny neurons regulates the function of both the direct and indirect pathways differentially (DeLong and Wichmann, 2007). Activation of dopaminergic D1 receptors in the direct pathway leads to excitation of striatonigral neurons and thereby facilitates motor output by the thalamus. DA activation of the dopaminergic D2 receptors on the striatopallidal neurons inhibits these neurons also facilitating motor output (Squire, 2003; Benarroch, 2007).

The Basal Ganglia in PD

Degeneration of the NSDA neurons within the basal ganglia leads to dysfunction of the basal ganglia and over-activation of the indirect pathway and an overall inhibition of motor facilitation by the thalamus (DeLong and Wichmann, 2007). This process occurs through the loss of dopaminergic inhibition on striatopallidal GABAergic neurons, which (in turn) leads to inhibition of the GABAergic GPe neurons. Inhibition of the GPe leads to firing of the glutamatergic STN neurons onto the GPi/SNpr and inhibition of the motor output by the thalamus (Brotchie, 2003; DeLong and Wichmann, 2007). Overall inhibition of motor output by thalamus is responsible for the slowness of movement which occurs in PD patients.

D. DA Synthesis, Release, and Metabolism

DA is a catecholamine which is made up of a benzene ring, an amine group, and two hydroxyl groups. The synthesis of DA occurs when the dietary amino acid L-tyrosine is transported into the DA neuron via the large neutral amino acid transporter (Squire, 2003). L-tyrosine is converted to 3,4-dihydroxyphenylalanine (DOPA) by the enzyme tyrosine hydroxylase (TH) via the addition of a hydroxyl group to the benzene ring of tyrosine (Dunkley et al., 2004). TH synthesis of DOPA is considered the rate limiting step in DA synthesis because brain levels of L-tyrosine are high enough that TH is saturated and not limited by substrate availability. The synthesis of DA is completed when DOPA is rapidly decarboxylated by the enzyme DOPA decarboxylase (DDC) to form DA, which is primarily sequestered in synaptic vesicles to be released on demand (Squire, 2003).

DA also serves as the precursor for the neurotransmitters norepinephrine and epinephrine in other catecholaminergic neurons. The formation of norepinephrine occurs via the addition of a hydroxyl group to one of the carbon atoms of the amine group on DA by the enzyme DA β-hydroxylase. Norepinephrine serves as the substrate for the synthesis of epinephrine by the enzyme phenylethanolamine N-methyltransferase (Squire, 2003).

TH is the key rate limiting enzyme in the synthesis of DA and its activity can be regulated in dopaminergic neurons by various mechanisms. TH has 4 serine phosphorylation sites critical for enzyme activation including serine 8, 19, 31, and 40. Phosphorylation of these serine sites is important for regulation of TH activity, though TH serine 40 phosphorylation is key to maximal activation of the enzyme.

Phosphorylation of TH at the various serine residues occurs via kinases such as protein kinase A and protein kinase C, both of which phosphorylate serine 40 (Dunkley et al., 2004; Bobrovskaya et al., 2007). Activated TH uses the cofactor tetrahydrobiopterin (BH_4), oxygen (O_2), and Fe^{+2} to hydroxylate L-tyrosine. In this reaction the Fe^{2+} component of TH binds L-tyrosine and in the presence of BH_4 and O_2, L-tyrosine is hydroxylated to DOPA, BH_4 is converted to dihydrobiopterin (BH_2), and one molecule of H_2O is produced (Figure 1-2) (Fitzpatrick, 2003). Regulation of TH involves end-product (DA) feedback inhibition, where DA competition with BH_4 for the Fe^{2+} site on TH reduces TH activity. The availability of BH_4 (either limited or in excess) can reduce TH activity as does limitations in availability of the substrate L-tyrosine (Dunkley et al., 2004). However, the extent and threshold for initiation of end product inhibition by DA on TH activity depends on the dopaminergic neuronal population (Figure 1-3).

Following its release into the synapse, DA binds to either pre- or post-synaptic DA receptors or is taken back up into the DA neuronal terminal via the DA transporter (DAT) (Storch et al., 2004). Following reuptake by DAT, DA is either re-sequestered into synaptic vesicles via the vesicular monoamine transporter 2 (VMAT2) or is metabolized within the mitochondria by monoamine oxidase B (MAO B) to 3,4-dihydroxyphenylacetaldehyde (DOPAL), and then to the metabolite 3,4-dihydroxyphenylacetic acid (DOPAC) via aldehyde dehydrogenase (AD) (Figure 1-3). DOPAC diffuses out of the neuron and is converted to homovanillic acid (HVA) by catechol-O-methyltransferase (COMT) in glial cells. Alternatively DA is converted via COMT to 3-methoxytyramine (3-MT) in glial cells, 3-MT is converted to HVA aldehyde

(HVAA) by MAO, and HVAA is metabolized to HVA via AD (Figure 1-4) (Squire, 2003; Galvin, 2006).

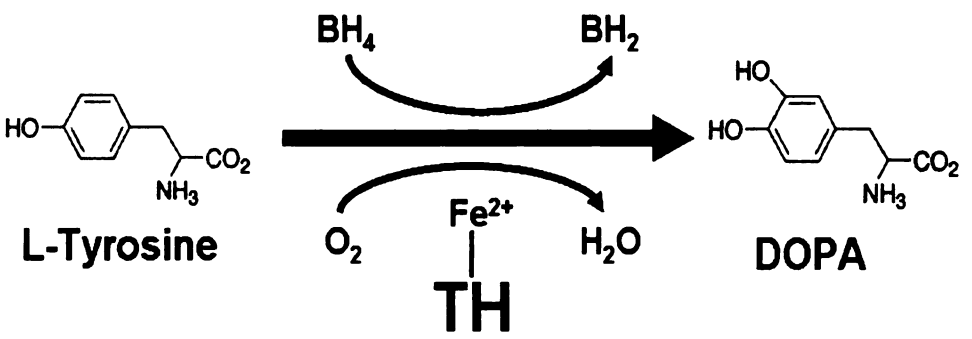

Figure 1-2. TH synthesis of DOPA from dietary tyrosine. DOPA is synthesized from L-tyrosine by oxidation of L-tyrosine in the presence of tetrahydrobiopterin (BH_4) and O_2 by TH. Figure is adapted from (Fitzpatrick, 2003).

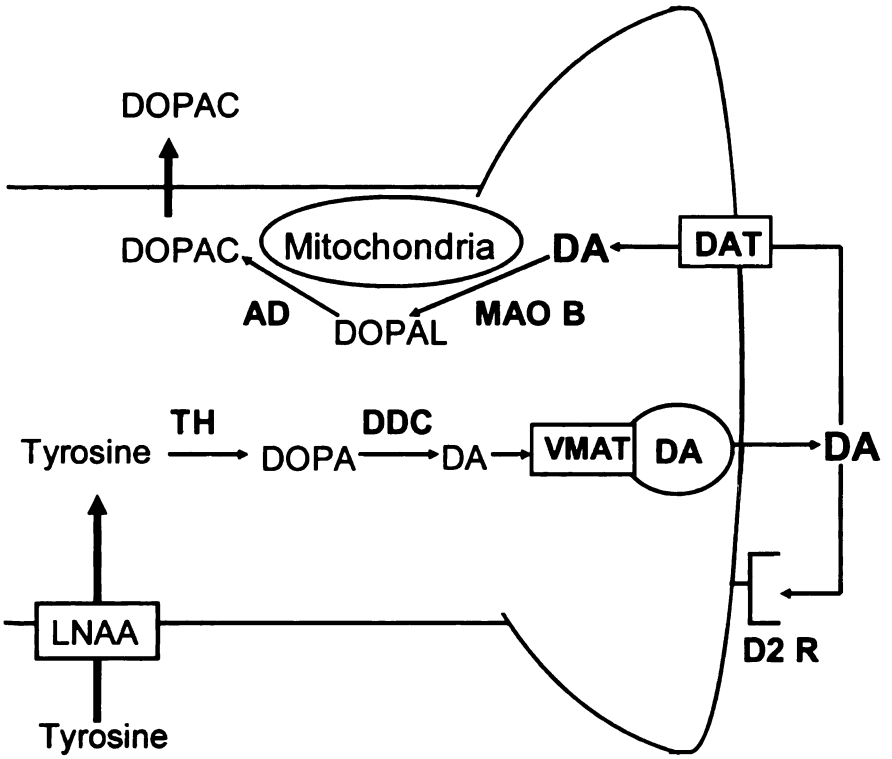

Figure 1-3. DA synthesis, release, reuptake, and metabolism at the NSDA axon terminal. DA is synthesized by hydroxylation of L-tyrosine by TH to form DOPA which is decarboxylated by DDC to form DA. DA is sequestered into synaptic vesicles by uptake by VMAT. DA is released with the arrival of an action potential into the synapse, taken up by DAT, and either metabolized by MAO B and AD to DOPAC or re-sequestered into synaptic vesicles for re-release by VMAT.

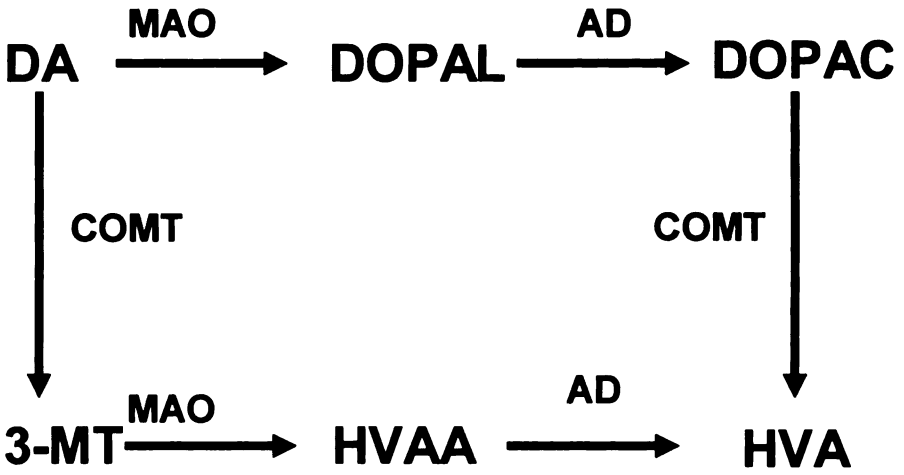

Figure 1-4. DA is metabolized by one of two pathways to HVA. DA is converted from DA to DOPAL to DOPAC to HVA or to 3-MT to HVAA to HVA. Figure is adapted from (Galvin, 2006).

E. DA Neuronal Populations

Dopaminergic neurons are divided into one of ten different neuronal populations that constitute part of the catecholamine neuronal system within the brain made up of 17 catecholaminergic neuronal groups classified in a caudal to rostral numerical system (A1-A17) (Figure 1-5). The A1-A7 groups are noradrenergic neurons, whereas the A8-A17 groups are dopaminergic neurons. The mesencephalic dopaminergic neurons consist of the A8 (retrorubal), A9 (nigrostriatal), and A10 (ventral tegmental) populations that are found within the midbrain. The diencephalic dopaminergic neurons include A11 (diencephalspinal), A12 (tuberoinfindibular), A13 (incertohypothalamic), A14 (periventricular-hypophysial/periventricular), and A15 (ventral lateral hypothalamic) neurons (Bjorklund, 1984a; Lookingland, 2005; Pappas et al., 2008). Two other dopaminergic neuronal populations the A16 and A17 are found within the glomerular layer of the olfactory bulb and the retina, respectively (Hida et al., 1999; Chen et al., 2000). The function and regulation of the nigrostriatal, ventral tegmental, and tuberoinfindibular systems have been well characterized (Moore and Wuerthele, 1979; Roth, 1984; Lookingland et al., 1987b; Lookingland et al., 1987a; Murrin and Roth, 1987; Eaton et al., 1992; Eaton et al., 1994; Lookingland, 2005).

The A9 nigrostriatal dopaminergic (NSDA) neurons originate in the SNpc, project their axons via the medial forebrain bundle, and primarily terminate in the striatum (caudate-putamen) of the forebrain. The A8 dopaminergic neurons originating in the ventral tegmental area (VTA) project through the medial forebrain bundle to both the nucleus accumbens and prefrontal cortex via the mesolimbic DA (MLDA) and mesocortical DA pathways (Fallon and Moore, 1978; Bjorklund, 1984a). The A12

tuberoinfindibular dopaminergic (TIDA) neurons originate in the arcuate nucleus of the hypothalamus and terminate in the median eminence (Moore and Wuerthele, 1979)

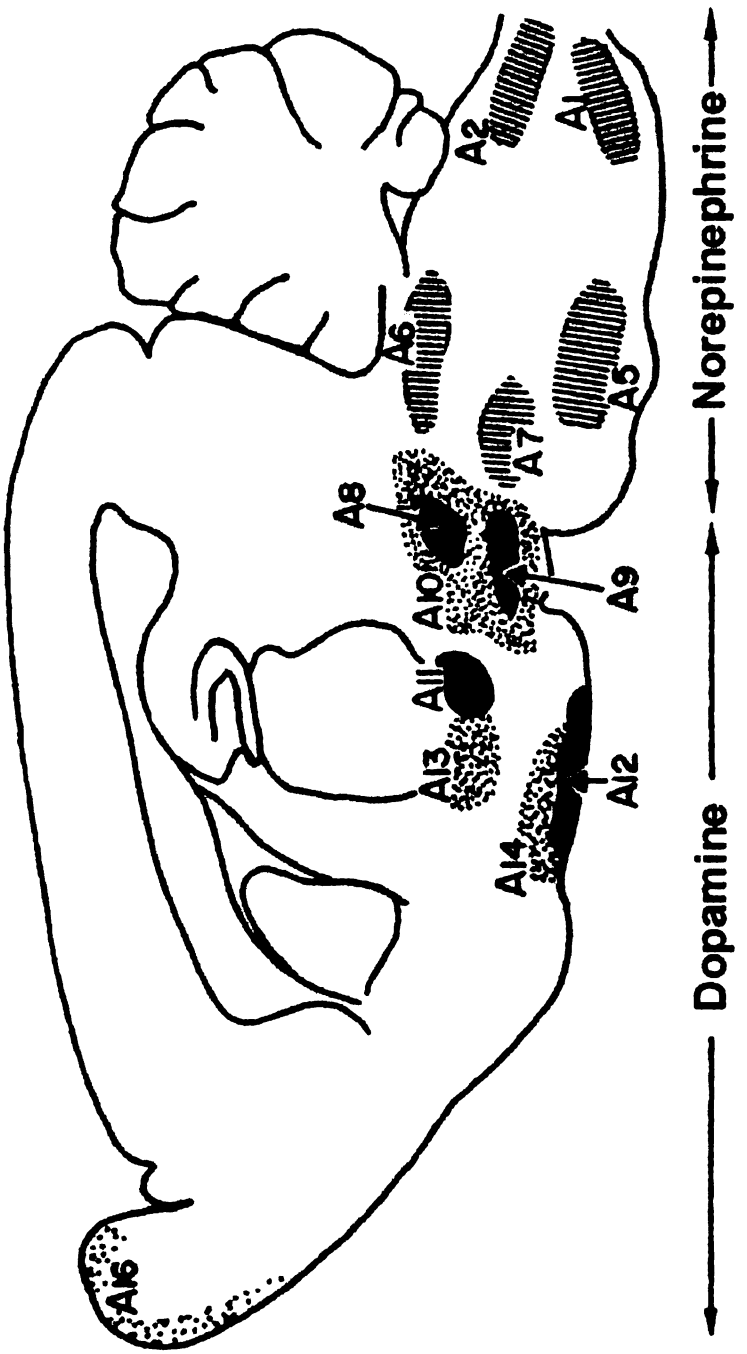

Figure 1-5. Catecholaminergic neuronal populations in the rodent brain. A1-A7 populations are noradrenergic and A8-A16 are dopaminergic. Catecholamine neuronal populations and are located in numerical order in a caudal to rostral direction (Moore, 1987).

F. DA Receptors

DA receptors are found throughout the brain and five different subtypes of DA receptors have been cloned and characterized. All DA receptors are G protein linked primarily to either G inhibitory (G_i) or G stimulatory (G_s). The receptors have been classified into two families D1-like and D2-like (Sealfon and Olanow, 2000). These two families of DA receptors were first characterized by their functions and ligand binding properties. The family of D1 receptors (D1 and D5) were determined to stimulate adenylate cyclase and D2 the receptors (D2, D3, & D4) inhibited adenylate cyclase (Onali et al., 1985; Missale et al., 1998). These classifications are still maintained today and have since been well characterized as described.

The D1 receptor is a G_s linked protein which stimulates adenylate cyclase and was the first of its family to be cloned The D5 receptor was cloned and found to have similar properties to the D1 and thus was grouped in the D1 like family (Sunahara et al., 1991). D1 receptor localization was initially determined by ligand binding studies (Dubois et al., 1986; Savasta et al., 1986), but since D1 receptor mRNA and protein within the brain has been determined. D1 receptors have the highest expression level within the brain, and are mainly found within the striatum, nucleus accumbens, olfactory tubercle, limbic system, hypothalamus, and thalamus (Missale et al., 1998; Sealfon and Olanow, 2000). D5 receptor expression is very limited in the brain and is exclusively found on neurons mainly in the limbic regions, olfactory tubercle, hippocampus, and mammillary nucleus (Sunahara et al., 1991; Missale et al., 1998; Sealfon and Olanow, 2000).

The D2 receptor is G_i linked and inhibits adenylate cyclase. Similar to the D1 family receptor localization studies, initially location of the D2 family of receptors was determined using ligand binding studies (Onali et al., 1985; Camus et al., 1986). However, these findings were later confirmed or expanded using mRNA and protein expression studies within the brain. The D2 receptor is expressed widely throughout the brain including the basal ganglia, pituitary, striatum, olfactory tubercle, nucleus accumbens, hypothalamus, VTA, and SNpc (Bunzow et al., 1988; Sesack et al., 1994; Missale et al., 1998; Sealfon and Olanow, 2000). D3 receptor expression is mainly found within the nucleus accumbens, olfactory tubercle, hypothalamus, and limbic areas of the brain, with low expression in the striatum, VTA, and substantia nigra (Sokoloff et al., 1990; Sealfon and Olanow, 2000). D4 receptors are mainly found in the frontal cortex, amygdala, olfactory bulb, and hypothalamus (Sealfon and Olanow, 2000).

The D3 and D4 receptors were later cloned and found to have similar properties to the D2 receptor and were classified in the D2-like family of DA receptors (Bunzow et al., 1988; Sokoloff et al., 1990; Van Tol et al., 1991). One of the main differences between the D1 and D2 families of receptors is that the D1 family does not have any introns and only comes in one form. However, the D2 family contain at least one intron thus allowing more then one splice variant to exist for each receptor (Sesack et al., 1994; Missale et al., 1998).

The role of D1 and D2 receptors in the basal ganglia is important for the regulation of locomotion and (in the case of D2 receptors) regulation of dopaminergic neuronal activity (Missale et al., 1998). D1 receptors are located on GABAergic medium spiny neurons within the striatum that project via the striatonigral pathway to the SNpr

and the GPi. These GABAergic medium spiny neurons express substance P and dynorphin, and D1 receptor stimulation increases the expression of these neuropeptides in these neurons. D2 receptors are also located on GABAergic medium spiny neurons within the striatum that project via the striatopallidal pathway to the GPe and release the neuropeptide enkephalin (Ariano et al., 1992; Yung et al., 1995; Missale et al., 1998). Stimulation of D2 receptors inhibits the expression of the enkephalin precursor peptide preproenkephalin in striatopallidal neurons (Missale et al., 1998).

D2 receptors are also on the cell bodies, dendrites, and axon terminals of NSDA and MLDA neurons, and these "D2 autoreceptors" regulate the synthesis and release of DA (Roth, 1984; Bozzi and Borrelli, 2006). D2 receptors are also expressed by anterior pituitary lactotrophs. DA released from TIDA neurons terminating in the median eminence binds to these receptors and inhibits the release of prolactin from these lactotrophs (Borgundvaag and George, 1985; Moore, 1987).

G. Regulation of DA Synthesis in Central Dopaminergic Neurons

There are three primary regulatory mechanisms of DA synthesis in central dopaminergic neurons including post-synaptic long loop feedback, pre-synaptic short loop feedback, and end product inhibition (Moore and Wuerthele, 1979; Roth, 1984; Ogren et al., 1986). Post-synaptic long loop feedback involves DA action on post-synaptic DA receptors that inhibit the release of DA from the pre-synaptic terminal via afferent neuronal inhibition of dopaminergic neuronal activity. Short loop feedback involves DA in the synapse binding pre-synaptic D2 autoreceptors leading to direct inhibition of TH activity and the release of DA from the pre-synaptic terminal. End-product inhibition occurs within DA neurons when the concentration of intracellular DA suppresses TH activity.

Regulation of dopaminergic neurons can vary amongst groups and these neurons may be regulated by one or more of these mechanisms. NSDA neurons possess all three mechanisms of feedback inhibition (Figure 1-6). DA binding to D2 receptors on post-synaptic medium spiny neurons leads to post-synaptic long loop feedback inhibition of NSDA neuronal activity (Ogren et al., 1986; Eaton et al., 1992). D2 autoreceptors on the axonal terminals of NSDA neurons inhibit TH activity within the cell and the release of DA into the synapse (Walters and Roth, 1976; Bannon et al., 1981; Foreman et al., 1989; Eaton et al., 1994; Pappas et al., 2008). End product inhibition occurs when cytoplasmic concentrations of DA within NSDA neurons increases due to DA synthesis or reuptake of released DA by DAT. Non-sequestered DA can directly inhibit the activity of TH by competitively inhibiting the binding of tyrosine to the Fe^{2+} site on TH (Demarest and Moore, 1979).

MLDA neurons also possess all 3 mechanisms of DA neuronal regulation, although MLDA neuronal D2 autoreceptor function is more sensitive than NSDA neurons (Demarest and Moore, 1979; Demarest et al., 1983; Ogren et al., 1986; Eaton et al., 1992). In contrast to NSDA and MLDA neurons, TIDA neurons exhibit only end-product inhibition and lack both short and long loop feedback mechanisms (Demarest and Moore, 1979; Berry and Gudelsky, 1991; Pappas et al., 2008).

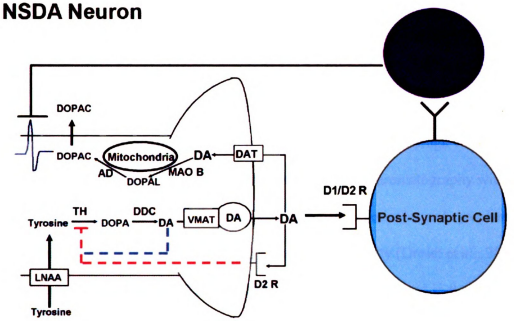

Figure 1-6. Feedback regulation of NSDA neuronal activity. Feedback mechanisms **include** post-synaptic long loop feedback, pre-synaptic short loop feedback (red dashed **line**), and end product inhibition (blue dashed line).

H. Indices of DA Neuronal Integrity and Activity

Several indices are commonly used to determine the integrity of dopamine neurons. The integrity of dopaminergic terminals can be determined by measuring the concentrations of DA and/or protein content of TH and DAT in the dopaminergic axon terminal region. DA concentrations are primarily located in synaptic storage vesicles in axon terminals and are measured using high performance liquid chromatography with electrochemical detection (HPLC-EC). A decrease in synaptic vesicular and cytoplasmic DA concentrations reflects a loss in dopaminergic terminal integrity (Drolet et al., 2004). The protein content of cytoplasmic TH and membrane-bound DAT found in the striatum are measured using Western blotting and have been used as an index of terminal integrity (Tillerson et al., 2002; Jakowec et al., 2004). A decrease in either TH or DAT protein reflects a loss of dopaminergic neuronal terminals, especially DAT which is almost exclusively expressed by dopaminergic neurons.

Cell body integrity of dopaminergic neurons is determined by counting the number of TH immunoreactive cells in regions of the brain containing cell bodies of these neurons (Jackson-Lewis et al., 1995; Petroske et al., 2001). However, if a change in TH cell body number is found in a region, it is critical to count cells in this region using another neuronal cell marker that labels all neuronal cell bodies such as Nissl/Cresyl Violet. By doing this and comparing the number of TH immunoreactive cells to the number of Nissl positive cells one can discern if there is clearly a reduction in cell number or if there is a decrease in the number of cells expressing TH (Jackson-Lewis et al., 1995). The amount of TH protein determined by Western blotting in cell body

regions of the dopaminergic neurons is also used as an indicator of TH cell body integrity.

The ratio of either of the two major DA metabolites DOPAC or HVA to DA itself (DOPAC/DA or HVA/DA) is used as an index of DA neuronal activity (Moore and Wuerthele, 1979). Activity of the DA neuron consists of synthesis, release, reuptake, and metabolism of DA. Increased activity is indicated by an increased ratio due to a decrease in DA stores and/or an increase in metabolism of DA to DOPAC or HVA due to greater release and reuptake of DA. A decrease in either of the ratios would be reflective of a reduction in dopaminergic neuronal activity (Moore and Wuerthele, 1979; Lookingland, 2005).

I. Serotonin Synthesis and Neuronal Function

The dorsal and median raphe nuclei is the location of cell bodies for the neurons which project to the forebrain and release the neurotransmitter serotonin (5-hydroxytryptamine; 5HT), another biogenic amine neurotransmitter. Serotoninergic neurons project axons via ascending and descending pathways throughout the brain, but mainly in a rostral direction. Specific regions that 5HT neurons terminate include the striatum, nucleus accumbens, cerebral cortex, substantia nigra, hypothalamus and spinal cord (Moore et al., 1978; Bjorklund, 1984b).

5HT is an indolamine synthesized from the amino acid L-tryptophan, which (like tyrosine) is taken up by the large neutral amino acid transporter. Synthesis of 5HT is substrate limited by the low concentrations of dietary L-tryptophan (Wurtman and Fernstrom, 1975; Squire, 2003). L-tryptophan is hydroxylated by the rate limiting enzyme tryptophan hydroxylase to L-5-hydroxytryptophan, and decarboxylated by aromatic-L-amino acid decarboxylase to 5HT. 5HT is taken up into synaptic vesicles by VMAT2 and stored until release (Squire, 2003). Following its release 5HT binds to pre- and post-synaptic 5HT receptors (Cerrito and Raiteri, 1979; Fink and Gothert, 2007), and is inactivated by re-uptake into pre-synaptic terminals by the serotonin reuptake transporter (SERT). 5HT can be metabolized within the serotoninergic neuron by MAO to 5-hydroxyindole acid aldehyde and oxidized to 5-hydroxyindole acetic acid (5HIAA) (Squire, 2003).

Similar to dopaminergic neurons, the integrity of serotoninergic neurons can be determined by measuring the concentrations of 5HT within brain regions containing axonal terminals of serotoninergic neurons, including the striatum or nucleus accumbens.

The activity of serotoninergic neurons can also be estimated like dopaminergic neurons by determining the ratio of the 5HT metabolite 5HIAA to 5HT (5HIAA/5HT) ratio (Tian et al., 1992; Darmani et al., 2003).

J. Neurotoxic Models of PD

MPTP

MPTP is a relatively selective neurotoxin for dopaminergic neurons. MPTP was discovered to cause a Parkinson's like movement disorder in 1982 when a group of heroin users in California accidentally injected themselves with the neurotoxin that was a by-product of an attempted synthesis of a meperidine analog (Langston et al., 1983). The patients presented soon after with a movement disorder resembling PD. Later it was determined that MPTP was the offending agent following analysis of samples of the drugs the patients injected. The use of MPTP as a potential model of PD followed the incidental finding of Parkinson's like symptoms in these drug users (Dauer and Przedborski, 2003).

MPTP is a lipophilic compound that readily crosses the blood brain barrier. MPTP is converted to MPDP+ (1-methyl-4-phenyl-2,3-dihydropyridine) primarily in glial cells by the enzyme MAO B and is oxidized to its active metabolite MPP+ (1-methyl-4-phenylpyridinium) (Markey et al., 1984; Dauer and Przedborski, 2003). MPP+ has a high affinity for DAT and is selectively transported by DAT into dopaminergic neurons (Figures 1-7 & 1-8) (Javitch et al., 1985; Gainetdinov et al., 1997; Dauer and Przedborski, 2003). Once inside the DA neuron, MPP+ blocks Complex I of the mitochondrial respiratory chain thereby inhibiting the synthesis of ATP causing energy depletion and oxidative stress (Vyas et al., 1986). MPP+ is also sequestered into synaptic vesicles containing DA via uptake in to vesicles by the VMAT2 (Liu et al., 1992). Oxidative stress also occurs by MPP+ oxidation of DA forming DA quinones which are a free radical species of DA that induce further production of other free radical species and

can modify proteins altering neuronal function (Figure 1-8) (Klaidman et al., 1993; Dauer and Przedborski, 2003; Lee et al., 2003). The method of cell death attributed to MPTP induced neurotoxicity is dependent on the dosing paradigm and frequency of administration but apoptosis (programmed cell death), autophagy, and necrosis have all been implicated (Zhu et al., 2007).

MPTP is likely the most common model used to study PD. MPTP can elicit its neurotoxic effects not only in humans but also in monkeys and mice (Burns et al., 1983; Heikkila et al., 1984). The differences in MPTP dosage, dosing frequency, interval between injections, and time point following MPTP treatment when the animals are killed can produce differential effects on dopaminergic terminal degeneration (Sundstrom et al., 1987; Sundstrom et al., 1990; Behrouz et al., 2007).

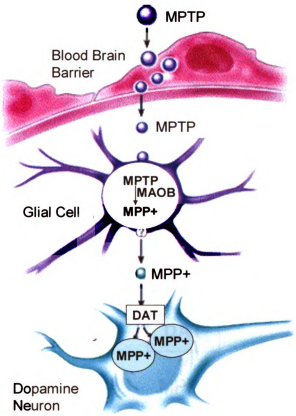

Figure 1-7. Metabolism of MPTP to MPP+ and transport of MPP+ into DA neurons. **MPTP** crosses the blood brain barrier as a lipophilic compound and is metabolized by **MAOB**, than oxidized to its active metabolite MPP+ and released via an unknown **mechanism** by glial cells to be taken up into the dopaminergic neuron. Figure is taken **from** (Dauer and Przedborski, 2003).

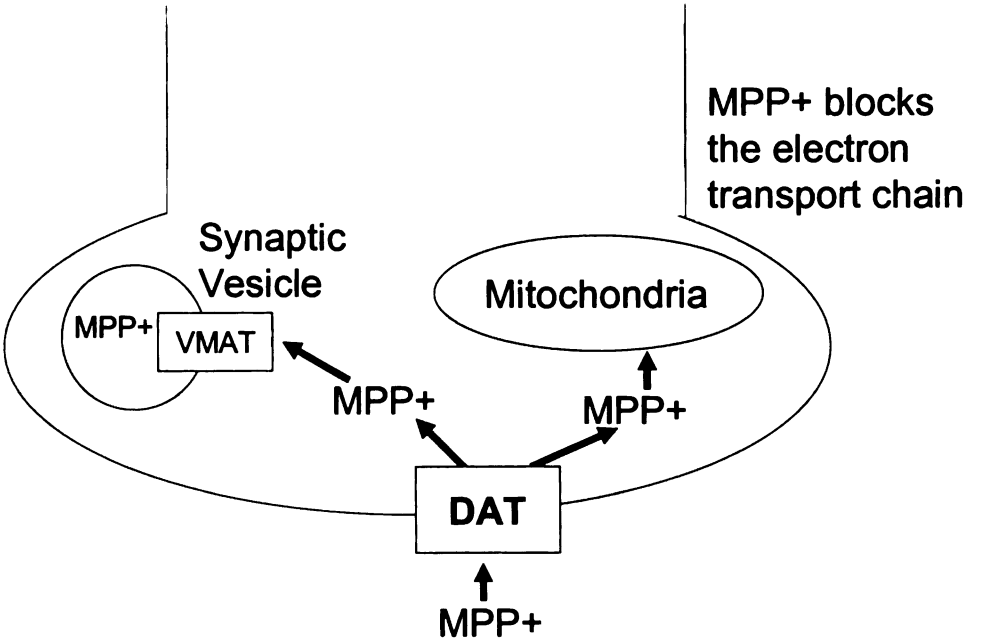

Figure 1-8. Effects of MPP+ at the dopaminergic neuronal terminal. MPP+ is transported into the dopaminergic neuronal terminal by DAT and inhibits Complex I in the mitochondrial respiratory chain or is sequestered into synaptic vesicles by uptake into vesicles by VMAT.

6-Hydroxydopamine (6-OHDA)

The 6-hydroxydopamine (6-OHDA) model was the first established rodent model for PD. 6-OHDA is a hydroxylated analogue of DA and is taken up by both DAT and the norepinephrine transporter (NET) into catecholaminergic neurons (Bove et al., 2005). 6-OHDA accumulates in the cytosol and upon oxidation induces reactive oxygen species production and the formation of quinone species within the cell (Heikkila and Cohen, 1973). Although reactive oxygen species are the primary cause of 6-OHDA mediated death, the quinone species also contribute by reacting with cellular DNA and proteins causing cellular damage (Jonsson and Sachs, 1975; Bove et al., 2005; Drechsel and Patel, 2008). The death of dopaminergic neurons induced by 6-OHDA can also activate microglial cells within the brain which in turn directly induce the loss of NSDA neurons (Rodriguez-Pallares et al., 2007).

6-OHDA does not easily cross the blood brain barrier and accordingly needs to be administered directly into the brain by stereotaxic injection. In the various 6-OHDA rodent models of PD, the neurotoxin is injected directly into the substantia nigra, medial forebrain bundle or striatum, either unilaterally or bilaterally. Injection into the substantia nigra or medial forebrain leads to a more substantial and rapid loss of NSDA neurons, compared to injection into the striatum which involves a more progressive retrograde loss of NSDA neurons and axonal terminals over 1-3 weeks (Bove et al., 2005). Unilateral injection of 6-OHDA is advantageous in that it selectively lesions one side of the NSDA neuronal system causing DA agonist induced turning behavior which is proportional to the extent of the lesion (Przedborski et al., 1995). This model system is therefore used to test potential anti-parkinson's drugs, by quantifying the circling

behavior of the rodent. Although, 6-OHDA is not completely selective for dopaminergic neurons, it is still used frequently as a rodent model of PD.

Rotenone

Rotenone is a common pesticide which (like MPTP) is lipophilic and inhibits Complex I of the mitochondrial respiratory chain (Bove et al., 2005). Rotenone has only recently been used as a model of PD by a limited number of investigators (Betarbet et al., 2000). The primary mechanism of rotenone toxicity is its ability to inhibit Complex I and induce ATP depletion and ROS formation (Bove et al., 2005; Drechsel and Patel, 2008). Rotenone also directly activates microglial cells, which contributes to microglial mediated induced death of NSDA neurons (Gao et al., 2002a; Sherer et al., 2003). Since rotenone is the active form of the neurotoxin and is lipophilic, it is not selective for dopaminergic neurons. Preferential loss of NSDA (as opposed to MLDA) neurons has been demonstrated following rotenone administration, likely do the higher sensitivity of NSDA neurons to the deleterious effects of oxidative stress (Drechsel and Patel, 2008). Rotenone administration causes protein aggregates within NSDA neurons that are similar to Lewy bodies, suggesting that this model may be ideal for studying pathology associated with proteosome and related protein metabolism deficits (Betarbet et al., 2000; Dauer and Przedborski, 2003). The use of the rotenone model is considered limiting, however, due the lack of selectivity and the extent of disruption of NSDA neurons.

K. Inflammation in the Brain

Microglial Cells

Microglial cells are the resident immune cells in the brain that are derived from a myeloid lineage and are similar to macrophage cells found outside of the central nervous system (Rock et al., 2004). Microglia are estimated to constitute about 15% of all cells within the brain, but the number of microglia can vary among brain regions with some areas having a higher number of microglia than others (Kim et al., 2000; Rock et al., 2004). Microglial cells serve as a form of immune surveillance in the central nervous system in their resting state and have a ramified morphology (Vilhardt, 2005). Activation of microglial cells leads to a rapid transformation from a ramified shape to an amoeboid circular shape. Microglial activation also results in a significant increase in the number of cell membrane receptors involved in the inflammatory response and an increase in the release of inflammatory cytokines and free radical species (Rock et al., 2004; Vilhardt, 2005).

Microglial activation can occur in response to infection, brain injury and neuronal cell death, and leads to microglial proliferation and migration, increased phagocytic activity, and ability to present antigens to other immune cells (Vilhardt, 2005; Liu, 2006). Activated microglia also release pro-inflammatory mediators including tumor necrosis factor alpha (TNF-α), interleukin-1 beta (IL-1β), prostaglandins, chemokines, ROS and reactive nitrogen species (Hanisch, 2002). Activated microglia release the anti-inflammatory cytokine IL-10 and neurotrophic factors (Vilhardt, 2005). The ability of microglia to identify infection, injury, or cell death is beneficial in that an immune reaction is initiated which recruits other microglia via cytokines to remove dead or dying

cells. The detrimental effects of microglial activation include increased numbers of activated microglial which prolongs the release of pro-inflammatory mediators and free radical species. This process termed "microgliosis" continues throughout the cycle of microglial activation and induces death of surrounding neurons (Block and Hong, 2005).

Microglial Activation and PD

Inflammation induced neuronal death mediated by activated microglia has been implicated in the process of neurodegeneration in several diseases including PD, Alzheimer's disease, multiple sclerosis, and stroke. PD patients and animal models of PD demonstrate a greater number of microglia within the substantia nigra region compared to controls (McGeer et al., 1988; Imamura et al., 2003; Barcia et al., 2004; Ouchi et al., 2005), making NSDA neurons more likely to experience microgliosis (Kim et al., 2000). Microglial mediated cell death of NSDA neurons likely occurs in humans and is seen in several animal models of PD.

Several different neurotoxins and inflammatory mediators are used in animal models to study PD, and have yielded valuable information concerning potential factors which lead to the development of the disease. Several of these animal models either directly or indirectly activate microglia (Figure 1-9). The MPTP and 6-OHDA neurotoxin models of PD indirectly activate microglia by inducing NSDA neuronal cell loss (Gao et al., 2003; Block and Hong, 2005). The neurotoxin rotenone induces NSDA neuronal cell death, but also activates microglia directly (Gao et al., 2002a). However, the lipopolysaccharide (LPS) model of PD allows the exclusive activation of microglia

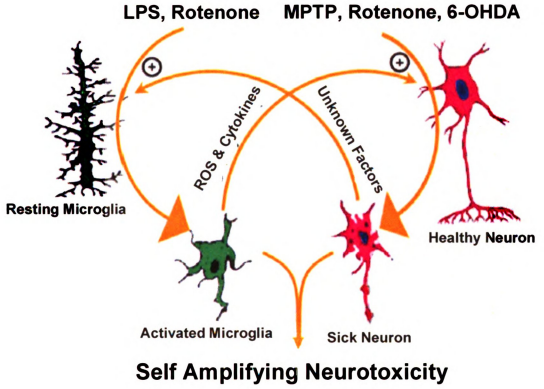

Figure 1-9. Direct and indirect activation of microglia induces microgliosis in models of **PD.** LPS and rotenone directly activate resting microglial cells and the neurotoxins 6-**OHD**A, MPTP, and rotenone indirectly activate microglial cells by inducing neuronal **death** leading to microgliosis. Figure taken from (Hald and Lotharius, 2005).

without direct induction of NSDA neuronal cell death (Liu et al., 2000a; Iravani et al., 2005; Roy et al., 2006).

LPS as an Inflammatory Model of PD

LPS is a component of the cell wall of gram negative bacteria which directly activates resident microglia in the brain via the Toll-like receptor 4 (TLR4) (Lehnardt et al., 2003; Qin et al., 2005). LPS is able to exclusively induce microglia activation because neurons lack TLR4 receptors (Lehnardt et al., 2003). This allows study of microglial mediated loss of NSDA neurons, without concurrently inducing NSDA neuronal loss by a neurotoxic mechanism. Most studies using LPS in *in vivo* models of PD directly inject LPS into the substantia nigra or striatum of rodents (Castano et al., 1998; Kim et al., 2000; Hsieh et al., 2002; Iravani et al., 2002; Zhou et al., 2005). This allows a relatively localized activation of microglia in these regions leading either to loss of NSDA neuronal cell bodies followed by retrograde loss of axon terminals. In contrast, LPS can also be injected systemically but induces an inflammatory reaction throughout the brain and does not cause loss of NSDA neurons till at least 7 months (Qin et al., 2007).

L. Neurogenesis and Sildenafil

Neurogenesis and stem cell replacement therapy have been proposed as ways to replace NSDA neurons lost in PD. Stimulation of endogenous neural stem cells within the brain would be most ideal as this would prevent a host-immune response to donor stem cells (Borlongan et al., 1996). One potential mechanism to induce neurogenesis is through inhibition of the enzyme phosphodiesterease 5 (PDE5). PDE5 catalyzes the break down of 3',5'-cyclic guanosine monophosphate (cGMP) to 5'-guanosine monophosphate (Corbin and Francis, 1999; Kulkarni and Patil, 2004). Increased cGMP levels following inhibition of PDE5 using the drug sildenafil increases neurogenesis of subventricular derived stem cells (Wang et al., 2005). Sildenafil also increases the concentrations of cGMP in the brain, promotes neurogenesis from the subventricular zone within the brain, and improves neurological recovery following ischemic stroke in rodents (Zhang et al., 2002; Zhang et al., 2005; Zhang et al., 2006a). This information suggests that sildenafil may be a potential mechanism to induce neurogenesis in a rodent model of PD. Studies outlined in Chapter 3 of this disseration tested this possibility.

M. The Role of Nicotinamide Adenine Dinucleotide Phosphate (NADPH) Oxidase in Microglial Mediated Death of NSDA Neurons

The ability of microglia to produce the ROS superoxide in models of PD has been attributed to the activation of the enzyme NADPH oxidase (Gao et al., 2002a; Gao et al., 2003). NADPH oxidase is found in several cell types in the central nervous system including microglia, astrocytes, and neurons (Serrano et al., 2003; Abramov et al., 2005; Block and Hong, 2005). The activation of microglial NADPH oxidase contributes to the process of microgliosis which is detrimental to NSDA neurons.

As shown in Figure 1-10, NADPH oxidase is composed of the cytosolic GTPase protein Rac1 and subunits in the cytosol (p67Phox, p47Phox, p40Phox) or plasma membrane (gp91Phox, p22Phox). The cytosolic subunits of NADPH oxidase exist as a complex under resting conditions, and the plasma membrane bound subunits exist as a complex known as cytochrome b_{558} (Babior, 1999; Groemping and Rittinger, 2005; Sumimoto et al., 2005). NADPH oxidase is activated when the serine residues on the cytosolic subunit p47Phox are phosphorylated inducing a conformational change of the protein. This change allows sites that interact with the membrane bound subunit p22Phox to be accessible, enabling the cytosolic complex to bind to the membrane. The p67Phox subunit bound to p47Phox and the GTPase protein Rac1 function together to activate the enzyme. The binding of Rac1 to p67Phox, leads to the interaction of p67Phox with gp91Phox, resulting in superoxide production. The cytosolic subunit p40Phox aids in translocation of the cytosolic subunits to the membrane and is involved in binding the complex to the membrane (Groemping and Rittinger, 2005; Sumimoto et al., 2005).

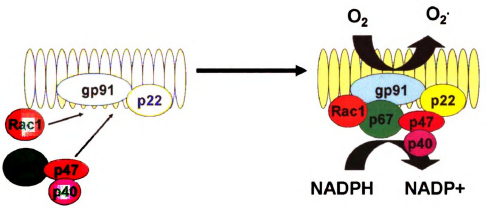

Figure 1-10. NADPH oxidase activation and production of superoxide in microglial cells. The cytosolic NADPH oxidase subunits p67Phox, p47Phox, and p40Phox translocate along with the GTPase protein Rac1 to the membrane bound subunits gp91Phox and p22Phox inducing the production of superoxide (O_2^-) by the transfer of an electron from NADPH to molecular oxygen (O_2).

NADPH induced superoxide or its metabolites hydrogen peroxide and hydroxyl radical play a large role in microgliosis. Hydrogen peroxide induces the expression of the protein inducible nitric oxide synthase (iNOS) that synthesizes the reactive nitrogen species, nitric oxide. Nitric oxide can react with superoxide to produce another reactive nitrogen species, peroxynitrite (Pawate et al., 2004). Nitric oxide and peroxynitrite both inhibit the mitochondrial respiratory chain thereby inducing ATP depletion, free radical species production, and oxidative stress which contributes to the loss of NSDA neurons (Ebadi and Sharma, 2003; Tieu et al., 2003).

Microglial NADPH oxidase activation also induces the production of pro-inflammatory cytokines such as TNF-α and IL-1β. TNF-α release recruits other microglial cells to the site of activation and induces the release of more TNF-α (Kariko et al., 2004; Block and Hong, 2005; Doyle and O'Neill, 2006). IL-1β similar to TNF-α can induce the production of more pro-inflammatory cytokines and activation of microglia (Basu et al., 2004). Microglial proliferation and release of pro-inflammatory cytokines leads to the migration of other resident microglial in the brain that may initially be beneficial, but the activation of microglial can lead to microgliosis (Block and Hong, 2005).

N. Cannabinoids (CB) and Endocannabinoids (ECB)

CB are the psychoactive compounds derived from the plant *Cannabis sativa* also known as marijuana. The primary active compound obtained from marijuana is Δ^9-tetrahydrocannabinol (Δ^9-THC) a lipophilic compound originally isolated from the plant in 1964 (Gaoni, 1964). Other psychoactive, but less potent CB compounds were later isolated. The properties of CB include anti-emetic, anti-inflammatory, and psychoactive effects raising the possibility of the existence of ECB (Svizenska et al., 2008). The first ECB, anandamide was discovered in 1992 and others followed including 2-arachidonoylglycerol (2-AG), noladin ether, and virodhamine (Devane et al., 1992; Mechoulam et al., 1995; Hanus et al., 2001; Porter et al., 2002).

ECB are lipophilic compounds derived from the lipid precursor arachidonic acid. The two main ECB anandamide and 2-AG are found within the brain and several other tissues (Rodriguez de Fonseca et al., 2005). ECB are generally produced in an on demand manner and function in several different biological systems including but not limited to neuronal, inflammatory, cardiovascular, gastrointestinal, and pain pathways (Rodriguez de Fonseca et al., 2005; Svizenska et al., 2008).

Anandamide is synthesized by the transfer of arachidonic acid from phosphatidylcholine within biologic membranes to phosphatidylethanolamine via the calcium dependent enzyme N-acyltransferase (NAT) forming the anandamide precursor N-arachidonylphosphatidylethanolamine (NArPE). NAT is regulated by cAMP which increases enzyme activity via the phosphorylation of protein kinase A (PKA). A NAPE specific phospholipase D then synthesizes anandamide and phosphatidic acid from NAPE (Di Marzo et al., 1994; Rodriguez de Fonseca et al., 2005; Basavarajappa, 2007).

2-AG is synthesized by one of two possible mechanisms where either phospholipase C (PLC) hydrolyzes membrane phospholipids forming diacylglycerol (DAG) or DAG is formed by hydrolysis of phosphatidic acid via Mg^{2+} or Ca^{2+} dependent phoshpatidic acid phosphohydrolase activity. DAG is converted to 2-AG by DAG lipase (Bisogno et al., 1999; Basavarajappa, 2007).

Inactivation of ECB begins with uptake of anandamide or 2-AG into the cell via the anandamide membrane transporter (AMT). Following uptake anandamide is metabolized via hydrolysis by fatty acid amidohydrolase (FAAH) within neurons (Cravatt et al., 1996; Giang and Cravatt, 1997; Thomas et al., 1997; Egertova et al., 2003). 2-AG is also taken into neurons via the AMT and is metabolized by monoacylgycerol lipase (MAGL) to 2-arachidonyl lysophosphatidic acid (Dinh et al., 2002; Blankman et al., 2007). 2-AG can also be degraded by FAAH like anandamide, or via enzymatic oxygenation by cyclooxygenase-2 (COX-2) into prostaglandins (Basavarajappa, 2007).

Localization of CB Receptors within the Central Nervous System

CB receptors are found throughout the central nervous system and are involved in both neuronal and immune function. Within the brain CB activity has mainly been associated with two receptors, the CB1 and CB2 receptors. CB1 receptors are found widely throughout the brain with especially high concentrations in the basal ganglia including the striatum, globus pallidus (GP), and substantia nigra pars reticulata (SNpr). CB1 is also expressed in the hippocampus, cerebellum, cerebral cortex, hypothalamus,

and olfactory bulb (Herkenham et al., 1990; Herkenham et al., 1991b; Hohmann and Herkenham, 2000; Liu et al., 2003; Wittmann et al., 2007).

CB2 receptors are primarily located on microglial cells within the central nervous system and are upregulated by neuronal inflammation and microglial activation (Benito et al., 2003; Maresz et al., 2005; Mukhopadhyay et al., 2006; Ashton et al., 2007; Nunez et al., 2008). CB2 mRNA and protein expression have also been found within and on neurons in the cerebellum and hippocampus (Van Sickle et al., 2005; Gong et al., 2006; Onaivi et al., 2006). CB2 receptors on one population of neurons plays a role in emesis regulation, but others have only minimally been characterized (Van Sickle et al., 2005).

Mechanism of Induced Synthesis and Release of ECB within the Brain

ECB are synthesized *de novo* from lipid precursors and are not stored in synaptic vesicles like typical neurotransmitters. ECB involved in neuronal regulation are typically released from post-synaptic neurons and act on CB1 receptors on the pre-synaptic terminals of inhibitory gamma-aminobutyric acid (GABA) and excitatory glutamate neurons (Mackie, 2008). CB1 and CB2 receptors are G_i protein linked receptors which inhibit adenylate cyclase thereby reducing production of the second messenger cAMP. CB1 receptors are also linked to G_s proteins (Demuth and Molleman, 2006).

The type of pre-synaptic cell, method of ECB production, and post-synaptic cell receptor type determines the terminology of the specific ECB mediated feedback inhibition occurring at a synapse. The predominate form of CB inhibition is depolarization induced suppression of neurotransmission involving a transient suppression of GABA or glutamate release from the pre-synaptic cell (Mackie, 2008).

GABA or glutamate induced depolarization of the post-synaptic cell causes an increase in intracellular dendritic Ca^{2+} concentrations which triggers the production of ECB (Diana and Marty, 2004; Mackie, 2008). ECB are released retrogradely and inhibit Ca^{2+} channels on the pre-synaptic terminal via CB1 receptors and inhibit the release of GABA or glutamate (Figure 1-11) (Kreitzer and Regehr, 2001; Wilson et al., 2001; Wilson and Nicoll, 2001).

A second method of ECB feedback inhibition is metabotropic induced suppression of neurotransmission which occurs when post-synaptic metabotropic glutamate receptors activate phopholipase Cβ and diacylglycerol lipase, thereby triggering the formation of ECB from phospholipids of the membrane. ECB retrogradely feedback on pre-synaptic CB1 receptors reducing GABA or glutamate release. This process requires little calcium (Ca^{2+}) in the post-synaptic cell (Mackie, 2008).

A third form of ECB feedback is long term depression where prolonged low frequency stimulation of glutamatergic postsynaptic cell metabotropic receptors causes high levels of ECB production. This results in prolonged CB1 receptor activation leading to long term inhibition of glutamate release (Robbe et al., 2002). One other mechanism is

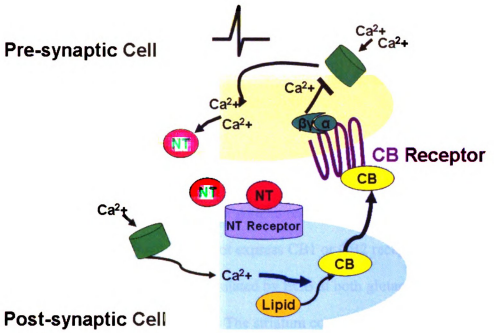

Figure 1-11. Depolarization induced suppression of neurotransmission by cannabinoids. Release of neurotransmitter (NT) from a pre-synaptic cell triggers Ca^{2+} entry into the post-synaptic cell leading to ECB synthesis from lipid precursors. ECB are then released from the post-synaptic cell to inhibit release of NT from the pre-synaptic terminal via action at the CB1 receptor.

ECB inhibition of neuronal excitation where repeated depolarization of a neuron triggers increased intracellular Ca^{2+} concentration inducing ECB production. ECB are released and act on CB1 receptors on the same cell activating inwardly rectifying K+ channels causing hyperpolarization of the neuron (Mackie, 2008).

Role of ECB in the Basal Ganglia

NSDA neurons are part of the basal ganglia regulating motor output from the thalamus. Although NSDA neurons do not express CB1 or CB2 receptors the complex network of the basal ganglia is highly regulated by ECB at both glutamatergic and GABAergic synapses via CB1 receptors. The striatum contains glutamatergic terminals projecting from the motor cortex which possess pre-synaptic CB1 receptors that regulate the release of glutamate by ECB feedback from medium spiny neurons within the striatum (Julian et al., 2003; Matyas et al., 2006; Narushima et al., 2006; Matyas et al., 2008). GABA release from medium spiny neurons in the striatum is also regulated by post-synaptic feedback of CB from the GPe, GPi, and SNpr. The STN making up part of the indirect pathway of the basal ganglia projects glutamatergic neurons to the GPi and SNpr which have CB1 receptors and are regulated by ECB release within the GPi and SNpr (Figure 1-12) (Benarroch, 2007). The many parts of the basal ganglia which possess CB1 receptors indicates the important role ECB function can play in NSDA neuronal regulation.

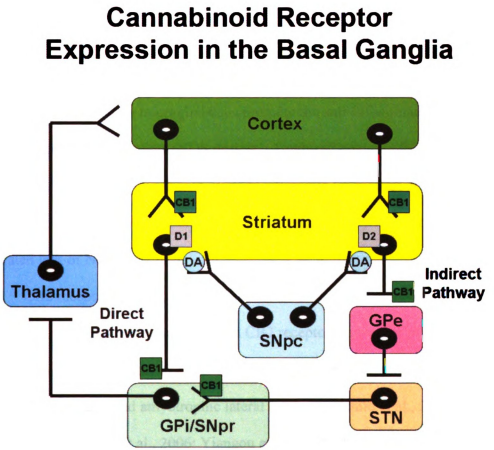

Figure 1-12. CB1 receptor expression within the basal ganglia. CB1 receptors are located on both glutamatergic (^) and GABAergic (⊥) terminals within the basal ganglia. CB1 receptors are on cortical neurons terminating in the striatum. Medium spiny neurons projecting to the globus pallidus interna (GPi), substantia nigra pars reticulata (SNpr), and globus pallidus externa (GPe) have axonal terminal CB1 receptors. Glutamatergic neurons originating in the subthalamic nucleus (STN) and terminating in the GPi and SNpr also have terminal CB1 receptors. ECB action at different locations within the basal ganglia can alter the activity of the direct (excitatory) pathway or the indirect (inhibitory) pathway on the thalamus, and also indirectly effect NSDA neurons originating in the substantia nigra pars compacta (SNpc) and terminating in the striatum.

CB Receptors and Microglial Function

Microglial cells express both CB1 and CB2 receptors (Waksman et al., 1999; Franklin and Stella, 2003). CB1 and CB2 receptors on microglial cells primarily mediate anti-inflammatory functions upon stimulation, although recently they were also suggested to induce inflammation (Roche et al., 2008).

CB1 receptors on microglial cells promote the anti-inflammatory effects of CB by reducing the expression of the iNOS protein. A reduced content of iNOS leads to a reduction in the production of nitric oxide by microglia (Waksman et al., 1999). This effectively reduces the production of peroxynitrite potentially limiting microglial mediated loss of NSDA neurons.

CB2 receptors are responsible for most of the anti-inflammatory effects of CB in the brain. Microglial activation increases CB2 receptor expression *in vitro* and in several neuroinflammatory diseases or conditions such as multiple sclerosis, hypoxic stroke, Alzheimer's disease, and amyotrophic lateral sclerosis (Benito et al., 2003; Maresz et al., 2005; Mukhopadhyay et al., 2006; Yiangou et al., 2006; Ashton et al., 2007). CB2 agonists act as anti-inflammatory agents by reducing the production of TNF-α and nitric oxide, but induce microglial cell migration and proliferation (Franklin and Stella, 2003; Walter et al., 2003; Carrier et al., 2004; Ehrhart et al., 2005; Eljaschewitsch et al., 2006; Fernandez-Lopez et al., 2006). Microglia produce ECB that may act in an autoregulatory fashion on CB2 receptors on microglial cells thereby feeding back to reduce the production of inflammatory mediators (Walter et al., 2003; Carrier et al., 2004). CB2 agonist use in neuropathological models involving significant activation of microglia, leads to an attenuation of microglial activation and slows the progression of disease

demonstrating the anti-inflammatory effects of CB acting at the CB2 receptor (Ramirez et al., 2005; Kim et al., 2006).

The pro-inflammatory effects of CB have recently been suggested, whereby elevation of ECB led to increased TNF-α plasma concentrations. TNF-α which induces activation and migration of microglia and the production of pro-inflammatory cytokines is therefore detrimental. These pro-inflammatory effects of ECB are reversed in the presence of CB1 or CB2 antagonist (Roche et al., 2008). These differential findings make the role of CB in microglial function controversial.

O. Dissertation Objectives

Several mechanisms or pharmacological agents to slow or halt the progression of PD have been evaluated. Most of these potential treatments were aimed at reducing inflammation, oxidative stress, mitochondrial dysfunction, or protein aggregation in an attempt to maintain the integrity of remaining NSDA neurons. Alternatively, administration of neurotrophic factors, implantation of stem cells, or stimulation of adult stem cells already residing in the brain have been attempted to induce the production of new dopaminergic progenitor cells.

Three potential mechanisms of neuroprotection are tested in this dissertation, which are:

Specific Aim #1: Determine if sildenafil induces neurogenesis of NSDA neurons following chronic MPTP treatment by increasing cGMP concentrations in the brain.

Hypothesis: Sildenafil will attenuate the MPTP induced loss of NSDA neurons when treatment is initiated before, during, or after the completion of chronic MPTP treatment.

Specific Aim #2: Determine the pharmacokinetics of apocynin in the brain and examine if apocynin is neuroprotective in an MPTP model of PD by reducing activation of NADPH oxidase.

Hypothesis #1: Apocynin rapidly crosses the blood brain barrier following systemic administration.

Hypothesis #2: MPTP will induce activation of NADPH oxidase that will contribute to the loss of NSDA neuronal terminals, and thus be attenuated with apocynin treatment.

Specific Aim #3: Determine if mice lacking CB1 and CB2 receptors have normal dopaminergic and serotoninergic neuronal integrity, activity, and/or regulation.

Hypothesis #1: A lack of functional CB1 and CB2 receptors will alter the integrity of NSDA, MLDA, TIDA, or serotoninergic neurons.

Hypothesis #2: The activity and/or regulation of dopaminergic and serotoninergic neurons will be altered in mice lacking functional CB1 and CB2 receptors.

Specific Aim #4: Determine the effects of CB1 and CB2 receptor mutation deletion and pharmacological blockade on NSDA neuronal integrity and activity following acute or sub-chronic MPTP or peripheral LPS treatment.

Hypothesis #1: Lack of CB1 and CB2 receptors will increase MPTP induced loss of NSDA axon terminals and cell bodies, and compensatory activation of these neurons.

Hypothesis #2: Acute peripheral LPS treatment of WT and CB1/CB2 KO mice will alter dopaminergic neuronal integrity or neuronal activity.

Each of these specific aims is investigated and hypotheses tested in this dissertation by examining if NSDA neuronal integrity, activity, or microglial activation is altered with either pharmacological treatment or genetic knockout of CB1 and CB2 receptors within the mouse models of PD.

Chapter 2: Materials and Methods

A. Animals

Animals

Male C57BL/6 mice (Jackson Labs, Bar Harbor, ME) age 8-10 weeks were used in most experiments, and as wildtype (WT) controls (CB1 (+/+), CB2 (+/+)) for all studies using mice lacking both CB1 and CB2 receptors (CB1 (-/-), CB2 (-/-)) on a C57BL/6 background. CB1 (-/-)/CB2 (-/-) (CB1/CB2 knockout (KO)) mice were obtained from Drs. Norbert Kaminski and Barbara Kaplan who maintain a breeding colony of CB1/CB2 KO mice at Michigan State University. Mice used for some preliminary pharmacology experiments were obtained from a laboratory colony at Michigan State University maintained by Drs. John Goudreau and Keith Lookingland and are derived from a cross of the B6-129X and C57BL/6 mouse strains.

CB1/CB2 Receptor KO Mice

The sequence for the CB1 receptor in the mouse is located within one exon on chromosome 4 (Zimmer et al., 1999). CB1 receptor KO mice were previously created by replacing most of the CB1 receptor coding sequence between amino acids 32 and 448 with a phosphoglycerate kinase (PGK)-neomycin (neo^r) cassette in MPI2 embryonic stem cells using homologous recombination (Zimmer et al., 1999). These stem cells were used to create chimeric mice which were bred with C57BL/6 mice to create heterozygote CB1 receptor (+/-) mice. Heterozygote CB1 (+/-) mice, were bred to create CB1 receptor (-/-) KO mice (Jarai et al., 1999; Zimmer et al., 1999; Gerald et al., 2006).

The CB2 receptor DNA encoding sequence is also contained within a single exon on chromosome 4. The CB2 gene was inactivated (Buckley et al., 2000) by insertion of a PGK- neo^r cassette into the gene replacing 341 base pairs in the 3' coding exon of the CB2 receptor gene using homologous recombination in the embryonic stem cell line 129. Chimeric mice were generated with embryonic stem cells and crossed with C57BL/6 mice to create heterozygote CB2 (+/-) mice. CB2 receptor KO mice were created by breeding heterozygote CB2 (+/-) mice (Buckley et al., 2000).

Double KO (CB1 (-/-)/CB2 (-/-) mice) were obtained by breeding CB1 (-/-) mice with CB2 (-/-) mice to create double heterozygote CB1 (+/-)/CB2 (+/-) mice. Double heterozygote mice were then bred with one another to obtain CB1 (-/-)/CB2 (-/-) mice which were continually bred with one another to maintain a double KO mouse colony (Jarai et al., 1999). CB 1 (-/-)/CB2 (-/-) were originally obtained by Drs. Kaminski and Kaplan from Dr. Andreas Zimmer of the University of Bonn, and were used to establish a breeding colony at Michigan State University.

CB1 (-/-)/CB2 (-/-) mice were genotyped using tail samples. Approximately 1 cm of the terminal tail was digested using 0.5 mg of Proteinase K (Roche, Basel, Switzerland) in nuclei lysis buffer (25 mM ethylenediaminetetraacetic acid (EDTA), 75 mM NaCl) incubated overnight in a water bath at 58°C with gentle shaking. The following day digested samples were vortexed to homogenize remaining tissue and 30 ug of RNase (Roche) was added to tubes containing lysates and inverted 5 times. Lysates were incubated for 30 min at 37°C in a water bath. Next, 200 ul of protein precipitation solution (4.21 M NaCl, 0.63 M KCl, 8 mM Tris-HCl, pH 8.0) was added to 650 uL of lysate, vortexed for 20 s, chilled on ice for 5 min, and centrifuged for 4 min at 16,000 x g

at 4°C in a Microfuge 18 Centrifuge (Beckman Coutler Inc., Fullerton, CA). Supernatants were removed and placed in new tubes with 600 uL of isopropranol and inverted until DNA strands could be visualized. Samples were centrifuged at room temperature for 1 min to pellet DNA, which was resuspended in 600 uL of ethanol and washed by inversion. Samples were re-centrifuged at room temperature to pellet DNA, followed by an additional ethanol wash. Ethanol was decanted from tubes, DNA pellets dried, and incubated in 100 uL of DNA rehydration solution (1 mM EDTA, 10 mM Tris-HCl) for 1 h at 65°C in a water bath. DNA concentration was determined using a NanoDrop 1000 Spectrophotometer (Thermo Scientific, Wilmington, DE) and further diluted in DNA rehydration solution to a final concentration of 50 ng/uL.

Polymerase chain reaction (PCR) was used to confirm knockout of CB1 and CB2 receptor genes. PCR exponentially amplified base pair products of the CB1 or CB2 genes using 3' and 5' primers (Table 2-1) specifically targeted to the mouse CB1 and CB2 receptor genes in the presence of a DNA polymerase and deoxynucleotide triphosphates (dNTP's). As a positive control, primers targeting the neomycin cassette inserted into the CB2 receptor gene were used to amplify a product of the neomycin cassette. DNA expression of CB1 and CB2 receptor transcripts in WT mice was determined using 250 ng of genomic DNA isolated from tail samples in a volume of 5 uL. A master mix of PCR reagents (1x PCR reaction buffer, 1 mM $MgCl_2$, 25 U/uL Taq DNA Polymerase, 0.2 mM dNTP's, and 0.2 mM of each forward and reverse primers for either CB1 WT positive or CB2 WT positive and CB2 KO positive) was made and 20 uL of master mix was added to the 5 uL of genomic DNA (50 ng/uL).

Table 2-1. PCR Primers for CB1 and CB2 Receptors and CB2 KO Neomycin Cassette

	Primer Sequence
CB1 (+/+)	
Forward	5′-AGGAGCAAGGACCTGAGACA-3′
Reverse	5′-GGTCACCTTGGCGATCTTAA-3′
CB2 (+/+)	
Forward	5′-CCTGATAGGCTGGAAGAAGTATCTAC-3′
Reverse	5′-ACATCAGCCTCTGTTTCTGTAACC-3′
CB2 (-/-)	
Forward	5′-ACCGCTGTTGACCGCTACCTATGTCT-3′
Reverse	5′-TAAAGCGCATGCTCCAGACTGCCTT-3′

Table 2-1. PCR primers for CB1 and CB2 receptors and CB2 KO neomycin cassette. If a gene of interest was present, primers produced a 183 base pair (bp) product of the CB1 gene, a 93 bp product of the CB2 gene, or a 359 bp product of the CB2 KO neomycin gene cassette.

PCR reaction was initiated in a PX2 Thermo Hybaid PCR machine (Thermo Scientific) using 40 cycles of 45 s at 94°C for denaturation of DNA, 30 s at 55°C for annealing, and 90 s at 72°C for extension. Amplified cDNA was then stored at -20°C until 10 uL of amplified DNA was run on a 2% agarose gel (75 V for 1 hr) to determine DNA transcript knockout of CB1 and CB2 receptor genes in CB1 (-/-)/CB2 (-/-). Amplified DNA was visualized on gels using a UV transilluminator (UVC Co., San Gabriel, CA) to confirm knockout of CB1 and CB2 receptor genomic DNA in knockout mice and presence in WT C57BL/6 mice (Figures 2-1 and 2-2).

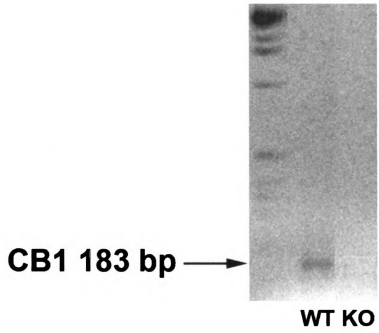

Figure 2-1. CB1 receptor product in WT mice, but not CB1/CB2 KO mice. WT and CB1/CB2 KO mice were genotyped to confirm absence of the CB1 receptor as revealed by lack of a CB1 receptor PCR product at 183 bp in CB1/CB2 KO mice seen in WT mice.

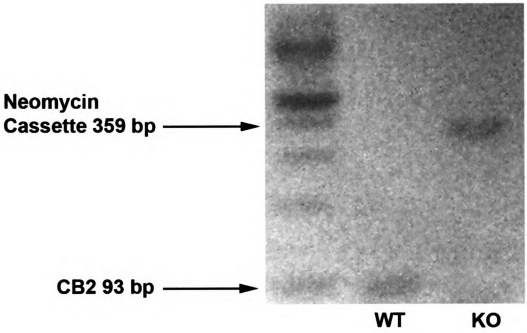

Figure 2-2. CB2 receptor product in WT mice, but not CB1/CB2 KO mice. WT and CB1/CB2 KO mice were genotyped to confirm KO of the CB2 receptor as revealed by lack of a CB2 receptor PCR product at 93 bp seen in WT mice. Mice were also genotyped for the neomycin cassette inserted into the CB2 receptor gene of CB2 KO mice, which produced a 359 bp PCR product observed only in CB1/CB2 KO mice.

Animal Housing and Maintenance

All animals were provided with food and water *ad libitum,* and housed individually or in groups of up to 5 mice per cage at 25°C with a 12 h light/dark cycle (lights on: 06:00). Mice receiving MPTP were housed in a separate room from saline treated control mice to prevent any contamination of saline treated mice with bedding or waste of MPTP treated mice. Mice that underwent stereotaxic surgery receiving vehicle or LPS were housed individually but within the same room.

All experiments used the minimal number of animals required, minimized suffering, and followed the guidelines of the National Institutes of Health Guide for the Care and use of Laboratory Animals. All drug treatments, surgical procedures, and methods of euthanasia were approved by the Michigan State Institutional Animal Care and Use Committee (IACUC). Animal use form (AUF) numbers for drug treatment and surgical procedures are: Sildenafil, apocynin, and MPTP treatment experiments AUF #: 08/04-112-00. CB1/CB2 KO and stereotaxic LPS surgery and peripheral LPS treatment experiments AUF#: 05/07-076-00.

B. Drugs

Saline or Vehicle Treatment

All saline or vehicle treatments were given as a 10 mL/kg volume either given subcutaneously (s.c.) or intraperitoneally (i.p.).

MPTP

MPTP-hydrochloride (Sigma-Aldrich, St. Louis, MO) was dissolved in 0.9% NaCl (saline). MPTP was administered in one of four different treatment paradigms with 0.9% saline serving as the vehicle control in all cases. All MPTP dosing was expressed as mg of MPTP free base per weight of the animal. One of 4 different MPTP dosing paradigms was used for experiments; acute, sub-chronic, chronic/probenecid, or repeated acute MPTP treatment (Table 2-2). MPTP was injected s.c. for acute, sub-chronic, and chronic/probenecid experiments, and i.p. for repeated acute treatment. For chronic/probenecid MPTP experiments probenecid (Sigma-Aldrich) was administered via i.p. injection.

Table 2-2. MPTP Treatment Paradigms

MPTP Paradigm	MPTP Dosage	Frequency
Acute MPTP	10 mg/kg	Once
Sub-Chronic MPTP	10 mg/kg	Once a day for 5 days
Chronic MPTP with Probenecid	20 mg/kg	One injection of MPTP and one injection of probenecid (250 mg/kg) every 3.5 days for 5 weeks for a total of 10 injections, probenecid injection was given 1 h prior to MPTP administration
Repeated Acute	16 mg/kg	One injection of MPTP every 2 h over a 6 h period for a total of 4 injections and cumulative MPTP dosage of (64 mg/kg)

Sildenafil

Sildenafil citrate (Pfizer, Ann Arbor, MI) was dissolved in 0.9% saline to a concentration of either 0.5 or 1 mg/mL. Mice received sildenafil 5 or 10 mg/kg s.c. every 12 h beginning 3 days prior to MPTP treatment (Pre-treatment), 3 days following the initiation of MPTP treatment (Concurrent treatment), or 3 days following the final MPTP injection (Post-treatment). Sildenafil administration continued daily from the point of initiation to the morning of sacrifice with the last injection given 30 min prior to decapitation.

Apocynin Administration

Apocynin (Sigma-Aldrich) was prepared as a 6 mg/mL solution dissolved in 0.1 N sodium hydroxide (NaOH), brought to a pH of 8.0 using 1 M Tris-HCl (pH 6.8) and q.s. to an appropriate volume with ddH_2O. Vehicle solution used as a control for apocynin was prepared as described for apocynin minus the drug. For the sub-chronic MPTP experiment mice received an injection of 100 mg/kg apocynin i.p. or vehicle 2 h prior to injection of 0.9% saline or MPTP, and a second injection of apocynin or vehicle 12 h later. Apocynin administration was initiated 2 days prior to the first MPTP injection and continued twice daily up to and including the day of sacrifice, which was 3 days following the last MPTP injection.

For the repeated acute MPTP experiment apocynin was constantly infused via an Alzet osmotic mini-pump 1007D (Durect, Cupertiono, CA) beginning 3 days prior to initiation of MPTP treatment. Apocynin was dissolved in 50 % dimethyl sulfoxide (DMSO) and 50% polyethylene glycol (PEG) to a concentration of 48 mg/mL apocynin.

The osmotic mini-pump delivered 0.26 uL/h of a vehicle 50% DMSO/50% PEG or 48 mg/mL apocynin solution. This infusion rate allowed the delivery of 250 mg/kg apocynin per day for a mouse weighing 30 g. Pumps were filled with either vehicle or apocynin solution, and placed in 0.9% saline for 18 h to prime pumps before s.c. implantation.

Mice were anesthetized with 80 mg/kg Ketamine/ 12 mg/kg Xylazine for sedation for pump implantation. Following sedation the incision site was cleaned with betadine before a midline s.c. one inch incision was made between the scapulas. Pumps were then placed underneath the skin, and the surgical site was closed with surgical staples. Mice normally recovered from sedation within 1-2 h following Ketamine/Xylazine administration.

Raclopride

The D2 receptor antagonist raclopride (Sigma-Aldrich) was dissolved in 0.9% saline at a concentration of 0.1 mg/mL. Raclopride (1 mg/kg) or 0.9% saline vehicle was injected i.p. 1 h prior to sacrifice.

γ-Butyrolactone (GBL) and Quinelorane

GBL (Sigma-Aldrich) which inhibits firing of DA neurons was diluted to a 0.75 mg/mL solution in 0.9% saline from a 1 g/ml stock solution and quinelorane (Sigma-Aldrich) was dissolved in 0.9% saline to concentration of 0.01 mg/mL. Saline vehicle or the D2 receptor agonist quinelorane 0.1 mg/kg was given to mice i.p. 1 min prior to either

saline or GBL 750 mg/kg i.p. administration and mice were sacrificed 1 h following saline or quinelorane administration.

CB Receptor Antagonists

The CB1 receptor antagonist, rimonabant (SR141716A), and the CB2 receptor antagonist, SR144528 both obtained from the National Institute of Drug Abuse (NIDA) by Dr. Norbert Kaminski were individually dissolved in a solution of 10% Tween-80, 10% Ethanol, and 80% saline. The 10% Tween-80/ 10% Ethanol/ 80% saline served as the vehicle solution for both rimonabant and SR144528. Mice were injected once daily s.c. 1 h prior to 0.9% saline or MPTP administration with either the vehicle solution, rimonabant 1 mg/kg, SR144528 2.5 mg/kg, or both rimonabant 1 mg/kg and SR144528 2.5 mg/kg. Mice continued to receive either the appropriate vehicle solution or one or both CB antagonists once daily in the morning each day following the termination of 0.9% saline or MPTP administration until 3 days following the last MPTP injection when mice were decapitated.

Lipopolysaccharide (LPS)

LPS or bacterial endotoxin can induce significant activation of microglial cells within the brain inducing localized or widespread inflammation within the brain depending on the method of delivery. In order to induce localized inflammation within the substantia nigra, LPS was injected unilaterally into the left side of the substantia nigra as described below. Alternatively, inflammation throughout the brain was initiated with the injection of LPS intraperitoneally.

Unilateral Stereotaxic LPS Injection into the Mouse Substantia Nigra

LPS or phosphate buffered saline (PBS) (0.14 M NaCl, 3.4 mM NaH_2PO_4, 6.8 mM Na_2HPO_4, pH 7.4) vehicle was injected unilaterally into the left substantia nigra to induce localized inflammation. Mice were lightly sedated with 50 mg/kg Ketamine/2.5 mg/kg Xylazine and approximately 15 min later were completely anesthetized with isoflurane using a Vapomatic Vaporizer (A. M. Bickford, Wales Center, NY). The surgical area was shaved and the mouse was positioned in a stereotaxic apparatus under continuous isoflurane flow via a modified nose cone mask. The surgical area was cleaned with alcohol and betadine, a midline incision was made in the scalp along the mid-saggital line, the skull was exposed, and both Bregma and lambda were marked on the surface of the skull with a pencil.

Vertical measurements were taken at bregma and lamda using a 30 gauge blunt tipped needle attached to the stereotaxic apparatus. If vertical measurements were not equivalent at both of these points the toothbar was adjusted appropriately to make the measurements equivalent. Medial/lateral and anterior/posterior plane measurements were taken in reference to Bregma to determine the coordinates for stereotaxic injection. The injection needle was raised from the surface of the skull and positioned to +1.3 mm (lateral/medial plane) and -3.0 mm (anterior/posterior plane) with regard to Bregma, coordinates corresponding to location of the left substantia nigra (Franklin and Paxinos, 1996). A dremel drill was used to drill a hole through the skull at the site of injection. The blunt tipped 30 gauge needle was flushed with PBS and either PBS (vehicle) or LPS was drawn up through the needle/tubing attached to a 1 uL Hamilton syringe. The needle was lowered into the skull -4.7 mm (dorsal/ventral plane) with regard to Bregma.

The specified volume of PBS or LPS 2.5, 5, or 10 ug (Sigma Aldrich) was injected into the substantia nigra over a period of 2 min. LPS was obtained from escherichia coli O111:B4 (catalog #: L3012-10 mg batch #: 067K4139, L3012-5 mg batch #: 047K4089, and L2880-100 mg batch #: 066K4039, Sigma-Aldrich). The needle was left in place for 5 min following the period of PBS/LPS injection before being removed from the brain to reduce backflow of PBS/LPS. The hole in the skull was closed using bone wax and the scalp sutured using wound clips. Mice were carefully observed for any signs of pain or distress over the entire time period following surgery until they were euthanized. Mice did not receive any anti-inflammatory agents as this would interfere with the inflammatory effects of LPS in the brain.

Peripheral LPS Administration

Mice received either 0.9% NaCl vehicle or LPS 5 mg/kg (Sigma Aldrich) administered in a 0.5 mg/mL LPS solution via i.p. injection 1 h prior to sacrifice by decapitation. LPS was obtained from escherichia coli O111:B4 (catalog # L3012-5 mg batch #: 047K4089, Sigma-Aldrich).

C. Brain Tissue Preparation

Euthanasia

Mice were killed by one of two methods for all experiments. Mice were decapitated using a guillotine for collection of brain tissue used for either neurochemistry and/or Western Blot analysis. For immunohistochemistry analyses mice were given a lethal dose of Ketamine 266 mg/kg and Xylazine 4 mg/kg and perfused with saline followed by 4% paraformaldehyde. Brains were subsequently removed and placed in 4% paraformaldehyde for at least 24 h, then stored in 20% sucrose for cryoprotection.

Preparation of Brain Tissue

After mice were sacrificed by decapitation for neurochemistry and Western blot analyses the brain was immediately removed and the median eminence was dissected from the brain and placed in 50 uL of tissue buffer (0.05 M sodium phosphate, 0.03 M citrate, 15% methanol, pH 2.5). The median eminence was stored at -20°C until preparation for neurochemical analysis. Whole brains were immediately frozen on dry ice and stored at -80 °C until they were sectioned in a cryostat at -10°C (HM525 Microtome Cryostat, Microm International or CTD-Model Harris, International Equipment Co., Needham, MA).

Brain tissue used for immunohistochemistry analysis was fixed in 4% paraformaldehyde either by drop fixation or perfusion. For drop fixation mice were decapitated, the brain removed, and dissected at the mid-coronal plane through the hypothalamus. The caudal portion of the brain (hindbrain) was placed in 4% paraformaldehyde for 7 days and stored at 4°C. Hindbrains were subsequently

cryoprotected in 20% sucrose following paraformaldehyde incubation. Mice perfused with 4% paraformaldehyde were decapitated following perfusion, brains removed and placed in 4% paraformaldehyde and stored at 4°C for 24 h. Brains were later placed in 20% sucrose for at least 24 h before sectioning. Both drop fixed and perfused brains were sectioned in a cryostat at -25°C.

D. Assay of Amines, Amine Metabolites, and Apocynin in Brain Tissue

Amines and apocynin were measured in brain extracts using high performance liquid chromatography with amperometric electrochemical detection (HPLC-EC). HPLC-EC measures amines and apocynin by oxidation at an electrode held at a constant voltage or potential. The oxidation of an amine or apocynin at the electrode produces a current that is proportional to the concentration of compound in the brain extract. In order to detect an amine or apocynin the potential must be high enough to oxidize the compound. The optimal potential for oxidation of amines is 0.4 V (Eaton et al., 1994), but no information is available for apocynin. Accordingly, the ability of apocynin to be oxidized at various potentials was examined and the resulting voltamogram is depicted in Figure 2-3 (see section below entitled *Measurement of Apocynin within the Brain*). The optimal voltage to measure apocynin was determined to be 0.47 V.

The higher the current produced as the brain extract passes through the electrode detector, the more of the compound of interest is present in the brain extract, as reflected by a higher peak height. By comparing peak height of a standard to the peak height of a compound in a brain extract, the concentration of the compound within a sample can be calculated. Different compounds that are oxidized at similar potentials can be distinguished by the retention time of compound on a C-18 column. The more hydrophobic a compound is the longer it will remain on the column and the longer the retention time of the compound.

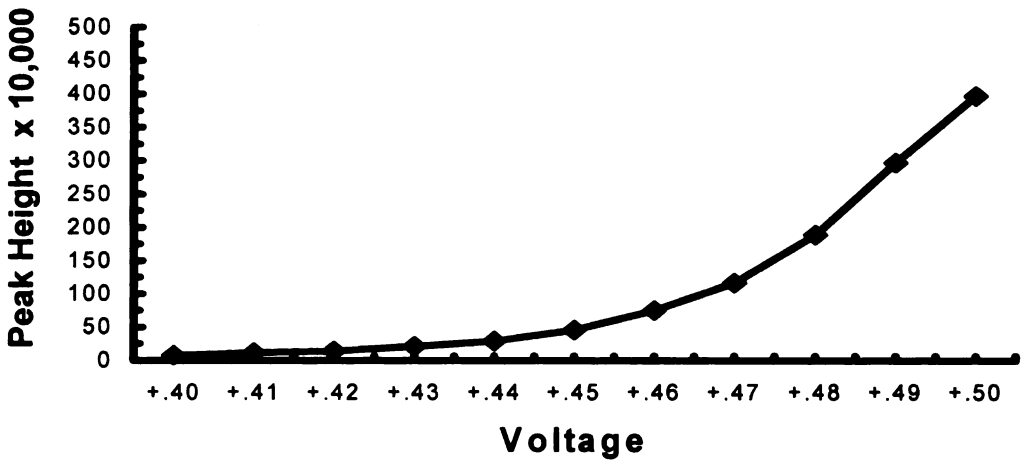

Figure 2-3. Apocynin voltamogram. Apocynin (25 ng) standards were measured at a sensitivity of 10 x 50 and voltages ranging from +0.40 to +0.50 using HPLC-EC to determine an ideal voltage to detect apocynin.

Tissue Collection and Preparation

Frozen brain tissue was sectioned coronally in a cryostat at -10 °C at 500 μM going from the rostral to caudal brain beginning at approximately Bregma +1.94 mm (Franklin and Paxinos, 1996). Brain tissue sections were mounted directly onto slides and slides were placed on dry ice. Brain regions including the striatum and nucleus accumbens were microdissected under a Stereo Master Microscope (Fisher Scientific, Pittsburgh, PA) at 4x magnification using a modification of the Palkovits method (Palkovits and Brownstein, 1983). The nucleus accumbens was sampled using a 21 gauge (0.5 mm inner diameter) circular punch tool and striatum an 18 gauge (1 mm inner diameter) circular punch tool. Tissue punch sites for specified brain regions are pictured in (Figure 2-4). Tissue punches were placed in 50 uL of tissue buffer and stored at -20°C until preparation for neurochemical analysis.

Samples were thawed and centrifuged for 30 s at 18,000 x g in a Microfuge 18 Centrifuge (Beckman Coutler Inc., Fullerton, CA) and tissue was sonicated with three 1 s bursts (Heat Systems Ultrasonics, Plainview, NY). Tissue samples were again centrifuged for 30 s at 18,000 x g to pellet tissue. Tissue buffer containing neurochemicals released with sonication was collected using a beveled tip 100 uL Hamilton syringe and q.s. using tissue buffer to a final volume of 100 uL for striatum samples and 65 uL for median eminence and nucleus accumbens samples. Samples were placed in new tubes for analysis of neurochemicals using high performance liquid chromatography with electrochemical detection (HPLC-EC) (Eaton et al., 1994).

Remaining tissue pellets were placed in 100 uL of 1 N sodium hydroxide (NaOH). Tissue pellets were sonicated and vortexed to homogenize samples. Protein

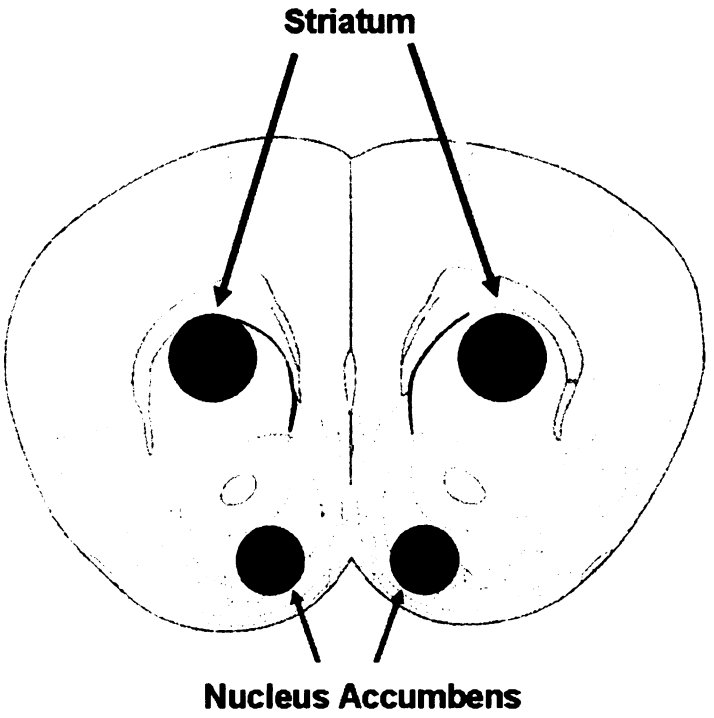

Figure 2-4. Diagram showing striatum and nucleus accumbens sampling sites. Bilateral samples were taken from both the striatum and nucleus accumbens using an 18 gauge (1 mm inner diameter) and 21 gauge (0.5 mm inner diameter) circular punch tool respectively. Pictorial coronal section of the mouse brain at Bregma +1.42 (Franklin and Paxinos, 1996).

content of tissue samples was determined using a Lowry protein assay (Lowry et al., 1951). Samples were reacted with 1 mL of reagent A solution (0.18 M sodium carbonate, 0.63 mM cupric sulfate, 0.95 mM KNA tartrate) for 10 min, and with 100 uL of reagent B solution (2 N Folin-Ciocalteau's phenol reagent diluted 1:1 with ddH_20) for 30 min to produce a colorimetric reaction. Protein content was determined using a standard curve of 0, 12.5, 25, and 50 ug bovine serum albumin (BSA) protein (Sigma) dissolved in 1 N NaOH. The absorbance of standards and samples was read at 700 nm using a U-Quant plate reader (BioTek Instruments Inc., Winooski, VT). Protein content in samples was quantified by normalizing sample absorbance to absorbencies of protein standards.

Measurement of Amines and Amine Metabolites in the Brain

Content of DA, DOPAC, HVA, 5HT, and 5HIAA in samples was determined using HPLC-EC. A Waters 515 HPLC pump was used to circulate the HPLC-EC mobile phase (0.05 M sodium phosphate, 0.03 M citrate, 0.1 mM EDTA, pH 2.65) at a flow rate of 1 mL/min through an ESA Coulochem 5100A electrochemical detector set at +0.4 volts. Brain sample extracts were injected onto a C18 reverse phase analytical column (Bioanalytical Systems, West Lafayette, IN). Standards (1 ng) of DA, DOPAC, HVA, 5HT, and 5HIAA were used to determine brain tissue neurochemical content. Separation of compounds was achieved using 15-25% methanol and 0.02-0.05% sodium octylsulfate. Peak heights of standards (Figure 2-5; Panel A) were used to determine neurochemical content in brain samples (Figure 2-6; Panels A & B) using sample peak heights. Neurochemical sample content was normalized to protein content of samples and expressed as ng of neurochemical per mg of protein.

Measurement of Apocynin within the Brain

Tissue punches of the striatum were taken from 500 μm brain tissue sections using an 18 gauge punch tool and placed in tissue buffer. Striatum tissue punches were sonicated with three 1 s bursts, centrifuged for 30 s at 18,000 x g to pellet tissue, and supernatants were removed and q.s. using tissue buffer to a final volume of 100 uL. Apocynin was measured using HPLC-EC by injecting striatum supernatant extracts onto a C18 reverse phase analytical column coupled with ESA Coulochem 5100A electrochemical detector set at +0.47 V. The optimal voltage to measure apocynin was determined by measuring 25 ng apocynin standards at specified voltages between (+0.4 V to +0.5 V) creating a voltamaogram (Figure 2-3). Apocynin concentration was minimally detected at lower voltages but the standard curve of the voltamogram was relatively linear to about +0.47 V which there after the curve became exponential (Lookingland, Goudreau and Sayed, unpublished results). Apocynin content in samples was quantified by comparing sample peak heights (Figure 2-6; Panel C) to standards (Figure 2-5; Panel B) and normalized to tissue sample protein content determined using a Lowry protein assay (Lowry et al., 1951).

Measurement of MAO B Activity in vitro

MAO B activity was measured *in vitro* to determine if apocynin inhibits MAO B metabolism of DA to DOPAL. The synthesis of DOPAL from DA in the presence of MAO B (Sigma-Aldrich) was measured at 15, 30, 45, and 60 min following the initiation of the reaction. The reaction solution contained 5 uM DA in phosphate buffer (pH 7.5) and synthesis of DOPAL was initiated by the addition of 2.8 units of MAO B to 250 uL

of the reaction solution. MAO B enzyme activity was stopped at the indicated time points with the addition of tissue buffer (100 uL) for every 50 uL of the reaction mixture. The concentrations of DA and DOPAL were measured in reacted samples using HPLC-EC (Figure 2-6, Panel D) as described in this section (Measurement of Amines and Amine Metabolites in the Brain).

The synthesis of DOPAL was also measured in the presence of apocynin 60 min following the addition of MAO B to the reaction mixture to determine if apocynin inhibited MAO B activity by decreasing the synthesis of DOPAL. The reaction mixture contained 5 uM DA in phosphate buffer (pH 7.5) and apocynin (1, 10, or 100 uM), and synthesis of DOPAL was initiated by the addition of 2.8 units of MAO B to 250 uL of the reaction mixture. The reaction was terminated 60 min later as described above and DA and DOPAL concentrations determined using HPLC-EC.

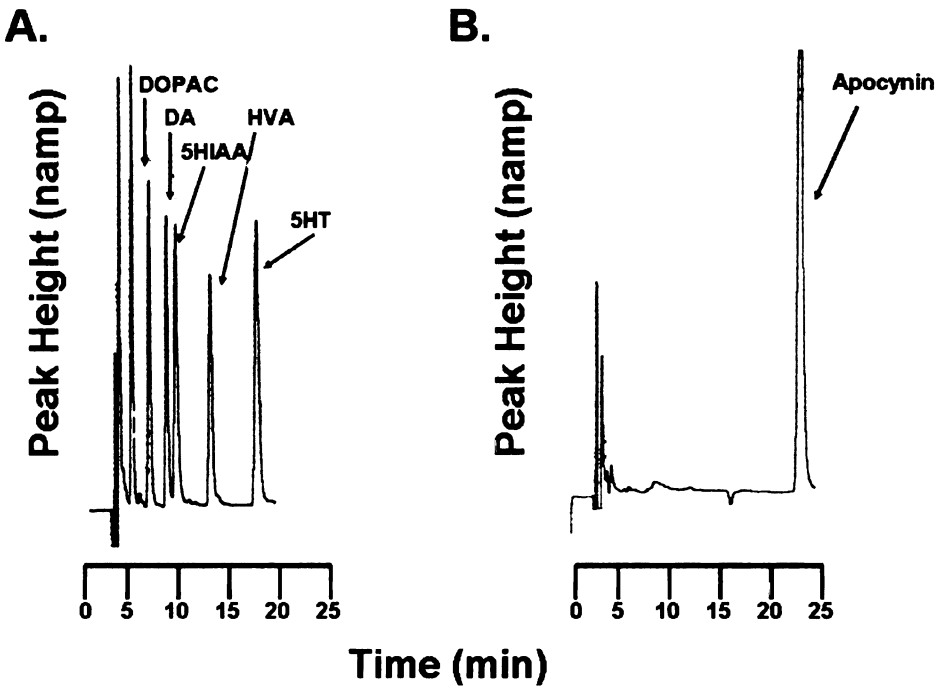

Figure 2-5. Chromatograms show peak height and retention time for the respective neurochemicals or apocynin. Representative HPLC-EC chromatograms for 1 ng DA, DOPAC, HVA, 5HIAA, and 5HT standards (Panel A) and 25 ng apocynin standard (Panel B).

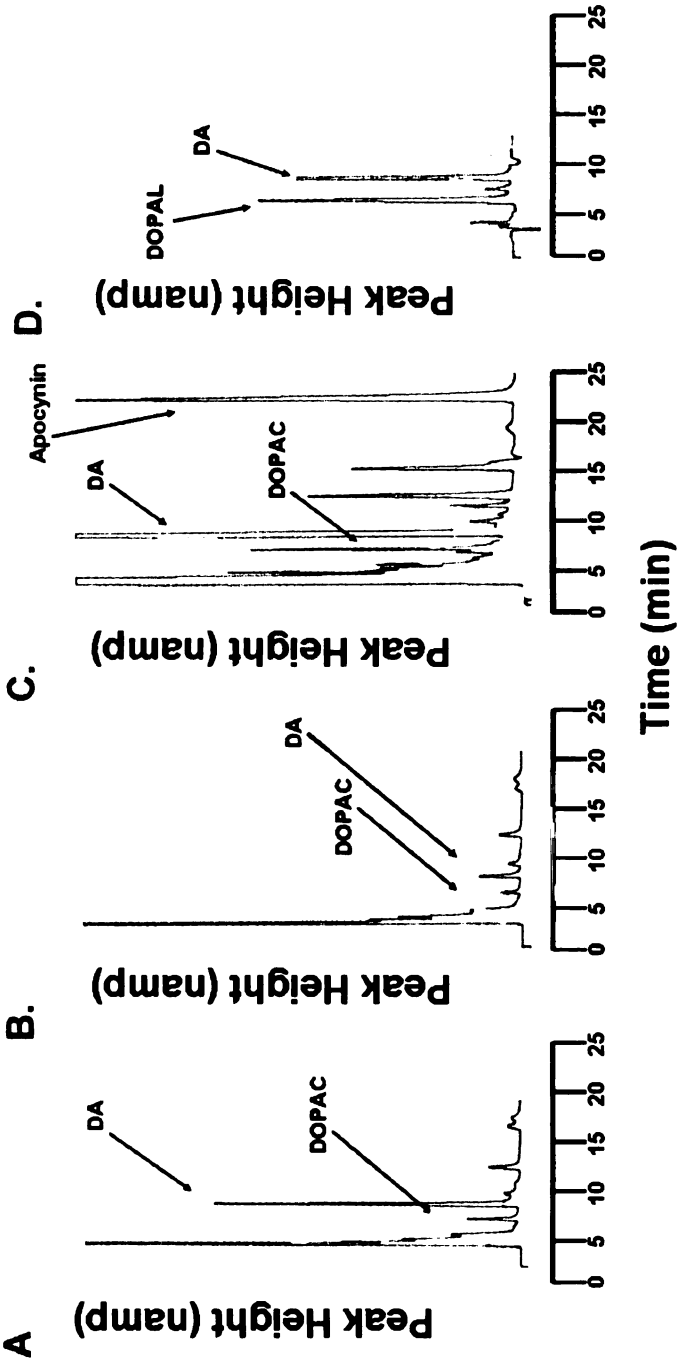

Figure 2-6. Chromatograms showing peak height and retention times for DA, DOPAC and apocynin in striatum samples. Representative HPLC chromatograms of DA and DOPAC in the striatum obtained from saline (Panel A), sub-chronic MPTP treated (10 mg/kg once a day for 5 days; Panel B), and apocynin (100 mg/kg 2.5 min prior to decapitation; Panel C) mice. Representative HPLC chromatogram of DA and DOPAL 30 min following initiation of DA metabolism by MAO B (Panel D).

E. cGMP Assay

cGMP concentrations were measured in the brain to determine if sildenafil inhibition of PDE5 increased cGMP levels in the brain. Following decapitation the brain was removed and sectioned mid-coronally. The hindbrain was frozen on dry ice, weighed, and placed in liquid nitrogen. Brain tissue was homogenized in liquid nitrogen with a mortar and pestel, and placed in a 1.5 mL tube with 0.1 N HCl with 1 mM of 3-isobutyl-1-methylxanthine (IBMX) in a 20% weight per volume solution and vortexed to disperse tissue within solution. Samples were centrifuged for 15 min at 600 x g at 4°C and supernatants were removed and assayed for cGMP content. Pelleted brain tissue was resuspended in 800 uL of 1 N NaOH and protein content determined using a Lowry protein assay (Lowry et al., 1951). cGMP content of supernatants were determined in duplicate as per directions of the acetylation method of the low cGMP kit (R&D Systems, Minneapolis, MN). cGMP content of individual samples was determined by extrapolation from a standard cGMP curve (Figure 2-7). Colorimetric reaction of individual samples used to determine cGMP content was read on U-Quant plate reader at 405 nm with background subtraction of 570 nm.

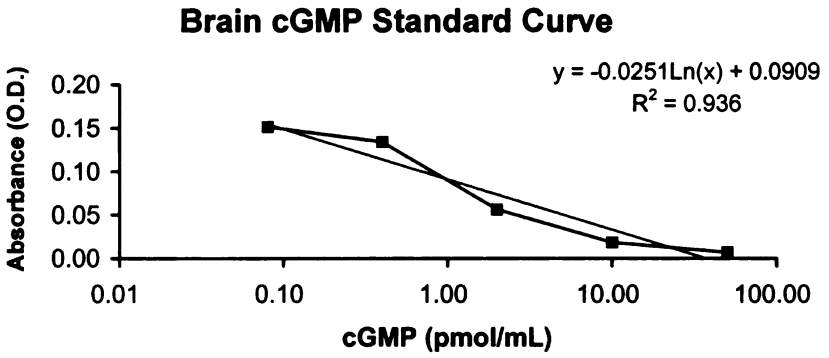

Figure 2-7. cGMP standard curve. Standard cGMP concentrations were plotted against the mean of duplicate standard absorbances (optical density or O.D.). The cGMP concentration of samples was extrapolated by the use of the linear equation of the line obtained by known cGMP concentration of standards to standard absorbances.

F. Plasma Sildenafil Determination

Trunk blood was collected following decapitation and placed in heparinzed tubes for analysis of free sildenafil levels. Plasma was isolated and collected from blood by centrifugation of heparinzed tubes at 2,000 rpm for 20 min at 4°C in a 3000R Centrifuge (Fisher-Scientific). The concentrations of free sildenafil in plasma were determined 30 min after a single (5 or 10 mg/kg s.c.) sildenafil dose. Concentrations of free sildenafil in plasma were measured by Pfizer (Sandwich, United Kingdom) using HPLC with ultraviolet detection (UV). UV detection of sildenafil was obtained at an absorbance of 290 nm (Walker et al., 1999).

G. Western Blot Analysis

Western blotting was used to determine the TH content of NSDA neuronal cell bodies and proteins (TH, serine 40 phosphorylated TH, and DAT) in axon terminals. TH and DAT protein content were used as indices of NSDA neuronal cell body and or terminal integrity. Proteins associated with microglial cells (p67Phox, gp91Phox) and dopaminergic neurons (DA and cAMP regulated phosphoprotein; DARPP-32) and alpha-synuclein were also measured by Western blot. All proteins of interest were normalized to homogenously expressed proteins (β-III tubulin, synaptosomal-associated protein 25 (SNAP-25), or glyceraldehyde-3-phosphate dehydrogenase (GAPDH)) to control for protein loading variations.

Brain Tissue Preparation

Brains were sectioned at 500 μm in a cryostat at -10°C and mounted onto room temperature slides. Striatum tissue was obtained by taking two 12 gauge tissue punches, or ventral midbrain tissue was dissected from coronal brain sections with a razor blade (Figure 2-8). Brain tissue was placed in a sucrose homogenization (0.25 M sucrose, 10 mM HEPES, 10 mM $MgCl_2$, pH 7.4) or a lysis buffer (1% sodium dodecyl sulfate (SDS), 20 mM Tris-HCl, pH 7.4). Cytosolic and membrane protein fractions were obtained using one of two serial centrifugation methods.

One method of isolating membrane and cytosolic fractions of brain tissue used was a serial centrifugation and sucrose gradient method (Figure 2-9) (Leng et al., 2001). Tissue was sonicated and centrifuged for 10 min at 500 x g at 4°C to pellet membrane, nuclear, and cellular debris (P1). The supernatant (S1) was removed and centrifuged

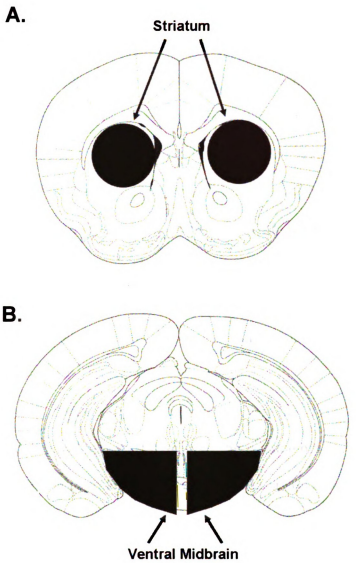

Figure 2-8. Pictorial diagram of striatum and ventral midbrain tissue sites taken by tissue punch or dissection. Striatum tissue punch sites (Panel A) and ventral midbrain area tissue (Panel B) dissected for Western blot, NADPH oxidase assay, and or Complex I activity assay. Striatum tissue punches were taken using a 12 gauge punch tool (1 mm inner diameter) and ventral midbrain tissue was dissected with a razor blade. Pictorial coronal sections of the mouse brain at Bregma +1.18 (striatum) and -3.08 (ventral midbrain) (Franklin and Paxinos, 1996).

at 18,000 x g for 20 min at 4°C. The supernatant (S2) obtained from the second centrifugation step was used to analyze cytosolic protein content. The pellet (P1) from the first centrifugation was resuspended in 200 uL of sucrose homogenization buffer. A membrane fraction was isolated by layering resuspended (P1) samples on top of 330 uL of a high density sucrose buffer (2.4 M sucrose, 10 mM HEPES, 10 mM $MgCl_2$, pH 7.4), and centrifuging samples for 7.5 h at 16,000 x g at 4°C. Following centrifugation the membrane fraction layer was located between the low and high density sucrose buffers and was drawn up in a volume of about 150 uL. Protein content of cytosolic and membrane fractions was determined using a bicinchoninic acid (BCA) protein assay. The BCA assay determines sample protein content by reacting 5 uL of tissue homogenate and 95 uL of ddH_2O with 2 mL of a protein reaction solution (50:1 bicinchoninic acid: copper (Cu) II sulfate). The BCA assay uses protein reduction of Cu II to Cu I in a protein concentration dependent manner, followed by the reaction of Cu I with bicinchoninic acid, a chromogen which was measured at 562 nm on a Beckman DU640 spectrophotometer (Beckman Coulter). Protein sample concentration was quantified using absorbencies of BSA protein standards of 2.5, 5, 10, 15, and 20 ug/uL.

Cytosolic and membrane fractions of brain tissue were also isolated using an ultracentrifugation method (Guillemin et al., 2005; Amadesi et al., 2006). Although the sucrose gradient method of membrane isolation was successful, the protein concentration per uL of membrane homogenate obtained using this method yielded low protein content. This problem was addressed by developing an ultracentrifugation method of cytosolic and membrane fraction isolation (Figure 2-10). Striatum and ventral midbrain tissue was taken, placed in 300 uL of lysis buffer, and sonicated to form a homogenous sample.

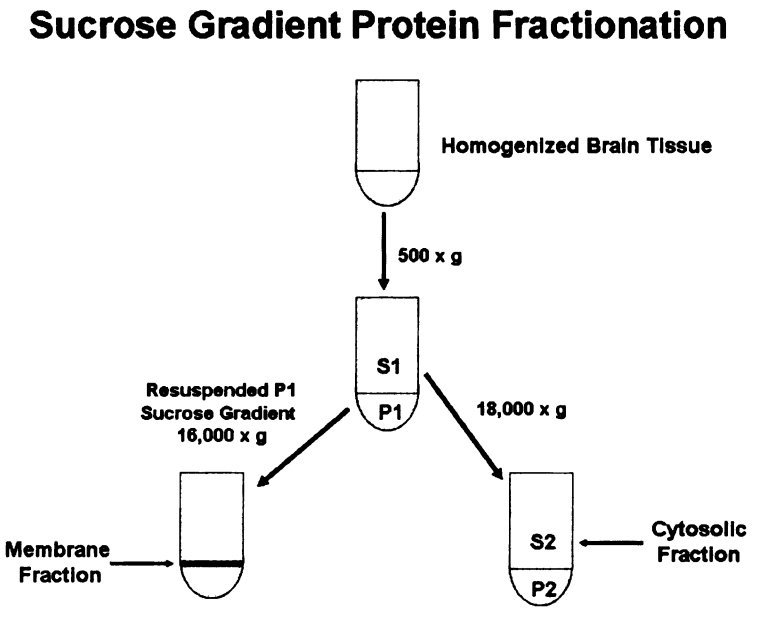

Figure 2-9. Pictorial diagram of sucrose gradient fractionation of membrane and cytosolic fractions. Homogenized brain tissue was centrifuged at 500 x g for 10 min. The supernatant (S1) was centrifuged at 18,000 x g for 20 min to obtain the S2 cytosolic fraction, and pellet (P1) was resuspended in sucrose homogenization buffer. The P1 pellet was layered onto a higher density sucrose buffer and centrifuged at 16,000 x g for 7.5 h to obtain a membrane fraction at the interface of the lower and higher density sucrose buffers.

Ultracentrifugation Protein Fractionation

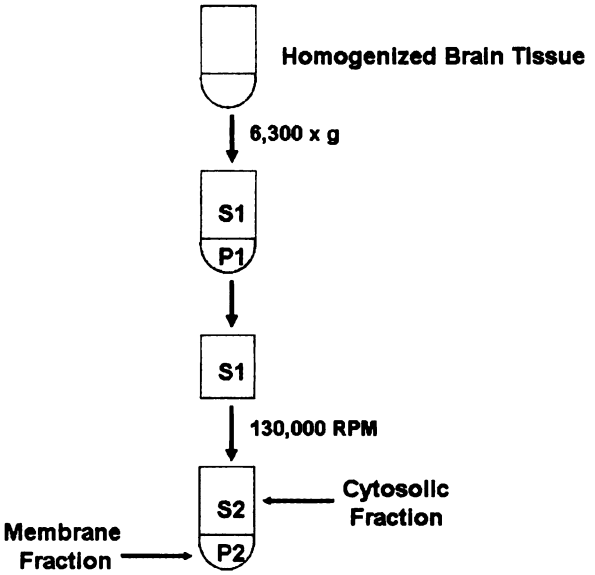

Figure 2-10. Pictorial diagram of isolation of membrane and cytosolic fractions using ultracentrifugation. Brain tissue was centrifuged at 6,300 x g for 10 min to obtain the supernatant (S1) and pellet (P1) fractions. S1 was centrifuged at 130,000 RPM to obtain the S2 (cytosolic) and P2 (membrane) fractions.

Samples were then centrifuged for 10 min at 6,300 x g at 4°C to pellet cellular and nuclear debris (P1). The supernatant (S1) from this initial centrifugation was removed and centrifuged using a T-120 rotor in an Optima Max Ultracentrifuge (Beckman Coutler) at 130,000 rpm for 30 min at 4°C. The supernatant (S2) from this centrifugation step was used as the cytosolic fraction and the pellet (P2) contained the membrane fraction and was resuspended in 50 uL of PBS. Protein content for all samples was determined using a BCA protein assay. Protein samples were prepared for electrophoresis by the addition of 1:10 or 1:4 dilution of loading dye (0.25 M Tris-HCl pH 6.8, 5% SDS, 0.05% Bromophenol blue, 45% glycerol, and 2-mercaptoethanol). Protein samples were boiled at 95-100°C for 5 min to denature proteins.

Electrophoresis and Transfer of Proteins

A total of 20-80 ug of protein/well was loaded on one of the following types of precast gels: 7.5%, 10%, 4-15%, or 4-20% Tris-HCl polyacrylamide gels (Bio-Rad Laboratories, Hercules, CA) with 10-15 wells for electrophoresis. The percentage of polyacrylamide in gels was adjusted depending on the molecular weight of the proteins of interest. A protein standard ladder was loaded to determine protein molecular weight of specific proteins of interest. The inner chamber formed by two precast gels placed within the mini-protean 3 cell (Bio-rad) was filled with electrophoresis running buffer (50 mM Tris-base, 0.38 M glycine, 3.5 mM SDS), and another 300 mL was placed outside of the chamber. Protein samples were separated by running 150 V through the mini-protean 3 cell until the lowest molecular weight protein standard reached the bottom of the each gel. Gels were removed from the electrophoresis chamber and placed on a 0.45 μm

nitrocellulose membrane for transfer of proteins using a trans-blot cell (Bio-rad). The trans-blot cell was filled with transfer buffer (25 mM Tris-base, 0.19 M glycine, 20% methanol) and 300 mV was applied for 90 min to transfer proteins to the membrane. Membranes were washed in Tris buffered saline (TBS) (50 mM Tris-base, 2.7 mM KCl, 0.14 M NaCl, pH 7.4) 3 x 5 min, and non-specific proteins on membranes were blocked using Oddyssey Blocking Buffer (LI-COR Biosciences, Lincoln, NE) for 1 h. Membranes were probed overnight for specific proteins including TH, phosphorylated serine 40 TH, p67Phox, gp91Phox, DAT, α-synuclein, DARPP-32, parkin, SNAP-25, GAPDH, and β-III tubulin using primary antibodies developed in rabbit, mouse or rat (Table 2-3). Primary antibodies were reacted with an appropriate secondary antibody with an infrared fluorescent tag for 1 h (Table 2-3).

Quantification of Protein Content and Normalization to Control Proteins

Proteins tagged with primary and secondary antibodies were visualized using an Oddyssey infrared imaging system (LI-COR Biosciences) which uses infrared fluorescence detection of secondary antibodies at either 700 or 800 nm to create a digital image of protein bands. Protein content was determined using densitometry analysis of digital images Protein content of TH, phosphorylated serine 40 TH, p67Phox, gp91Phox, DAT, α-synuclein, parkin, or DARPP-32 was normalized to cytosolic (GAPDH or β-III tubulin) or the membrane protein SNAP-25 all three of which are proteins homogenously expressed in brain tissue. Individual proteins normalized to cytosolic or membrane proteins are expressed as relative density units (RDU).

Protein	Species	Dilution	Source
Tyrosine hydroxylase (TH)	Rabbit	1:2,000	Millipore, Billerica, MA (AB152)
Phosphorylated Serine 40 TH	Rabbit	1:1,000	Cell Signaling Danvers, MA (2791)
Dopamine transporter (DAT)	Rat	1:1,000	Millipore (MAB369)
p67Phox	Mouse	1:500	BD Biosciences San Jose, CA (611415)
gp91Phox	Mouse	1:500	BD Biosciences (610913)
Alpha-synuclein	Rabbit	1:1,000	Cell Signaling (2642)
Dopamine and cyclic AMP-regulated phosphoprotein (DARPP-32)	Rabbit	1:1,000	Cell Signaling (2302)
Parkin	Mouse	1:1,000	Millipore (MAB5512)
Glyceraldehyde-3-Phosphate Dehydrogenase (GAPDH)	Mouse	1:5,000	Millipore (MAB374)
Beta-III tubulin	Mouse	1:2,000	Millipore (MAB1637)
Synaptosomal-associated Protein 25 (SNAP-25)	Mouse	1:2,000	Millipore (MAB331)
IRDye 800 conjugated goat anti-rabbit IgG	Goat	1:5,000-1:20,000	Rockland, Gilbertsville, PA (611-132-122)
ALEXA Fluor 680 goat anti-mouse IgG	Goat	1:5,000-1:20,000	Molecular Probes, Eugene, OR (A-21057)
IRDye 800 conjugated goat anti-rat IgG	Goat	1:10,000	Rockland (612-132-120)

Table 2-3. Primary and secondary antibodies used for Western blotting. The antibody the protein was directed against, species it was obtained from, dilution used, and company (source) it was obtained from is listed.

H. Immunohistochemistry and Stereology Cell Counts

Immunohistochemistry for TH

Hindbrains placed in 4% paraformaldehyde following decapitation or whole brains perfused with 4% paraformaldehyde were sectioned coronally at 60 μm in a cryostat at -25 °C. Every third tissue section was stained for TH with a rabbit polyclonal antibody to TH (1:2,000) (AB152, Chemicon, Temecula, CA). Brain tissue was reacted with a biotin conjugated goat anti-rabbit secondary antibody (1:500) (Vector Laboratories, Burlingame, CA). Secondary antibody was reacted with an avidin biotin complex using an ABC Vectastain kit (Vector Laboratories, Burlingame, VT), followed by 3,3′-diaminobenzidine (Sigma-Aldrich) to visualize the staining. All brain tissue sections were mounted on gelatin coated slides, and dehydrated using a series of steps through ethanol (70%, 95%, and 100%) and xylene (two steps) each for 10 min prior to being coverslipped.

Stereological TH Cell Counts

Brain sections stained for TH were visualized on a screen using a 4X objective and the substantia nigra was delineated with the aid of a mouse atlas using Stereoinvestigator Software version 6.55 (MicroBrightField, Inc., Williston, VT) (Franklin and Paxinos, 1996). The first section counted contained TH immunoreactive cell bodies from the rostral substantia nigra (Bregma -2.80), and subsequent sections were counted every 180 μm following this initial section until TH immunoreactive cells were no longer visualized.

TH positive cells were counted using the unbiased Optical Fractionator technique with a 20X objective on a Nikon Eclipse 80i microscope and an Optronics Microfire color CCD camera. This technique allows an unbiased estimation of the number of cells in a region using a three dimensional probe or optical disector, and a systematic sampling method or fractionator (Gundersen and Jensen, 1987; Schmitz and Hof, 2005). A (100 x 100 μm) counting frame was used and a fraction of the counting frames were sampled in the delineated region of each section. Mounted section thickness was estimated to be 18 μm and 2 μm guard zones were set at the top and bottom of sections, so approximately 78% of a section was counted. A cell was considered to be a TH immunoreactive neuron if the cytoplasm of the neuronal cell body stained positive for TH, the nucleus of the neuron could be clearly visualized, and the cell body was greater then 15 μm in diameter. Uniform antibody penetration was confirmed by the distribution of immunoreactive cell counts in the vertical (z) axis. To accurately calculate the number of TH immunoreactive cells in a unilateral substantia nigra every third section was analyzed (section periodicity of 3) and 8-9 sections were analyzed through the substantia nigra. The mean coefficient of error (C. E.) was calculated to be 0.1 or less for each treatment group (Gunderson, m=1) (Gundersen and Jensen, 1987).

I. NADPH Oxidase Activity Assay

Brain Tissue Preparation

NADPH oxidase activity was measured in striatum or ventral midbrain brain tissue samples. Brain tissue was removed and immediately frozen on dry ice, and sectioned in a cryostat at -10°C. Two 12 gauge tissue punches of striatum were taken from 500 μM tissue sections or dissected out for ventral midbrain tissue (Figure 2-8), and placed in 200 uL of lysis buffer (0.1 M K_2PO_4, 1 mM phenylmethanesulfonyl fluoride (PMSF), 0.002% Triton-X), and sonicated to disrupt cell membranes. Samples were centrifuged at 12,000 xg for 30 min at 4°C, supernatant was removed and the pellet resuspended in 150 uL of a reaction buffer (20 mM HEPES, 0.12 M NaCl, 4.6 mM KCl, 2 mM $MgSO_4$, 0.15 mM Na2HPO_4, 0.4 M KH_2PO_4, 5 mM $NaHCO_3$, 5.5 mM Glucose, 1.2 mM $CaCl_2$, and pH 7.4), and re-homogenized by sonication (Pagano et al., 1995; Li et al., 2003). Protein content of samples was determined using a BCA protein assay described in (Chapter 2, Section G, Brain Tissue Preparation).

NADPH Oxidase Activity Determination

NADPH oxidase activity was measured using 250 ug of protein for each sample placed in 500 uL of reaction buffer with 1 mM PMSF, 10 ug/mL of aprotinin, 10 ug/mL of leupeptin. Enzyme activity was measured by incubating protein samples in a water bath for 10 min at 37°C, 5 uL of 10 mM NADPH and 5 uL of 0.5 mM lucigenin was added to the sample and incubated for another 10 min in a water bath at 37°C. The 1.5 mL tube containing the sample was placed in a 20/20n luminometer (Turner BioSystems, Sunnyvale, CA) for 90 s before a total of 10 readings (5 s) each were taken and expressed

as relative light units (RLU), 5 uL of the superoxide scavenger (1 M tiron) was added to the sample to scavenge superoxide and after 5 min another set of 10 readings (5 s) each were taken. Results were calculated for NADPH oxidase activity of samples by the difference between the mean of readings 2 through 9 before and after the addition of tiron was taken, and a mean background subtraction of the reaction buffer with NADPH and lucigenin in the presence of no protein was performed. This value was multiplied by a factor of 12 to account for RLU per min (RLU/min) since each reading was taken over a 5 sec period. This value was divided by the total protein (250 ug) contained in each sample such that NADPH oxidase activity was expressed as RLU/min/ug of protein.

$$\text{NADPH oxidase activity} = \frac{12*((\text{mean 2-9 pre-tiron} - \text{mean 2-9 post-tiron})-(\text{mean 2-9 background}))}{250 \text{ ug of protein}}$$

J. Mitochondrial Complex I Assay

Complex I is the first in the series of the mitochondrial respiratory chain that involves the transfer of electrons from nicotinamide adenine dinucleotide (NADH) by oxidation (Greenamyre et al., 2001). The Complex I assay uses 2,6-dichloroindophenol (DCIP) as a terminal electron acceptor, where Complex I present in mitochondria isolated from brain tissue oxidizes NADH, producing electrons which are transferred to decylubiquinone (a ubiquinone analog electron carrier) that delivers the electrons to DCIP. This assay measures the reduction of DCIP at 600 nM every min over a 12 min period. After the fifth reading, rotenone is added to the reaction mixture to inhibit Complex I activity within the tissue sample. Complex I activity is determined using the difference in the absorbance decay before and after the addition of rotenone.

Brain Tissue Preparation

Brains were frozen and sectioned at 500 μm in a cryostat and striatum tissue was dissected from brain sections. Striatum samples were placed in 10 mM Tris buffer (pH 7.8), and homogenized with a Dounce homogenizer. Tissue homogenates were centrifuged for 10 min at 1000 x g, supernatant (S1) removed, frozen in liquid nitrogen and thawed in a water bath. The pellet (P1) from this centrifugation was discarded. Supernatant (S1) was centrifuged at 14,000 x g for 20 min and the pellet (P2) from this centrifugation contained mitochondria. The pellet (P2) was resuspended twice in 10 mM Tris buffer and re-centrifuged each time at 14,000 x g for 20 min to obtain a clean mitochondrial fraction. The pellet (P2) was resuspended in 100 mM KH_2PO_4 buffer pH

7.8 and the protein content determined using a BCA assay. Samples were stored at -80°C until time of the assay.

Optimization of Sample Size

The optimal amount of protein needed to measure Complex I activity was determined by measuring Complex I activity with 0, 2.5, 5, 10, or 15 ug of striatum protein. Complex I activity measured at the specified protein concentrations produced a linear standard curve by plotting the difference in the absorbance decay before and after the addition of rotenone against protein content within samples (Figure 2-11). A total of 5 ug of protein (within the linear range of Complex I activity) was used in all sample assays measuring Complex I activity.

Complex I Activity Assay

All samples were run in triplicate using 5 ug protein aliquots for each replicate. Samples were placed in reaction buffer containing 3.5 g/L bovine serum albumin, 25 mM KH_2PO_4, 70 uM decyclubiquinone, 60 uM 2,6-dichloroindophenol (DCIP), and 1 uM antimycin A (Sigma-Aldrich) and measured for Complex I activity (Janssen et al., 2007). Samples were placed in a Beckman DU460 spectrophotometer and NADH substrate (Sigma-Aldrich) was added in a final concentration of 0.2 uM. Using a kinetics program absorbance readings were taken over a 12 min period and rotenone was added to each sample following the 5 min reading for a concentration of 1 uM rotenone. The difference between the 2^{nd} and 5^{th} readings was taken and subtracted from the difference between the 8^{th} and 11^{th} readings, and divided by the 3 min time interval, and then divided by the

appropriate amount of protein added to each sample (5 ug), which was reported as Complex I activity.

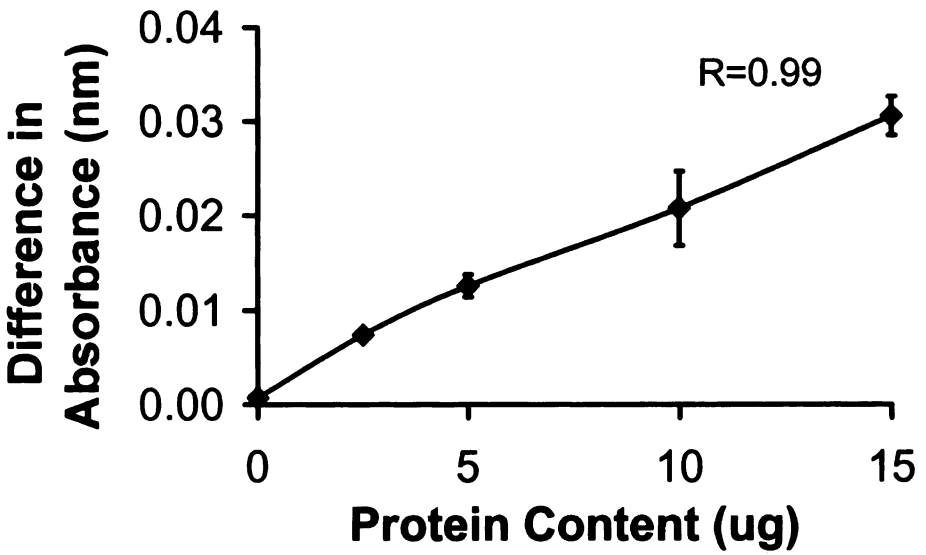

Figure 2-11. Plot of striatum brain tissue protein content verses the difference in absorbance decay before and after Complex I inhibition. Linearity of Complex I activity is seen across 2.5-15 ug of protein as indicated by the difference in the rate of absorbance decrease before and after rotenone addition to samples. Data points represent means and bars one SEM.

K. MPP+ Assay

MPP+ is the active metabolite of MPTP taken up into DA neurons by DAT. MPP+ can be measured in brain regions using liquid chromatography coupled to mass spectrometry (LC-MS). LC-MS is a very sensitive and quantitative method of measuring MPP+ because it uses HPLC to identify how long it adheres to a hydrophobic column (retention time) and MS to identify molecular fragmentations specific to MPP+. MS detection of MPP+ is done by providing mobile phase conditions that allow full ionization of MPP+, desolvation in an atmospheric pressure source for electrospray ionization, and acceleration into a tandem, i.e. triple stage quadrupole (TSQ), MS detector. The initial quadrupole radio frequency and direct current voltages are set to filter the mass/charge ratio specific to MPP+ (i.e. m/z 170.110). This precursor or parent ion continues into a second stage hexapole to undergo kinetic fragmentation imparted by collisions with argon gas, followed by mass analysis in the third quadrupole. When the third quadrupole is set to look only at specific fragments rather than scanning a range, then this is considered multiple reaction monitoring or selected reaction monitoring detection, depending on the manufacturer and its software conventions. Charged fragments bombard a conversion dynode, and the resultant generated electrons are in turn measured by a neighboring electron multiplier. The electrical signals from the electrons are measured as an amplified voltage, and the corresponding voltages are collected, stored and analyzed using computer software.

MPP+ fragment ions are m/z 127, 128 and 154, and quantitation is based on the m/z 170→ 127 fragmentation, whereas the m/z 170→128 and →154 fragmentations are used as qualifiers. Where necessary, the three ions are summed for maximum sensitivity.

The three ions arise specifically as: m/z 128, loss of CH_3N=CH; m/z 127, loss of H from m/z 128; and m/z 154, simultaneous loss of H and CH_3 from m/z 170, a loss that may be specific to methylated quarternary amines, since the related compound paraquat (1,1'-dimethyl-4,4'-dipyridinium) shows similar loss under ESI-MS conditions (Lee et al., 2004). Fragment identifications are tentative due to their unusual individual natures, but in any case agree with spectra generated by others under similar conditions (Boismenu et al., 1996).

Brain Tissue Preparation

Brain tissue was sectioned at 500 uM in a cryostat at -10°C, mounted directly onto room temperature glass slides, and refrozen on dry ice. Micropunches of the striatum were sampled for MPP+ determination. An 18 gauge circular punch tool (1 mm inner diameter) was used to obtain striatum tissue (Bregma +1.42) (Franklin and Paxinos, 1996). Brain tissue punches were placed in 30-50 uL of tissue buffer and centrifuged at 13,000 x g for 1 min to pellet tissue. Tissue was sonicated using three 1 s bursts and samples centrifuged again at 13,000 x g for 1 min to pellet brain tissue. Samples were q.s. to 60 uL with tissue buffer, and brain tissue pellets were placed in 100 uL of 1 N NaOH to determine protein content using a Lowry protein assay (Lowry et al., 1951). Samples were centrifuged again at 18,000 x g for 3 min, and then transferred to glass vials for LC-MS analysis.

LC-MS Analysis of MPP+

Brain tissue samples were prepared and 10 uL of each sample was injected onto a Thermo-Finnigan Surveyor HPLC connected to a Thermo-Finnigan TSQ Quantum ESI-MS/MS detector (Thermo-Fisher Scientific Inc., Waltham, MA). A series of known MPP+ standards (MPP+ 0, 0.5, 1, 2, 5, 10, 20, 50, and 100 ng/mL) were also measured, and the peak area of MPP+ standards was plotted against the known concentrations of individual standards (Figure 2-12). The linear equation of the line resulting from this plot was used to determine sample MPP+ concentrations by interpolating the peak area of samples in the equation of the line. The peak areas of standards and samples were measured using the analytical software Xcalibur (Thermo-Fisher Scientific). Individual sample concentrations of MPP+ were normalized to protein content of brain tissue samples and expressed as the concentration of MPP+ (ng) over the weight of brain tissue (mg). The limit of detection for MPP+ concentrations was approximately 5 ng/mL, thus any value below 5 ng/mL or approximately 6 ng/mg (assuming a tissue punch protein concentration of 50 ug) are essentially zero.

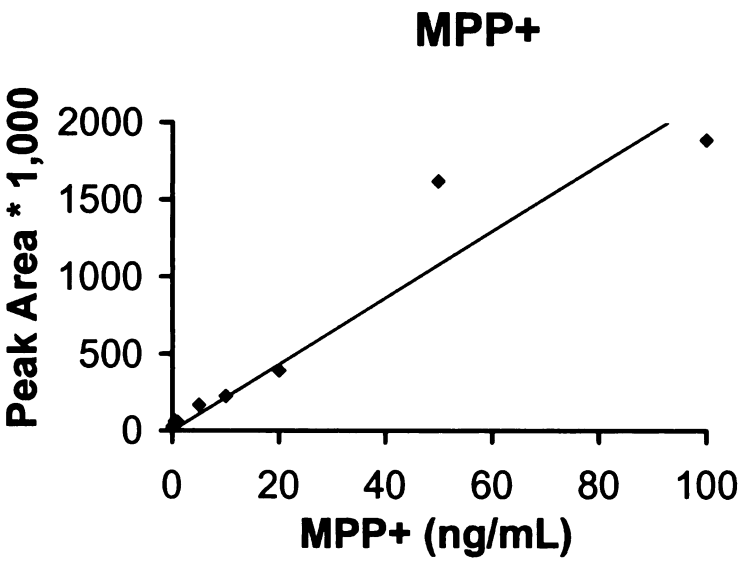

Figure 2-12. Standard curve of MPP+ concentrations measured using liquid chromatography mass spectrometry. MPP+ standards (MPP+ 0, 0.5, 1, 2, 5, 10, 20, 50, and 100 ng/mL) were measured, and the peak area of MPP+ standards was plotted against the known concentrations of individual standards.

L. Statistical Analysis

Power of studies was set at 0.8 and used to the determine number of animals or samples required for significant strength. Data analysis between only two sample groups concerning one variable used a Students T-test to determine if statistical significance was present. For data analysis in which one variable was investigated with more then two sample groups a one-way analysis of variance (ANOVA) test was used. Data from experiments involving more than two sample groups and having two or more variables were analyzed for statistical significance using a two-way ANOVA by a post hoc Tukey's test for multiple comparisons. For all statistical tests an alpha value of $p \leq 0.05$ was deemed statistically significant. All statistical tests used were done using Sigma Stat Statistical Software (Systat Software, Point Richmond, CA).

Notes

Images in this dissertation are presented in color.

Chapter 3: Effects of Sildenafil on Nigrostriatal Dopamine Neurons in a Murine Model of Parkinson's Disease

A. Introduction

Neurodegenerative diseases, like PD, progressively worsen in concert with the inexorable loss of specific neuronal populations. The motor symptoms of PD, slowness of movement, resting tremor, rigidity, and postural instability, are primarily due to the loss of the NSDA neurons (Fahn, 2003). Typically PD is not diagnosed until approximately 40-60% of NSDA neurons are already lost (Dauer and Przedborski, 2003). L-DOPA or DA agonists are currently used to ameliorate the motor symptoms that occur due to deficits of striatal DA in patients with PD, but these symptomatic treatments do not prevent the progressive loss of NDSA neurons or decline of motor function in PD (Lau and Meredith, 2003). Despite substantial advances in our understanding of molecular pathogenic mechanisms underlying cell death in PD and other neurodegenerative diseases, no treatments have proven neuroprotective efficacy in the clinical setting (Ravina et al., 2003). As such, validating a neuroprotective agent to slow or halt the progression of PD remains an important goal for therapy development.

Several animal models have been employed to study potential neuroprotective agents, one of these being the MPTP murine model of PD (Dauer and Przedborski, 2003). Various MPTP dosing paradigms have been used to model PD in mice and the chronic exposure paradigm may be particularly advantageous when screening for neuroprotective effects of target compounds (Petroske et al., 2001). MPTP readily crosses the blood brain barrier and is converted to its active metabolite MPP+ by the enzyme MAO B. MPP+ is a relatively selective NSDA neuronal toxicant and concurrent administration of

probenecid prevents the loss of MPP+ from the brain and extends its duration of action (Lau et al., 1990; Tipton and Singer, 1993; Przedborski et al., 2001). The chronic MPTP model of PD causes striatal DA depletion and a progressive loss of NSDA neurons over an extended period of time (Meredith et al., 2002). Taken together, the features of the chronic MPTP-probenecid murine model mirror the progressive nature NSDA neuronal loss in PD and provide an unique model to study potential neuroprotective agents for this disease (Chan et al., 2007).

Phosphodiesterases are intracellular enzymes that catalyze the breakdown of 3', 5'-cyclic nucleotides such as cGMP, into inactive 5'-monophosphate nucleotides (Kulkarni and Patil, 2004). Phosphodiesterases have varying specificities for 3', 5'-cyclic nucleotides; PDE5 is selective for cGMP, whereas others catabolize both cGMP and cyclic adenosine monophosphate (cAMP) (Corbin and Francis, 1999; Kulkarni and Patil, 2004). PDE5 (or its mRNA) is found in specific cell types in several brain regions including Purkinje cells of the cerebellum, motor and non-motor neurons of the spinal cord, and in adult stem cells of the subventricular zone (SVZ) (Kotera et al., 2000; Nakamizo et al., 2003; Shimizu-Albergine et al., 2003; Van Staveren et al., 2003; Wang et al., 2005). mRNA for PDE5 has also been found in the olfactory bulb, cortex, hippocampus, and substantia nigra, but the phenotypes of cells containing this enzyme are not known (Loughney et al., 1998; Van Staveren et al., 2003).

Sildenafil is a PDE5 inhibitor approved for the treatment of erectile dysfunction (ED), a common non-motor symptom in PD (Corbin and Francis, 1999; Michelakis et al., 2000; Kulkarni and Patil, 2004). In addition to its vasodilatory action on penile microcirculation, sildenafil also increases cortical concentrations of cGMP and promotes

neurogenesis in the SVZ of rats with ischemic stroke as demonstrated by an increase in the number of bromodeoxyuridine positive cells and immature neurons in the striatum (Corbin and Francis, 1999; Zhang et al., 2002; Zhang et al., 2006a). The neurogenic effect of sildenafil on SVZ cells is associated with cGMP-induced activation of the PI-3K/Akt pathway. This pathway has also been implicated in the cGMP-mediated survival of cerebellar granule cells and PC-12 cells (Ciani et al., 2002; Ha et al., 2003). Increased intracellular cGMP concentration also inhibits apoptosis of SH-SY5Y neuroblastoma cells (Andoh et al., 2003). Elevations in intracellular levels of cGMP in immune microglial cells following inhibition of PDE5 results in a decrease in the release of various pro-inflammatory cytokines from LPS stimulated microglia suggesting that sildenafil could potentially inhibit microglial activation that mediates the oxidative stress-induced damage to NSDA neurons in mice exposed to MPTP and in neurodegenerative diseases like PD and Alzheimer's disease (Paris et al., 1999; Paris et al., 2000; Wu et al., 2003).

The purpose of these experiments was to evaluate the potential of sildenafil as a neuroprotective agent for PD by examining the dose-response effects of three treatment paradigms of sildenafil on NSDA neurons in MPTP treated mice. These studies examined the effects of chronic sildenafil treatment, initiated before (pre-treatment), during (concurrent treatment) or after chronic MPTP administration (post-treatment). Once initiated, chronic sildenafil administration continued throughout the duration of these experiments. Endpoints of toxicity included TH protein levels, DA storage and metabolism in axon terminals of NSDA neurons in the striatum, in addition to the numbers of NSDA neurons in the substantia nigra.

Hypothesis: Sildenafil will attenuate the MPTP induced loss of NSDA neurons when treatment is initiated before, during, or after the completion of chronic MPTP treatment.

1) Effectiveness of sildenafil will be determined by correlating the amount of free sildenafil in plasma with concentrations of cGMP within the hindbrain following sildenafil injection.

2) The integrity of NSDA axonal terminals will be evaluated by measuring the concentrations of DA and TH protein content in the striatum following chronic MPTP and sildenifil treatment.

3) NSDA neuronal cell body integrity will be determined by counting the number of TH immunoreactive cells in the substantia nigra after chronic MPTP treatment and sildenafil pre-treatment.

B. Materials and Methods

Male C57BL/6 mice (Jackson Labs) aged 8-10 weeks were used. Mice that received MPTP were housed separately from saline treated control mice. Mice were injected with either 0.9% NaCl or MPTP (20 mg/kg, s.c) and probenecid (250 mg/kg, i.p. using a chronic treatment regimen every 3.5 days for 35 days as previously described (Chapter 2, Section B Drugs). Sildenafil citrate (5 or 10 mg/kg) or 0.9% NaCl were administered twice daily to mice via s.c. injection as previously described (Chapter 2, Section B Drugs).

Mice were killed by decapitation 21 days following the last MPTP injection. The forebrain was dissected at the coronal plane midway through the hypothalamus. The forebrain was prepared for neurochemical and Western blotting analysis of TH protein content as previously described (Chapter 2, Section D Assay of Amines, Amine Metabolites, and Apocynin in Brain Tissue and Section G Western Blot Analysis). The remaining hindbrain was dissected at the mid-saggital plane and half of the hindbrain was immersion fixed in 4% paraformaldehyde and stored at 4°C for TH staining and the other frozen on dry ice for analysis of cGMP content.

Unilateral hindbrains were sectioned at 60 μm using the Multiblock™ processing method and cells stained for TH by Neuroscience Associates (Knoxville, TN). Briefly, every other coronal tissue section was stained using rabbit anti-TH 1:1,500 (Pelfreez Biologicals, Rogers, AR). Primary antibody was bound with the appropriate biotin conjugated secondary antibody, followed by an avidin biotinylated enzyme complex (Vector Laboratories, Burlingame, VT). Bound peroxidase was visualized using 0.05% 3-3'-diaminobenzidine tetrahydrochloride with 0.01% hydrogen peroxide. The number of

immunoreactive TH cells was then determined using an unbiased stereological method as previously described (Chapter 2, Section H, Immunohistochemistry and Stereology Cell Counts). Brain tissue was also stained for the neuroblast marker doublecortin to determine if neurogenesis occurred within the substantia nigra, and doublecortin positive cells observed in the hippocampus were used as a positive control.

The concentrations of free sildenafil in plasma was determined 30 min after a single (5 or 10 mg/kg s.c.) sildenafil injection as previously described (Chapter 2, Section F, Plasma Sildenafil Determination). The concentrations of cGMP were measured in hindbrains 30 min following sildenafil administration as previously described (Chapter 2, Section E, cGMP assay).

C. Results

Blood levels of free sildenafil in mice 30 min following sildenafil administration are shown in (Figure 3-1). Subcutaneous administration of sildenafil resulted in a mean of 40-60 nM concentrations of free sildenafil in plasma following the 5 mg/kg dose, and approximately 80-85 nM concentrations following the 10 mg/kg sildenafil dose. Sildenafil was not detected in the plasma of saline treated mice. cGMP levels were increased in the brain with either 5 or 10 mg/kg sildenafil treatment 30 min following administration (Figure 3-1). Treatment with MPTP did not affect levels of sildenafil in plasma or alter sildenafil-induced increases in brain cGMP levels.

Chronic exposure to MPTP produced a marked decrease in DA concentrations in the striatum (Figures 3-2, 3-3, & 3-4). There was a corresponding, but less marked, decrease in striatal levels of TH protein (Figure 3-5). A decrease in TH immunoreactive neurons (Table 3-1, Figure 3-6) was observed in the substantia nigra following chronic MPTP. The loss of TH-immunoreactive cells parallels the loss of Nissl stained cells in previous studies (Petroske et al., 2001; Behrouz et al., 2007), indicating the loss of TH-immunoreactive cells is from cell death and not merely changes in TH protein expression. Striatal DOPAC concentrations were reduced (Figures 3-2, 3-3, & 3-4) and the ratio of DOPAC to DA increased (Figures 3-2, 3-3, & 3-4) following chronic MPTP treatment.

Sildenafil did not alter basal levels of striatal DA or DOPAC, or the ratio of DOPAC to DA (Figures 3-2, 3-3, & 3-4) at doses of 5 or 10 mg given twice daily. Similarly, sildenafil did not alter the levels of striatal TH protein content (Figure 3-5) or the numbers of TH immunoreactive neurons found in the substantia nigra (Table 3-1). Chronic MPTP exposure decreased striatal DA and DOPAC concentrations, and

increased the ratio of DOPAC to DA to a similar extent in animals treated with 5 or 10 mg/kg of sildenafil, regardless of whether sildenafil treatment was initiated before (Figure 3-2), concurrently or after (Figure 3-3 & 3-4) MPTP administration. Similarly, MPTP-induced decreases in striatal TH protein content (Figure 3-5) and numbers of TH immunoreactive cells in the substantia nigra (Table 3-1, Figure 3-6) were not affected by sildenafil pre-treatment, concurrent treatment, or post-treatment paradigms. Doublecortin staining used to indicate neurogenesis within the substantia nigra was not observed, whereas doublecortin positive control cells within the hippocampus were seen.

A.

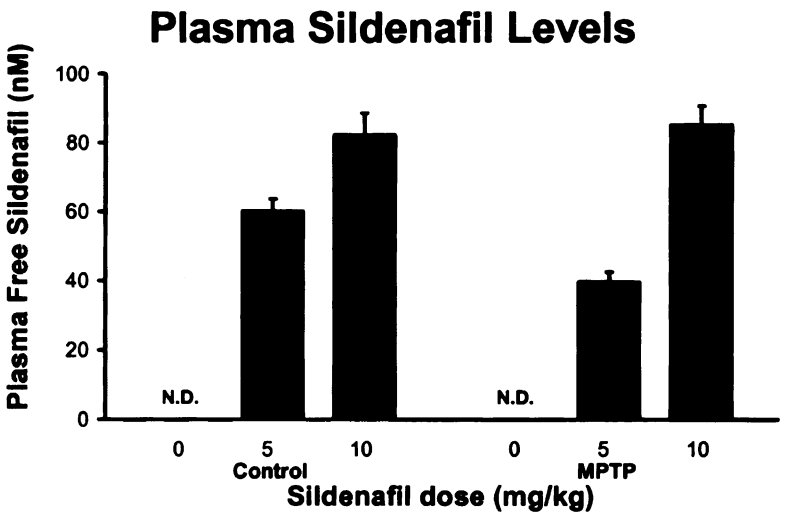

B.

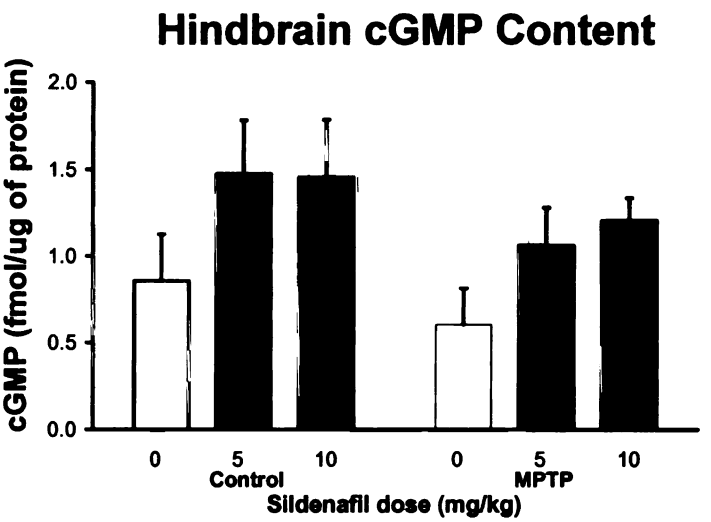

Figure 3-1. Plasma free sildenafil (Panel A) and brain cGMP levels (Panel B) 30 min after sildenafil administration. Mice were injected with either 5 or 10 mg/kg sildenafil, or 0.9% saline vehicle. Columns represent the means and vertical lines one standard error of the mean (S.E.M.), n=4-8. Plasma levels of free sildenafil were not detectable (N.D.) in vehicle controls, but were measurable following 5 and 10 mg/kg sildenafil treatment in both control and chronic MPTP treated mice. Hindbrain cGMP concentrations were increased following 5 and 10 mg/kg sildenafil administration in saline and MPTP treated mice.

A.

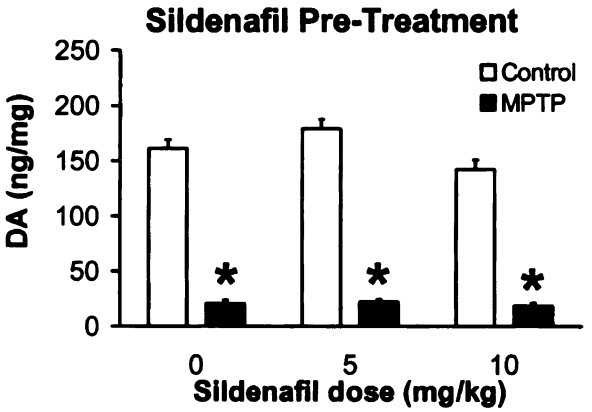

B.

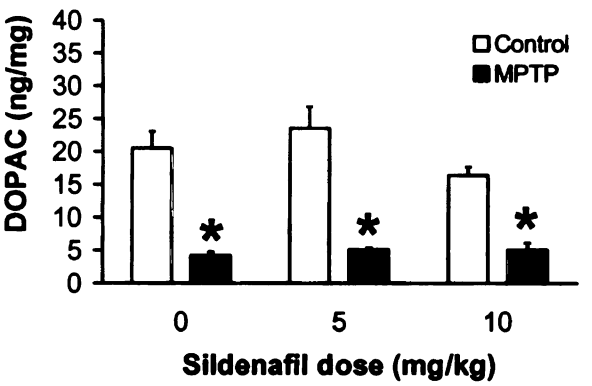

C.

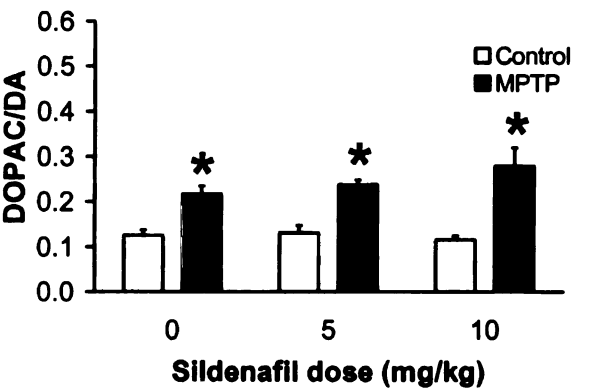

Figure 3-2. Effects of chronic MPTP administration (20 mg/kg s.c., every 3.5 days for 35 days) on DA and DOPAC concentrations, and the DOPAC/DA in the striatum of mice pre-treated with sildenafil. Mice were treated with either saline vehicle or sildenafil (5 or 10 mg/kg, s.c., twice daily) beginning 3 days before saline vehicle or MPTP administration and continuing until the day of decapitation. Columns represent means and vertical lines one standard error of the mean S.E.M. * $P<0.05$, n=4-9. DA and DOPAC concentrations (Panels A & B) significantly (*) decreased following chronic MPTP treatment, and were not affected by sildenafil treatment. The DOPAC/DA ratio (Panel C) increased significantly (*) increased with MPTP treatment, but was not affected by sildenafil treatment.

A.

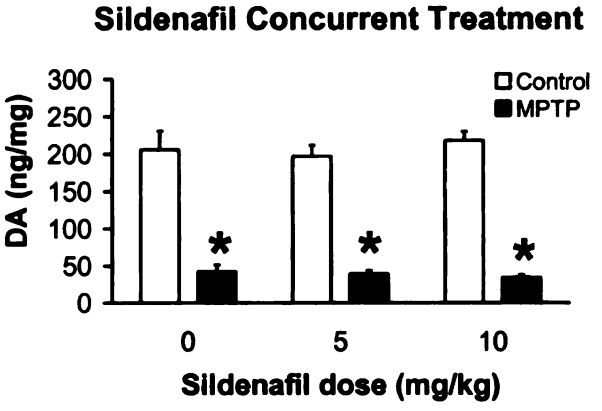

B.

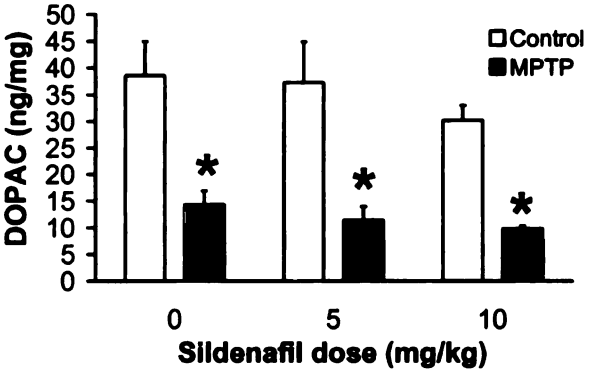

C.

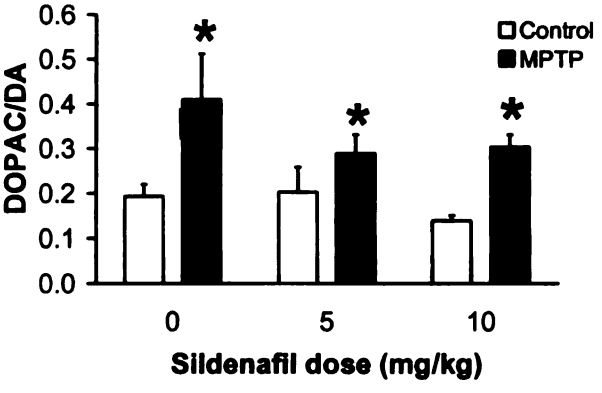

Figure 3-3. Effects of chronic MPTP administration (20 mg/kg s.c., every 3.5 days for 35 days) on DA and DOPAC concentrations, and the DOPAC/DA in the striatum of concurrent sildenafil treated mice. Mice were treated with saline vehicle or sildenafil (5 or 10 mg/kg, s.c., twice daily) beginning 3 days after saline vehicle or MPTP administration began (Concurrent Treatment) and continuing until the day of decapitation. Columns represent means, vertical lines one standard error of the mean S.E.M.. *, $P<0.05$, n=5-9. DA and DOPAC concentrations (Panels A & B) significantly (*) decreased with chronic MPTP treatment, but were not affected by sildenafil treatment. The DOPAC/DA ratio (Panel C) significantly (*) increased with MPTP treatment, but was not affected by sildenafil treatment.

A.

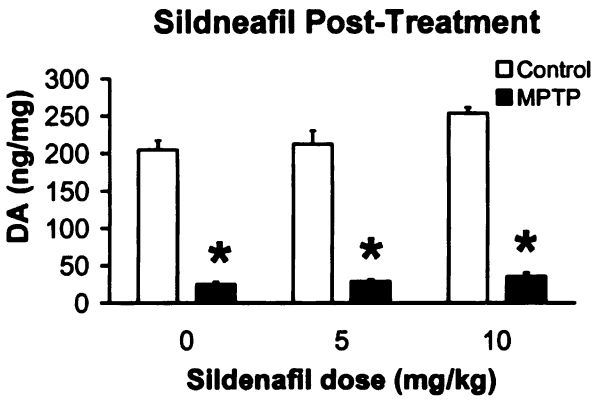

B.

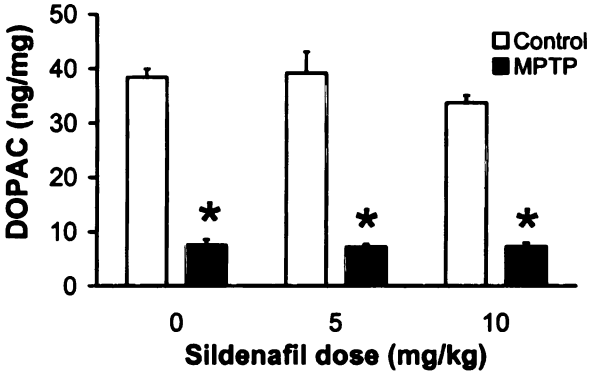

C.

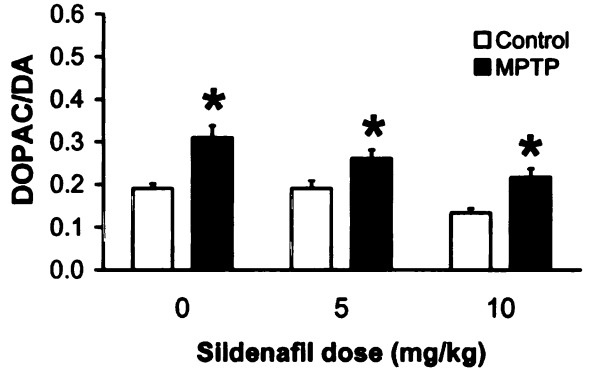

Figure 3-4. Effects of chronic MPTP administration (20 mg/kg s.c., every 3.5 days for 35 days) on DA and DOPAC concentrations, and the DOPAC/DA in the striatum of post-treatment sildenafil treated mice. Mice were treated with saline vehicle or sildenafil (5 or 10 mg/kg, s.c., twice daily) beginning 3 days after saline vehicle or MPTP administration ended (Post-Treatment) and continuing until the day of decapitation. Columns represent means, vertical lines one standard error of the mean S.E.M.. *, $P<0.05$, n=5-9. DA and DOPAC concentrations (Panels A & B) significantly (*) decreased with chronic MPTP treatment, but were not affected by sildenafil treatment. The DOPAC/DA ratio (Panel C) significantly (*) increased with MPTP treatment, but was not affected by sildenafil treatment.

A.

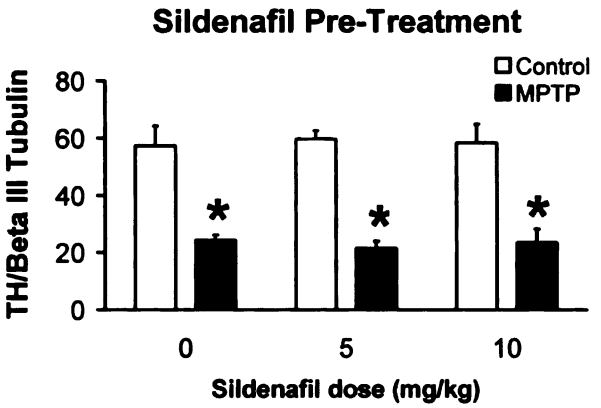

B.

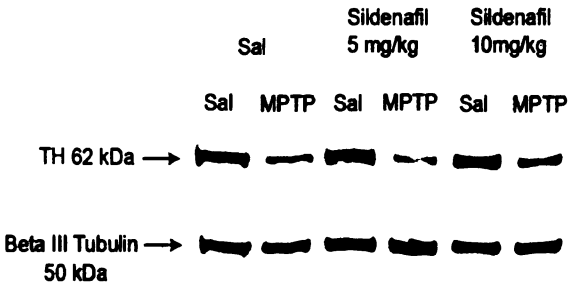

Figure 3-5. Effect of chronic MPTP administration (20 mg/kg s.c., every 3.5 days for 35 days) on TH protein content in the striatum of mice pre-treated with sildenafil. Mice were treated with either saline vehicle or sildenafil (5 or 10 mg/kg, s.c., twice daily) beginning 3 days before saline vehicle or MPTP administration and continuing until the day of decapitation. Columns represent means, vertical lines one standard error of the mean S.E.M., *, $P<0.05$, n=6-8. TH protein content (Panel A) significantly (*) decreased with chronic MPTP treatment, but was not affected by sildenafil treatment. Representative Western blots of TH and Beta III Tubulin (Panel B) in the striatal cytosolic fraction.

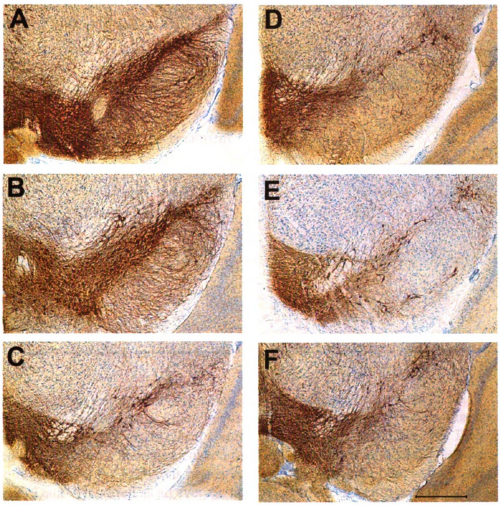

Figure 3-6. Effects of chronic MPTP administration (20 mg/kg s.c., every 3.5 days for 35 days) on TH immunoreactive cells in the substantia nigra. TH immunoreactive cell bodies and fibers are stained brown and bar = 500 μm. Representative pictures from selected treatment conditions are shown. Saline control and saline vehicle treated (Panel A), saline and 10 mg/kg sildenafil Pre-Treatment (Panel B), MPTP and saline vehicle treated (Panel C), MPTP and 10 mg/kg sildenafil Pre-Treatment (Panel D), MPTP and 10 mg/kg sildenafil Concurrent Treatment (Panel E), MPTP and 10 mg/kg sildenafil Post-Treatment (Panel F).

Table 3-1. Numbers of TH Immunoreactive Cells in the unilateral Substantia Nigra Pars Compacta of Sildenafil and/or MPTP treated Mice

Treatment	Mean ± S.E.M.	% Loss	C.E.
Saline/Vehicle	3094 ± 253	-	0.08
Saline/10 mg/kg Sildenafil Pre-Treatment	3254 ± 182	-	0.07
MPTP/Vehicle	2185 ± 113*	29	0.09
MPTP/10 mg/kg Sildenafil Pre-treatment	2150 ± 242*	31	0.09
MPTP/10 mg/kg Sildenafil Concurrent Treatment	1509 ± 106*	49	0.10
MPTP/10 mg/kg Sildenafil Post-Treatment	2128 ± 216*	31	0.09

Table 3-1. Data are presented as the mean ± the S.E.M. and percent loss of TH immunoreactive cell bodies of the saline/vehicle treated control. * Values that are significantly different ($P < 0.05$) from control. Neurons immunoreactive for TH were counted using unbiased stereological counts obtained using an optical fractionator technique to control for variations in neuronal size and volume of the region being analyzed. Data is reported as an average number of total TH positive neurons per unilateral substantia nigra.

D. Discussion

The results of this study reveal that chronic administration of MPTP causes a significant decrease in striatal DA and DOPAC concentrations and TH protein content, as well as a significant loss of TH positive cells in the substantia nigra. A decrease in the concentration of DA in the striatum of MPTP treated mice reflects a loss in the density of NSDA neuronal terminals that is supported by a decrease in striatal TH protein content. Sildenafil treatment did not prevent the MPTP-induced loss of DA, DOPAC, or TH content in the striatum, or alter basal levels of these parameters. The compensatory increase in function of remaining NSDA neurons, as indicated by the increased DOPAC/DA ratio with MPTP treatment, was also not altered with sildenafil treatment. Therefore, sildenafil did not affect the function or compensatory increase in activity of remaining NSDA neurons after MPTP treatment. A significant decrease in the number of TH immunoreactive cells in the substantia nigra of MPTP treated mice indicated a loss of NSDA neuronal cell bodies in this region, which was not affected by sildenafil treatment.

The data presented demonstrates the reliable and reproducible effects of chronic MPTP exposure on clearly defined endpoints of neurodegeneration, thus underscoring the utility of this model (Lau et al., 1990; Petroske et al., 2001; Drolet et al., 2004). The chronic and progressive nature of the MPTP-induced disruption of NSDA neurons observed recapitulates that of PD, which provides distinct advantages over acute dosing models for the study of potential neuroprotective agents. Several different MPTP treatment paradigms have been used to study PD in mice each with a different extent of loss of striatal DA and DOPAC concentrations and NSDA neuronal cell bodies in the substantia nigra (Lau et al., 1990; Przedborski et al., 2001; Schmidt and Ferger, 2001).

MPTP is converted to its toxic metabolite MPP+ which inhibits Complex I of the mitochondrial respiratory chain, causes ATP depletion, oxidative stress, and necrotic and apoptotic loss of NSDA neurons (Tipton and Singer, 1993; Dauer and Przedborski, 2003; Tretter et al., 2004; Novikova et al., 2006). However, the depletion of striatal DA and DOPAC concentrations and TH immunoreactivity in the striatum and substantia nigra have been demonstrated to be partially or completely reversible using some of these other MPTP treatment paradigms, suggesting that loss of neurons may not occur using these treatment paradigms (Lau et al., 1990; Petroske et al., 2001; Schmidt and Ferger, 2001). In contrast, the chronic MPTP paradigm used in this study causes a sustained loss of NSDA neurons, which allows a comparison of pre-treatment, concurrent treatment and post-treatment paradigms when screening for neuroprotective effects of lead compounds (Lau et al., 1990; Petroske et al., 2001).

Several lines of evidence suggest that sildenafil could be a neuroprotective agent for PD. Indeed, due to its ability to block PDE5 and increase cGMP concentrations in the brain, sildenafil promotes neurogenesis of SVZ cells in rats with ischemic stroke and inhibits the release of inflammatory cytokines from microglial cells (Paris et al., 1999; Paris et al., 2000; Zhang et al., 2002; Zhang et al., 2006a). Serum deprived human neurotrophic SH-SY5Y cells with elevated cGMP concentrations or following treatment with a cGMP analogue activate intracellular protein kinase G (PKG) thereby inducing the anti-apoptotic protein BCL-2, which has been shown to attenuate MPTP induced neuronal toxicity when overexpressed in mice (Yang et al., 1998; Andoh et al., 2000; Andoh et al., 2003). When these cells were treated with MPP+, they showed increased resistance to MPP+ toxicity thus implicating a neuroprotective mechanism via elevation

of cGMP concentrations (Andoh et al., 2000; Andoh et al., 2002; Andoh et al., 2003). A cGMP analogue, 8-Br-cGMP, that can activate PKG was shown to decrease 6-OHDA-induced PC-12 cell apoptosis, by suppressing a mitochondrial apoptosis signal which is associated with 6-OHDA cell death (Ha et al., 2003). 8-Br-cGMP also decreases NGF withdrawal- and β-amyloid-induced cell death in PC-12 cells (Wirtz-Brugger and Giovanni, 2000). Another cGMP analogue, dibutyryl cGMP, as well as a nonspecific PDE inhibitor, IBMX, was shown to elevate the release of brain-derived neurotrophic factor (BDNF) implicated in increased survival of NSDA neurons in a DA cell line, suggesting a that increased cGMP was neuroprotective (Chun et al., 2000). Taken together, this evidence suggests that sildenafil-induced elevations in cGMP concentrations could potentially be neuroprotective.

To determine if sildenafil was neuroprotective in the chronic MPTP model of PD three different treatment paradigms were used. Sildenafil administration was initiated either 3 days before (pre-treatment), three days following (concurrent treatment) the initiation of MPTP treatment, or 3 days following the last injection of MPTP (post-treatment) and continued until sacrifice. These various paradigms permitted the evaluation of sildenafil to prevent NSDA neuronal death before, during, or after the initiation of MPTP exposure. The post-treatment paradigm is particularly compelling, since it recapitulates the most likely scenario in which a neuroprotective drug would be employed in patients with PD; i.e., in the absence of a valid biomarker of PD to detect pre-clinical disease, most patients could only be administered a neuroprotective therapy after the disease process has been initiated.

The results from these experiments, however, do not support a neuroprotective effect of sildenafil on NSDA neurons in the chronic MPTP model. The administration of sildenafil was sufficient to produce an increase in brain cGMP concentrations, which is consistent with previous studies that found systemic administration of similar or lower doses of sildenafil increased rodent brain cGMP content (Zhang et al., 2002). That said, low basal PDE5 expression in the NSDA neurons could limit the sildenafil-induced increase of cGMP concentrations in NSDA neurons, which could attenuate any potential neuroprotective effects of sildenafil in the chronic MPTP model (Loughney et al., 1998; Wykes et al., 2002; Van Staveren et al., 2003). In addition, it should be noted that sildenafil has a relatively short-half life and PDE-5 inhibitors with a longer half-life could provide a more sustained change in cGMP levels. Finally, repeated administration of sildenafil could have down-regulated PDE-5 expression and limited the long-term efficacy of this compound.

Prolonged exposure to repeated sildenafil treatment alone did not adversely affect the integrity of NDSA neurons, both under basal conditions and in the context of NSDA damage. The MPTP-induced decrease in striatal DA concentration, TH protein content, and the loss of TH immunoreactive cells in the substantia nigra was similar in vehicle and sildenafil treated mice. Therefore sildenafil did not affect MPTP induced neurodegeneration of NSDA neurons that occurs with chronic MPTP treatment, suggesting that the use of sildenafil to treat PD patients with ED would not be deleterious. ED is a common problem in men with PD and its incidence is significantly greater in these men than age matched controls. The frequency of ED in PD is not surprising since the mesocortical and mesolimbic DA pathways affected in PD partly

mediate the maintenance of penile erection (Magerkurth et al., 2005; Papatsoris et al., 2006). Sildenafil administered to men with PD and other neurodegenerative diseases has been shown to improve sexual function with little or no short-term adverse side effects (Zesiewicz et al., 2000; Hussain et al., 2001). The results from the present study are in agreement with the conclusion that the repeated use of sildenafil in PD patients would not accelerate the loss of NSDA neurons or alter their function, even in the presence of ongoing neurodegeneration. As such, sildenafil administration would not be expected to adversely affect disease progression or motor function in patients with PD.

In summary, the results from this study indicate that sildenafil is not neuroprotective in a chronic MPTP murine model of PD when sildenafil treatment is initiated prior to, during or after neurotoxic insult. Our results also show no deleterious effects of sildenafil in the chronic MPTP murine model of PD. Accordingly, sildenafil could be considered a safe treatment for ED in men with PD.

Chapter 4: Apocynin as a Neuroprotective Agent in the MPTP Model of PD

A. Introduction

NADPH oxidase activation contributes to microglial induced loss of NSDA neurons through the production of superoxide. Although superoxide is not detrimental itself, it induces the production of secondary reactive oxygen species such as hydrogen peroxide and hydroxyl radical that promote microglial proliferation, and induce the synthesis and release of pro-inflammatory cytokines and reactive nitrogen species (Jekabsone et al., 2006; Mander et al., 2006). NADPH oxidase is also implicated in the pathogenesis of NSDA neuronal cell loss when microglia are either directly or indirectly activated in the substantia nigra (Wu et al., 2003; Qin et al., 2004; Purisai et al., 2007; Rodriguez-Pallares et al., 2007). MPTP treatment also induces the activation of NADPH oxidase, and mice lacking the key functional subunit gp91Phox are partially resistant to MPTP induced loss of NSDA neurons (Wu et al., 2003). These findings indicate the importance of NADPH oxidase activation to microglial induced loss of NSDA neurons.

A potential way to reduce NADPH oxidase activation and thereby attenuate microglial mediated loss of NSDA neurons is through the use of an inhibitor of this enzyme such as apocynin (acetovanillone, 4-hydroxy-3-methoxyacetophonone). Apocynin is isolated from the roots of *Apocynum cannabinum* or Canadian hemp (Felter and Lloyd, 1898). The roots of Apocynum cannabinum were used by native Americans for its various medicinal purposes including use as a laxative, anti-rheumatoid agent, and for coughing and asthma (Moerman, 1998). The active compound can also be isolated from the roots of the Himalayan plant *Picrorhiza kurroa* which is used for its anti-

inflammatory properties in the Himalayan region (Anonymous, 2001). Apocynin inhibits NADPH oxidase activation by preventing translocation of the cytosolic subunits p47Phox and p67Phox to the plasma membrane (Stolk et al., 1994; Barbieri et al., 2004). It has been suggested that apocynin itself does not inhibit the enzyme but rather one of its metabolites is responsible for this action (Muller et al., 1999; Ximenes et al., 2007). One possible mechanism is the oxidation of apocynin by cellular peroxidases, which produces apocynin radicals that dimerize forming diapocynin. Diapocynin may be the primary compound responsible for the inhibition of p47Phox translocation to the membrane (Ximenes et al., 2007).

There are several potential neuroprotective mechanisms of microglial derived NADPH oxidase inhibition using apocynin. Inhibition of hydrogen peroxide formation from NADPH oxidase derived superoxide induces microglial cell proliferation and may attenuate the microgliosis associated with the loss of NSDA neurons (Mander et al., 2006). Apocynin inhibition of NADPH oxidase derived superoxide production may also decrease iNOS induction and consequent nitric oxide and peroxynitrite formation as demonstrated *in vitro* (Zhou et al., 1999; Lomnitski et al., 2000; Muijsers et al., 2000). Metabolites of apocynin are also implicated in inhibiting the migration of cells (Muller et al., 1999; Klees et al., 2006), which may be beneficial in inhibiting microglial invasion of the site of inflammation.

Apocynin is a lipophilic molecule which readily crosses the blood brain barrier and therefore is an ideal candidate to inhibit NADPH oxidase within the brain following peripheral administration. Apocynin inhibits microglial NADPH oxidase activation in a rodent model of stroke and reduces the number of activated microglia and degenerating

cortical neurons suggesting a potential to reduce microglial activation and loss of NSDA neurons (Wang et al., 2006). Apocynin also reduces the loss of NSDA neuronal cell bodies and axon terminals in the 6-OHDA model of PD in rats (Rey et al., 2006), revealing a potential for it to attenuate or inhibit the loss of NSDA neurons in the MPTP model of PD.

Hypothesis #1: Apocynin rapidly crosses the blood brain barrier following systemic administration.

This hypothesis will be tested by:

1) Measuring the concentration of apocynin in the striatum using HPLC-EC to establish the pharmacokinetics of the drug including how rapidly it crosses the blood brain barrier and how long it remains within the brain.

2) Investigating the potential effects on dopaminergic neuronal activity by determining the concentrations of DA and DOPAC in the striatum following apocynin treatment.

Hypothesis #2: MPTP will induce activation of NADPH oxidase that will contribute to the loss of NSDA neuronal terminals, and thus be attenuated with apocynin treatment.

This hypothesis will be tested by:

1) Measuring the concentrations of DA in the striatum following MPTP treatment in the presence of apocynin to determine if NSDA axonal terminal loss reflected by reduced DA concentrations in the striatum is attenuated with apocynin treatment.

2) Determining the activity of NSDA neurons by measuring the concentrations of DOPAC and the DOPAC/DA ratio within the striatum following MPTP with and without apocynin treatment.

3) Evaluating NADPH oxidase activation in the striatum and ventral midbrain following MPTP with and without apocynin treatment by determining the amount of membrane bound p67Phox protein, the protein content of the

NADPH oxidase membrane subunit gp91Phox, and the activity of NADPH oxidase.

For comparison, the effects of MPTP and apocynin treatment on MLDA, TIDA, and serotoninergic neuronal integrity and activity will also be determined.

B. Materials and Methods

Male C57BL/6 mice (Jackson Labs), age 8-10 weeks were used in all experiments in which mice were treated with MPTP. B6-129X/C57BL/6 crossed mice obtained from a colony maintained by Drs. John Goudreau and Keith Lookingland were used for apocynin time course and dose response experiments.

Mice used in apocynin pharmacokinetic experiments were injected i.p. with apocynin (30, 100, or 300 mg/kg) at various time points prior to decapitation. Brains were removed and used for analysis of neurochemical and apocynin concentrations which were measured in the striatum using HPLC-EC as previously described (Chapter 2, Section D, Assay of Amines, Amine Metabolites, and Apocynin in Brain Tissue).

MAO B activity was measured in the presence of apocynin *in vitro* to determine if apocynin inhibits activity of this enzyme. MAO B was added to a reaction mixture of DA (5 uM) and apocynin (1, 10, or 100 uM) and stopped 1 h later. The concentrations of DA and its MAO B metabolite DOPAL were measured by HPLC-EC in reaction samples as previously described (Chapter 2, Section D, Assay of Amines, Amine Metabolites, and Apocynin in Brain Tissue) (Legros et al., 2004).

MPTP was administered by one of two paradigms: sub-chronic MPTP (10 mg/kg, s.c. once a day for 5 days) or repeated acute MPTP treatment (16 mg/kg given i.p. once every 2 h over a 6 h period for a total of 4 injections; see Chapter 2, Table 2-2). Mice were killed either 3 days following the last MPTP injection for sub-chronic MPTP treatment or 2 days following the last MPTP injection for repeated acute MPTP treatment, and brain tissue was used for neurochemical, Western blotting, or NADPH oxidase activity assay.

The sub-chronic MPTP model was used in the first study since it induces microglial activation but does not cause as severe of a loss of NSDA axon terminals as the repeated acute MPTP model. If apocynin was neuroprotective this may be more apparent in the sub-chronic MPTP model. However, lack of an observed neuroprotective effect in the sub-chronic model led to the use of the repeated acute MPTP model with the thought that perhaps a greater microglial reaction was needed to observe a potential a neuroprotective effect of apocynin. Apocynin (100 mg/kg, i.p.) or vehicle administration for sub-chronic MPTP treated mice was administered every 12 h beginning 2 days prior to the beginning of MPTP treatment up to the day of decapitation. Vehicle or apocynin (250 mg/kg per day) was administered via osmotic mini-pump beginning two days prior to repeated acute MPTP treatment and continuing until decapitation as previously described (Chapter 2 Section B, Drugs).

Brain tissue from these experiments was processed for neurochemical analysis of DA, DOPAC, HVA, 5HIAA, and 5HT concentrations in select brain regions as previously described (Chapter 2 Section D, Assay of Amines, Amine Metabolites, and Apocynin in Brain Tissue). The protein content of TH, p67Phox, and gp91Phox was measured in the striatum or ventral midbrain as previously described (Chapter 2, Section G, Western Blot Analysis). The activity of NADPH oxidase was measured in the striatum and ventral midbrain following repeated acute MPTP treatment as previously described (Chapter 2, Section I, NADPH Oxidase Assay).

C. Results

Pharmacokinetics of Apocynin in the Brain

The concentrations of apocynin in the striatum were measured using HPLC-EC at several time points (2.5, 5, 10, 20, and 30 min; Figure 4-1, Panel A) or (2.5, 30, 120, 240, and 480 min; Figure 4-1, Panel B) following administration of apocynin (100 mg/kg i.p.) to determine the length of time apocynin remained in the brain. Apocynin concentrations in the striatum were measurable at the first 2.5 min time point. However, the drug was rapidly eliminated from the brain essentially being undetectable by 20 min following administration indicating that apocynin has a half-life of only a few minutes (Figure 4-1) (unpublished results of Lookingland, Goudreau, and Pappas). The concentration of apocynin was also measured in the striatum at incremental dosages (0, 30, 100, or 300 mg/kg) at the 2.5 min time point to determine if apocynin crossed the blood brain barrier in a dose dependent manner. The concentrations of apocynin in the striatum revealed that apocynin could be measured in the brain in a dose dependent manner, since the dosage of apocynin formed a linear relationship with the amount of the drug measured in the striatum (Figure 4-1; Panel C). These results indicated that apocynin is a lipophilic compound that readily crossed the blood brain barrier, but was quickly eliminated from the brain possibly due to metabolism or redistribution of apocynin to other tissues.

The concentrations of DA and its metabolite DOPAC were measured in the striatum at 2.5, 30, 120, 240, and 480 min following apocynin (100 mg/kg, i.p.) administration to determine if apocynin altered the activity of NSDA neurons. As shown in Figure 4-2 (Panels A & B) DA concentrations were not altered compared to vehicle treated mice, but DOPAC concentrations were significantly decreased at 2.5 min

following apocynin treatment. DOPAC concentrations returned to vehicle control concentrations by 30 min following apocynin administration. The DOPAC/DA ratio was also decreased at 2.5 min due to reduced DOPAC concentrations at that time point indicating a decrease in NSDA neuronal activity (Figure 4-2; Panel C). DA and DOPAC concentrations were also measured in the striatum of vehicle and apocynin (30, 100, or 300 mg/kg, i.p.) treated mice at 2.5 min to determine if apocynin effected the activity of NSDA neurons in a dose dependent manner. A shown in Figure 4-3 (Panels A & B) the concentrations of DA were not altered with apocynin treatment, but DOPAC concentrations were significantly decreased in a dose dependent manner with apocynin treatment. The decrease in DOPAC concentrations in the striatum following apocynin treatment was associated with a significant decrease in the DOPAC/DA ratio in the striatum (Figure 4-3; Panel C). The decrease in DOPAC following apocynin could reflect a change in NSDA neuronal activity or apocynin inhibition of MAO B metabolism.

Apocynin inhibition of MAO B was tested by an *in vitro* cell free experiment measuring the activity of MAO B in the presence or absence of apocynin (Legros et al., 2004). MAO B activity was measured over time (15, 30, 45, and 60 min) initially to determine an ideal time point that MAO B metabolism of DA to DOPAL could be measured. As shown in Figure 4-4 (Panel A), the reaction over time produced a linear decrease in DA concentrations and a linear increase in DOPAL concentrations, and based on these results a 60 min time point was chosen to terminate the reaction in the presence of apocynin.

As shown in Figure 4-4 (Panels B & C), the synthesis of DOPAL was measured in the presence of various concentrations of apocynin (1, 10, or 100 uM). Apocynin treatment alone did not alter the concentrations of DA within the reaction mixture in the absence of MAO B. The addition of MAO B to the reaction mixture of DA and apocynin (1, 10, or 100 uM) did not alter the synthesis of DOPAL from DA compared to samples only containing DA and MAO B at 1 h following the initiation of the reaction. The results indicated that apocynin likely does not alter metabolism of DA to DOPAC by MAO B in the brain.

A.

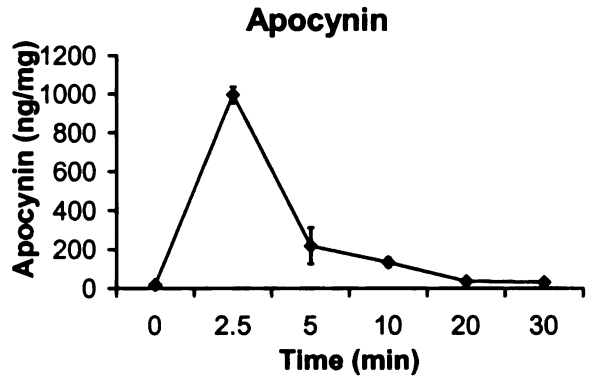

B.

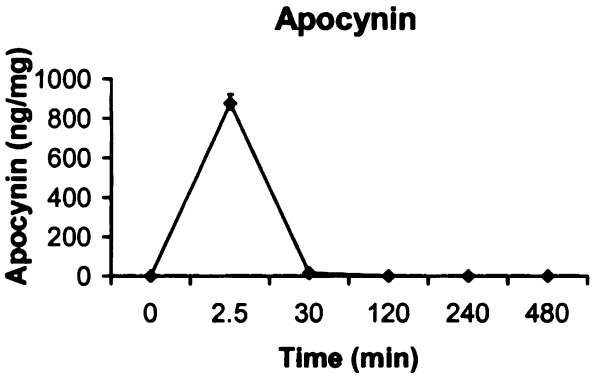

C.

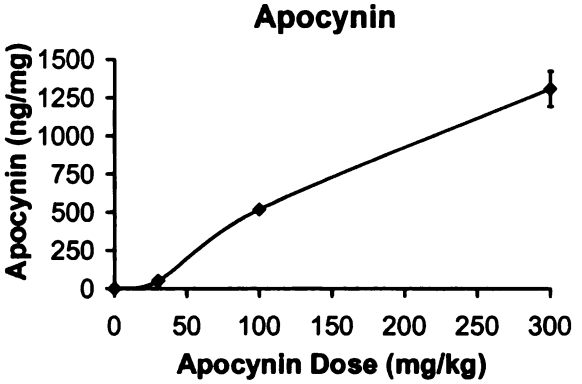

Figure 4-1. Measurement of apocynin in the brain using HPLC-EC. Apocynin was measured in the striatum of mice at 2.5, 5, 10, 20, and 30 min (Panel A) or 2.5, 30, 120, 240, 480 min (Panel B) following an i.p. injection of 100 mg/kg apocynin, vehicle treated mice were considered the 0 time controls were injected with vehicle and killed 2.5 min later, n=4-8. Dose dependent increase of apocynin in the striatum following vehicle, 30, 100, or 300 mg/kg apocynin i.p. injection given 2.5 min prior to decapitation (Panel C), n=4. Data points represent means and bars one SEM.

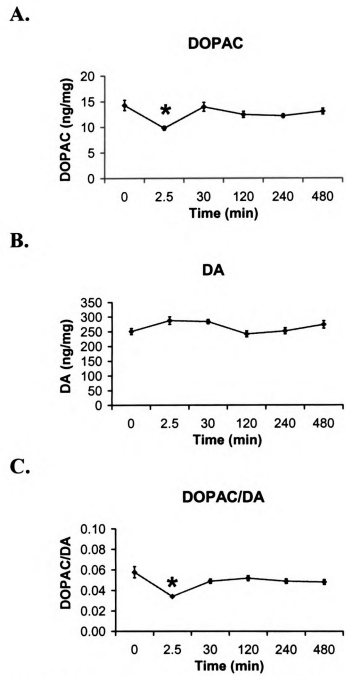

Figure 4-2. Apocynin decreases the concentrations of DOPAC and the DOPAC/DA ratio in the striatum. Mice were injected with apocynin 100 mg/kg, i.p. and decapitated 2.5, 30, 120, 240, or 480 min later, vehicle treated mice were considered the 0 time controls were injected with vehicle and killed 2.5 min later, n=7-8. The concentrations of DOPAC (Panel A) and DA (Panel B), and the DOPAC/DA (Panel C). Data points represent means and bars one SEM. *Significantly less DOPAC or the DOPAC/DA ratio compared to vehicle treated mice.

A.

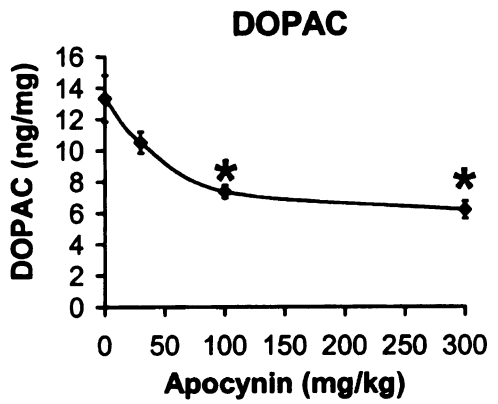

B.

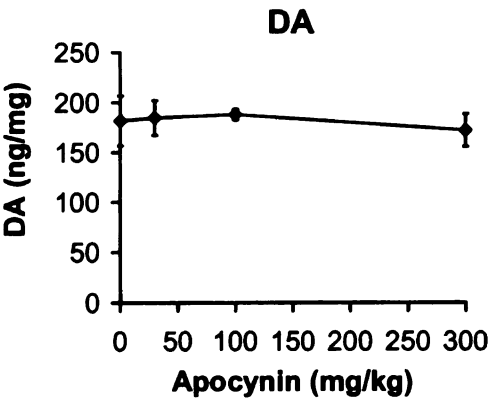

C.

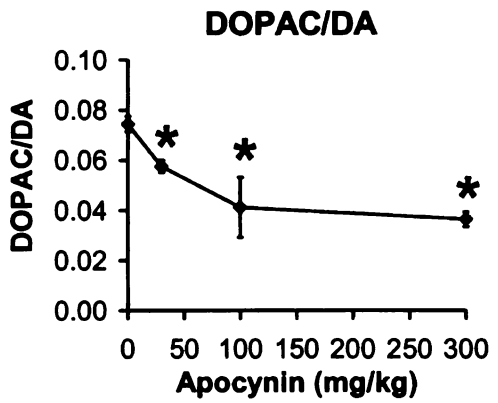

Figure 4-3. Apocynin dose dependently decreases DOPAC concentrations and reduces the DOPAC/DA ratio in the striatum. Mice were injected with vehicle, 30, 100, or 300 mg/kg apocynin i.p. and sacrificed 2.5 min later, n=4. The concentrations of DOPAC (Panel A) and DA (Panel B), and the DOPAC/DA (Panel C) at specified dosages. Data points represent means and bars one SEM. *Significantly reduced DOPAC concentrations or the DOPAC/DA ratio compared to vehicle treated mice.

A.

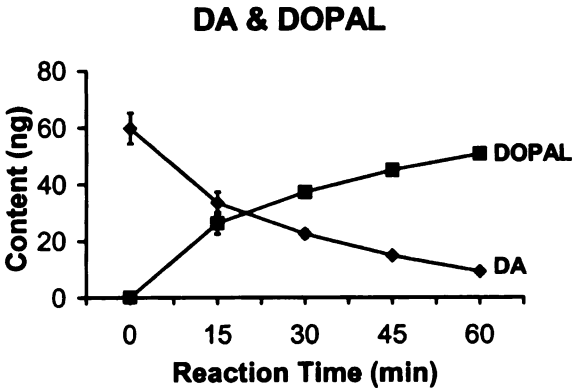

B.

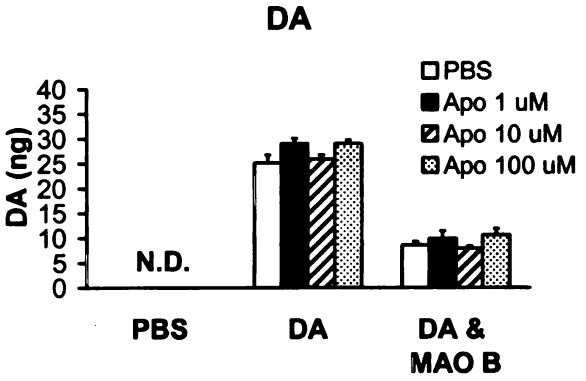

C.

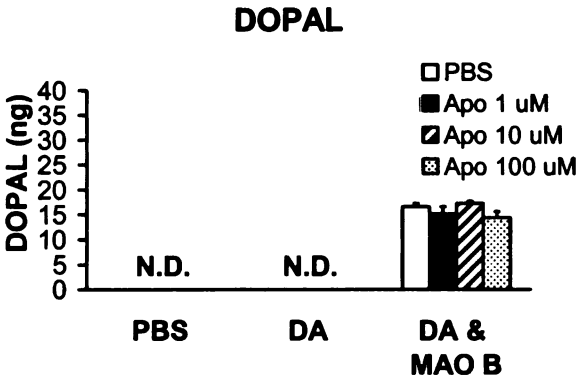

Figure 4-4. Apocynin (Apo) does not inhibit MAO B *in vitro* in a cell free system. Time course of MAO B conversion of DA to DOPAL (Panel A). Lack of an effect on DA depletion (Panel B) or the synthesis of DOPAL (Panel C) by apocynin in the presence of MAO B and DA 1 h following reaction initiation, n=3. Columns represent means and bars one SEM.

Apocynin as a Neuroprotective Agent in the Sub-Chronic MPTP Model of PD

The concentrations of DA and its metabolites DOPAC and HVA were measured in the striatum of mice treated with saline or sub-chronic MPTP (10 mg/kg, s.c., once a day for 5 days) treatment and given either vehicle or apocynin (100 mg/kg, i.p. every 12 h) to determine if apocynin prevented the loss of NSDA neuronal terminals. As shown in Figures 4-5 & 4-6, DA, DOPAC, and HVA concentrations were similar in control mice given either vehicle or apocynin. DA concentrations were significantly decreased in MPTP treated mice and MPTP treated mice given apocynin. DOPAC and HVA concentrations in the striatum were also significantly decreased with MPTP treatment in both vehicle and apocynin treated mice. The DOPAC/DA and HVA/DA ratios in the striatum were not altered with apocynin treatment alone, and were significantly increased with MPTP treatment in vehicle and apocynin treated mice (Figure 4-5; Panel C & Figure 4-6; Panel B). These results reveal that apocynin did not prevent the loss of NSDA neuronal terminals, or the compensatory activity of remaining NSDA neurons typically seen with sub-chronic MPTP treatment.

The extent of microglial activation was assessed in the striatum using content of membrane bound p67Phox. The activation of NADPH oxidase involves the translocation of the cytosolic subunit p67Phox to the cell membrane (Bianca et al., 1999; Groemping and Rittinger, 2005). The content of membrane bound p67Phox can be used to determine if there is an increase in microglial activation with MPTP treatment (Wu et al., 2002; Wu et al., 2003). As shown in Figure 4-7, Membrane bound p67Phox protein in the striatum was similar between vehicle and apocynin treated mice given saline vehicle. MPTP treatment induced a significant increase in membrane bound p67Phox protein in vehicle

treated mice, consistent with activation of NADPH oxidase (Figure 4-7, Panel A). In the presence of apocynin this increase was not present indicating that apocynin reduced activation of NADPH oxidase.

The neurochemical concentrations of DA, DOPAC, and HVA were also measured in the nucleus accumbens to determine if sub-chronic MPTP treatment and/or apocynin altered MLDA neuronal activity. As shown in Table 4-1, the concentrations of DA were not different in the nucleus accumbens following MPTP or apocynin treatment suggesting that MLDA neuronal integrity was maintained with MPTP treatment. DOPAC concentrations in the nucleus accumbens were significantly decreased with MPTP treatment in vehicle treated mice, but not altered with MPTP treatment in the presence of apocynin. The HVA concentrations in the nucleus accumbens were not changed in the presence of MPTP or apocynin. The DOPAC/DA and HVA/DA ratios were similar in MPTP and/or apocynin treatment compared to saline and/or vehicle treated mice. These results suggest that sub-chronic MPTP treatment does not alter MLDA neuronal integrity or activity.

TIDA neuronal integrity and activity were also assessed in the presence of sub-chronic MPTP and/or apocynin treatment. DA concentrations were similar in the median eminence between saline and sub-chronic MPTP treated mice within both vehicle and apocynin groups of mice (Table 4-2). The concentrations of DOPAC and HVA in the median eminence were also not altered with MPTP and/or apocynin treatment. The activity of TIDA neurons as determined by the DOPAC/DA and HVA/DA ratios were similar between saline treated mice given either vehicle or apocynin. These findings

indicate that sub-chronic MPTP or apocynin treatment do not alter TIDA neuronal integrity or activity.

Lack of an Effect on Serotoninergic Integrity and Activity with Sub-Chronic MPTP or Apocynin Treatment

The concentrations of 5HT were measured in the nucleus accumbens and median eminence to determine if sub-chronic MPTP or apocynin treatment altered serotoninergic neuronal integrity. The concentrations of 5HT were similar in mice treated with saline or MPTP given vehicle or apocynin in both the nucleus accumbens and median eminence. Apocynin treatment also did not affect 5HT concentrations in either axonal terminal region. The 5HIAA concentrations were also determined in both terminal regions and were not different with either MPTP or apocynin administration. The ratio of 5HIAA/5HT in the nucleus accumbens and median eminence were also similar in the presence or absence of MPTP and apocynin within each axonal terminal region (Table 4-1 & 4-2). This data indicates that serotoninergic neuronal integrity and activity are maintained in the presence of either sub-chronic MPTP or apocynin treatment.

A.

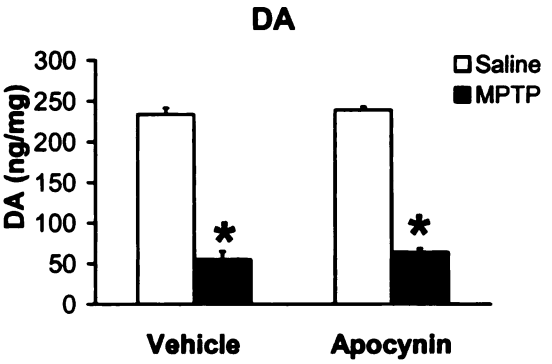

B.

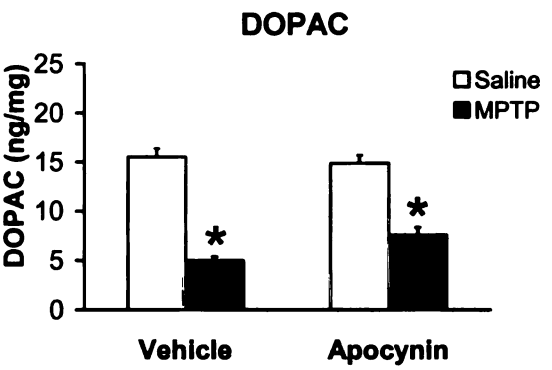

C.

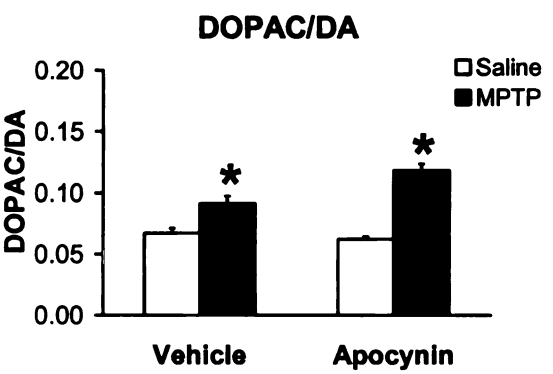

Figure 4-5. Apocynin does not alter MPTP induced DA depletion in the striatum. Mice were treated with saline or a sub-chronic MPTP treatment paradigm (10 mg/kg once a day for 5 days) and sacrificed 3 days later. Mice were treated with either vehicle or apocynin (100 mg/kg, i.p.) twice a day prior to and following MPTP treatment. Concentrations of DA (Panel A), DOPAC (Panel B), and the DOPAC/DA ratio (Panel C) in the striatum. Columns represent means and bars one SEM. *Significant difference between saline and MPTP treated mice.

A.

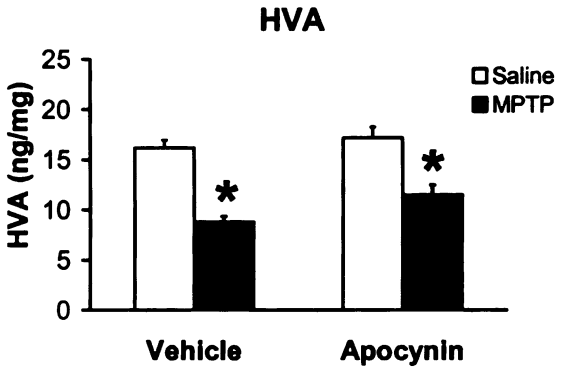

B.

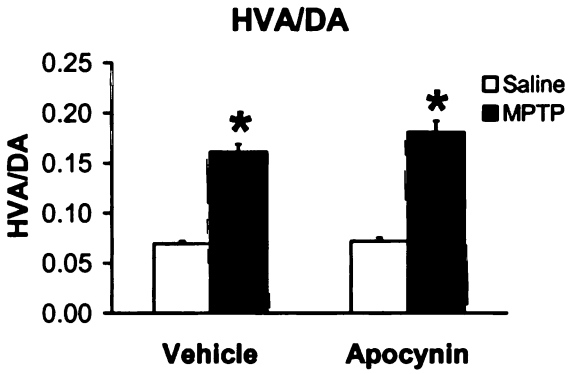

Figure 4-6. Apocynin does not alter MPTP induced HVA depletion in the striatum. Mice were treated with saline or a sub-chronic MPTP treatment paradigm (10 mg/kg once a day for 5 days) and sacrificed 3 days later. Mice were treated with either vehicle or apocynin (100 mg/kg, i.p.) twice a day prior to and following MPTP treatment. Concentrations of HVA (Panel A) and the HVA/DA ratio (Panel B) in the striatum. Columns represent means and bars one SEM. *Significant difference between saline and MPTP treated mice.

A.

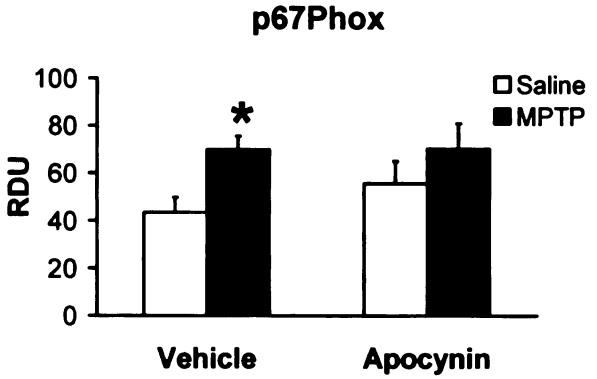

B.

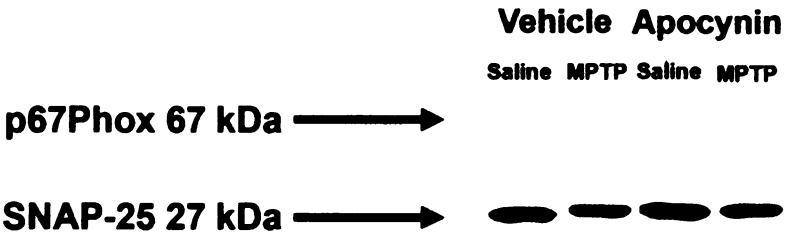

Figure 4-7. Membrane bound p67Phox protein in the striatum. Mice were treated with saline or a sub-chronic MPTP treatment paradigm (10 mg/kg once a day for 5 days) and sacrificed 3 days later. Mice were treated with either vehicle or apocynin (100 mg/kg, i.p.) twice a day prior to and following MPTP treatment. p67Phox protein normalized to the membrane protein SNAP-25 and multiplied by a factor of 1000 and expressed as relative density units (RDU) (Panel A). Pictorial representation of p67Phox and SNAP-25 protein bands from each respective treatment group (Panel B). Columns represent means and bars one SEM. *Significant difference between saline and MPTP treated mice.

Table 4-1. Neurochemical Concentrations in the Nucleus Accumbens Following Sub-Chronic MPTP and Apocynin Treatment

Nucleus Accumbens	Saline/Vehicle	MPTP/Vehicle	Saline/Apocynin	MPTP/Apocynin
DA	117.5 ± 6.0	89.9 ± 10.4	104.1 ± 11.5	92.0 ± 11.8
DOPAC	13.5 ± 1.2	8.7 ± 0.8 *	10.8 ± 1.1	9.1 ± 1.0
DOPAC/DA	0.12 ± 0.01	0.10 ± 0.01	0.11 ± 0.01	0.11 ± 0.2
HVA	12.0 ± 0.4	10.4 ± 0.6	10.9 ± 0.6	10.0 ± 0.7
HVA/DA	0.11 ± 0.01	0.13 ± 0.02	0.11 ± 0.01	0.13 ± 0.04
5HT	10.3 ± 1.6	10.8 ± 1.0	10.3 ± 1.4	10.7 ± 1.4
5HIAA	3.5 ± 0.5	4.6 ± 0.5	3.4 ± 0.4	3.9 ± 0.6
5HIAA/5HT	0.35 ± 0.02	0.44 ± 0.04	0.35 ± 0.02	0.38 ± 0.04

Table 4-1. Mice were treated with saline or a sub-chronic MPTP treatment paradigm (10 mg/kg once a day for 5 days) and sacrificed 3 days later. Mice were treated with either vehicle or apocynin (100 mg/kg, i.p.) twice a day prior to and following MPTP treatment. The concentrations of DA, DOPAC, HVA, 5HT, 5HIAA, and the DOPAC/DA, HVA/DA, and 5HIAA/5HT ratios were determined in the nucleus accumbens. Values are the mean ± the SEM. *Significant difference between saline and MPTP treated mice within either vehicle or apocynin treatment groups.

Table 4-2. Neurochemical Concentrations in the Median Eminence Following Sub-Chronic MPTP and Apocynin Treatment

Median Eminence	Saline/Vehicle	MPTP/Vehicle	Saline/Apocynin	MPTP/Apocynin
DA	112.2 ± 11.6	146.9 ± 5.9	119.2 ± 8.0	116.3 ± 16.3
DOPAC	7.1 ± 0.5	6.5 ± 0.3	7.7 ± 0.4	6.6 ± 0.7
DOPAC/DA	0.07 ± 0.01	0.05 ± 0.01	0.07 ± 0.01	0.06 ± 0.01
HVA	11.7 ± 0.8	14.8 ± 1.3	11.7 ± 0.8	12.9 ± 1.1
HVA/DA	0.11 ± 0.01	0.10 ± 0.01	0.10 ± 0.01	0.13 ± 0.03
5HT	13.3 ± 1.3	12.6 ± 1.4	14.5 ± 2.8	13.4 ± 2.0
5HIAA	14.0 ± 1.4	15.7 ± 0.5	13.6 ± 1.3	13.9 ± 1.2
5HIAA/5HT	1.08 ± 0.10	1.31 ± 0.08	1.05 ± 0.11	1.10 ± 0.09

Table 4-2. Mice were treated with saline or a sub-chronic MPTP treatment paradigm (10 mg/kg once a day for 5 days) and sacrificed 3 days later. Mice were treated with either vehicle or apocynin (100 mg/kg, i.p.) twice a day prior to and following MPTP treatment. The concentrations of DA, DOPAC, HVA, 5HT, 5HIAA, and the DOPAC/DA, HVA/DA, and 5HIAA/5HT ratios were determined in the median eminence. Values are the mean ± the SEM.

Apocynin as a Neuroprotective Agent in the Repeated Acute MPTP Model

The rapid elimination of measurable apocynin from the brain and the finding that apocynin failed to attenuate or prevent the loss of NSDA axon terminals suggested that apocynin administration may need to be delivered continuous over time rather than twice daily. Although p67Phox membrane was significantly increased following sub-chronic MPTP treatment, lack of a neuroprotective effect may be due to limited microglial activation. Therefore, if microglial activation is limited, the MPTP induced loss of axonal terminals in the striatum may be due exclusively to neurotoxic effects of MPTP without the additive effects of microglial mediated cell death. The use of the repeated acute MPTP model was employed to induce a more severe neurotoxic insult over a shorter period of time and a greater extent of microglial activation. Due to its short half-life, apocynin (250 mg/kg per day) was administered continuously via osmotic mini-pump to maintain constant levels of apocynin in the brain.

The repeated acute MPTP model consists of injections of either saline vehicle or MPTP (16 mg/kg, i.p.) every 2 h over a 6 h period for a total of 4 injections of MPTP, and mice were killed 2 days later when microglial activation is maximal (Wu et al., 2003). The activity of NADPH oxidase was measured in the striatum and ventral midbrain of mice following saline or MPTP administration using brain homogenates from each region. Repeated acute MPTP treatment induced a significant increase in NADPH oxidase activity in the striatum (Figure 4-8; Panel A) that was more pronounced than in the ventral midbrain (Figure 4-8; Panel B). An increase in NADPH oxidase activity indicates that repeated acute MPTP induces a significant activation of microglia.

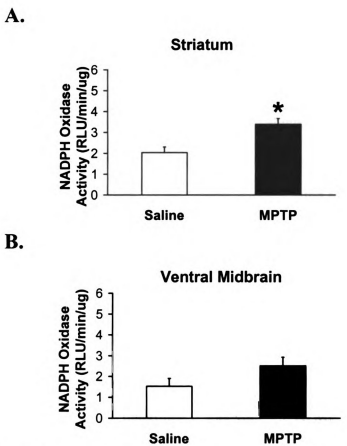

Figure 4-8. NADPH oxidase activation following repeated acute MPTP treatment. Mice were treated with either saline or a repeated acute MPTP paradigm (4 injections of 16 mg/kg MPTP given i.p. every 2 h over a 6 h period). NADPH oxidase activity in the striatum (Panel A) and ventral midbrain (Panel B). Columns represent means and bars one SEM. *Significant increase with repeated acute MPTP treatment versus saline.

In a subsequent experiment, mice were treated with apocynin (250 mg/kg per day) beginning 2 days prior to repeated acute MPTP treatment and continued for an additional 2 days until the time of decapitation. The concentrations of DA were measured in the striatum of saline and MPTP treated mice given either vehicle solution or apocynin via osmotic mini-pump. DA concentrations were significantly decreased following MPTP treatment to a similar extent in both vehicle and apocynin treated mice (Figure 4-9; Panel A). MPTP induced a significant decrease in the content of TH in the striatum, which was not attenuated with apocynin administration (Figure 4-10). These results indicate that apocynin does not prevent a loss of NSDA axonal terminals seen with repeated acute MPTP treatment.

DOPAC concentrations and the DOPAC/DA ratio (Figure 4-9; Panels B & C) were examined in the striatum to determine if apocynin altered MPTP induced increases in NSDA neuronal activity. DOPAC concentrations were significantly decreased to a similar extent following repeated acute MPTP treatment in both vehicle and apocynin treated mice. MPTP induced a significant increase the DOPAC/DA ratio in both vehicle and apocynin treated mice (Figure 4-9; Panel C). These results indicate that apocynin does not attenuate the compensatory activity of NSDA neurons seen with repeated acute MPTP treatment.

NADPH oxidase activation was evaluated in the striatum following repeated acute MPTP treatment by measuring membrane bound p67Phox and gp91Phox proteins. MPTP treatment significantly induced an increase p67Phox and gp91Phox proteins in the striatum of vehicle treated mice (Figure 4-11). A similar increase was seen in both MPTP and apocynin treated mice (Figure 4-11). Thus, apocynin failed to block MPTP

induced translocation of p67Phox to the membrane, or increase in gp91Phox at the membrane of microglial cells.

MLDA Neuronal Integrity and Activity with Repeated Acute MPTP and Apocynin Treatment

DA and DOPAC concentrations were also measured in the nucleus accumbens following repeated acute MPTP treatment (Table 4-3). MPTP induced a significant decrease in DA and DOPAC concentrations, which was not different in MPTP/apocynin treated mice. The DOPAC/DA ratio was not altered with MPTP administration in vehicle treated mice, but was significantly increased following MPTP treatment in mice given apocynin.

Serotoninergic Neuronal Integrity and Activity with Repeated Acute MPTP and Apocynin Treatment

5HT and 5HIAA concentrations in the nucleus accumbens were also measured to determine if repeated acute MPTP and/or apocynin treatment affected serotoninergic neuronal integrity or activity (Table 4-3). The concentrations of 5HT were significantly decreased with MPTP treatment in mice given either vehicle or apocynin suggesting a loss of serotoninergic axonal terminals in the nucleus accumbens. The 5HIAA concentrations were similar in the presence or absence of MPTP and/or apocynin treatment. However, serotoninergic neuronal activity was increased in the nucleus accumbens of MPTP/apocynin treated mice.

A.

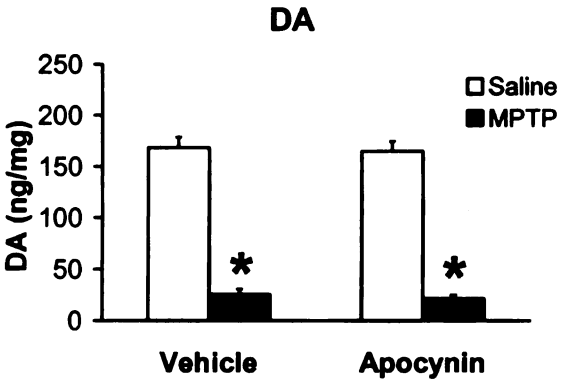

B.

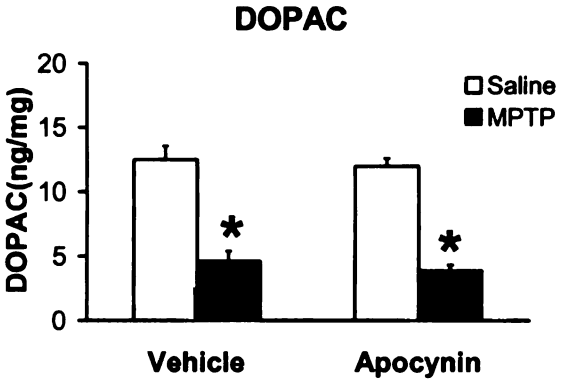

C.

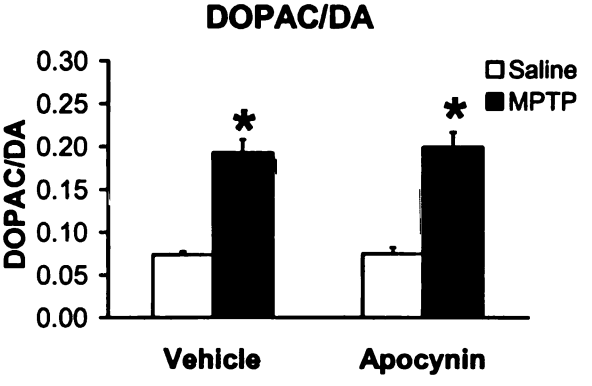

Figure 4-9. Apocynin does not alter repeated acute MPTP induced DA depletion in the striatum. Mice were treated with either saline or a repeated acute MPTP treatment paradigm (4 injections of 16 mg/kg MPTP given every 2 h over a 6 h period) and given vehicle or apocynin 250 mg/kg per day via osmotic mini-pump. Concentrations of DA (Panel A), DOPAC (Panel B), and the DOPAC/DA ratio (Panel C) in the striatum 2 days following saline/MPTP treatment. Columns represent means and bars one SEM. *Significant difference between saline and MPTP treated mice.

A.

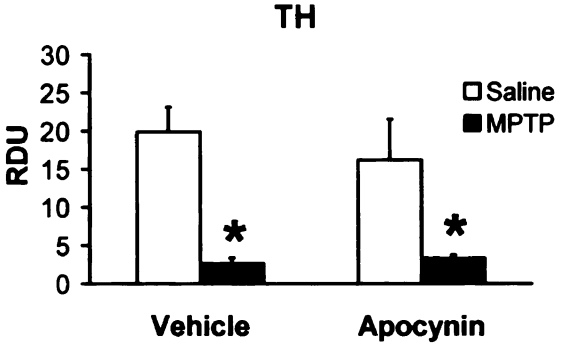

B.

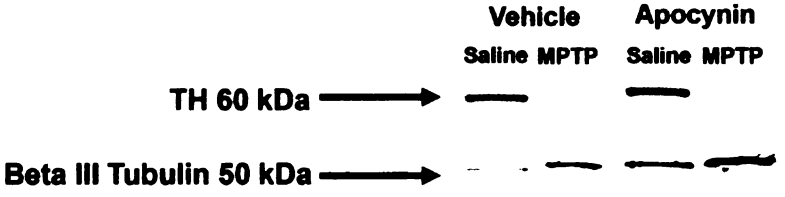

Figure 4-10. Loss of TH protein content in the striatum with repeated acute MPTP treatment is not attenuated with apocynin. Mice were treated with either saline or a repeated acute MPTP paradigm (4 injections of 16 mg/kg MPTP given every 2 h over a 6 h period) and given either vehicle or apocynin 250 mg/kg per day via osmotic mini-pump. TH protein content was normalized to β-III tubulin protein content (Panel A). Pictorial representation of TH and β-III tubulin bands for each treatment group (Panel B). Columns represent means and bars one SEM. *Significant difference between saline and MPTP treated mice.

A.

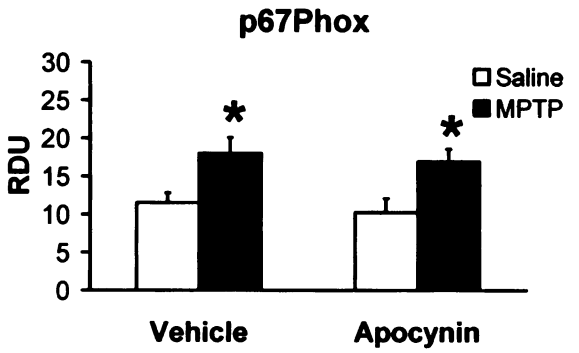

B.

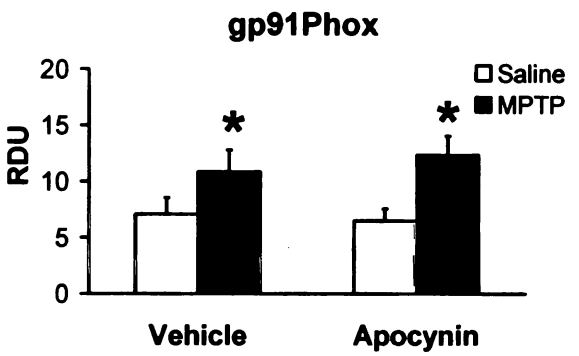

C.

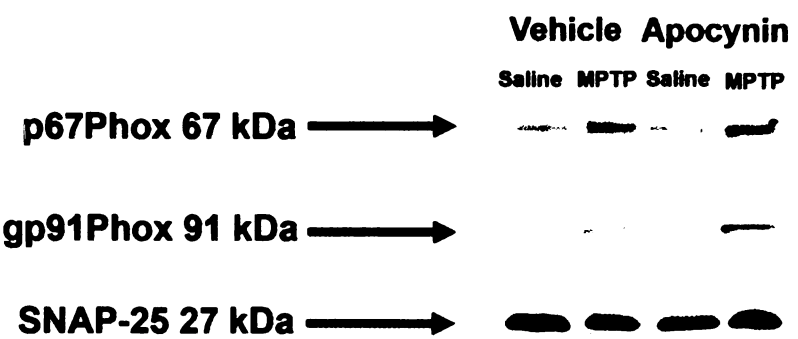

Figure 4-11. Apocynin does not reduce p67Phox translocation to the membrane or an increase in gp91Phox subunit membrane expression in the striatum observed with repeated acute MPTP treatment. Mice were treated with either saline or a repeated acute MPTP paradigm (4 injections of 16 mg/kg MPTP given every 2 h over a 6 h period) and given vehicle or apocynin 250 mg/kg per day via osmotic mini-pump. p67Phox and gp91Phox subunit expression were normalized to the membrane protein SNAP-25 and multiplied by a factor of 1000. p67phox (Panel A) and gp91Phox (Panel B) protein expression in the striatum membrane fraction. Pictorial representation of p67Phox, gp91Phox, and SNAP-25 bands in treatment group (Panel C). Columns represent means and bars one SEM. *Significant difference between saline and MPTP treated mice.

Table 4-3. Neurochemical Concentrations in the Nucleus Accumbens Following Repeated Acute MPTP and Apocynin Treatment

Nucleus Accumbens	Saline/Vehicle	MPTP/Vehicle	Saline/Apocynin	MPTP/Apocynin
DA	130.0 ± 10.5	81.1 ± 10.4 *	111.9 ± 5.7	73.0 ± 7.8 *
DOPAC	15.8 ± 1.4	9.3 ± 0.6 *	13.2 ± 1.3	10.1 ± 0.9 *
DOPAC/DA	0.12 ± 0.01	0.13 ± 0.01	0.12 ± 0.01	0.15 ± 0.02 *
5HT	11.2 ± 1.1	7.9 ± 0.9 *	12.3 ± 0.9	8.0 ± 0.9 *
5HIAA	4.7 ± 0.2	3.6 ± 0.3	4.9 ± 0.5	4.6 ± 0.5
5HIAA/5HT	0.44 ± 0.02	0.50 ± 0.05	0.41 ± 0.05	0.60 ± 0.08 *

Table 4-3. Mice were treated with saline or a repeated acute MPTP paradigm (4 injections of 16 mg/kg MPTP given i.p. every 2 h over a 6 h period) and given vehicle or apocynin 250 mg/kg per day via osmotic mini-pump. The concentrations of DA, DOPAC, 5HT, 5HIAA, and the DOPAC/DA and 5HIAA/5HT ratios were determined in the nucleus accumbens. Values are the mean ± the SEM. *Significant difference between saline and MPTP treated mice within either vehicle or apocynin treatment groups.

D. Discussion

The use of apocynin as a neuroprotective agent for NSDA neurons in the MPTP model of PD was examined due to its pharmacological property of inhibiting NADPH oxidase. NADPH oxidase is a key enzyme responsible for the production of superoxide by microglial cells (Pawate et al., 2004). Activation of NADPH oxidase is involved in the microglial mediated death of NSDA neurons due to its role in the production of reactive oxygen and nitrogen species and pro-inflammatory cytokines, and induction of microglial proliferation and migration (Pawate et al., 2004; Jekabsone et al., 2006; Mander et al., 2006). Indeed, mice lacking a functional gp91Phox subunit (the primary membrane bound subunit) are partially resistant to both MPTP and LPS induced loss of NSDA neurons (Wu et al., 2003; Qin et al., 2004). Apocynin is considered an ideal candidate for neuroprotection of NSDA neurons because its lipophilic properties allows it to cross the blood brain barrier readily and it has a high lethal dose (LD50) when 50% of animals die due to toxicity (Van den Worm et al., 2001). Apocynin also reduces oxidative stress, microglial activation, and loss of neurons seen in *in vitro* and/or *in vivo* models of stroke, amyotrophic lateral sclerosis, Alzheimer's disease, and PD, which strongly supported its potential as a neuroprotective agent (Gao et al., 2003; Jekabsone et al., 2006; Rey et al., 2006; Wang et al., 2006; Rodriguez-Pallares et al., 2007; Tang et al., 2007; Harraz et al., 2008; Tang et al., 2008).

In the present study, the pharmacokinetics of apocynin in the brain were examined to determine if apocynin crosses the blood brain barrier and to establish the length of time it was present in the brain following systemic administration. The measurement of apocynin in the brain using HPLC-EC in these studies was a novel

method in the laboratory. The results indicated that apocynin readily crosses the blood brain barrier within 2.5 min following drug administration. Surprisingly, apocynin was hardly detectable after 20 min in the brain following administration of a 100 mg/kg dose to mice. This result was unexpected since apocynin is reported to reduce superoxide production and neuronal death within the brain for a much longer period at even lower doses, but unfortunately, these studies did not measure the concentrations of apocynin within the brain (Rey et al., 2006; Wang et al., 2006). Recently a metabolite of apocynin known as diapocynin has been implicated as a more potent inhibitor of NADPH oxidase than apocynin *in vitro* (Ximenes et al., 2007). Rapid metabolism of apocynin in the brain may therefore explain why apocynin can only be measured in the brain for such a short period of time in this study. The ability of apocynin metabolites to inhibit NADPH oxidase would explain the potential reduction of superoxide production in the brain long after it was no longer measurable.

The potential time and dose dependent effects of apocynin on NSDA neuronal activity were also examined by measuring the concentrations of DA and DOPAC within the striatum. DA concentrations were not altered with apocynin treatment at any time point. DOPAC concentrations and the DOPAC/DA ratio were significantly decreased in a dose dependent manner by 2.5 min following apocynin administration. These findings could be attributed to one potential cause, that apocynin may inhibit the metabolism of DA to DOPAC by blocking MAO B activity which has not been described in the literature. This hypothesis of MAO B inhibition was tested using an *in vitro* cell free assay system measuring the catabolism of DA to DOPAL in the presence of apocynin. The results from this study reveal that apocynin does not inhibit MAO B.

The implication of MAO B inhibition in the presence of MPTP treatment is that apocynin could inhibit the metabolism of MPTP to its active metabolite MPP+. This possibility could indicate a neuroprotective property of apocynin that would be attributed to NADPH oxidase inhibition, but rather could also be due to a reduced neurotoxic effect of MPTP.

Although the half-life of apocynin is relatively short in the brain, it was decided that apocynin would be given 2 h prior to MPTP administration, since other studies which revealed a neuroprotective effect of apocynin administered the drug at least 30 min prior to neurological insult. Apocynin (100 mg/kg, i.p.) was injected twice a day 12 h apart beginning 2 days prior to the initiation of sub-chronic MPTP administration and continued up to the morning the mice were killed. MPTP treatment induced a significant and similar loss of DA in the striatum with either vehicle or apocynin treatment indicating that apocynin failed to attenuate the loss of axon terminals. Apocynin did not alter the increased activity of NSDA neurons seen with MPTP treatment, which is due to the compensation of the remaining unlesioned neurons for the loss of axon terminals (Sundstrom et al., 1987; Drolet et al., 2004). These findings contradict others that showed apocynin to be neuroprotective in a rat model of PD using the neurotoxin 6-OHDA (Rey et al., 2006).

Lack of a neuroprotective effect of apocynin in the sub-chronic MPTP model could be due to a limited amount of microglial induced loss of NSDA axonal terminals in this MPTP model. Another possibility is that apocynin (or potentially one of its active metabolites) may not be available for sufficient time to cause a significant reduction in NADPH oxidase activity and subsequent microglial mediated cell death. However, in the

present study apocynin administration blunted MPTP-induced NADPH oxidase activation of membrane bound p67Phox in the striatum suggesting that this was not the case.

The increase in p67Phox at the membrane seen with MPTP treatment though significant may still be below the threshold to observe any neuroprotective effects of apocynin. Another MPTP model, the repeated acute MPTP model was therefore employed as it induces significant microglial activation (demonstrated by increased p67Phox translocation) within 2 days following a series of 4 injections of MPTP (16 mg/kg) over a 6 h time period (Wu et al., 2002; Wu et al., 2003). Continuous delivery of apocynin using an osmotic mini-pump was used with the repeated acute MPTP model in an effort to maintain apocynin concentrations in the brain. The idea for this method of MPTP and apocynin administration was that in the presence of a more significant lesioning of NSDA neuronal terminals and microglial reaction, apocynin would be more likely to exhibit a neuroprotective effect.

Indeed, repeated acute MPTP treatment increases the amount of NADPH oxidase activity as determined by an *in vitro* NADPH oxidase activity assay using brain tissue from saline and MPTP treated mice and by an increase in membrane bound p67Phox agreeing with others (Wu et al., 2002; Wu et al., 2003). The membrane bound subunit gp91Phox (which is critical for NADPH oxidase production of superoxide) was also significantly increased with MPTP treatment as others have shown in an animal model of PD and human PD brains (Wu et al., 2003), which suggests either an upregulation of the protein or an increase in microglial number.

The repeated acute MPTP model also induces a significant decrease in DA concentrations and TH protein in the striatum of vehicle treated mice demonstrating a loss of NSDA axonal terminals. However, even with constant infusion (250 mg/kg per day), apocycnin failed to attenuate the loss of NSDA neuronal terminals as indicated by a similar loss in DA and TH protein with MPTP treatment compared to MPTP/vehicle treated mice. Similarly, membrane p67Phox was increased with repeated acute MPTP treatment, but delivery of apocynin using the osmotic mini-pump did not reduce NADPH oxidase activation with MPTP treatment.

Although MPTP clearly induced activation of NADPH oxidase it is possible that with infusion of apocynin the concentrations present in the brain at any one time were too low to inhibit the enzyme, but others have shown that at dosages much lower (apocynin 3 mg/kg per day) osmotic mini-pump delivery of apocynin inhibited NADPH oxidase mediated effects (Zhan et al., 2005). Another possibility in regard to the dosage is that there may be a narrow therapeutic window of apocynin, since this compound is reported to be neuroprotective in a stroke model at 2.5 mg/kg (but not at 3.75 mg/kg) when administered intravenously 30 min before the stroke was induced (Tang et al., 2008).

The integrity and activity of MLDA and TIDA neurons was also examined with MPTP and apocynin treatment. The findings that apocynin itself did not alter MLDA or TIDA neuronal terminal integrity or neuronal activity has not previously been noted in the literature. These results are not surprising in that apocynin injection did not alter the NSDA neurons activity following acute injection or with mini-pump administration.

Sub-chronic MPTP treatment did induce a slight decrease in DOPAC concentrations in the nucleus accumbens, but otherwise failed to alter the integrity or

activity of NSDA or MLDA neurons demonstrating that these neurons are resistant to MPTP treatment with this dosing paradigm. In contrast, repeated acute MPTP treatment induced a significant loss of MLDA axon terminals and cause increased compensatory neuronal activity in the presence of both MPTP and apocynin. Repeated acute MPTP treatment clearly leads to a more severe lesioning of dopaminergic neurons than the sub-chronic MPTP paradigm.

The integrity and activities of serotoninergic neurons terminating in the nucleus accumbens and median eminence were evaluated in the presence of apocynin, since there has not been any reports as to any potential effects or lack of apocynin on serotoninergic neurons in the central nervous system. Similar to dopaminergic neurons, apocynin did not alter serotoninergic neurons with either an acute apocynin injection or delivery by osmotic mini-pump.

MPTP treatment typically either does not effect serotoninergic neurons or only to a minimal extent in high dosing paradigms of MPTP in mice (Hallman et al., 1985; Date et al., 1990; Rousselet et al., 2003). Indeed, sub-chronic MPTP treatment did not alter serotoninergic terminals or neuronal activity in either the nucleus accumbens or median eminence. In agreement with the more severe MPTP paradigms inducing a loss of serotoninergic neuronal terminals (Rousselet et al., 2003), repeated acute MPTP treatment induced a significant loss in 5HT concentrations within the nucleus accumbens. The 5HIAA concentrations were also decreased with MPTP treatment with this paradigm, and with MPTP/apocynin treatment the 5HIAA/5HT ratio was increased indicating an increase in the activity of remaining serotoninergic neuronal terminals.

These studies are in agreement with others showing that NADPH oxidase activation increases with MPTP treatment due to indirect activation of microglia by the direct neurotoxin induced loss of NSDA neurons (Gao et al., 2003). The production of superoxide and consequent formation of other reactive oxygen species and induction of iNOS and pro-inflammatory cytokines is incredibly detrimental to NSDA neurons (Wu et al., 2002; Wu et al., 2003). The use of the NADPH oxidase inhibitor apocynin seemed therefore to be an ideal method to reduce microglial NADPH oxidase mediated death of NSDA neurons. This theory was supported by others who demonstrated that apocynin was neuroprotective in models of other diseases associated with microglial NADPH oxidase induced death of neurons (Rey et al., 2006; Wang et al., 2006). However, complications of the complex pharmacokinetics of apocynin and little knowledge about its proposed active metabolites made it challenging to choose the appropriate dosage, frequency, and method of administration of the drug. The equivalent loss of NSDA axonal terminals seen with apocynin treatment in the face of MPTP induced microglial activation, therefore indicates that apocynin was not neuroprotective in either the sub-chronic or repeated acute MPTP models of PD.

Chapter 5: The Characterization of the Neurochemical Properties and Neuromodulation of Dopaminergic Neurons in Wildtype and Cannabinoid 1 and 2 Receptor Knockout Mice

A. Introduction

Endocannabinoid (ECB) regulation of DA neuronal populations within the central nervous system is complex, and the effects of ECB on dopaminergic function vary by population. ECB regulate NSDA, MLDA, and TIDA neurons either directly or indirectly through afferent upstream neuronal systems.

ECB are involved in the regulation of NSDA neurons, but these neurons do not express CB1 receptors (Herkenham et al., 1991a). The presence of CB1 receptors throughout the basal ganglia and ECB action at both glutamatergic and GABAergic synapses within the basal ganglia leads to the complexity of ECB regulation of NSDA neurons (Figure 5-1). CB can facilitate NSDA neuronal activity by increasing the firing rate of the neurons and release of DA using a CB1 receptor mediated mechanism within the basal ganglia (French et al., 1997; Melis et al., 2000; Price et al., 2007; Morera-Herreras et al., 2008). Cannabinoids (CB) in contrast can also inhibit synthesis of DA and decrease its release from NSDA neurons (Cadogan et al., 1997; Moranta et al., 2004). The differential roles CB have in NSDA neuronal regulation are likely due to actions at different populations of CB1 receptors within the basal ganglia.

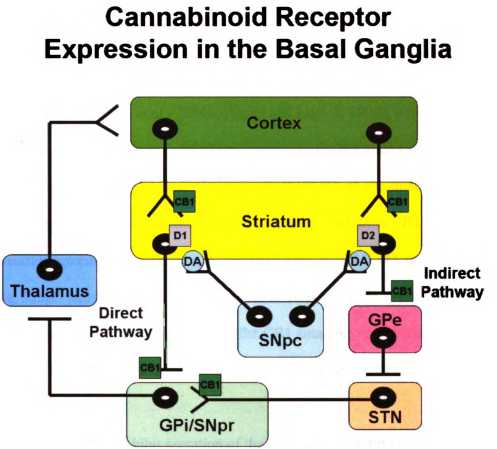

Figure 5-1. CB1 receptor expression within the basal ganglia. CB1 receptors are located on both glutamatergic (^) and GABAergic (⊥) terminals within the basal ganglia. CB1 receptors are on glutamatergic cortical neurons terminating in the striatum. Medium spiny GABAergic neurons projecting to the globus pallidus interna (GPi), substantia nigra pars reticulata (SNpr), and globus pallidus externa (GPe) have axonal terminal CB1 receptors. Glutamatergic neurons originating in the subthalamic nucleus (STN) and terminating in the GPi and SNpr also have terminal CB1 receptors. ECB action at different locations within the basal ganglia can alter the activity of the direct (excitatory) pathway or the indirect (inhibitory) pathway on the thalamus, and also indirectly effect NSDA neurons originating in the substantia nigra pars compacta (SNpc) and terminating in the striatum.

MLDA neurons comprise the dopaminergic component portion of the reward pathway and increased DA release contributes to the addictive properties of several drugs of abuse including alcohol, nicotine, and cocaine. CB increase MLDA neuronal activity and release of DA into the nucleus accumbens (French et al., 1997; Gessa et al., 1998; Cheer et al., 2004; Melis et al., 2004b; Riegel and Lupica, 2004), which is likely due to modulation of depolarization induced suppression of GABA and/or glutamate release within the ventral tegmental area. Suppression of GABA or glutamate release occurs through release of ECB from MLDA neurons that feedback onto CB1 receptors within the ventral tegmental area resulting in increased activity of MLDA neurons (Melis et al., 2004a; Riegel and Lupica, 2004). CB and ECB induction of DA release in the nucleus accumbens is reversed in the presence of the CB1 antagonist rimonabant indicating the importance of ECB in MLDA neuronal function (Gessa et al., 1998; Melis et al., 2000; Cheer et al., 2007).

TIDA neurons inhibit secretion of the hormone prolactin from the anterior pituitary by releasing DA from the median eminence into the hypophyseal-portal system that transports DA to the anterior pituitary (Sellix and Freeman, 2003). CB1 receptors are present in the arcuate nucleus and median eminence implicating ECB in the regulation of TIDA neurons (Wittmann et al., 2007). The administration of the ECB anandamide differentially regulates prolactin secretion depending on sex and estrogen levels, indicating that ECB indeed actively regulate TIDA neurons. Anandamide significantly increases the release of prolactin in ovariectomized female rats given estrogen replacement that is accompanied by a reduction in TIDA neuronal activity. Ovariectomized female rats without estrogen replacement do not have altered prolactin

levels, but do have reduced TIDA neuronal activity following anandamide treatment (Scorticati et al., 2003). In contrast, male rats demonstrate a reduction in prolactin release following anandamide treatment that corresponds to an increase in activity of TIDA neurons (Scorticati et al., 2003). The sex and hormonal differential regulation of TIDA neurons by ECB suggests that estrogen and other hormones or neurotransmitters may play a role in the effects of ECB on TIDA neurons.

ECB can also regulate serotoninergic neurons within the central nervous system. 5HT neuronal cell bodies are located in the dorsal and median raphe nuclei of the brainstem and project to regions throughout the brain including to the striatum and nucleus accumbens (Moore et al., 1978). CB1 receptors are localized on serotoninergic neurons within the raphe nuclei, and CB decrease the synthesis of 5HT in the striatum and reduce 5HT release in the nucleus accumbens and cortex via a CB1 receptor dependent mechanism (Nakazi et al., 2000; Moranta et al., 2004; Sano et al., 2008). CB can also increase 5HT neuronal activity and reduce depression which is typically associated with lower 5HT levels in the brain (Bambico et al., 2007). The differential findings concerning 5HT neuronal function indicates that (similar to dopaminergic neurons) serotoninergic neurons may be regulated by more than one CB mechanism.

The role of CB receptors in the central nervous system has mainly been studied in CB1 KO mice because of the abundant expression of CB1 receptors in the brain. CB1 KO mice have TH mRNA expression similar to WT mice within the substantia nigra and ventral tegmental area (the cell body regions of NSDA and MLDA neurons) and have similar DA concentrations in the nucleus accumbens (Steiner et al., 1999; Hungund et al., 2003). This finding suggests that CB1 KO mice have normal NSDA and MLDA

neuronal integrity compared to WT mice. CB1 KO mice also have normal expression of mRNA for the D2 receptor in the striatum suggesting that CB1 KO mice may have intact D2 receptor regulation of NSDA neurons (Gerald et al., 2006). Evaluation of the motor activity of CB1 KO mice reveals that they have normal motor coordination, but are hypoactive in an exploratory behavior test and experience increased catalepsy (Steiner et al., 1999; Zimmer et al., 1999). Catalepsy (inhibition of movement) is typically a consequence of CB treatment and thus contradicts findings in the CB1 KO mice that would be expected to have increased locomotion.

CB2 KO mice dopaminergic neuronal integrity and activity have not previously been studied to our knowledge. However, CB2 KO mice are more prone to induction of inflammation within the brain in a rodent model of multiple sclerosis (Maresz et al., 2007). Therefore since the integrity and function of dopaminergic and serotoninergic neurons in CB1/CB2 KO mice is unknown, the characterization of the integrity and activity of these neuronal populations in CB1/CB2 KO mice is of interest.

Hypothesis #1: A lack of functional CB1 and CB2 receptors will alter the integrity of NSDA, MLDA, TIDA, or serotoninergic neurons.

This hypothesis was tested by examining:

1) The concentrations of DA in the terminal regions of NSDA, MLDA, and TIDA neurons (striatum, nucleus accumbens, and median eminence, respectively) as an index of the integrity of dopaminergic neuron axon terminals.
2) The integrity of NSDA neuronal cell bodies and axon terminals by assessing the number of TH immunoreactive cells within the substantia nigra and protein content of TH in the ventral midbrain (cell bodies) and TH and DAT in the striatum (neuronal terminals).

Hypothesis #2: The activity and/or regulation of dopaminergic and serotoninergic neurons will be altered in mice lacking functional CB1 and CB2 receptors.

This hypothesis was tested by examining:

1) The activity of NSDA, MLDA, and TIDA neurons by measuring the DA metabolites DOPAC and HVA and determining the ratio of DOPAC/DA and HVA/DA.
2) Dopaminergic receptor regulation of NSDA, MLDA, and TIDA neurons by assessing long loop and short loop feedback regulation in CB1/CB2 KO mice using the concentrations of DOPAC and the ratio of DOPAC/DA as an index of DA neuronal activity.
3) The activity and axon terminal integrity of serotoninergic neurons terminating in the striatum and nucleus accumbens was examined by determining the concentrations of 5HT and its metabolite 5HIAA in the specified terminal regions.

B. Materials and Methods

Male C57BL/6 referred to as wildtype (WT) mice were obtained from (Jackson Labs) and used as controls for male CB1/CB2 receptor KO mice bred by our collaborators at Michigan State University. Mice used for all experiments were between 8-12 weeks of age and did not differ in average body weight (Figure 5-2). In neurochemical studies mice were sacrificed by decapitation and brain tissue processed for neurochemistry or Western blot analysis as previously described (Chapter 2, Section C, Euthanasia and Brain Tissue Preparation). In immunohistochemical studies hindbrains were dissected at the mid-coronal plane following decapitation, and drop fixed and stored in 4% paraformaldehyde for 7 days and placed in 20% sucrose for 24 h before being processed. TH cell counts in the substantia nigra using unbiased stereology were done as previously described (Chapter 2, Section H, Stereology TH Cell Counts).

D2 autoreceptor regulation in WT and CB1/CB2 KO mice was tested by treating mice with γ-butyrolactone (GBL) (750 mg/kg; ip) alone or in combination with quinelorane (0.1 mg/kg; ip) 1 h prior to decapitation. CB1/CB2 KO and WT mice were also treated with the D2 receptor antagonist raclopride to determine if CB1/CB2 KO mice had normal post-synaptic D2 receptor regulatory mechanisms. Mice were injected with either saline vehicle or raclopride (1 mg/kg/ip) 1 h prior to decapitation. Brains were immediately frozen on dry ice following removal of the median eminence for neurochemical analysis as previously described (Chapter 2, Section C, Preparation of Brain Tissue).

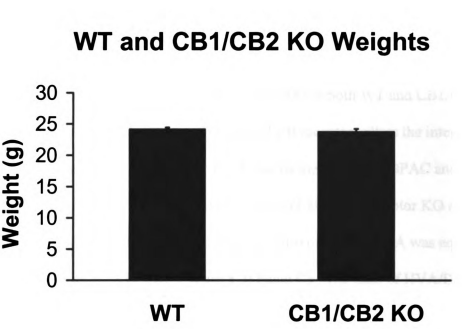

Figure 5-2. WT and CB1/CB2 KO mouse body weight (g), n=8. Columns represent means and bars one SEM.

C. Results

Comparison of NSDA neurons in WT and CB1/CB2 Receptor KO Mice

Several indices of NSDA neurons were evaluated in both WT and CB1/CB2 receptor KO mice to determine if lack of functional CB receptors alters the integrity and function of NSDA neurons. Basal levels of DA and its metabolites DOPAC and HVA in the striatum (Figures 5-3 and 5-4) were not different in CB1/CB2 receptor KO mice. The basal activity of NSDA neurons as indicated by the ratio of DOPAC/DA was equivalent in both WT and CB1/CB2 KO mice (Figure 5-3; Panel C). The ratio of HVA/DA was similar in WT and CB1/CB2 KO mice suggesting that a lack of CB receptors does not alter glial metabolism of DOPAC to HVA via the enzyme COMT (Figure 5-4; Panel B).

Vesicular DA concentrations measured within the striatum is used as an indirect index of axonal integrity and density of innervation of NSDA neurons (Drolet et al., 2004). The lack of a difference in DA concentration within the striatum was complementary to other axonal terminal markers of NSDA neurons, which included striatum protein expression of TH and DAT that were similar in WT and CB1/CB2 KO mice (Figure 5-5). Phosphorylation of serine 40 on TH protein is the key step in activation of TH synthesis of DA to replenish neurotransmitter released by NSDA neurons. No difference in phosphorylated serine 40 TH was observed by Western blot (Figure 5-5).

NSDA neuronal cell body integrity was evaluated in CB1/CB2 KO mice as determined by analysis of TH protein expression in the ventral midbrain by Western blot and the numbers of TH-immunoreactive cells within the substantia nigra. The amount of TH protein expression in the ventral midbrain and distribution of TH immunoreactive

cells within the substantia nigra was comparable in CB1/CB2 KO and WT mice (Figure 5-6). A higher powered (20 X) view of NSDA neuronal cell bodies demonstrated normal cell morphology in CB1/CB2 KO mice (Figure 5-6). Unbiased stereology cell counts of TH-immunoreactive cells within the bilateral substantia nigra demonstrated similar TH cell numbers (Figure 5-7; Panel A). Western blot analysis of ventral midbrain TH protein content (Figure 5-7; Panel B) did not differ between WT and CB1/CB2 KO mice.

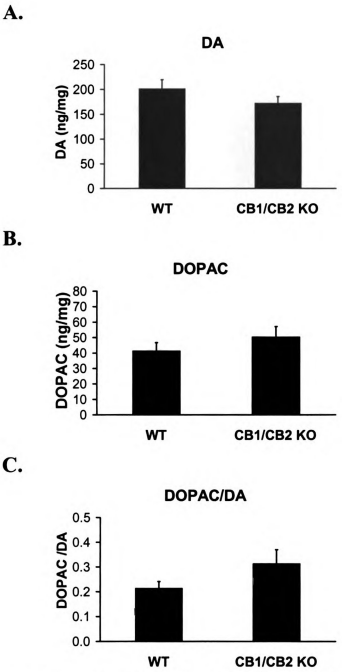

Figure 5-3. Concentrations of DA (Panel A) and DOPAC (Panel B) and the DOPAC/DA ratio (Panel C) in the striatum of male WT and CB1/CB2 KO mice, n=9-10. Columns represent means and bars one SEM.

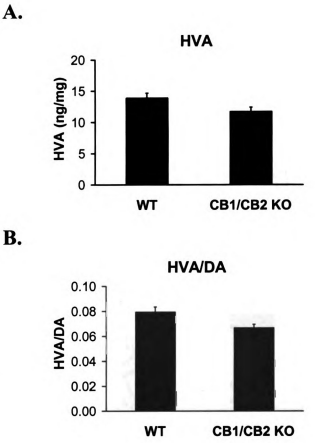

Figure 5-4. Concentrations of HVA (Panel A) and the HVA/DA ratio (Panel B) in the striatum of WT and CB1/CB2 receptor KO mice, n=7-8. Columns represent means and bars one SEM.

A.

B.

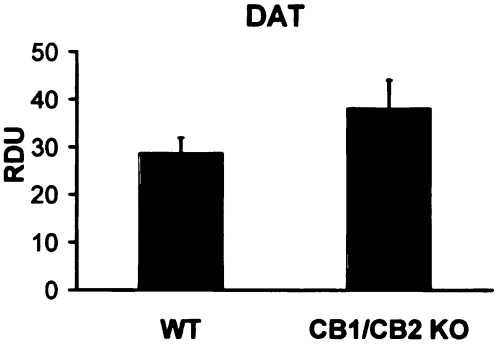

C.

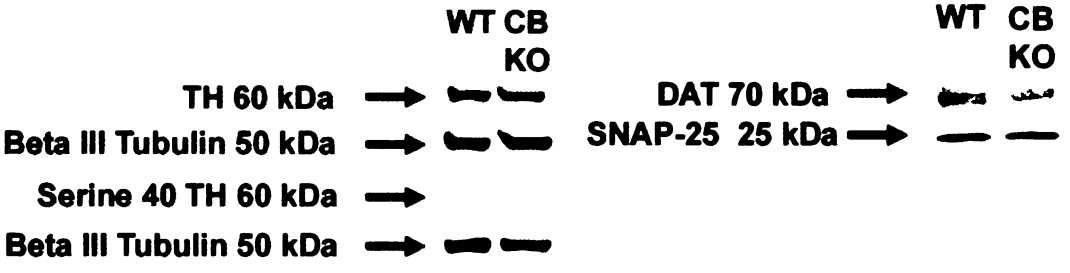

Figure 5-5. Expression of TH, phosphorylated serine 40 TH, and DAT in the striatum of WT and CB1/CB2 KO mice as determined by Western blot. TH and phosphorylated serine 40 TH protein expression normalized to β-III tubulin times a factor of 100 in the striatum (Panel A) and DAT protein expression normalized to SNAP-25 times a factor of 1000 (Panel B) and expressed as relative density units (RDU) of protein bands, n=8-11. Columns represent means and bars one SEM. Pictorial representation of TH, phosphorylated serine 40 TH, β-III tubulin, DAT, and SNAP-25 protein bands from the striatum of WT and CB1/CB2 KO mice (Panel C).

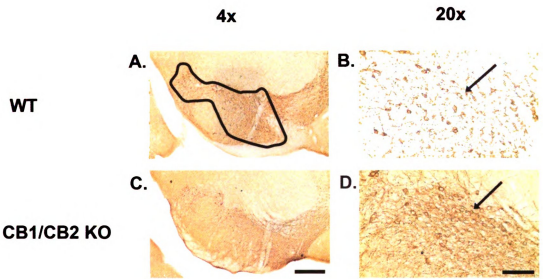

Figure 5-6. TH immunoreactive neurons within the substantia nigra of WT (Panels A & B) and CB1/CB2 KO mice (Panels C & D). Photomicrographs depict TH staining (in brown) of neurons within the substantia nigra of WT and CB1/CB2 KO mice. Black outline surrounds the area of the substantia nigra that was delineated to count TH cells within in all animals (Panel A). Arrows appearing in (Panels B & D) indicate NSDA neuronal cell bodies immunopositive for TH within the substantia nigra. Bar pictured in (Panel C) is 500 uM and bar pictured in (Panel D) is 100 uM.

A.

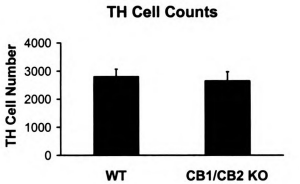

B.

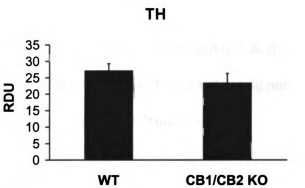

Figure 5-7. Bilateral TH cell body stereological counts in the substantia nigra and TH protein expression in the ventral midbrain of WT and CB1/CB2 KO mice. The number of TH cells within the substantia nigra was determined by counting cells using an unbiased stereology method (Panel A), n=3-7. TH protein expression in the ventral midbrain (Panel B) normalized to β-III tubulin expression multiplied by a factor of 100 and expressed as relative density units (RDU) of protein bands, n=9-10. Columns represent means and bars one SEM.

Comparison of MLDA and TIDA neurons in WT and CB1/CB2 KO Mice

The concentration of DA and one or more of its metabolites was measured in the terminal regions (nucleus accumbens and median eminence) of MLDA and TIDA neurons. The concentration of DA and its metabolites DOPAC and HVA did not differ between WT and CB1/CB2 KO mice in the nucleus accumbens (Figures 5-8; Panels A &B and 5-9; Panel A). The DOPAC/DA and HVA/DA ratios were similar in both WT and CB1/CB2 KO mice (Figures 5-8; Panel C and 5-9; Panel B).

In the median eminence the concentrations of DA and DOPAC was similar between WT and CB1/CB2 KO mice (Figure 5-10; Panels A & B). The DOPAC/DA ratio was also similar in WT and CB1/CB2 KO mice indicating normal TIDA neuronal activity in CB1/CB2 KO mice (Figure 5-10; Panel C).

A.

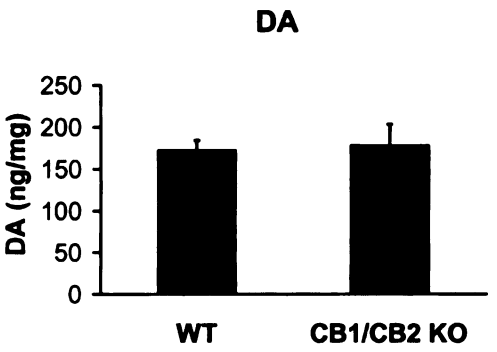

B.

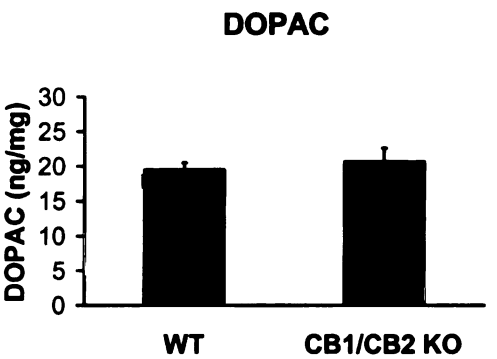

C.

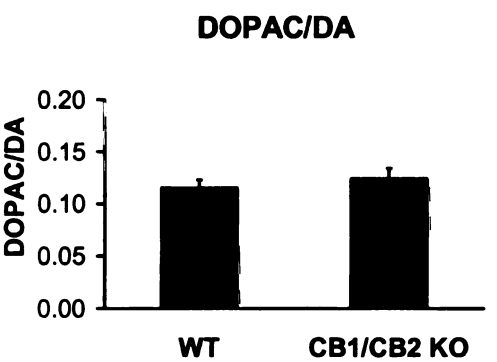

Figure 5-8. Concentrations of DA (Panel A) and DOPAC (Panel B) and the DOPAC/DA ratio (Panel C) in the nucleus accumbens of WT and CB1/CB2 KO mice. Columns represent means and bars one SEM.

A.

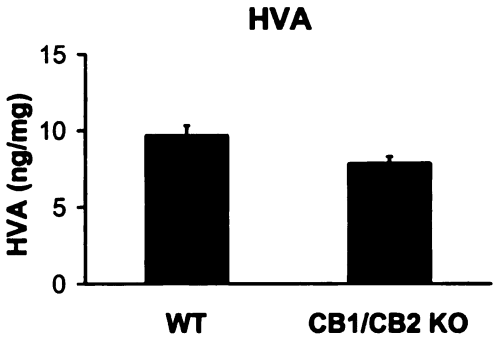

B.

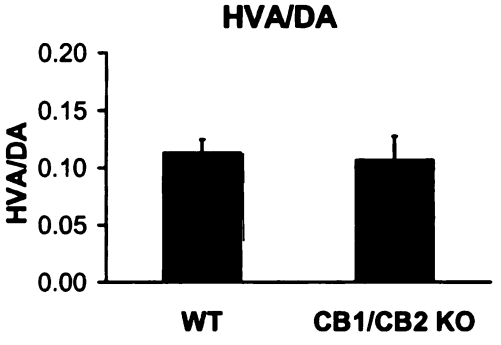

Figure 5-9. Concentrations of HVA (Panel A) and the HVA/DA ratio (Panel B) in the nucleus accumbens of WT and CB1/CB2 KO mice. Columns represent means and bars one SEM.

A.

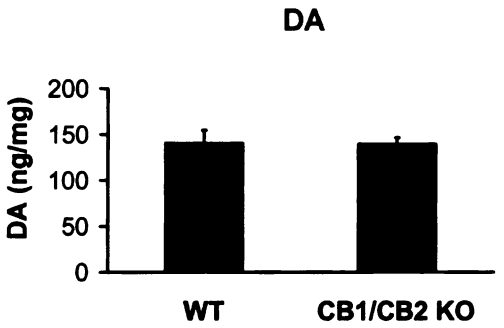

B.

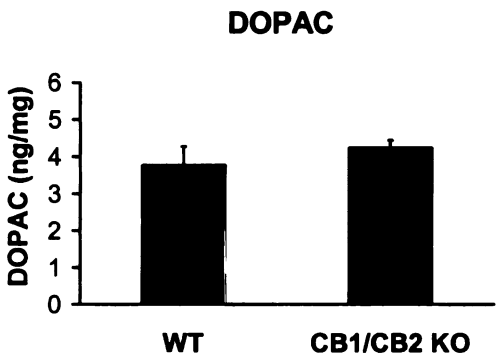

C.

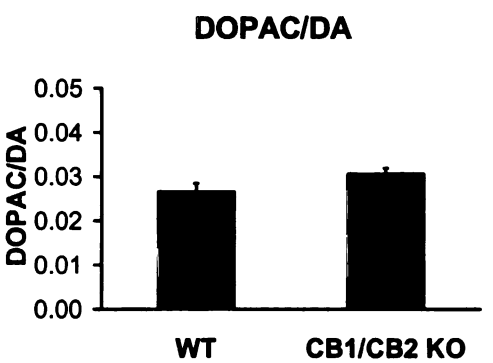

Figure 5-10. Concentrations of DA (Panel A) and DOPAC (Panel B) and the DOPAC/DA ratio (Panel C) in median eminence of WT and CB1/CB2 KO mice. Columns represent means and bars one SEM.

DA Autoreceptor Regulation of Central DA Neurons in WT and CB1/CB2 KO Mice

GBL treatment in the presence of quinelorane is commonly used as a model to study DA autoreceptor feedback regulation of dopaminergic neurons (Walters and Roth, 1976; Foreman et al., 1989; Eaton et al., 1994). Pre-synaptic D2 auto-receptor function was evaluated in CB1/CB2 KO mice by treating mice with either saline/vehicle, GBL (750 mg/kg i.p.)/vehicle, or GBL/quinelorane (0.1 mg/kg i.p.). Vehicle or quinelorane were administered 1 min prior to saline/GBL injection. In the striatum DA and DOPAC concentrations were significantly increased in WT and CB1/CB2 KO mice to an equal extent in the presence of GBL alone. These increases were significantly attenuated in the presence of quinelorane restoring DA and DOPAC concentrations almost to control levels in both WT and CB1/CB2 KO mice (Figure 5-11; Panels A & B). The DOPAC/DA ratio in WT and CB1/CB2 KO mice was not changed in the presence of GBL alone, but when quinelorane was given prior to GBL there was a similar reduction in the ratio for both WT and CB1/CB2 KO mice due to restoration of DA autoreceptor feedback inhibition (Figure 5-11; Panel C).

In vehicle treated controls the concentration of DOPAC in the nucleus accumbens was significantly higher in CB1/CB2 KO mice (Figure 5-12; Panel B). DA concentrations were not changed with GBL/vehicle or GBL/quinelorane treatment compared to saline/vehicle treated WT or CB1/CB2 KO mice. DOPAC concentrations following GBL/vehicle treatment were not changed in WT mice, but were significantly lower in CB1/CB2 KO mice due to higher DOPAC concentrations in saline/vehicle CB1/CB2 KO mice. Both WT and CB2/CB2 KO mice treated with GBL/quinelorane had significantly lower DOPAC concentrations within the nucleus accumbens compared

to either saline/vehicle or GBL/vehicle treated mice. The DOPAC/DA ratio within the nucleus accumbens was significantly decreased in both WT and CB1/CB2 KO mice in the presence of either GBL/vehicle or GBL/quinelorane. However, the decrease with GBL/quinelorane treatment was more pronounced than with GBL alone (Figure 5-12; Panel C).

As shown in Figure 5-13 (Panels A & B), GBL treatment alone failed to alter the concentrations of DA or DOPAC in the median eminence of WT or CB1/CB2 KO mice. DA and DOPAC concentrations were higher in CB1/CB2 KO mice compared to WT mice. The DOPAC/DA ratio was not different among any of the treatment groups in WT or CB1/CB2 KO mice (Figure 5-13; Panel C).

A.

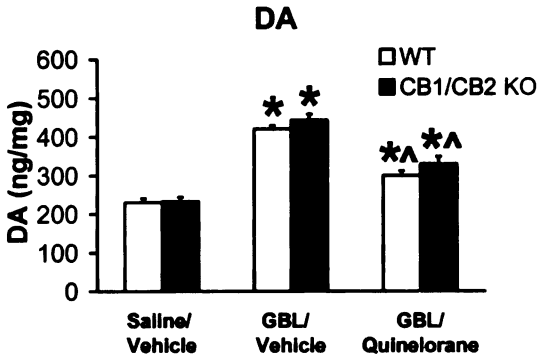

B.

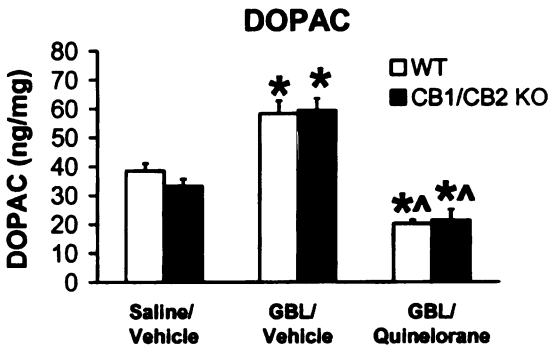

C.

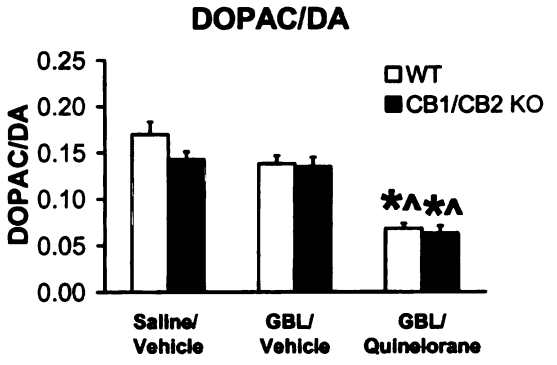

Figure 5-11. D2 autoreceptor regulation in the striatum of WT and CB1/CB2 KO mice. Concentrations of DA (Panel A), DOPAC (Panel B), and the DOPAC/DA (Panel C) in WT and CB1/CB2 KO mice given saline/vehicle, GBL (750 mg/kg)/vehicle, or GBL/quinelorane (0.1 mg/kg) 1 h prior to decapitation, n=7-8. Columns represent means and bars one SEM. *Saline/vehicle treated mice are significantly different from GBL/vehicle or GBL/quinelorane treated mice. ^GBL/quinelorane mice are significantly different from GBL/vehicle treated mice $p \leq 0.05$.

A.

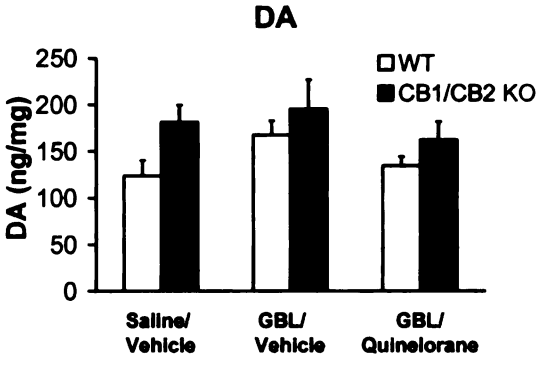

B.

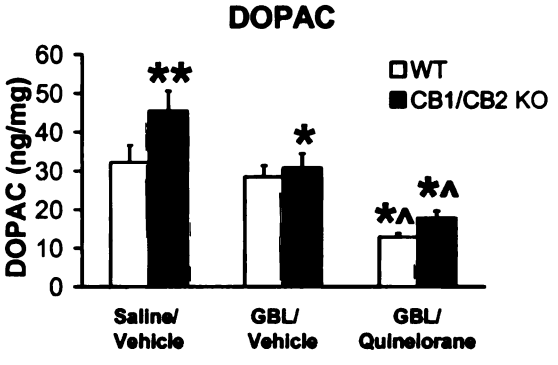

C.

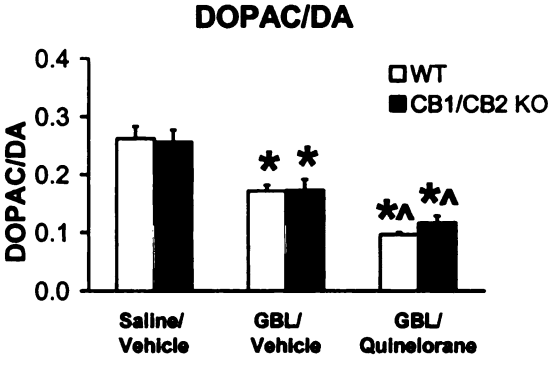

Figure 5-12. D2 autoreceptor regulation in the nucleus accumbens of WT and CB1/CB2 KO mice. Concentrations of DA (Panel A), DOPAC (Panel B), and the DOPAC/DA ratio (Panel C) in WT and CB1/CB2 KO mice given saline/vehicle, GBL (750 mg/kg)/vehicle, or GBL/quinelorane (0.1 mg/kg) 1 h prior to decapitation, n=6-8. Columns represent means and bars one SEM. *Significant difference between saline/vehicle and treatment groups within either WT or CB1/CB2 KO. ^ Significant difference between GBL/vehicle and GBL/quinelorane groups for either WT or CB1/CB2 KO mice. *Significant difference between WT and CB1/CB2 KO mice within a treatment group $p \leq 0.05$.

A.

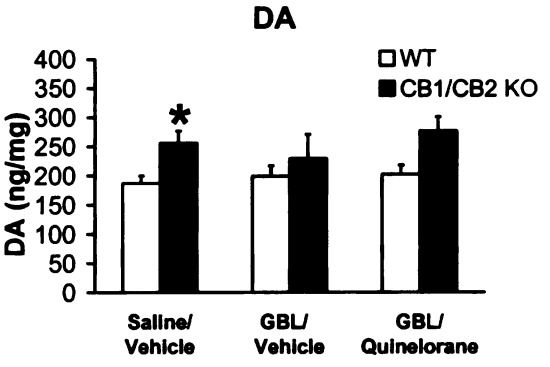

B.

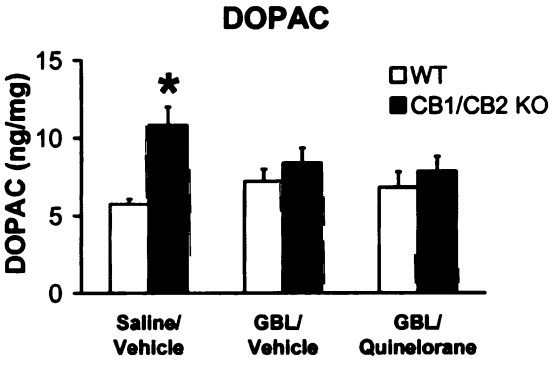

C.

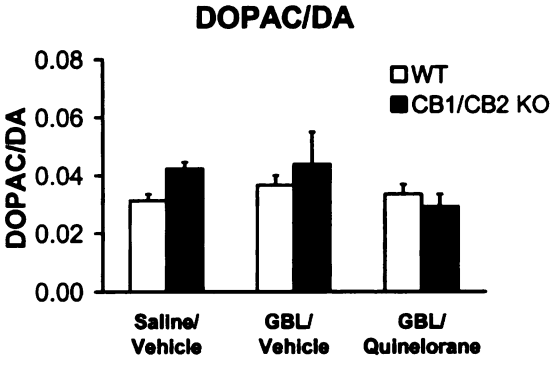

Figure 5-13. D2 autoreceptor regulation in the median eminence of WT and CB1/CB2 KO mice. Concentrations of DA (Panel A), DOPAC (Panel B), and the DOPAC/DA (Panel C) in WT and CB1/CB2 KO mice given saline/vehicle, GBL (750 mg/kg)/vehicle, or GBL/quinelorane (0.1 mg/kg) 1 h prior to decapitation, n=7-8. Columns represent means and bars one SEM. *Significant difference between WT and CB1/CB2 KO mice, $p \leq 0.05$.

DA Receptor Regulation of DA Neuronal Activity in CB1/CB2 Receptor KO Mice

The stimulatory effects of the D2 receptor antagonist raclopride (which blocks both pre- and post-synaptic D2 receptors) was observed by a significant increase in DOPAC concentrations within the striatum of WT and CB1/CB2 KO mice (Figure 5-14; Panel A). DA concentrations in the striatum were significantly decreased to a minimal, but similar extent with raclopride treatment in both WT and CB1/CB2 KO mice (Figure 5-14; Panel B). WT and CB1/CB2 KO mice also had a similar significant increase in the DOPAC/DA ratio (Figure 5-14; Panel C).

The concentrations of DOPAC and the DOPAC/DA ratio within the nucleus accumbens were also significantly increased to a similar extent in both WT and CB1/CB2 KO mice following raclopride treatment (Figure 5-15; Panels A & C). DA concentrations were not changed by raclopride treatment in WT or CB1/CB2 KO mice (Figure 5-15; Panel B).

DOPAC concentrations within the median eminence were decreased in WT mice, but remained unchanged in CB1/CB2 KO mice (Figure 5-16; Panel A). DA concentrations or the ratio of DOPAC/DA were not altered following raclopride in the median eminence of either WT or CB1/CB2 KO (Figure 5-16; Panels B & C).

A.

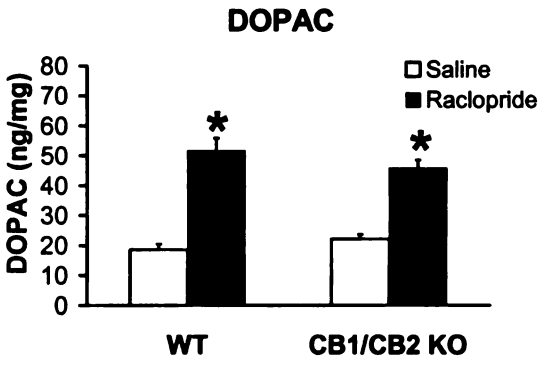

B.

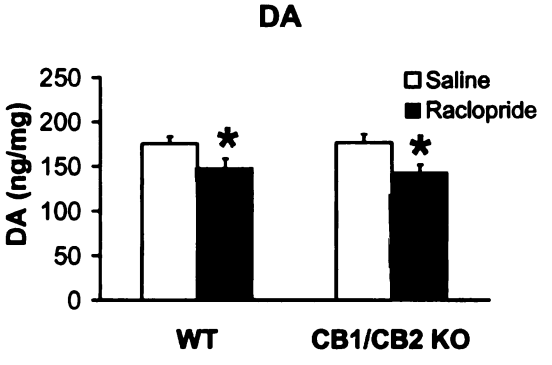

C.

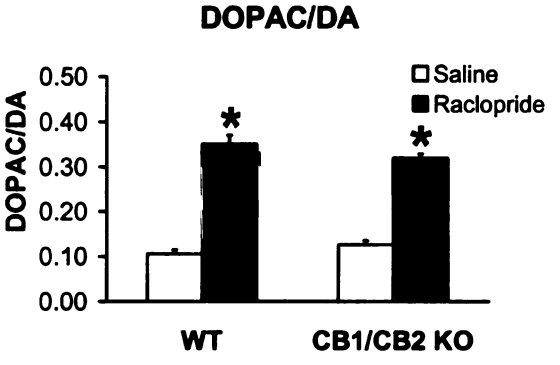

Figure 5-14. DA receptor regulation in the striatum of WT and CB1/CB2 KO mice. Concentrations of DOPAC (Panel A) and DA (Panel B) and the DOPAC/DA ratio (Panel C) in the striatum of WT and CB1/CB2 KO mice given saline or the D2 receptor antagonist raclopride (1 mg/kg) 1 h prior to decapitation, n=7-8. Columns represent means and bars one SEM. *Saline treated mice are significantly different from raclopride treated mice, $p \leq 0.05$.

A.

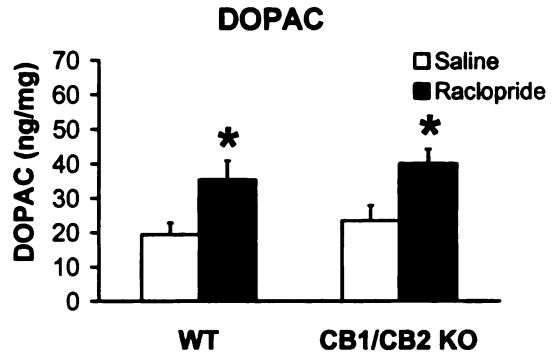

B.

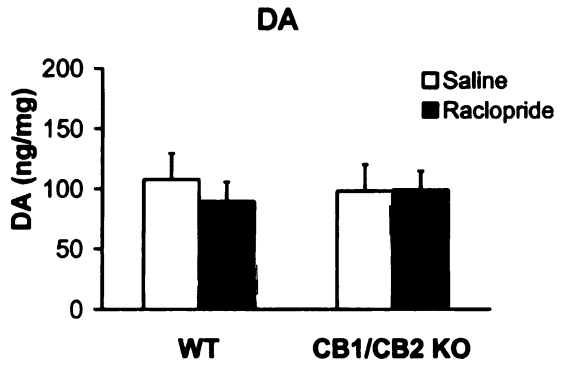

C.

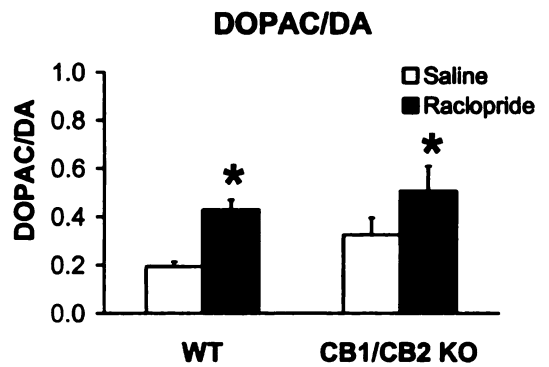

Figure 5-15. DA receptor regulation in the nucleus accumbens of WT and CB1/CB2 KO mice. Concentrations of DOPAC (Panel A) and DA (Panel B) and the DOPAC/DA ratio (Panel C) in the nucleus accumbens of WT and CB1/CB2 KO mice given saline or the D2 receptor antagonist raclopride (1 mg/kg) 1 h prior to decapitation, n=7-8. Columns represent means and bars one SEM. *Saline treated mice are significantly different from raclopride treated mice, $p \leq 0.05$.

A.

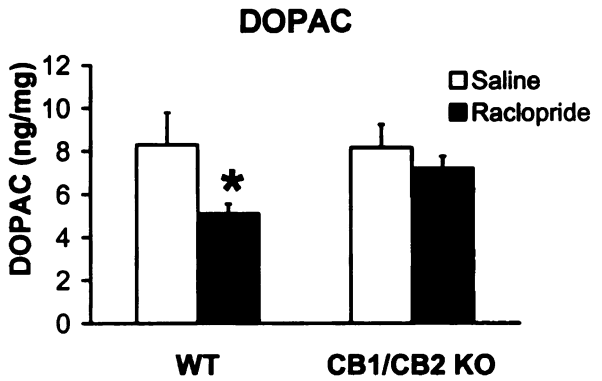

B.

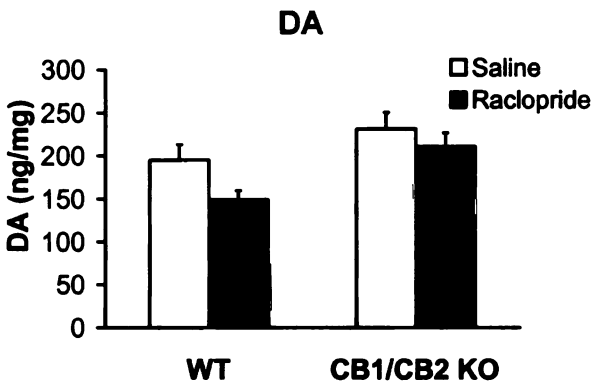

C.

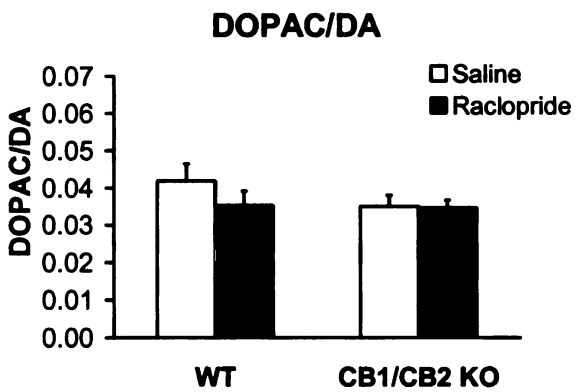

Figure 5-16. DA receptor regulation in the median eminence of WT and CB1/CB2 KO mice. Concentrations of DOPAC (Panel A) and DA (Panel B) and the DOPAC/DA ratio (Panel C) in the median eminence of WT and CB1/CB2 KO mice given saline or the D2 receptor antagonist raclopride (1 mg/kg) 1 h prior to decapitation, n=7-8. Columns represent means and bars one SEM. *Saline treated mice are significantly different from raclopride treated mice, $p \leq 0.05$.

Comparison of Serotoninergic Neuronal Function in WT and CB1/CB2 KO Mice

5HT neurons of the raphe nuclei project axons that terminate in various regions of the forebrain including both the striatum and nucleus accumbens (Moore et al., 1978). 5HT can facilitate the release of DA in both the striatum and nucleus accumbens and has been implicated in the regulation of NSDA and MLDA neurons that innervate these regions (Gudelsky and Nash, 1996; Zangen et al., 2001). 5HT concentrations are commonly used as an index of serotoninergic neuronal terminal integrity, and the ratio of the 5HT metabolite 5HIAA to 5HT (5HIAA/5HT ratio) is considered to be the "gold standard" for neurochemical estimation of serotoninergic neuronal activity (Tian et al., 1992; Darmani et al., 2003). In the present study, 5HT concentrations were compared in the striatum and nucleus accumbens of WT and CB1/CB2 KO mice. In both brain regions CB1/CB2 KO mice had similar basal levels of 5HT compared to WT mice (Figures 5-17; Panel A & 5-18; Panel A). The 5HT metabolite 5HIAA was also measured in both brain regions and was found not to be different in CB1/CB2 KO mice (Figures 5-17; Panel B & 5-18; Panel B). The 5HIAA/5HT ratio was similar in both WT and CB1/CB2 KO mice suggesting that the lack of CB1 and CB2 receptors does not alter serotoninergic neuronal activity in these brain regions (Figure 5-17; Panel C & 5-18; Panel C).

A.

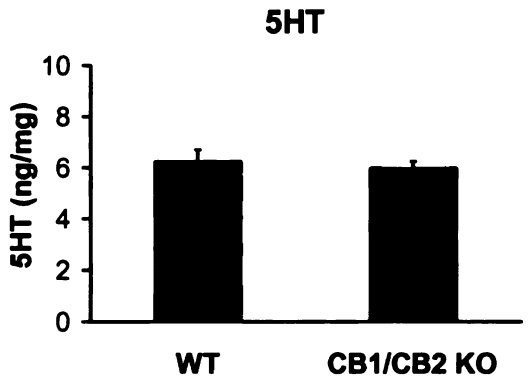

B.

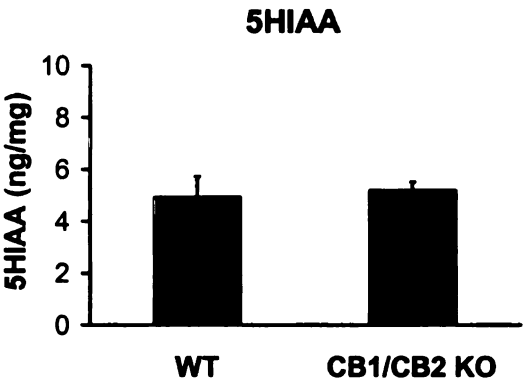

C.

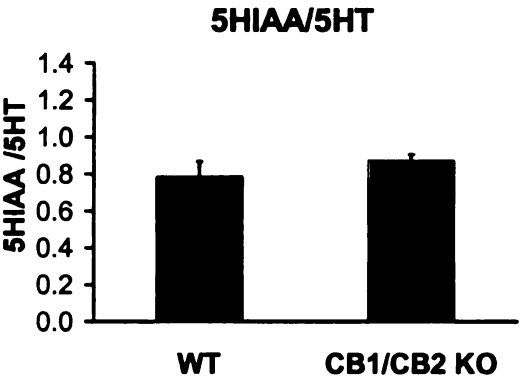

Figure 5-17. Concentrations of 5HT (Panel A), 5HIAA (Panel B), and the 5HIAA/5HT ratio (Panel C) in the striatum of WT and CB1/CB2 KO mice, n=8-10. Columns represent means and bars one SEM.

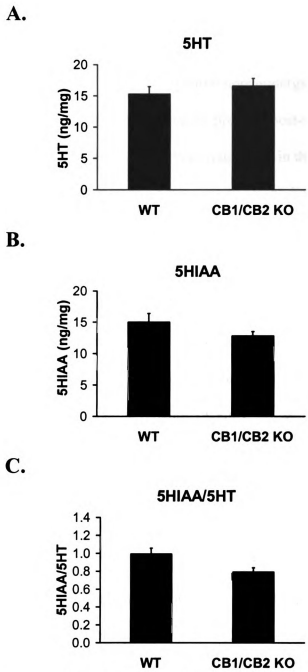

Figure 5-18. Concentrations of 5HT (Panel A), 5HIAA (Panel B), and the 5HIAA/5HT ratio (Panel C) in the nucleus accumbens of WT and CB1/CB2 KO mice, n=8-10. Columns represent means and bars one SEM.

D. Discussion

The purpose of these studies was to determine if the lack of functional CB1 and CB2 receptors in knockout mice affected central dopaminergic neuronal integrity and/or activity, and the regulation of these neurons by pre- and post-synaptic DA receptor mediated mechanisms. Since ECB have been implicated in their regulation three different populations of dopaminergic neurons with cell bodies residing in either the mesencephalon or diencephalon were studied. NSDA neurons originating in the SNpc of the mesencephalon are regulated by ECB indirectly via ECB action at CB1 receptors (Narushima et al., 2006; Morera-Herreras et al., 2008). MLDA neurons originating in the VTA of the mesencephalon are regulated by GABAergic and glutamatergic neurons possessing CB1 receptors. MLDA neuronal production of ECB inhibits pre-synaptic neurons thus altering dopaminergic function (Melis et al., 2004b; Riegel and Lupica, 2004). TIDA neuronal activity is differentially regulated by CB depending on the animals sex and estrogen levels at the time of CB administration, and is reflected by alteration in prolactin concentrations (Scorticati et al., 2003). The results from the present investigation of NSDA, MLDA, TIDA, and serotoninergic neuronal integrity and activities in CB1/CB2 KO mice has demonstrated normal structure and functionality, and DA receptor mediated regulation of these neuronal populations compared to WT mice.

Determining Dopaminergic Neuronal Integrity in CB1/ CB2 KO Mice

The integrity of dopaminergic neurons was determined by comparing the concentrations of DA in the striatum, nucleus accumbens, and median eminence of WT and CB1/CB2 KO mice. DA concentrations in the terminal regions of dopaminergic

neurons reflects the amount of DA in synaptic vesicular stores, thus a change in striatum DA concentrations could indicate a change in terminal integrity (Drolet et al., 2004). The concentrations of DA measured in the striatum, nucleus accumbens and median eminence were not different between WT and CB1/CB2 KO mice consistent with normal dopaminergic terminal integrity of all three neuronal populations examined. CB1 KO mice are known to have extracellular DA concentrations in the nucleus accumbens comparable to WT mice (Hungund et al., 2003; Soria et al., 2005), which corroborates the lack of difference in DA concentrations within the nucleus accumbens of WT and CB1/CB2 KO mice.

The protein concentration of TH and DAT in the striatum can also be used as indices of NSDA neuronal terminal integrity (Tillerson et al., 2002; Jakowec et al., 2004). TH and DAT are expressed in the axonal terminals of NSDA neurons and neurotoxin lesioning of these terminals significantly decreases the content of both proteins within the striatum (Storch et al., 2004). TH and DAT can therefore be considered reliable indicators of NSDA neuronal integrity. CB1/CB2 KO mice had similar protein content of TH and DAT compared to WT mice, correlating with similar DA concentrations within the striatum of WT and CB1/CB2 KO mice. Taken together these results reveal that CB1/CB2 KO mice have normal integrity of NSDA axon terminals.

The effects of CB on DA uptake by DAT have demonstrated that CB can inhibit DAT activity (Steffens and Feuerstein, 2004; Price et al., 2007). The treatment with either a CB or a CB1 receptor antagonist (AM251) reduced DA uptake by DAT in both *in vitro* and *in vivo* settings. This would suggest that CB reduction in DAT uptake of DA is not due to a CB1 receptor mechanism, but rather a non-CB receptor mechanism (Price et

al., 2007). These findings support that the lack of differential DAT expression in the striatum of CB1/CB2 KO mice is not surprising.

NSDA neuronal cell bodies are located within the substantia nigra and are immunoreactive for TH. Immunohistochemistry quantitative analysis of cells with TH protein within the substantia nigra can therefore be used to identify and determine the number of NSDA neurons. The numbers of TH immunoreactive in the substantia nigra of WT mice were lower than those reported previously possibly due to light staining (Liberatore et al., 1999). CB1 KO mice have typical mRNA expression of TH in the substantia nigra (Steiner et al., 1999), which supports the findings that CB1/CB2 KO mice have a similar number of TH neurons with the substantia nigra compared to WT mice, and protein content of TH within the ventral midbrain. Although the number of MLDA and TIDA neuronal cell bodies were not determined in the present study, it is reasonable to presume that since DA concentrations were not different in either neuronal axon terminal region, CB1/CB2 KO mice would have similar numbers of TH cells in the ventral tegmental area and arcuate nucleus compared to WT mice. CB1 KO mice also have similar TH mRNA levels in the ventral tegmental area further supporting that CB1/CB2 KO mice likely have a normal number of MLDA neurons (Steiner et al., 1999).

The activity of dopaminergic neurons was determined in the present study by measuring the DA metabolites DOPAC and HVA, and the ratio of either metabolite to DA. The DOPAC/DA or HVA/DA ratio is reflective of DA release, reuptake, and metabolism (Lookingland, 2005). A change in the concentrations of DOPAC, HVA, or DA within a dopaminergic neuronal terminal region can increase or decrease the

DOPAC/DA or HVA/DA ratio indicating an alteration in the synthesis, release, reuptake, and/or metabolism of DA at the neuronal terminal (Moore and Wuerthele, 1979).

CB can increase dopaminergic activity by acting at CB1 receptors in the brain (French et al., 1997; Price et al., 2007). CB1 receptor antagonist treatment in the presence of a CB agonist typically inhibits CB induced effects on dopaminergic neurons (Souilhac et al., 1995; Cadogan et al., 1997; Diana et al., 1998; Gessa et al., 1998; Melis et al., 2000; Pistis et al., 2002; Morera-Herreras et al., 2008), but by itself CB1 antagonist treatment does not alter dopaminergic function (Gueudet et al., 1995; Cadogan et al., 1997; Giuffrida et al., 1999; Ferrer et al., 2007). Thus, the basal activity of DA neurons is not tonically regulated by ECB. The finding that CB1/CB2 KO mice have normal activity of dopaminergic neurons is consistent with this conclusion. Some evidence though indicates that lack of functional CB receptors could reduce overall activity of dopaminergic neurons since chronic administration of the CB1 receptor antagonist rimonabant reduces activity of NSDA neurons (Gueudet et al., 1995). Nonetheless, the results from this study support the hypothesis that CB1/CB2 KO mice have normal NSDA, MLDA, and TIDA neuronal activity, since CB1/CB2 KO and WT mice had similar DOPAC and/or HVA concentrations (and DOPAC/DA and/or HVA/DA ratios) in the striatum, nucleus accumbens, and median eminence.

Since there is a coupling between the synthesis and release of NSDA neurons, the relative activity of these neurons can also be determined by measuring the amount of TH protein with phosphorylated amino acid serine 40 (Bobrovskaya et al., 2007). Serine 40 is the primary serine residue on TH responsible for maximal TH activity (Dunkley et al., 2004). Differences in serine 40 phosphorylated TH in the striatum of CB1/CB2 KO mice

could be indicative of differences in activity of NSDA neurons because alteration in TH activation can affect the synthesis of DA. Protein content of serine 40 phosphorylated TH was similar in the striatum of WT and CB1/CB2 KO mice suggesting that CB1/CB2 KO mice have comparable TH activity, contributing to a similar basal NSDA neuronal activity.

Determining the DA Receptor Mediated Regulation of Dopaminergic Neurons in CB1/CB2 KO Mice

Although CB1/CB2 KO mice had normal NSDA neuronal cell number, axon terminal integrity, and basal activity, they could still have altered DA receptor regulation mechanisms. NSDA, MLDA, and TIDA neurons have one or more forms of feedback inhibition including pre-synaptic short loop, post-synaptic long loop, and end product inhibition as previously described (Chapter 1, Section G, Regulation of DA Synthesis in Central Dopaminergic Neurons).

Pre-synaptic short loop D2 autoreceptor function can be determined by blocking DA impulse release in the presence or absence of a D2 receptor agonist. GBL is a precursor to γ-hydroxybutyrate (GHB) a $GABA_B$ agonist that can block DA impulse release from dopaminergic neurons (Walters and Roth, 1976; Demarest and Moore, 1979; Nowycky and Roth, 1979; Lookingland et al., 1987b). Inhibition of DA release following GBL administration removes feedback inhibition of DA synthesis by D2 autoreceptors on the pre-synaptic axon terminal. A lack of D2 autoreceptor stimulation removes inhibition of TH, increases DA synthesis and vesicular and non-vesicular DA content at the pre-synaptic axon terminal. DA short loop feedback can be maintained in

the presence of a D2 receptor agonist such as quinelorane. GBL treatment in the presence of quinelorane is used commonly as a model to study short loop feedback of dopaminergic neurons (Walters and Roth, 1976; Foreman et al., 1989; Eaton et al., 1994).

D2 autoreceptor regulation of NSDA, MLDA, and TIDA neurons was examined in CB1/CB2 KO mice using the GBL/quinelorane model. DA and DOPAC concentrations were increased in the striatum of WT and CB1/CB2 KO mice treated with GBL and this was attenuated or prevented by quinelorane treatment. The DOPAC/DA ratio was similar in WT and CB1/CB2 KO mice given GBL reflecting increased synthesis and metabolism of DA following loss of autoreceptor inhibition of DA synthesis. Quinelorane reduced this by maintaining autoreceptor inhibition of TH thereby decreasing synthesis and metabolism of DA.

The maintenance of short loop D2 autoreceptor regulation in the striatum of CB1/CB2 KO mice is not surprising since CB1 receptors are not found on NSDA axon terminals (Julian et al., 2003), and thus it is unlikely that these receptors modulate D2 pre-synaptic receptor regulation of DA synthesis. On the other hand, CB1 receptors are found along with post-synaptic D2 receptors on striatum medium spiny neurons (Julian et al., 2003). CB1 and D2 receptors are known to form heterodimers on medium spiny striatum neurons, and CB likely act as a mechanism to regulate D2 receptor induced motor activity, since the CB decrease D2 receptor agonist mediated movement is enhanced with the CB1 antagonist rimonabant (Giuffrida et al., 1999; Ferrer et al., 2007; Marcellino et al., 2008). Based on this information post-synaptic D2 receptor long loop feedback would be more likely to be affected by a lack of CB1 receptors.

D2 autoreceptor regulation of MLDA neurons was also evaluated in WT and CB1/CB2 KO mice. MLDA neurons maintain short loop D2 feedback inhibition which is even more sensitive to changes in DA concentration as compared to NSDA neurons (Demarest et al., 1983). Surprisingly, DA concentrations were not changed with GBL treatment in the nucleus accumbens as expected in either WT or CB1/CB2 KO mice. DOPAC concentrations significantly decreased with GBL/quinelorane treatment in both WT and CB1/CB2 KO mice demonstrating that quinelorane was indeed acting at D2 autoreceptors to suppress MLDA neurons terminating in the nucleus accumbens. The discrepancy as to why DA concentrations were not increased with GBL treatment may be attributed to slightly greater variability in DA concentrations in the nucleus accumbens in this study.

The DOPAC/DA ratio was significantly decreased with GBL treatment in both WT and CB1/CB2 KO mice. These data indicate that MLDA neurons (which are more sensitive to D2 autoreceptor regulation) (Demarest et al., 1983); are likely reducing the activity in response to blockade of DA impulse release. Quinelorane reduced the DOPAC/DA ratio in the nucleus accumbens to a greater extent than GBL alone demonstrating that MLDA neurons indeed respond to short loop feedback inhibition as previously reported (Demarest et al., 1983). Lack of functional CB1 and CB2 receptors in KO mice did not alter short loop feedback inhibition of MLDA neurons which would be expected as MLDA neurons to not possess CB1 receptors (Herkenham et al., 1991b; Melis et al., 2004a; Riegel and Lupica, 2004).

TIDA neurons lack pre-synaptic D2 receptors and thus are not regulated by D2 receptor mediated mechanisms (Demarest and Moore, 1979; Lookingland, 2005; Pappas

et al., 2008). In agreement, in the present study there was no change in DA, DOPAC, or the DOPAC/DA ratio within the median eminence of WT and CB1/CB2 KO mice with either GBL or GBL/quinelorane treatment. In this study CB1/CB2 KO mice had significantly higher DA and DOPAC concentrations in the median eminence, which was not repeated in subsequent studies (see Chapter 6) suggesting a spurious result. The absence of CB1 and CB2 receptors does not change the inability of GBL to alter DOPAC/DA ratio in the median eminence indicating that TIDA neurons in knockout mice also lack autoreceptor regulation.

The present observations demonstrate that CB1/CB2 KO mice have normal D2 autoreceptor regulation in the striatum and nucleus accumbens, but do not address whether CB1/CB2 KO mice have post-synaptic D2 receptor long loop feedback regulatory mechanisms. Post-synaptic long loop feedback patency can be determined by treating CB1/CB2 KO mice with the D2 receptor antagonist raclopride. Raclopride inhibits both pre-synaptic and post-synaptic D2 receptors (Ogren et al., 1986; Eaton et al., 1992; Eaton et al., 1994), but since CB1/CB2 KO mice have normal D2 autoreceptor function, any differential effects seen in CB1/CB2 KO mice following raclopride treatment could be linked to changes in post-synaptic D2 receptor regulatory mechanisms.

NSDA and MLDA neurons are both regulated by post-synaptic long loop feedback whereas TIDA neurons are not (Eaton et al., 1992; Eaton et al., 1994; Pappas et al., 2008). Possible differences in D2 receptor regulation in CB1/CB2 KO mice would most likely be seen in post-synaptic D2 receptor long loop feedback, since D2 receptors are localized in the striatum on medium spiny neurons that express CB1 receptors

(Martin et al., 2007). The inhibitory role CB play in dopaminergic induced activity in the striatum (Giuffrida et al., 1999) would support the idea that a lack of CB1 receptors would affect D2 receptor regulation of NSDA neurons.

Conflicting evidence suggests that the expression and activity of D2 receptors in the striatum of CB1/CB2 KO mice may or may not be normal since the D2 receptor is reported to be upregulated in one CB1 KO mouse line. However, the mRNA expression for the D2 receptor is similar to WT mice in the line of CB1 KO mice used to create the CB1/CB2 KO mice used in these studies (Houchi et al., 2005; Gerald et al., 2006). Like WT controls treatment of CB1/CB2 KO mice with raclopride led to a significant reduction in DA concentrations, and an increase in DOPAC concentrations and the DOPAC/DA ratio in the striatum all due to increased release, reuptake, and metabolism of DA. These results indicate that a lack of CB1 and CB2 receptors does not alter long loop post-synaptic D2 receptor feedback in the striatum of CB1/CB2 KO mice.

MLDA neurons are also regulated by D2 receptor mediated post-synaptic long loop feedback mechanisms (Eaton et al., 1992; Pappas et al., 2008). The nucleus accumbens contains neurons with co-localized CB1 and D2 receptors indicating a possible post-synaptic regulatory role of CB in D2 receptor long loop regulation of MLDA neurons (Pickel et al., 2006). The interaction of D2 and CB1 receptors could either augment or reduce D2 receptor long loop feedback. However, in the present study CB1/CB2 KO mice show a similar increase in DOPAC concentrations in the nucleus accumbens with raclopride treatment and a resulting increase in the DOPAC/DA ratio compared to WT mice. These results indicate that MLDA neurons in CB1/CB2 KO mice

are normally regulated by D2 post-synaptic receptors, and that a lack of functional CB1 receptors does not affect long loop feedback onto MLDA neurons.

TIDA neurons lack post-synaptic D2 receptor regulation and typically do not exhibit any changes in DA, DOPAC, or the DOPAC/DA ratio following pharmacological blockade of D2 receptors (Moore and Wuerthele, 1979; Berry and Gudelsky, 1991; Pappas et al., 2008). Indeed, both WT and CB1/CB2 KO mice did not have a change in DOPAC or DA concentrations or the DOPAC/DA ratio in the median eminence following raclopride treatment, indicating a typical lack of post-synaptic long loop feedback inhibition of TIDA neurons.

Serotoninergic Neuronal Integrity and Activity in CB1/CB2 KO and WT Mice

CB are also involved in the regulation of serotoninergic neurons and like dopaminergic neurons are influenced by CB through more than one mechanism and results in the differential roles CB have on serotoninergic neuronal activity (Darmani et al., 2003; Bambico et al., 2007). In the present study, the integrity and activity of serotoninergic neurons terminating in the striatum and nucleus accumbens of WT and CB1/CB2 mice were examined by measuring the concentrations of 5HT and 5HIAA in these regions. Neither neurochemical was different between WT and CB1/CB2 KO mice in the striatum and nucleus accumbens. These results are in agreement with a lack of a role of ECB in the regulation of 5HT neurons terminating in the striatum of another line of CB1 KO mice (Thiemann et al., 2007). CB are reported to alter the proper development of serotoninergic neurons within the brain (Molina-Holgado et al., 1996; Molina-Holgado et al., 1997), but the lack of a difference in concentrations of 5HT and

5HIAA in the striatum and nucleus accumbens of CB1/CB2 KO mice would suggest that CB1/CB2 KO have normal serotoninergic neuronal development.

The activity of serotoninergic neurons terminating in the striatum and nucleus accumbens was evaluated by determining the 5HIAA/5HT ratio in each brain region. CB are reported to decrease the synthesis of 5HT in the striatum and reduce the release in the nucleus accumbens and cortex (Nakazi et al., 2000; Moranta et al., 2004; Sano et al., 2008), and inhibition of CB1 receptors increases 5HT and 5HIAA concentrations in the frontal cortex (Darmani et al., 2003; Tzavara et al., 2003). These effects on serotoninergic neurons may be mediated by 5HT induced ECB release and feedback inhibition on pre-synaptic CB1 receptors (Best and Regehr, 2008). In contrast to these findings CB can also increase 5HT neuronal activity (Bambico et al., 2007). The 5HIAA/5HT ratios in the striatum and nucleus accumbens in CB1/CB2 KO mice were similar to WT mice indicating no change in the activity of serotoninergic neurons in CB1/CB2 KO mice. In contrast, pharmacological blockade of CB1 receptors is reported to increase the 5HIAA/5HT ratio in the forebrain (Darmani et al., 2003). The results presented here are in agreement with a report showing that the 5HIAA/5HT ratio in the striatum was not altered CB1 KO mice (Thiemann et al., 2007), and suggest that CB1/CB2 KO mice have normal serotoninergic integrity and function.

The results from these studies reveal that mice lacking functional CB1 and CB2 receptors have typical dopaminergic innervation of the striatum, nucleus accumbens, and median eminence by NSDA, MLDA, and TIDA neurons, respectively. The activity and DA receptor mediated regulation (or lack of in the case of TIDA neurons) are also maintained in CB1/CB2 KO mice. Serotoninergic neurons terminating in the striatum

and nucleus accumbens also exhibit typical innervation and activity in CB1/CB2 KO mice. These results suggest that the presence of CB1 or CB2 receptors is not crucial for development of these neuronal systems or maintenance in adulthood. Lack of any changes in these neuronal systems makes CB1/CB2 KO mice an ideal tool to determine if the lack of ECB activity at CB1 and CB2 receptors is beneficial or detrimental in the MPTP model of PD.

Chapter 6: The Effects of a Lack of Cannabinoid Receptors in the MPTP Model of PD

A. Introduction

CB1 receptors are located throughout the basal ganglia and activation of these receptors differentially regulates DA concentrations in the striatum depending on which population of CB1 receptors within the basal ganglia are involved (Figure 6-1) (Herkenham et al., 1990; Herkenham et al., 1991b; Hohmann and Herkenham, 2000). PD results in alterations in the basal ganglia function due to the loss of NSDA neurons, including over-activation of the indirect pathway of the basal ganglia leading to inhibition of motor output by the thalamus expressed as one of the hallmark symptoms of PD, slowness of movement (Dauer and Przedborski, 2003). ECB levels and expression of CB1 receptors changes within the central nervous system in rodent and non-human primate models of PD as well as in PD patients in response to a loss of NSDA neurons. These alterations in the ECB system may contribute to the delayed development of PD symptoms which often does not occur until 50-60% of NSDA neurons have been lost (Dauer and Przedborski, 2003).

Expression of CB1 receptor mRNA and protein increases in the striatum of the rodent 6-OHDA model, in non-human primates treated with MPTP, and in the brain of humans with PD (Romero et al., 2000; Lastres-Becker et al., 2001; Gonzalez et al., 2006). Elevation of ECB levels in the striatum of rodents and non-human primates indicates that ECB system activity occurs with lesioning of NSDA neurons (Gubellini et al., 2002; van der Stelt et al., 2005). The enzymatic activity of fatty acid amide hydrolase (FAAH; which metabolizes ECB) and the uptake of ECB into cells by the anandamide

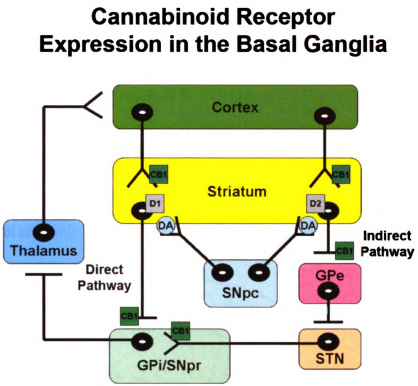

Figure 6-1. Schematic depicting the location of CB1 receptors within the basal ganglia. CB1 receptors are located on both glutamatergic (^) and GABAergic (⊥) terminals within the basal ganglia. CB1 receptors are on glutamatergic cortical neurons terminating in the striatum. Medium spiny GABAergic neurons projecting to the globus pallidus interna (GPi), substantia nigra pars reticulata (SNpr), and globus pallidus externa (GPe) have axonal terminal CB1 receptors. Glutamatergic neurons originating in the subthalamic nucleus (STN) and terminating in the GPi and SNpr also have terminal CB1 receptors. ECB action at different locations within the basal ganglia can alter the activity of the direct (excitatory) pathway or the indirect (inhibitory) pathway on the thalamus, and also indirectly effect NSDA neurons originating in the substantia nigra pars compacta (SNpc) and terminating in the striatum.

transporter (AMT) are both reduced in the striatum following 6-OHDA lesioning, thereby contributing to increased levels of ECB (Gubellini et al., 2002). An increase in CB1 receptor expression and ECB levels in the striatum is likely a mechanism to reduce glutamate release from corticostriatal neurons. Typically CB1 and D2 receptors are involved in the inhibitory regulation of glutamatergic corticostriatal inputs (Gerdeman and Lovinger, 2001; Meschler and Howlett, 2001). Loss of DA activation at D2 receptors in the striatum could explain an increase in CB1 activity in the striatum (Gubellini et al., 2002; van der Stelt et al., 2005).

CB1 receptor expression also increases in the substantia nigra of a rodent model of PD similar to the striatum (Gonzalez et al., 2006), and levels of the ECB 2-AG increase in a primate MPTP model indicating ECB alterations in another portion of the basal ganglia with NSDA neuronal loss (van der Stelt et al., 2005). The implications of these findings is that within the SNpc region increased ECB activity could enhance the release of DA from remaining NSDA neurons by reducing GABA release (Benarroch, 2007). In the SNpr, CB1 receptor stimulation could inhibit motor output if ECB were acting on CB1 receptors on GABAergic striatonigral neurons of the direct pathway, or stimulate motor output via inhibition of the indirect pathway by action on glutamatergic axonal terminals of neurons originating in the STN. Therefore, it is not known if the enhancement of the ECB system could be beneficial or detrimental in the treatment of PD.

The role of the ECB system within the basal ganglia in PD or models of the disease is complex and the effects of its activation varies depending on the region of CB1 receptor activation. If ECB system activity is enhanced in PD and leads to a dampening

of the indirect pathway output thereby facilitating movement and increased activity of remaining NSDA neurons, than this could be incredibly beneficial for PD patients. However, increased activity of remaining NSDA neurons could also contribute to the progressive loss of these neurons due to over-activity and oxidative stress. ECB enhancement could also lead to a worsening of PD symptoms if CB action at CB1 receptors leads to increased activation of the indirect pathway. The use of CB1/CB2 KO mice therefore provides an ideal tool to explore the lack of CB receptor activity within the basal ganglia in a model of PD. CB1/CB2 KO mice which were previously shown to have typical integrity, activity, and DA receptor regulation of NSDA neurons will be used along with WT mice to examine the effects of MPTP treatment, in the absence of functional CB1 and CB2 receptors.

Hypothesis #1: Lack of CB1 and CB2 receptors will increase MPTP induced loss of NSDA axon terminals and cell bodies and compensatory activation of these neurons. This hypothesis was tested by examining:

1) The concentrations of DA and TH protein content in the striatum as an index of NSDA axon integrity following MPTP treatment.
2) The number of TH immunoreactive cells in the substantia nigra following sub-chronic MPTP treatment.
3) The concentrations of DOPAC and HVA in the striatum and the DOPAC/DA and HVA/DA ratios as indices of NSDA neuronal activity, and protein content of phosphorylated serine 40 on TH.

Hypothesis #2: MPTP treatment will not alter the integrity or activity of MLDA, TIDA, and serotoninergic neurons in CB1/CB2 KO mice following MPTP treatment compared to WT mice.

This hypothesis will be tested by evaluating:

1) The concentrations of DA in the axon terminal regions of MLDA and TIDA neurons to determine the integrity of neuronal terminals following MPTP treatment.
2) The concentrations of DOPAC and HVA and the DOPAC/DA and HVA/DA ratios to examine the activities of MLDA and TIDA neurons following MPTP administration.
3) The concentrations of 5HT and 5HIAA and the 5HIAA/5HT ratio in the striatum and nucleus accumbens to determine serotoninergic axon terminal integrity and neuronal activity following MPTP treatment.

B. Materials and Methods

WT male mice obtained from (Jackson Labs) were used as controls for male CB1/CB2 KO mice, and in CB antagonist experiments and were between 8-12 weeks of age. All mice used for neurochemical, Western blot, or Complex I activity experiments were sacrificed by decapitation, brains removed and immediately frozen on dry ice following the removal of the median eminence. Tissue was processed as previously described in (Chapter 2, Section C, Euthanasia and Brain Tissue Preparation). The concentrations of the neurochemicals DA, DOPAC, HVA, 5HT, and 5HIAA were determined using HPLC-EC as previously described (Chapter 2, Section D, Measurement of Amines and Amine Metabolites in the Brain). The concentrations of MPP+ were measured by LC-MS as previously described (Chapter 2, Section K, LC-MS Analysis of MPP+). The content of proteins of interest (TH, DAT, alpha-synuclein, parkin, DARPP-32, and p67Phox) was determined using Western blotting as previously described (Chapter 2, Section G, Western Blotting). Complex I activity within striatum mitochondrial tissue fractions was measured as previously described (Chapter 2, Section J, Complex I Activity).

Hindbrain tissue used for immunohistochemical analysis of TH cell numbers was dissected at the mid-coronal plane from the forebrain following decapitation, and drop fixed in 4% paraformaldehyde for 7 days. Fixed brain tissue was sectioned in a cryostat, stained for TH, and mounted on slides for TH cell counts of the substantia nigra using unbiased stereology as previously described (Chapter 2, Section H, Stereology TH Cell Counts).

WT and CB1/CB2 KO mice were treated with either an acute or sub-chronic MPTP treatment paradigm to evaluate the neurotoxic effects of MPTP. Acute MPTP treatment consisted of a single injection of saline given 4 h prior to or MPTP (10 mg/kg, s.c.) given 1, 2, 4, or 8 h prior to decapitation. Sub-chronic MPTP treatment involved administration of either an injection of saline or MPTP (10 mg/kg) once a day for 5 days and mice were decapitated 3 days following the last MPTP injection. WT mice treated with the CB1 antagonist rimonabant (1 mg/kg, s.c.) and/or the CB2 antagonist SR144528 (2.5 mg/kg, s.c.) were used to determine if pharmacologic inhibition of either one or both CB receptors attenuated the loss of NSDA axon terminals with sub-chronic MPTP treatment. Mice were injected with either one or both CB antagonists once a day beginning one hour prior to the first MPTP injection. CB antagonist treatment continued once a day up to an including the morning of decapitation.

C. Results

Effects of Acute MPTP Treatment on the Neurochemical Activity of NSDA Neurons in WT and CB1/CB2 KO Mice

The concentrations of DA and its metabolites DOPAC and HVA were measured in the striatum of WT and CB1/CB2 KO mice treated with saline or MPTP (10 mg/kg) and killed either 4 or 8 h later. As shown in Figure 6-2 (Panel A), saline treated WT and CB1/CB2 KO mice had similar DA concentrations in the striatum. The concentrations of DA significantly decreased in the striatum of both WT and CB1/CB2 KO mice by 4 h following MPTP administration. DA concentrations remained decreased 8 h after MPTP treatment in WT mice, but began to return to levels seen with saline treatment in CB1/CB2 KO mice (Figure 6-2; Panel A).

The concentrations of DOPAC and HVA were significantly decreased in the striatum 4 and 8 h following MPTP treatment in both WT and CB1/CB2 KO mice compared to saline controls (Figures 6-2; Panel B & 6-3; Panel A). The depletion of DOPAC within the striatum was similar at 4 h in WT and CB1/CB2 KO mice and remained decreased at the 8 h time point for both (Figure 6-2; Panel B). HVA concentrations in the striatum of WT and CB1/CB2 KO mice was significantly decreased 4 and 8 h following acute MPTP treatment, although at 4 h CB1/CB2 KO mice had a greater reduction in HVA concentrations compared to WT mice (Figure 6-3; Panel A).

The activity of NSDA neurons in WT and CB1/CB2 KO mice was evaluated 4 and 8 h after acute MPTP treatment by calculating the DOPAC/DA and HVA/DA ratios. As shown in Figure 6-2 (Panel C), the DOPAC/DA ratio was not altered by MPTP treatment 8 h later in the striatum of WT or CB1/CB2 KO mice, but by 4 h CB1/CB2 KO

mice did have a significant decrease in the ratio. The HVA/DA ratio in the striatum of WT mice was significantly increased 4 h following MPTP treatment compared to saline treated mice, but returned to a value similar to saline treated mice by 8 h. The HVA/DA ratio in CB1/CB2 KO mice was not altered following MPTP treatment compared to saline treated mice (Figure 6-3; Panel B).

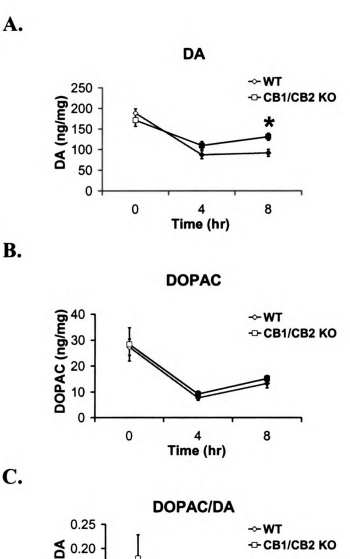

Figure 6-2. Time course effects of acute MPTP treatment on DA, DOPAC and the DOPAC/DA ratio in the striatum of WT and CB1/CB2 KO mice. Mice were treated with either saline or MPTP (10 mg/kg; s.c.) and decapitated 4 or 8 h later. Concentrations of DA (Panel A) and DOPAC (Panel B), and the DOPAC/DA ratio (Panel C) in the striatum of WT and CB1/CB2 KO mice, n=8-11. Data points represent means and bars ± one SEM. Filled in black data points indicate a significant difference between saline treated and MPTP treated mice within either WT or CB1/CB2 groups. *Significant difference between WT and CB1/CB2 KO mice within a treatment group, $p \leq 0.05$.

A.

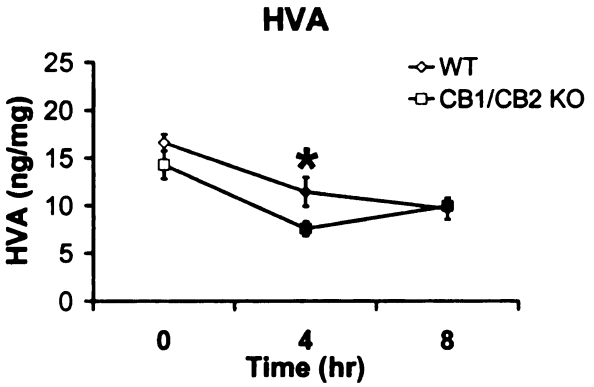

B.

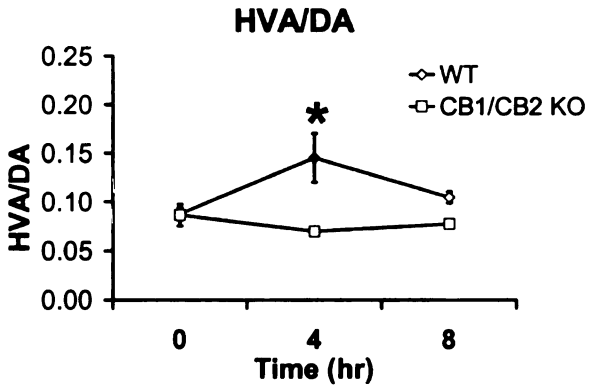

Figure 6-3. Time course effects of acute MPTP treatment on HVA and the HVA/DA ratio in the striatum of WT and CB1/CB2 KO mice. Mice were treated with either saline or MPTP (10 mg/kg; s.c.) and decapitated 4 or 8 h later. Concentrations of HVA (Panel A) and the HVA/DA ratio (Panel B) as determined in the striatum of WT and CB1/CB2 KO mice, n=8-11. Data points represent means and bars ± one SEM. Filled in black data points indicate a significant difference between saline treated and MPTP treated mice within either WT or CB1/CB2 groups. *Significant difference between WT and CB1/CB2 KO mice within a treatment group, $p \leq 0.05$.

Expression of NSDA Axon Terminal and Striatal Proteins in WT and CB1/CB2 KO Mice following Acute MPTP Treatment

NSDA axon terminal integrity was evaluated by determining the protein content of TH and DAT in the striatum of WT and CB1/CB2 KO mice treated with saline or acute MPTP (10 mg/kg, s.c.), and normalized to cytosolic (GAPDH) and membrane (SNAP-25) proteins, respectively. TH and DAT protein content in the striatum was similar in saline treated WT and CB1/CB2 KO mice. As shown in Figure 6-4, acute MPTP treatment did not alter TH or DAT content 4 or 8 h following MPTP administration in WT or CB1/CB2 KO mice.

Alpha-synuclein protein is one of the major components in Lewy bodies, the pathological hallmark of PD (Dauer and Przedborski, 2003). The content of alpha-synuclein was determined in the striatum following acute MPTP treatment. As shown in Figure 6-5 (Panels A & C), CB1/CB2 KO mice had significantly more alpha-synuclein protein within the striatum compared to WT mice. Acute MPTP treatment did not affect protein content of alpha-synuclein in WT mice 4 or 8 h following administration, but CB1/CB2 KO mice showed a significant loss in alpha-synuclein in the striatum following acute MPTP treatment at both time points (Figure 6-5; Panels A & C).

The protein content of the NADPH oxidase cytosolic subunit p67Phox associated with microglial cells was examined in the striatum of WT and CB1/CB2 KO mice and normalized to GAPDH as an index of microglial activation. As shown in Figure 6-5 (Panels B & C), WT and CB1/CB2 KO saline treated mice had similar levels of p67Phox content, and acute MPTP treatment did not alter cytosolic p67Phox content in WT or CB1/CB2 KO mice 4 or 8 h later.

Parkin is an E3 ligase protein associated with the ubiquitin proteasome system which degrades and recycles damaged or mutated proteins. A mutation in the parkin protein is associated with an autosomal recessive form of PD (Winklhofer, 2007). Membrane bound parkin was measured in the striatum of WT and CB1/CB2 KO mice treated with saline or an acute injection of MPTP. As shown in Table 6-1 and Figure 6-6, Parkin content normalized to the membrane protein SNAP-25 was similar between saline treated WT and CB1/CB2 KO mice and was not altered by acute MPTP treatment.

DA and cAMP regulated phosphoprotein of 32 kDa (DARPP-32) is a protein highly expressed in medium spiny neurons of the striatum. DARPP-32 phosphorylation is stimulated by ECB, and inhibited following pharmacological activation of D2 receptors (Andersson et al., 2005). Phosphorylated DARPP-32 cytosolic protein content was determined in the striatum of control and MPTP treated WT and CB1/CB2 KO mice. As shown in Table 6-1 and Figure 6-6, phosphorylated DARPP-32 protein in the striatum was similar between WT and CB1/CB2 KO mice treated with saline, and was not altered by acute MPTP treatment in WT or CB1/CB2 KO mice.

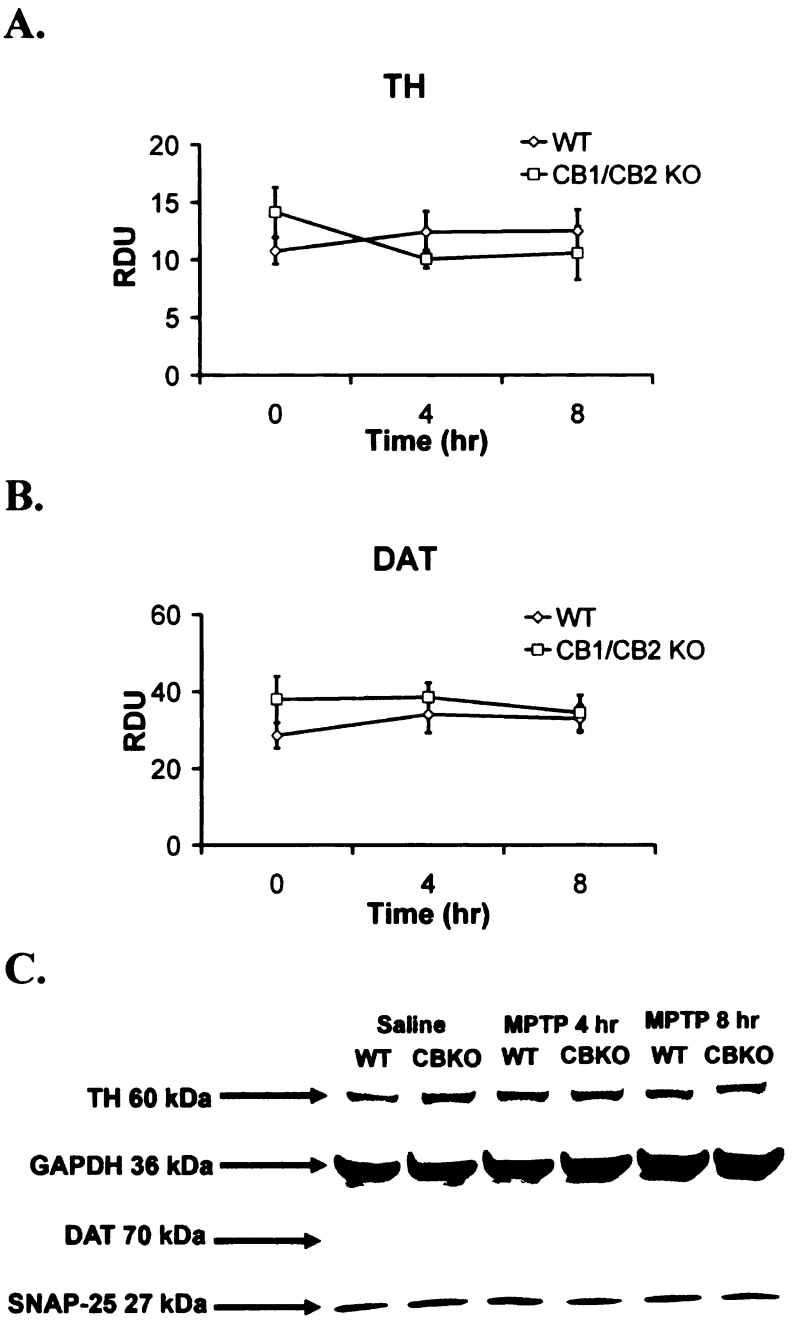

Figure 6-4. Lack of an effect of acute MPTP treatment on TH and DAT protein content in the striatum of WT and CB1/CB2 KO. Mice were treated with either saline or MPTP (10 mg/kg; s.c.) and decapitated 4 or 8 h later. Cytosolic TH protein was normalized to GAPDH and multiplied by a factor of 100 (Panel A) and membrane bound DAT protein was normalized to SNAP-25 and multiplied by a factor of 1,000 (Panel B) to be expressed as relative density units (RDU), n=6-11. Representative TH, GAPDH, DAT, and SNAP-25 protein bands for each treatment group (Panel C). Data points represent the mean and bars ± one SEM.

A.

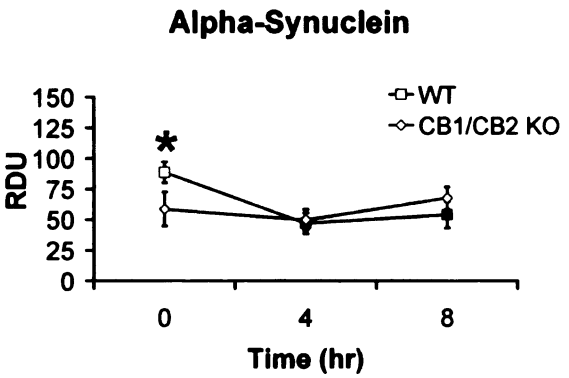

B.

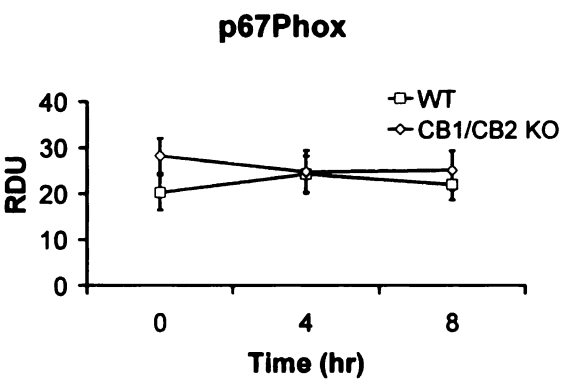

C.

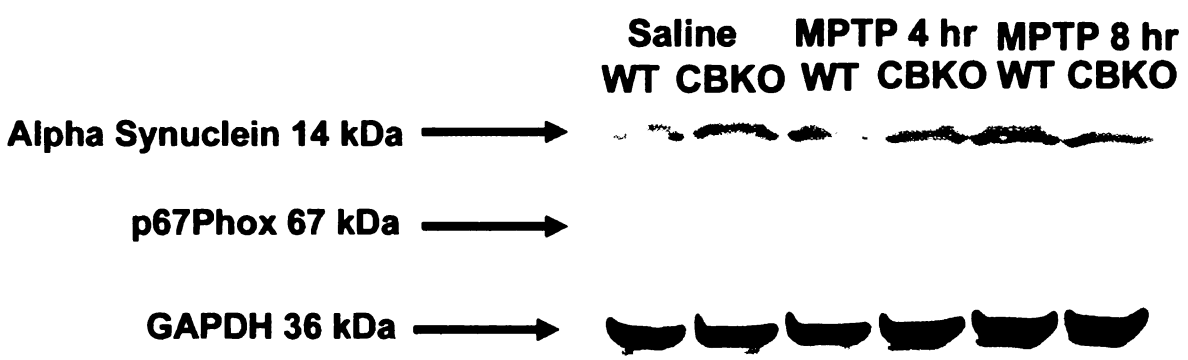

Figure 6-5. Alpha-synuclein and p67Phox cytosolic protein content in the striatum of WT and CB1/CB2 KO mice over time following saline or MPTP treatment. Mice were treated with either saline or MPTP (10 mg/kg; s.c.) and decapitated 4 or 8 h later. Cytosolic alpha-synuclein protein (Panel A) and p67Phox protein (Panel B) was normalized to GAPDH and multiplied by a factor of 1,000 to be expressed as RDU of the protein of interest to GAPDH, n=8-11. Representative alpha-synuclein, p67Phox, and GAPDH protein bands for each treatment group (Panel C). Data points represent the mean of each treatment group and bars ± one SEM. Filled in black data points indicate that MPTP treated mice were significantly different from saline treated mice within WT or CB1/CB2 KO mice. *Significant difference between WT and CB1/CB2 KO mice within a specific treatment group, $p \leq 0.05$.

Table 6-1. Parkin and DARPP-32 Protein in the Striatum Following Acute MPTP Treatment

	Parkin	DARPP-32
WT/ Saline	23.8 ± 3.0	23.7 ± 3.0
WT/ MPTP 4 hr	24.8 ± 2.7	25.9 ± 3.5
WT/ MPTP 8 hr	23.6 ± 2.5	20.3 ± 1.7
CB1/CB2 KO/ Saline	25.9 ± 3.8	26.3 ± 5.0
CB1/CB2 KO/ MPTP 4 hr	26.7 ± 2.2	23.0 ± 2.5
CB1/CB2 KO/ MPTP 8 hr	24.2 ± 1.9	26.1 ± 4.5

Table 6-1. Mice were treated with either saline or MPTP (10 mg/kg; s.c.) and decapitated 4 or 8 h later. Membrane bound parkin was normalized to SNAP-25 and multiplied by a factor of 100, n=9-11. Cytosolic phosphorylated DARPP-32 protein was normalized to GAPDH and multiplied by a factor of 100, n=8-11. Values displayed in the table are the mean of each group ± one SEM.

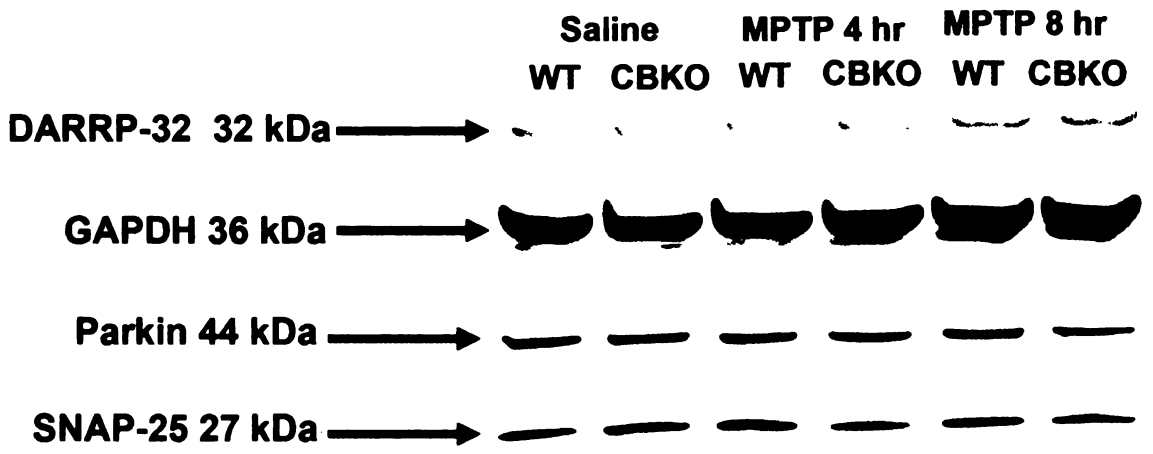

Figure 6-6. DARPP-32 and Parkin protein expression in the striatum in WT and CB1/CB2 KO mice following saline or MPTP treatment. WT and CB1/CB2 KO mice were treated with saline or acute MPTP (10 mg/kg, s.c.) and sacrificed 4 or 8 h later. DARPP-32 protein content was normalized to the cytosolic protein GAPDH, and Parkin the membrane protein SNAP-25. Representative cytosolic DARPP-32 and membrane Parkin protein bands for each treatment group.

Acute MPTP Treatment Effects on MLDA Neurons

DA concentrations were measured in the nucleus accumbens (the axon terminal region of MLDA neurons) in WT and CB1/CB2 KO mice treated with saline or acute MPTP (10 mg/kg, s.c.). DA concentrations in the nucleus accumbens were similar in saline treated WT and CB1/CB2 KO mice. As shown in Figure 6-7 (Panel A), acute MPTP treatment significantly decreased DA concentrations in the nucleus accumbens 4 and 8 h following administration in WT mice, but not CB1/CB2 KO.

The metabolites DOPAC and HVA, and the DOPAC/DA and HVA/DA ratios were also determined in the nucleus accumbens following acute MPTP treatment in WT and CB1/CB2 KO mice to evaluate MLDA neuronal activity. As demonstrated in Figure 6-7 (Panel B), DOPAC concentrations were significantly decreased following MPTP treatment in the nucleus accumbens of both WT and CB1/CB2 KO mice 4 and 8 h later, but this decrease was significantly attenuated in CB1/CB2 KO mice. HVA concentrations were also similar in WT and CB1/CB2 KO saline treated mice, and were not altered following acute MPTP treatment in CB1/CB2 KO mice. However, 4 h following MPTP treatment WT mice had a significant decrease in HVA concentrations (Figure 6-7, Panel A). The ratios of DOPAC/DA and HVA/DA in the nucleus accumbens were examined to determine the effects of acute MPTP treatment on neuronal activity. As shown in Figure 6-7 (Panel C), the DOPAC/DA ratio was significantly decreased following MPTP treatment at 8 h in CB1/CB2 KO mice, but WT mice failed to show any change in the ratio following MPTP treatment. The HVA/DA ratio was not altered with MPTP treatment at 4 or 8 h in WT or CB1/CB2 KO (Figure 6-8; Panel B).

A.

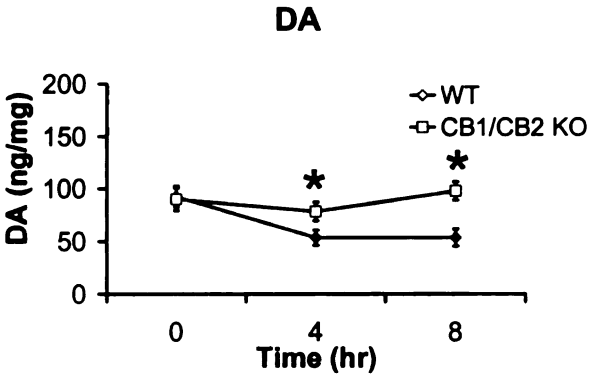

B.

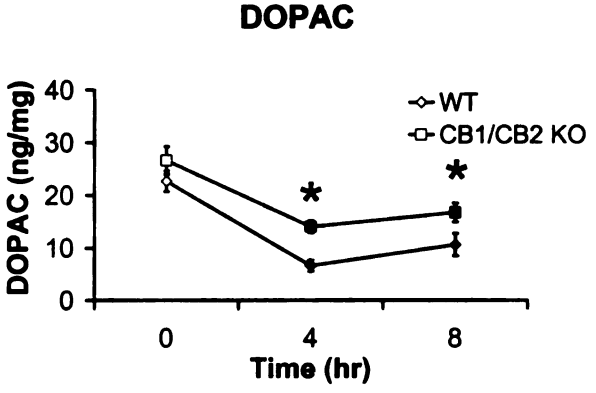

C.

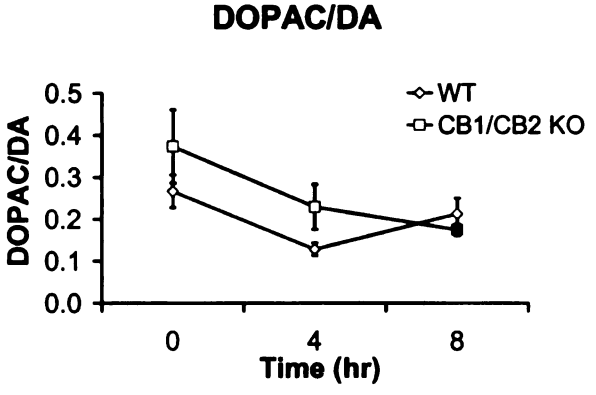

Figure 6-7. Time course effects of acute MPTP treatment on DA, DOPAC and the ratio of DOPAC/DA in the nucleus accumbens of WT and CB1/CB2 KO mice. Mice were treated with either saline or MPTP (10 mg/kg, s.c.) injection. The concentrations of DA (Panel A) and DOPAC (Panel B), and the DOPAC/DA ratio (Panel C) in the nucleus accumbens of WT and CB1/CB2 KO mice, n=8-11. Data points represent means and bars ± one SEM. Filled in black data points indicate a significant difference between saline treated and MPTP treated mice within either WT or CB1/CB2 groups. *Significant difference between WT and CB1/CB2 KO mice within a treatment group, $p \leq 0.05$.

A.

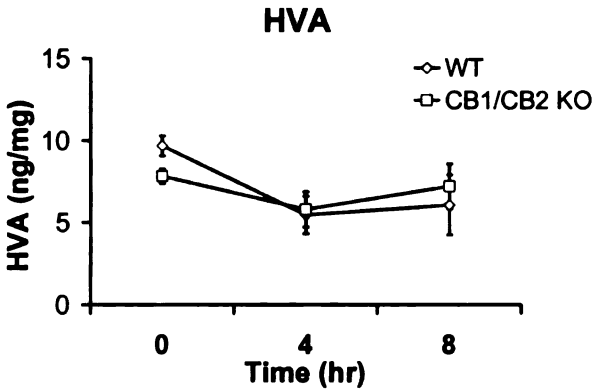

B.

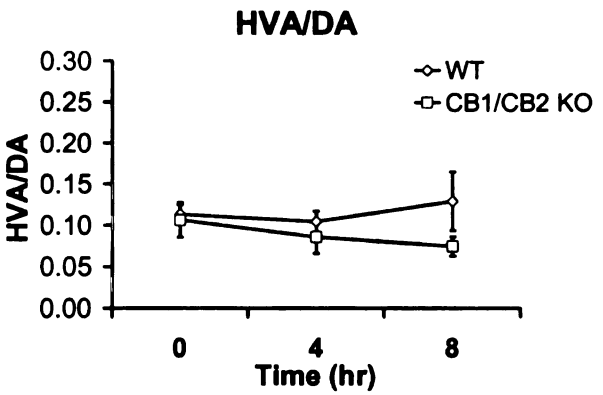

Figure 6-8. Time course effects of acute MPTP treatment on HVA and the ratio of HVA/DA in the nucleus accumbens of WT and CB1/CB2 KO mice. Mice were treated with either saline or MPTP (10 mg/kg, s.c.) injection. The concentrations of HVA (Panel A) and the HVA/DA ratio (Panel B) in the nucleus accumbens of WT and CB1/CB2 KO mice, n=8-11. Data points represent means and bars ± one SEM. Filled in black data points indicate a significant difference between saline treated and MPTP treated mice within either WT or CB1/CB2 groups, $p \leq 0.05$.

Time Course Effects of MPTP Treatment on TIDA Neurons in WT and CB1/CB2 KO Mice

The concentrations of DA were measured in the median eminence 4 and 8 following saline or acute MPTP treatment (10 mg/kg, s.c.) in WT and CB1/CB2 KO mice. DA concentrations were similar in the median eminence of saline treated WT and CB1/CB2 KO mice. As shown in Figure 6-9 (Panel A), acute MPTP treatment induced a significant decrease in DA concentrations in WT mice 4 h following MPTP administration which returned to control levels by 8 h. However, CB1/CB2 KO mice were resistant to DA depletion in the median eminence at both 4 and 8 h following acute MPTP treatment (Figure 6-9; Panel A).

The concentrations of DOPAC and the DOPAC/DA ratio in the median eminence were determined to evaluate TIDA neuronal activity after acute MPTP treatment. As shown in Figure 6-9 (Panels B & C), DOPAC concentrations and the DOPAC/DA ratio were both significantly reduced 4 and 8 h following MPTP administration.

A.

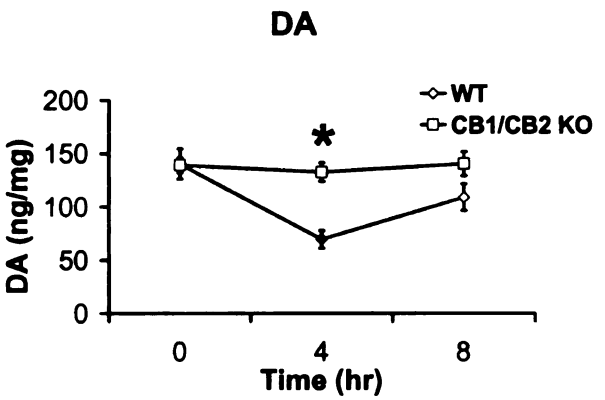

B.

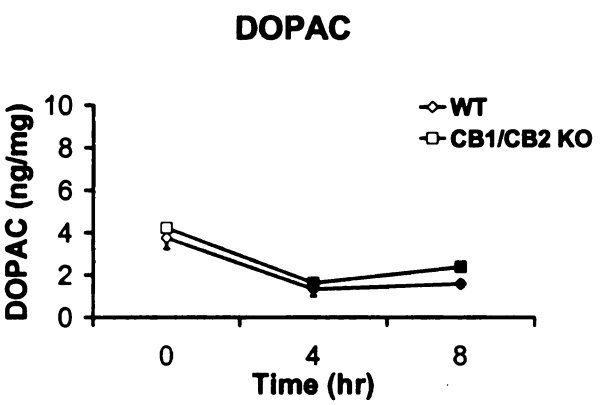

C.

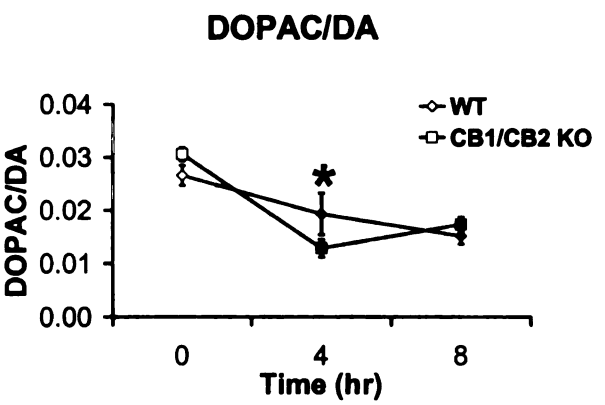

Figure 6-9. Time course effects of acute MPTP treatment on DA, DOPAC and the ratio of DOPAC/DA in the median eminence of WT and CB1/CB2 KO mice. Mice were treated with either saline or an acute MPTP (10 mg/kg, s.c.) injection. The concentrations of DA (Panel A) and DOPAC (Panel B), and the DOPAC/DA ratio (Panel C) in the median eminence of WT and CB1/CB2 KO mice, n=8-11. Data points represent means and bars ± one SEM. Filled in black data points indicate a significant difference between saline treated and MPTP treated mice within either WT or CB1/CB2 groups. *Significant difference between WT and CB1/CB2 KO mice within a treatment group, $p \leq 0.05$.

Time Course Effects of Acute MPTP Treatment on Serotoninergic Neurons in WT and CB1/CB2 KO Mice

The striatum and nucleus accumbens contain serotoninergic axon terminals of neurons originating in the dorsal and median raphe nuclei (Moore et al., 1978). The effects of acute MPTP treatment on 5HT axon terminals and serotoninergic neuronal activity were determined in each region. As shown in Panel A of Figures 6-10 and 6-11, concentrations of 5HT in both the striatum and nucleus accumbens following saline treatment were similar in WT and CB1/CB2 KO mice. Acute MPTP treatment did not alter 5HT concentrations in the striatum of either WT or CB1/CB2 KO mice, but in the nucleus accumbens 5HT concentrations were significantly increased in CB1/CB2 KO mice with MPTP treatment (Figure 6-11; Panel A).

The concentrations of 5HIAA and the 5HIAA/5HT ratio were examined in both the striatum and nucleus accumbens to determine the effects of acute MPTP treatment on serotoninergic neuronal activity. As shown in Panel B of Figures 6-10 and 6-11, 5HIAA concentrations were not different between saline treated WT and CB1/CB2 KO mice and were not altered following MPTP treatment in either region. However, the 5HIAA/5HT ratio indicated the serotoninergic neuronal activity was reduced following MPTP treatment in the striatum of CB1/CB2 KO mice at 4 h and in both regions at 8 h. In contrast, the 5HIAA/5HT ratio was not altered following acute MPTP treatment in WT mice (Figure 6-10; Panel C, & 6-11; Panel C).

A.

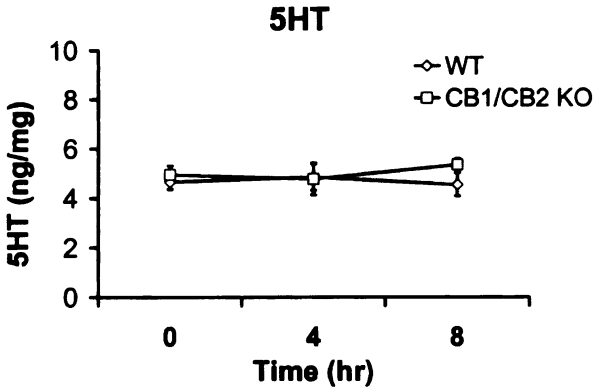

B.

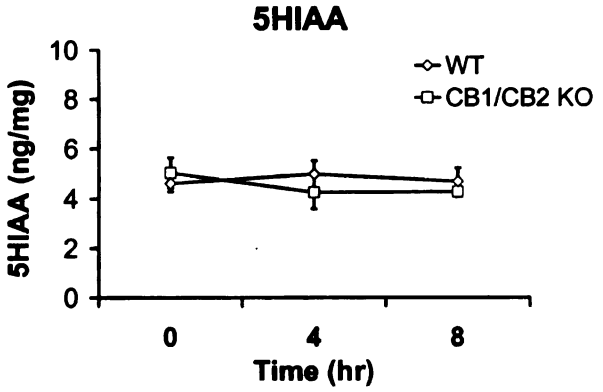

C.

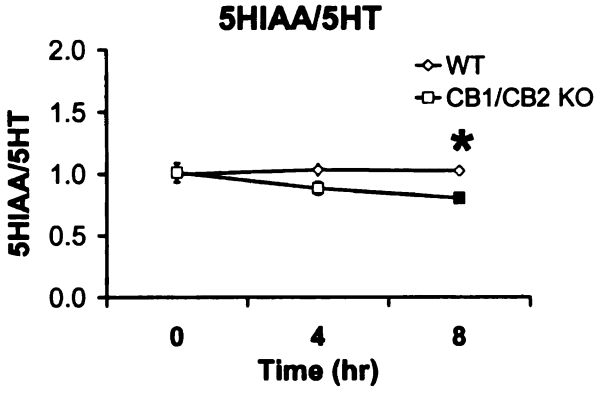

Figure 6-10. Time course effects of acute MPTP treatment in the striatum of WT and CB1/CB2 KO mice. Mice were treated with either saline or an acute MPTP (10 mg/kg, s.c.) injection. Concentrations of 5HT (Panel A) and 5HIAA (Panel B), and the 5HIAA/5HT ratio (Panel C) in the striatum of WT and CB1/CB2 KO mice, n=7-8. Data points represent means and bars ± one SEM. Filled in black data points indicate a significant difference between saline treated and MPTP treated mice within either WT or CB1/CB2 groups. *Significant difference between WT and CB1/CB2 KO mice within a treatment group, $p \leq 0.05$.

A.

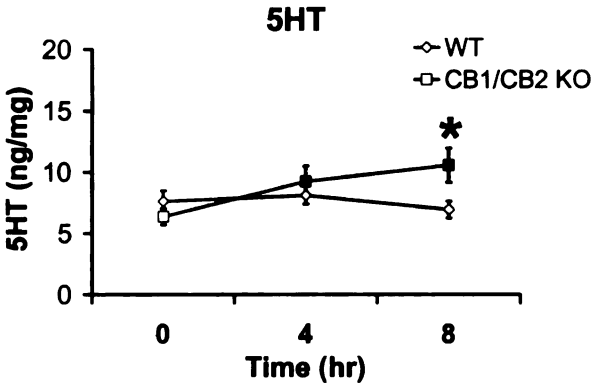

B.

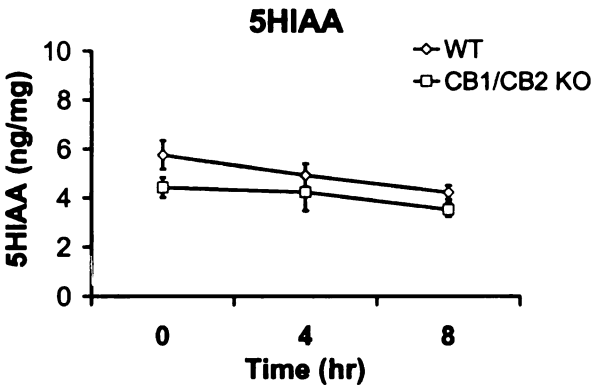

C.

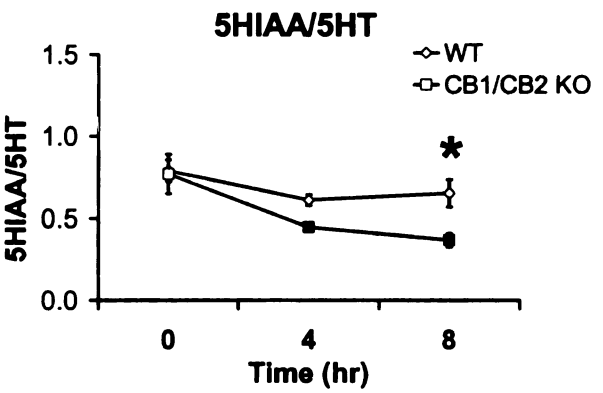

Figure 6-11. Time course effects of acute MPTP treatment in the nucleus accumbens of WT and CB1/CB2 KO mice. Mice were treated with either saline or an acute MPTP (10 mg/kg, s.c.) injection. Concentrations of 5HT (Panel A) and 5HIAA (Panel B), and the 5HIAA/5HT ratio (Panel C) in the nucleus accumbens of WT and CB1/CB2 KO mice, n=7-10. Data points represent means and bars ± one SEM. Filled in black data points indicate a significant difference between saline treated and MPTP treated mice within either WT or CB1/CB2 groups. *Significant difference between WT and CB1/CB2 KO mice within a treatment group, $p \leq 0.05$.

Lack of Cannabinoid Receptors Partially Protects NSDA Neurons from Sub-Chronic MPTP Neurotoxic Insult

WT and CB1/CB2 KO mice were injected with MPTP using a sub-chronic treatment paradigm (10 mg/kg; s.c. once a day for 5 days) and killed 3 days following the last MPTP injection to determine if a lack of CB receptors would be beneficial or detrimental with repeated neurotoxic insult to NSDA neurons. DA concentrations and TH protein content were measured in the striatum as indices of neuronal terminal integrity. DOPAC concentrations, the DOPAC/DA ratio, and phosphorylation of serine 40 TH was evaluated in the striatum of WT and CB1/CB2 KO mice, to determine the effects of sub-chronic MPTP treatment on NSDA neuronal activity. The number of TH immunoreactive cells within the substantia nigra and TH protein content in the ventral midbrain were examined to see if MPTP treatment induced a loss of NSDA cell bodies within the substantia nigra.

DA concentrations and TH content in the striatum were not different between saline treated WT and CB1/CB2 KO mice. As shown in Figure 6-12 (Panel A), sub-chronic MPTP treatment induced a significant loss in DA concentrations in the striatum of both WT and CB1/CB2 KO mice, but the loss of DA with MPTP treatment was attenuated in CB1/CB2 KO mice. This finding suggests that CB1/CB2 KO mice are partially resistant to MPTP induced DA depletion. However, sub-chronic MPTP treatment induced a significant and similar loss in TH protein in the striatum of both WT and CB1/CB2 KO mice (Figure 6-13; Panels A & C).

DOPAC concentrations and the DOPAC/DA ratio were similar between saline treated WT and CB1/CB2 KO mice (Figure 6-12; Panels B & C). Both WT and

CB1/CB2 KO mice treated sub-chronically with MPTP had a significant loss in DOPAC concentrations in the striatum (Figure 6-12; Panel B), and the ratio of DOPAC/DA was significantly increased in WT mice with MPTP treatment (Figure 6-12; Panel C). In contrast, MPTP treatment did not change the ratio of DOPAC/DA in the striatum of CB1/CB2 KO mice.

The protein content of serine 40 phosphorylated TH was also determined in the striatum of WT and CB1/CB2 KO mice treated sub-chronically with MPTP, as an additional index of NSDA neuronal activity. Phosphorylation of serine 40 on TH can increase with increased activity of NSDA neurons (Bobrovskaya et al., 2007). The compensatory increase in NSDA neuronal activity demonstrated in WT mice following MPTP treatment with the striatum DOPAC/DA ratio did not correspond with an increase in phosphorylated serine 40 in the striatum (Figure 6-13; Panels B & C). These results would suggest that measurement of serine 40 phosphorylation of TH protein may not be as sensitive as the DOPAC/DA ratio to detect an increase in NSDA neuronal activity following neurotoxin lesions.

NSDA neuronal cells were stained for TH and revealed similar morphology and distribution within the substantia nigra of CB1/CB2 KO mice treated with saline compared to WT mice (Figure 6-14). As shown in Figure 6-15 (Panel A), comparison of the number of NSDA neurons (as determined using an unbiased stereology cell counting method) revealed a similar number of TH positive cells in the substantia nigra of WT and CB1/CB2 KO mice treated with saline, which was not changed in WT or CB1/CB2 KO mice following sub-chronic MPTP treatment. The lack of a loss in NSDA neuronal cell bodies 3 days following the last injection of MPTP is not surprising, as a loss of cell

bodies with this treatment paradigm is not usually observed at 3 days following MPTP treatment termination (Petroske et al., 2001). The protein content of TH within the ventral midbrain containing NSDA neuronal cell bodies in the substantia nigra was similar in saline treated WT and CB1/CB2 KO mice corresponding to a similar number of TH immunoreactive cells in the substantia nigra (Figure 6-15; Panel B). Sub-chronic MPTP treatment induced a small but significant loss in TH protein content within the ventral midbrain of WT mice, which was not observed in CB1/CB2 KO mice.

A.

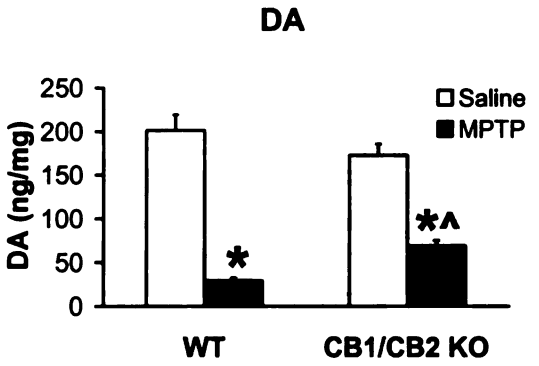

B.

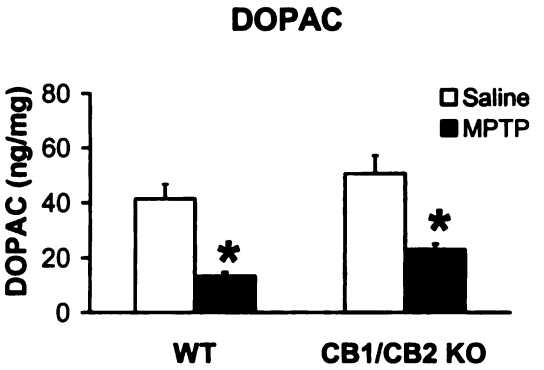

C.

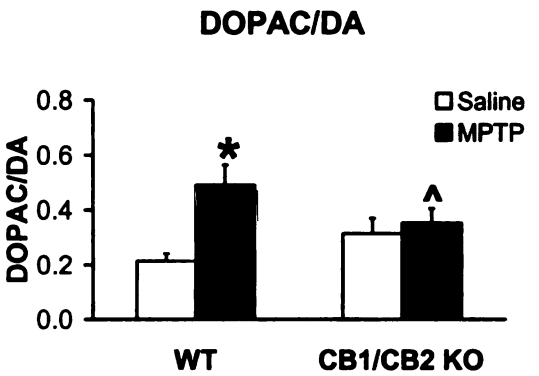

Figure 6-12. Effects of sub-chronic MPTP treatment on DA, DOPAC and the ratio of DOPAC/DA in the striatum of WT and CB1/CB2 KO mice. Mice were treated with saline or MPTP (10 mg/kg; s.c. per day for 5 days) and decapitated 3 days later. Concentrations of DA (Panel A) and DOPAC (Panel B), and the DOPAC/DA ratio (Panel C) were measured in the striatum of WT and CB1/CB2 KO mice, n=9-10. Columns represent means and bars ± one SEM. *Significant difference between saline and MPTP treated mice. ^Significant difference between WT and CB1/CB2 KO mice, $p \leq 0.05$.

A.

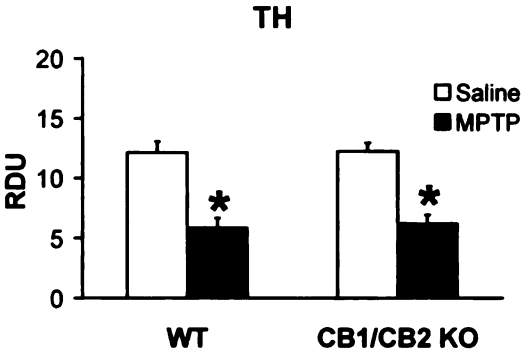

B.

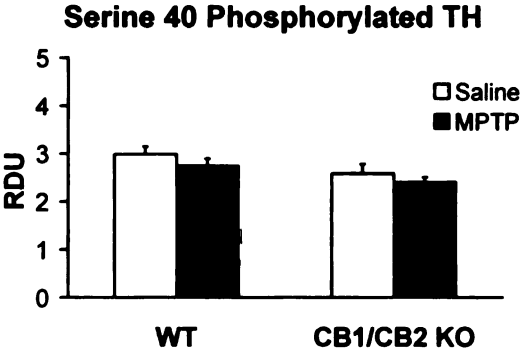

C.

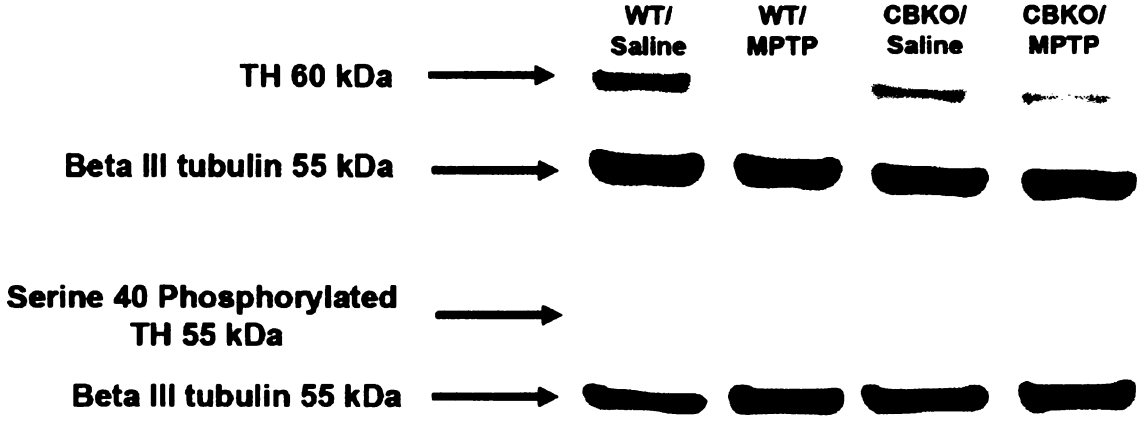

Figure 6-13. The effect of sub-chronic MPTP treatment on TH and phosphorylated serine 40 TH protein in the striatum of WT and CB1/CB2 KO mice. Mice were treated with saline or MPTP (10 mg/kg; s.c. per day for 5 days) and decapitated 3 days later. TH or phosphorylated serine 40 TH protein was normalized to β-III tubulin and multiplied by a factor of 100. TH protein (Panel A) and phosphorylated serine 40 TH (Panel B), and pictorial representation of TH and phosphorylated serine 40 TH bands in WT and CB1/CB2 KO mice (Panel C), n=6-10. Columns represent the mean and bars ± one SEM. *Saline treated mice are significantly different from MPTP treated mice, $p \leq 0.05$.

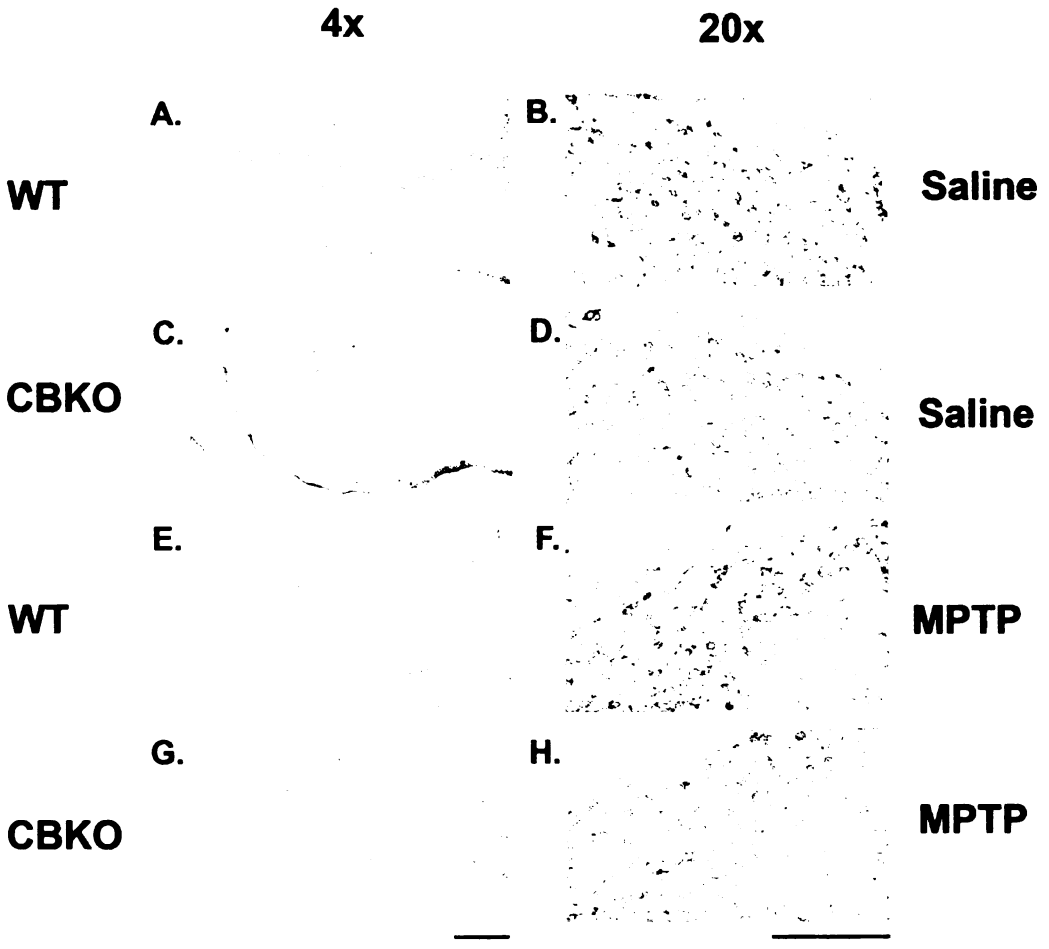

Figure 6-14. TH immunoreactive cells within the substantia nigra of WT and CB1/CB2 KO mice following sub-chronic MPTP treatment. Mice were treated with saline or MPTP (10 mg/kg per day for 5 days) and decapitated 3 days later. WT saline (Panels A & B), WT MPTP (Panels E & F), CB1/CB2 KO saline (Panels C & D), and CB1/CB2 KO MPTP (Panels G & H) treated mice. Panels (A, C, E, & G) were viewed at 4x, and Panels (B, D, F, & H) at 20x. Bar below panel G is equivalent to 500 uM and bar below panel H is 100 uM.

A.

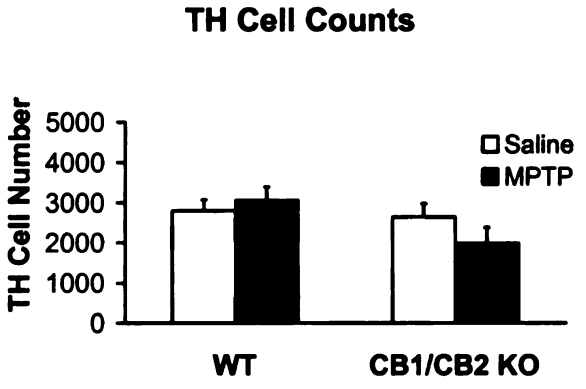

B.

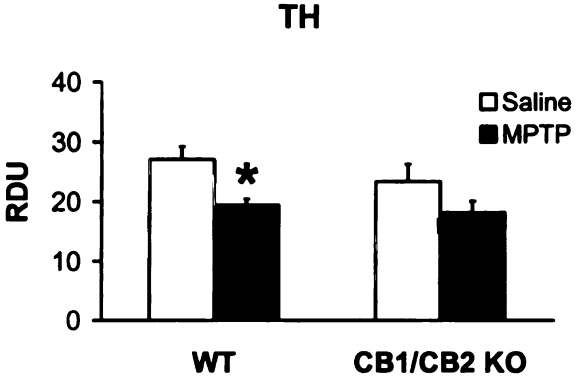

Figure 6-15. Bilateral TH cell counts in the substantia nigra and ventral midbrain TH protein content in WT and CB1/CB2 mice treated with MPTP using the sub-chronic treatment paradigm. Mice were treated with saline or MPTP (10 mg/kg; s.c. per day for 5 days) and decapitated 3 days later. Bilateral TH cell counts in the substantia nigra (Panel A), n=3-7. Cytosolic ventral midbrain TH protein content normalized to β-III tubulin and multiplied by a factor of 100 (Panel B), n=8-10. Columns represent means and bars ± one SEM. *Significant difference between saline and MPTP treated mice, $p \leq 0.05$.

Effects of Sub-Chronic MPTP Treatment on MLDA and TIDA Neurons

The integrity of MLDA axon terminals was determined by measuring the concentrations of DA in the nucleus accumbens of WT and CB1/CB2 KO mice following saline or sub-chronic MPTP (10 mg/kg s.c., once day or 5 days) treatment, and were found to be similar between saline treated WT and CB1/CB2 KO mice. As shown in Figure 6-16 (Panel A), sub-chronic MPTP treatment did not alter DA concentrations in the nucleus accumbens demonstrating no loss of axonal integrity of MLDA neurons.

The activity of MLDA neurons was determined by measuring DOPAC concentrations and the DOPAC/DA ratio in the nucleus accumbens. DOPAC concentrations were similar between saline treated WT and CB1/CB2 KO mice, but sub-chronic MPTP treatment caused a significant decrease in DOPAC concentrations in the nucleus accumbens of CB1/CB2 KO mice (Figure 6-16; Panel B). The DOPAC/DA ratio was similar in saline treated WT and CB1/CB2 KO mice, and did not change following MPTP treatment, suggesting that MLDA neuronal activity was not altered by MPTP treatment (Figure 6-16; Panel C).

DA concentrations were also measured in the median eminence of WT and CB1/CB2 KO mice following sub-chronic MPTP treatment. DA concentrations in the median eminence were higher in CB1/CB2 KO mice with saline treatment compared to WT mice (Figure 6-17; Panel A). CB1/CB2 KO (but not WT) mice had a significant decrease in DA concentrations following MPTP treatment.

DOPAC concentrations and the DOPAC/DA ratio were also measured in the median eminence to determine if sub-chronic MPTP treatment affected the activity of

TIDA neurons. DOPAC concentrations in the median eminence were similar in saline treated WT and CB1/CB2 KO mice, and DOPAC concentrations were not changed following MPTP treatment in WT mice (Figure 6-17; Panel B). In contrast, CB1/CB2 KO mice had a significant loss in DOPAC concentrations in the median eminence following MPTP treatment (Figure 6-17; Panel B). However, the DOPAC/DA ratio in the median eminence was similar between saline treated WT and CB1/CB2 KO mice, and sub-chronic MPTP treatment did not change the ratio for either (Figure 6-17; Panel C).

A.

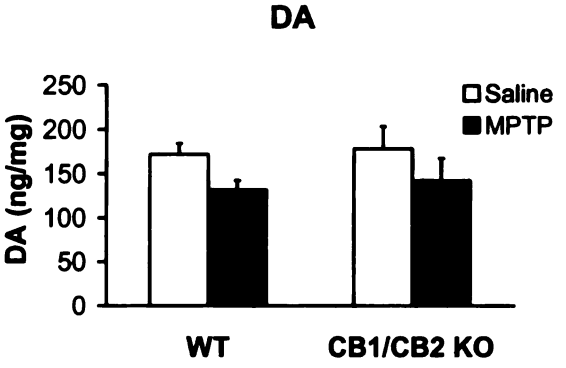

B.

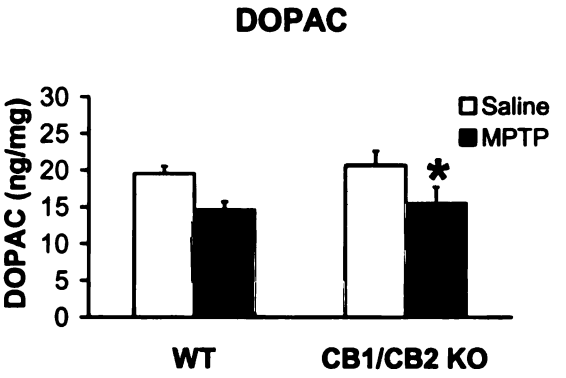

C.

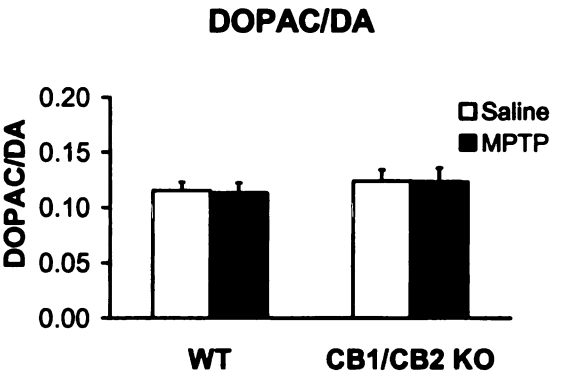

Figure 6-16. Effects of sub-chronic MPTP treatment on DA, DOPAC and the ratio of DOPAC/DA in the nucleus accumbens of WT and CB1/CB2 KO mice. Mice were treated with saline or MPTP (10 mg/kg; s.c. per day for 5 days) and decapitated 3 days later. Concentrations of DA (Panel A) and DOPAC (Panel B), and the DOPAC/DA ratio (Panel C) in the nucleus accumbens of WT and CB1/CB2 KO mice, n=6-10. Columns represent means and bars ± one SEM. *Significant difference between saline and MPTP treated mice, $p \leq 0.05$.

A.

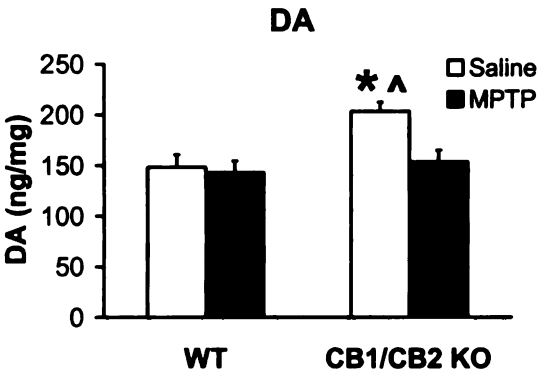

B.

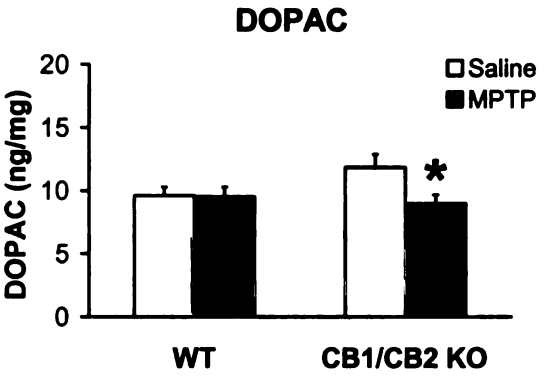

C.

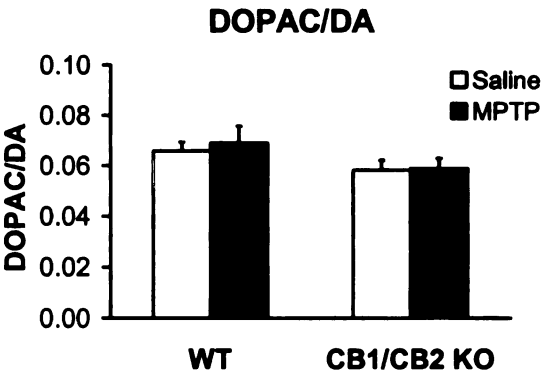

Figure 6-17. Effects of sub-chronic MPTP treatment on DA, DOPAC and the ratio of DOPAC/DA in the median eminence of WT and CB1/CB2 KO mice. Mice were treated with saline or MPTP (10 mg/kg; s.c. per day for 5 days) and decapitated 3 days later. Concentrations of DA (Panel A) and DOPAC (Panel B), and the DOPAC/DA ratio (Panel C) in the median eminence of WT and CB1/CB2 KO mice, n=7-10. Columns represent means and bars ± one SEM. *Significant difference between saline and MPTP treated mice. ^Significant difference between WT and CB1/CB2 KO mice within a treatment group, $p \leq 0.05$.

Effects of Sub-Chronic MPTP Treatment on NSDA Neurons in WT mice Treated with Cannabinoid Antagonists

The effects of pharmacological blockade of CB1 or CB2 receptors in the presence of sub-chronic MPTP treatment was tested to determine if partial resistance to MPTP induced DA depletion in the striatum of CB1/CB2 KO mice could be replicated in WT mice. The concentrations of DA and DOPAC were measured in the striatum of WT mice pre-treated with either a CB1 antagonist or CB2 receptor antagonist prior to saline or sub-chronic MPTP (10 mg/kg s.c., once a day for 5 days) administration. Mice were treated with the CB1 antagonist rimonabant (1 mg/kg s.c.) or the CB2 antagonist SR14428 (2.5 mg/kg) once a day beginning the day of the first MPTP injection and continuing until the day mice were killed, 3 days following the last MPTP injection.

DA concentrations were determined in the striatum of saline treated mice given rimonabant, SR144528 or vehicle injections, and it was determined that CB antagonist treatment alone did not alter DA concentrations (Figure 6-18; Panel A). As shown in Figure 6-18 (Panel A), sub-chronic MPTP treatment induced a significant loss in striatal DA concentrations in vehicle treated mice as compared to saline treated vehicle mice. However, mice treated with MPTP and either rimonabant or SR144528 had a similar loss in DA concentrations within the striatum. These results suggest that although rimonabant and SR144528 did not alter NSDA axon terminal integrity in the presence of saline treatment, both failed to attenuate or prevent MPTP induced loss of NSDA axon terminals.

The activity of NSDA neurons in the presence of either rimonabant or SR144528 was also evaluated by determining DOPAC concentrations and the DOPAC/DA ratio in

the striatum. Rimonabant or SR144528 had no effect on NSDA activity compared to vehicle treated mice as the DOPAC concentrations and the DOPAC/DA ratio was similar across all treatment groups (Figure 6-18; Panels B & C). Sub-chronic MPTP treatment induced a decrease in DOPAC concentrations and an increase in the striatum DOPAC/DA ratio in vehicle treated mice. However, as shown in Figure 6-18 (Panels B & C), rimonabant and SR144528 treated mice had a similar decrease in striatum DOPAC concentrations and increase in the DOPAC/DA ratio, indicating that individual blockade of CB1 or CB2 receptors did not attenuate the compensatory increase in NSDA neuronal activity typically seen with sub-chronic MPTP treatment.

Lack of a resistance to sub-chronic MPTP treatment in the striatum with blockade of either CB1 or CB2 receptors led to the question of whether dual blockade of both CB receptors was required to induce resistance to DA depletion in the presence of MPTP. To test this, WT mice were treated with saline or the sub-chronic MPTP paradigm and given both rimonabant (1 mg/kg, s.c.) and SR144528 (2.5 mg/kg, s.c.) once a day 1 h prior to saline or MPTP injection. CB antagonist treatment continued once daily including the day of sacrifice.

As previously shown with individual CB receptor antagonists, dual blockade of CB1 and CB2 receptors did not alter DA concentrations in saline treated mice, indicating that NSDA axonal terminal integrity was not altered with CB antagonists (Figure 6-19; Panel A). Similar to individual inhibition of CB receptors, concurrent rimonabant and SR144528 treatment did not attenuate the loss of axon terminals caused by sub-chronic MPTP treatment (Figure 6-19; Panel A), indicating that pharmacologic blockade of both

CB1 and CB2 receptors did not alter MPTP induced loss of DA in the striatum as observed in CB1/CB2 KO mice.

The concentrations of DOPAC and the DOPAC/DA ratio were also determined to see if dual CB receptor antagonist treatment affected the MPTP induced increase in NSDA neuronal activity. As shown in Figure 6-19 (Panels B & C), pharmacologic inhibition of both CB1 and CB2 receptors failed to attenuate MPTP induced decrease in DOPAC concentrations or increase in the DOPAC/DA ratio. Lack of an effect on loss of DA in the presence of either individual or simultaneous CB1 and CB2 receptor blockade suggests that the resistance to DA depletion seen in CB1/CB2 KO mice may be due to an unknown compensatory mechanism that occurs in CB1/CB2 KO mice.

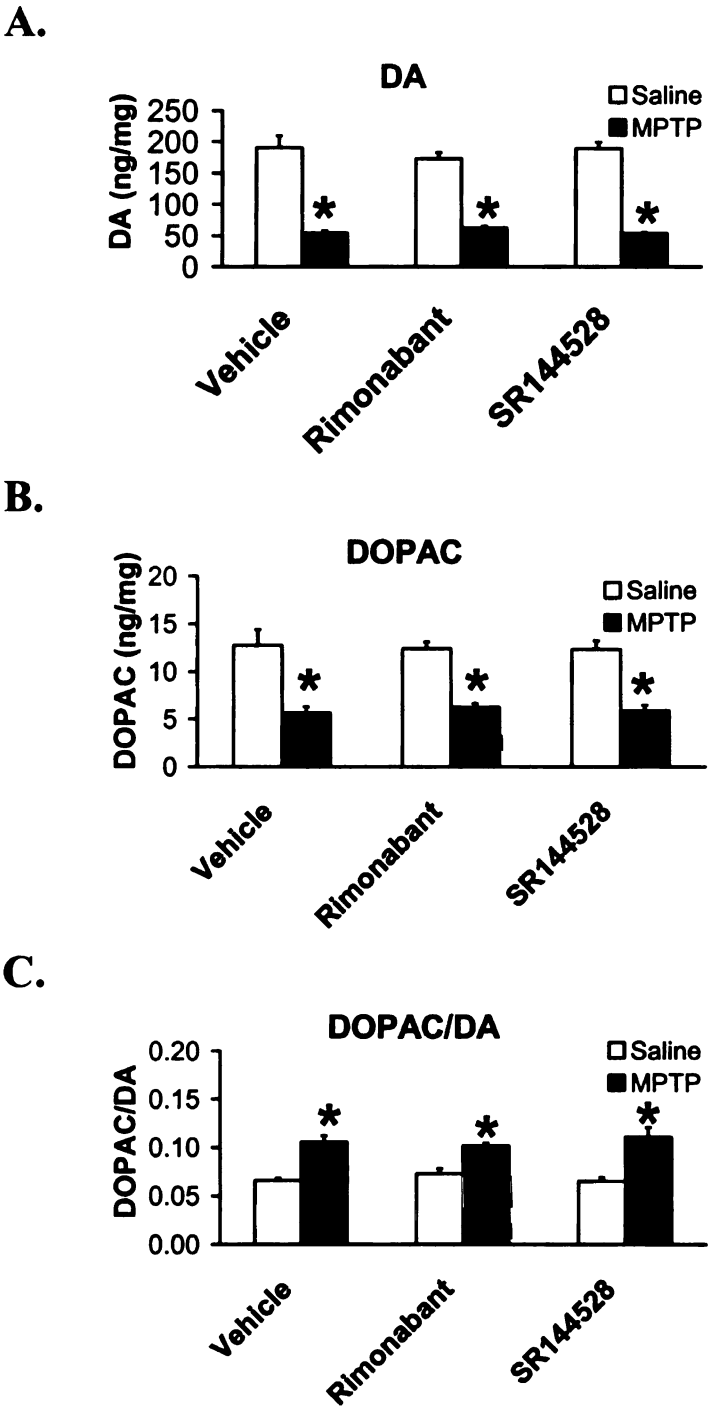

Figure 6-18. Lack of an effect of blockade of either CB1 or CB2 receptors on MPTP induced changes in DA, DOPAC and the ratio of DOPAC/DA in the striatum of WT mice. WT mice were treated with either vehicle, rimonabant (1 mg/kg; s.c.), or SR144528 (2.5 mg/kg; s.c.) 1 h prior to either saline or MPTP (10 mg/kg; s.c. once a day for 5 days) and continuing up until the time of decapitation, 3 days following the last injection of MPTP. Concentrations of DA (Panel A) and DOPAC (Panel B), and the DOPAC/DA ratio (Panel C) in the striatum, n=8-9. Columns represent means and bars ± one SEM. *Significant difference between saline and MPTP treated mice, $p \leq 0.05$.

A.

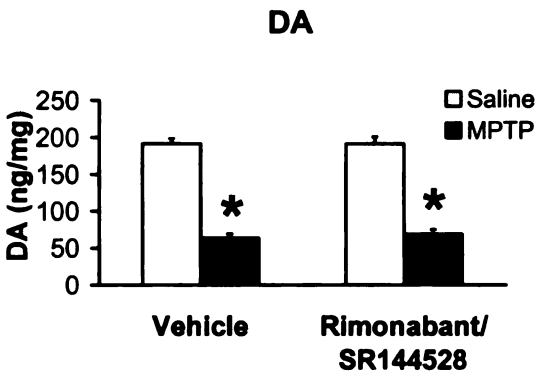

B.

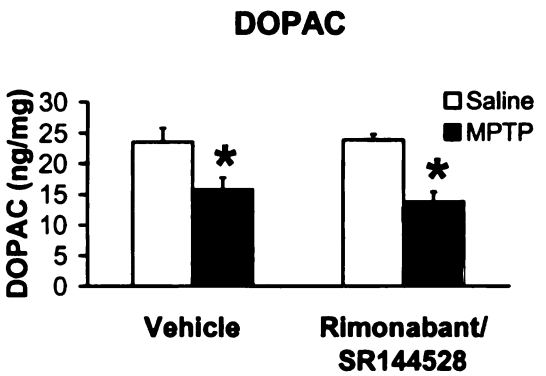

C.

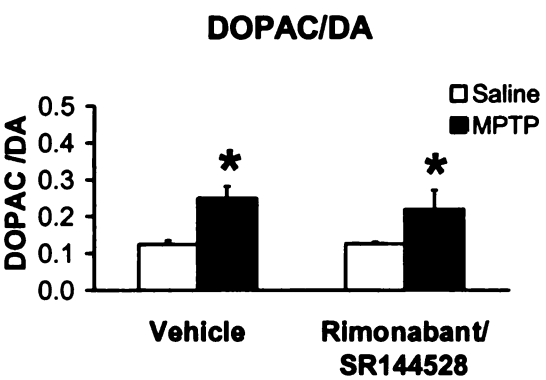

Figure 6-19. Lack of an effect of blockade of both CB1 and CB2 receptors on MPTP induced changes in DA, DOPAC and the ratio of DOPAC/DA in the striatum of WT mice. Mice were treated with vehicle or rimonabant (1 mg/kg; s.c.) and SR144528 (2.5 mg/kg; s.c.) 1 h prior to either saline or MPTP (10 mg/kg; s.c. once a day for 5 days) and continued until 3 days following the last injection of MPTP. Concentrations of DA (Panel A) and DOPAC (Panel B), and the DOPAC/DA ratio (Panel C) in the striatum, n=6-8. Columns represent means and bars ± one SEM. *Significant difference between saline and MPTP treated mice, $p \leq 0.05$.

Effects of Sub-Chronic MPTP Treatment on MLDA and TIDA Neurons in WT Mice Treated with CB Antagonists

MLDA and TIDA axon terminal integrity and neuronal activity were also examined following either individual or dual blockade of CB1 and CB2 receptors with rimonabant (1 mg/kg, s.c.) and/or SR144528 (2.5 mg/kg, s.c.). Mice were also treated with either saline or a sub-chronic MPTP (10 mg/kg s.c., once a day for 5 days) as previously described.

DA concentrations in the nucleus accumbens were not altered following CB antagonist treatment alone or in combination in saline treated WT mice. Sub-chronic MPTP treatment failed to alter DA concentrations except in combination with SR144528 treatment where MPTP induced a significant decrease in DA concentrations in the nucleus accumbens (Tables 6-2 & 6-3).

DOPAC concentrations and the DOPAC/DA ratio were not altered in the nucleus accumbens in saline treated mice given CB antagonists alone or in combination (Tables 6-2 & 6-3). DOPAC concentrations were significantly decreased in MPTP treated mice given MPTP plus SR144528 or MPTP and both CB antagonists. Sub-chronic MPTP treatment induced a small, but significant decrease in DOPAC concentrations (Tables 6-2 & 6-3). The DOPAC/DA ratio in the nucleus accumbens was similar across all treatment groups, suggesting that the overall activity of MLDA neurons was not altered by these treatments.

DA and DOPAC concentrations were similar in the median eminence in saline treated mice administered either rimonabant and/or SR144528 (Tables 6-2 & 6-3). Sub-chronic MPTP treatment also failed to change DA or DOPAC concentrations in the

presence of vehicle or either of the CB antagonists when administered individually (Table 6-2), although sub-chronic MPTP treatment did reduce DOPAC concentrations in the presence of both CB receptor antagonists. The lack of effect on the DOPAC/DA ratio in the median eminence indicated that CB antagonist treatment did not alter TIDA neuronal activity (Tables 6-2 & 6-3).

Table 6-2. Sub-chronic MPTP and CB1 or CB2 Receptor Antagonist Treatment Effects in the Nucleus Accumbens and Median Eminence

	Saline/ Vehicle	Saline/ Rimonabant	Saline/ SR144528	MPTP/ Vehicle	MPTP/ Rimonabant	MPTP/ SR144528
Nucleus Accumbens						
DA	118.0 ± 11.6	115.4 ± 13.0	132.7 ± 12.9	107.9 ± 8.1	101.6 ± 5.7	86.4 ± 6.9*
DOPAC	17.5 ± 2.1	14.7 ± 1.6	15.1 ± 0.8	14.0 ± 0.7*	12.4 ± 0.8	10.4 ± 0.6*
DOPAC/DA	0.16 ± 0.03	0.13 ± 0.01	0.12 ± 0.01	0.13 ± 0.01	0.12 ± 0.01	0.13 ± 0.01
Median Eminence						
DA	117.6 ± 15.2	129.6 ± 10.4	89.1 ± 7.3	117.8 ± 14.4	112.0 ± 9.5	120.1 ± 10.4
DOPAC	5.0 ± 0.9	7.3 ± 0.8	4.2 ± 1.0	4.8 ± 1.6	4.6 ± 0.9	5.9 ± 0.9
DOPAC/DA	0.04 ± 0.01	0.06 ± 0.01	0.05 ± 0.01	0.04 ± 0.01	0.04 ± 0.01	0.05 ± 0.01

Table 6-2. WT mice were treated with saline or sub-chronic MPTP (10 mg/kg, s.c., once a day for 5 days) treatment paradigm and either vehicle, rimonabant (1 mg/kg), or SR144528 (2.5 mg/kg) once a day 1 h prior to saline or MPTP administration and continuing for 3 days following the last injection of MPTP when mice were decapitated. The concentrations of DA, DOPAC, and DOPAC/DA ratios were determined in the nucleus accumbens and median eminence, n=6. Values displayed in the table are the mean of each group ± one SEM. *Significant difference between saline and MPTP treated mice within a specific vehicle or CB antagonist treatment group.

Table 6-3. Effects of Sub-chronic MPTP on DA, DOPAC and the DOPAC ratio in the Nucleus Accumbens and Median Eminence of Rimonabant and SR144528 Treated Mice

	Saline/ Vehicle	Saline/ Rimonabant & SR144528	MPTP/ Vehicle	MPTP/ Rimonabant & SR144528
Nucleus Accumbens				
DA	75.2 ± 9.1	87.3 ± 12.6	58.8 ± 8.8	59.0 ± 12.4
DOPAC	15.8 ± 2.1	20.7 ± 2.8	14.5 ± 1.5	14.0 ± 2.3*
DOPAC/DA	0.21 ± 0.02	0.25 ± 0.03	0.26 ± 0.03	0.27 ± 0.05
Median Eminence				
DA	79.7 ± 6.5	72.5 ± 6.9	57.9 ± 6.6	65.3 ± 10.1
DOPAC	2.6 ± 0.4	3.4 ± 0.6	1.8 ± 0.2	2.1 ± 0.4*
DOPAC/DA	0.03 ± 0.01	0.05 ± 0.01	0.03 ± 0.01	0.04 ± 0.01

Table 6-3. WT mice were treated with saline or MPTP (10 mg/kg, s.c., once a day for 5 days), and with vehicle or both rimonabant (1 mg/kg; s.c.) and SR144528 (2.5 mg/kg; s.c) 1 hr prior to saline or MPTP administration and continuing for 3 days following the last injection of MPTP. Concentrations of DA, DOPAC, and the DOPAC/DA ratios were determined in the nucleus accumbens and median eminence. Values displayed in the table are the mean of each group ± one SEM. *Significant difference between saline and MPTP treated mice within the respective vehicle or CB antagonist treatment group.

Complex I Activity and MPP+ Concentrations in the Striatum of WT and CB1/CB2 KO Mice

The partial resistance of CB1/CB2 KO mice to MPTP induced DA depletion in the striatum could be due to differences in intrinsic mitochondrial Complex I activity or differences in MPP+ to inhibit the activity of this enzyme. Complex I activity was therefore measured in the striatum of WT and CB1/CB2 KO mice treated with saline or MPTP (10 mg/kg, s.c.) injection and killed 4 or 8 h later. The activity of Complex I in the striatum of WT and CB1/CB2 KO mice treated with saline was similar (Figure 6-20). Complex I activity in the striatum following MPTP treatment was not different compared to saline treated controls in WT or CB1/CB2 KO mice (Figure 6-20). These results reveal that Complex I activity is similar between WT and CB1/CB2 KO mice, but the assay was likely not sensitive enough too detect a reduction in Complex I activity due to MPP+ inhibition.

Apparent partial resistance of CB1/CB2 KO mice to MPTP could be due to deficits in the conversion of MPTP to its bioactive metabolite MPP+. To test for this possibility, MPP+ concentrations were measured in the striatum of WT and CB1/CB2 KO mice 1, 2, 4, or 8 h following acute MPTP (10 mg/kg, s.c.) treatment. Zero time controls were injected with saline and killed 4 h later. As shown in Figure 6-21 (Panel A), concentrations of MPP+ in the striatum were significantly elevated at 1, 2 and 4 h after MPTP administration in both WT and CB1/CB2 KO mice, and by 8 h MPP+ was almost completely eliminated. WT mice had significantly more MPP+ in the striatum at 1, 2, and 4 h following MPTP treatment as compared with CB1/CB2 KO mice. These results indicate that although CB1/CB2 KO mice can convert MPTP to MPP+ in a similar

manner to that of WT controls, the efficacy of this conversion is somewhat reduced in CB1/CB2 KO mice.

DA concentrations in the striatum were also measured at 1, 2, 4, and 8 h following MPTP administration to determine the effects of acute MPTP treatment induced vesicular DA depletion at each of these time points. DA concentrations were similar in zero time point saline treated WT and CB1/CB2 KO mice, and were not changed 1 or 2 h following MPTP administration (Figure 6-21; Panel B). However, DA concentrations were significantly decreased 4 and 8 h after MPTP treatment in WT mice, but interestingly were not altered at these time points in CB1/CB2 KO mice (Figure 6-21; Panel B).

The DOPAC/DA ratio was also determined in the striatum at the specified time points following acute MPTP treatment. WT mice had a significant decrease in the ratio at 1 h with return to controls levels at 2 and 4 h, and finally increased compared to saline controls at 8 h (Figure 6-21; Panel C). CB1/CB2 KO mice had a significant decrease 1, 2, and 4 h following MPTP administration, but by 8 h activity of NSDA neurons returned to those of saline control animals (Figure 6-21; Panel C).

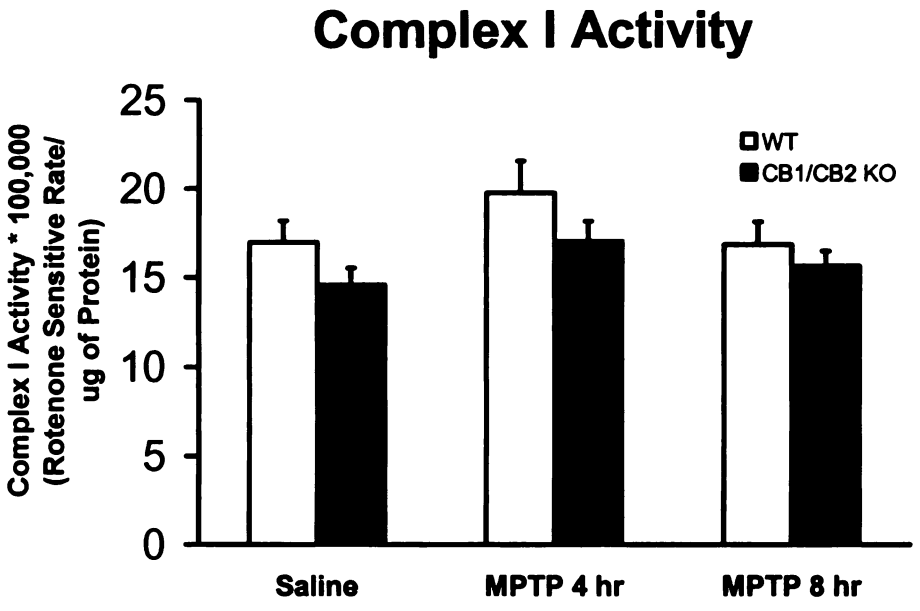

Figure 6-20. Mitochondrial Complex I activity in the striatum of MPTP treated WT and CB1/CB2 KO mice. Mice were treated either saline or an acute MPTP (10 mg/kg, s.c.) injection and decapitated 4 or 8 h later, n=10-11. Columns represent means and bars ± one SEM.

A.

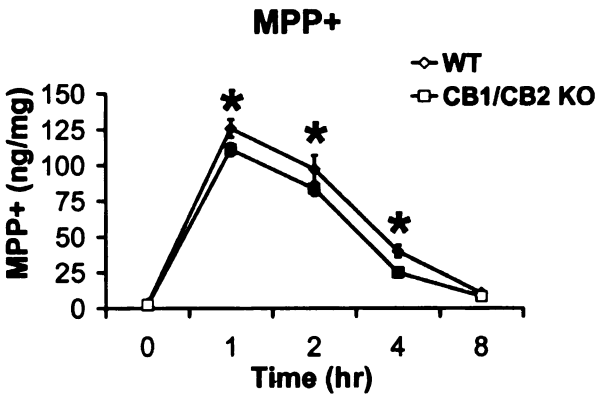

B.

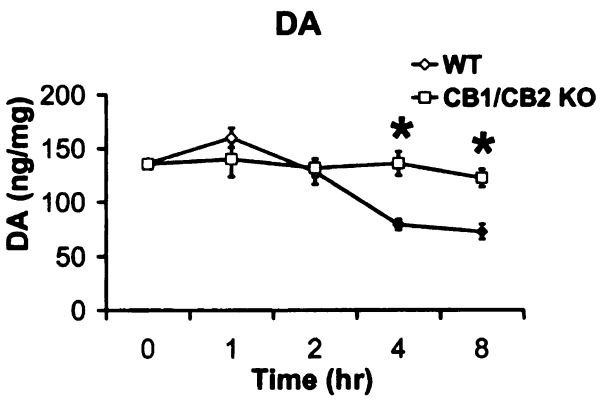

C.

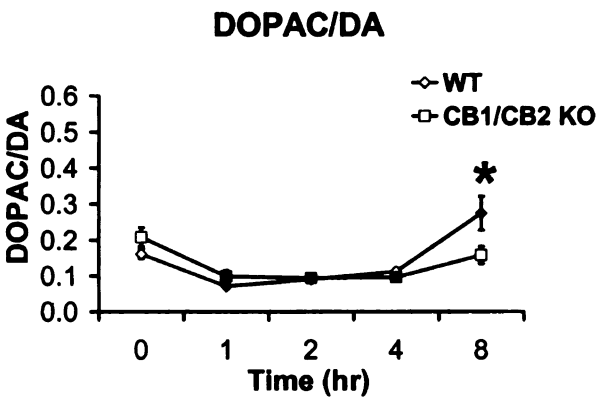

Figure 6-21. Time course effects of a single injection of MPTP on the concentrations of MPP+ and DA and the DOPAC/DA ratio in the striatum of WT and CB1/CB2 KO mice. WT and CB1/CB2 KO mice were injected with MPTP (10 mg/kg; s.c.) and killed at 1, 2, 4, or 8 h later. Saline treated controls served as the 0 time point and were killed at 4 h following injection, n=5. MPP+ concentrations were measured in the striatum using LC-MS (Panel A). Concentrations of DA (Panel B) and the DOPAC/DA ratio (Panel C) in the striatum, n=4-5. Filled in black data points indicate a significant difference between saline treated and MPTP treated mice within either WT or CB1/CB2 groups. *Significant difference between WT and CB1/CB2 KO mice within a treatment group, $p \leq 0.05$.

Discussion

The objective of these experiments was to determine if the presence of functional CB1 and CB2 receptors affected MPTP induced loss of NSDA neurons. CB1/CB2 KO mice were previously shown to have normal integrity, activity, and D2 receptor regulation of NSDA neurons (Chapter 5), thus making CB1/CB2 KO mice an ideal tool to investigate this topic.

The ECB system plays a role in the regulation of NSDA neurons due to the presence of CB1 receptors throughout the basal ganglia (Herkenham et al., 1990; Herkenham et al., 1991a; Hohmann and Herkenham, 2000). An upregulation of CB1 receptors, ECB, and changes in FAAH and AMT activity in the striatum of animal models and/or humans indicates that ECB system is hyperactive with the loss of NSDA neurons, especially with respect to regulation of the corticostriatal glutamatergic neurons (Romero et al., 2000; Lastres-Becker et al., 2001; Gubellini et al., 2002; van der Stelt et al., 2005; Gonzalez et al., 2006). An over activation of this portion of the basal ganglia reduces glutamate release in the striatum, which is typically increased in animal models of PD.

Upregulation in the ECB system activity in the substantia nigra in contrast could be either beneficial or detrimental. Animal models of PD have revealed enhanced CB receptor expression and increased ECB levels in the substantia nigra (van der Stelt et al., 2005; Gonzalez et al., 2006). The beneficial effects of this is that increased ECB activity in the substantia nigra pars compacta could enhance the activity of NSDA neurons and thus increase DA release in the striatum. Although this same effect could eventually also be detrimental if remaining NSDA neurons are over active for a long period of time,

which could cause a progressive loss of these neurons (Fitzmaurice et al., 2003). In the substantia nigra pars reticulata increased ECB activity could reduce motor activity if ECB were acting on CB1 receptors on striatonigral neurons of the direct pathway (dampening pathway activity), or alternatively enhance motor output by reduction in activity of the indirect pathway due to CB action on axonal terminals of glutamatergic subthalamic nucleus neurons (van der Stelt et al., 2005).

MPTP induced DA depletion in the striatum was evaluated following two different MPTP treatment paradigms. The acute MPTP paradigm induced a decrease in striatum DA within 4 h following a single injection of MPTP (Behrouz et al., 2007). The decrease in DA in this model likely reflects vesicular DA depletion at 4 h, as opposed to actual loss of NSDA neuronal integrity since there was no loss in TH or DAT protein content in the striatum of WT mice at this time point. In contrast, the sub-chronic MPTP model induces a significant loss in striatum DA concentrations accompanied by a loss in TH protein content, indicating a loss of axonal integrity (Petroske et al., 2001; Drolet et al., 2004; Shimoji et al., 2005).

Like in WT mice, acute MPTP treatment of CB1/CB2 KO mice revealed a decrease in DA concentrations in the striatum at 4 h, but these mice had significantly greater striatal DA concentrations at 8 h following MPTP treatment compared to WT mice. A recovery of DA concentrations in the striatum following an acute injection of MPTP is not apparent up to at least 32 h following administration in WT mice (Behrouz et al., 2007). These findings indicate that MPP+ is initially inducing a similar depletion in vesicular DA at the NSDA axon terminal presumably due to vesicular displacement of DA from synaptic storage vesicles by MPP+ (Reinhard et al., 1987; Liu et al., 1992) in

both WT and CB1/CB2 KO mice. However, the mechanisms that underlie persistent depletion in NSDA neurons terminating in the striatum of WT mice is lacking in CB1/CB2 KO mice.

DA metabolite concentrations in the striatum were significantly decreased following MPTP treatment consistent with a reduction in metabolism of DA, likely due to less uptake of DA at these time points through competition with MPP+ for DAT (Barc et al., 2002), or conversion of MPTP to MPP+ by mitochondrial MAO in NSDA axon terminals (Takamidoh et al., 1987). The DOPAC/DA and HVA/DA ratios indicated variable findings in regard to activity of NSDA neurons; NSDA neurons in WT mice had increased or lack of a change of their activity, while NSDA neurons in CB1/CB2 KO mice had reduced or no difference in their activity following acute MPTP administration. Since MPTP treatment alters DA metabolism through direct enzyme competitive inhibition, changes in metabolite levels do not accurately reflect neuronal activity in this experiment.

The recovery of MPTP induced DA depletion in CB1/CB2 KO mice in the acute MPTP model suggests that lack of CB receptors is beneficial in an animal model of PD. However, the acute model is not ideal to study the chronic effects of neurotoxin administration in CB1/CB2 KO mice. Accordingly, mice were repeatedly injected with MPTP following the sub-chronic MPTP model paradigm which induces a loss in NSDA neuronal terminals by 3 days following the last of 5 MPTP injections (Drolet et al., 2004).

Consistent with a previous report demonstrating that CB1 KO mice are resistant to severe MPTP treatment (Price, 2007), results from the present study reveal that

CB1/CB2 KO mice are partially resistant to sub-chronic MPTP induced striatal DA depletion compared to WT mice. This result was accompanied by a similar loss in striatum TH protein in both WT and CB1/CB2 KO mice. These results suggest that CB1/CB2 KO mice have a similar loss of NSDA axon terminals in the striatum in response to repeated MPTP administration, but that the DA storage capacity may be greater in the remaining unlesioned neurons in CB1/CB2 KO mice. If this is the case, then ECB may play a role in vesicular synthesis and/or re-cycling in NSDA neurons.

The DOPAC/DA ratio in the striatum shed some light on interpretation of these findings since this ratio is increased following sub-chronic MPTP treatment for WT mice, but was not altered in CB1/CB2 KO mice. This would suggest that CB1/CB2 KO mice have reduced activity of remaining NSDA neurons, which would explain a greater pool of vesicular DA. The ability of CB agonists acting via a CB1 receptor mediated mechanism to induce an increase in the firing of NSDA neurons and subsequent release of DA (French et al., 1997; Melis et al., 2000; Morera-Herreras et al., 2008), would agree with a lack of CB1 receptors leading to reduced activity of NSDA neurons. It is possible that either a lack of or inhibition of CB1 or CB2 receptors could therefore reduce the activity of NSDA neurons seen with MPTP treatment, thereby attenuating the progressive loss of remaining NSDA neurons.

The number of NSDA neuronal cell bodies was also determined in the substantia nigra along with the protein content of TH within the ventral midbrain containing the substantia nigra. The number of TH neuronal cell bodies within the substantia nigra was similar between saline and sub-chronic MPTP treated mice for both WT and CB1/CB2 KO, indicating that NSDA neuronal cell bodies are still intact. This corresponds to other

studies which have shown that MPTP does not induce a loss of NSDA neurons 3 days post treatment (Petroske et al., 2001). The significant loss in TH observed with sub-chronic MPTP treatment in WT mice suggests that TH protein expression may be decreasing at this time point, but as determined by cell counts the number of NSDA neuronal cell bodies is still intact.

The inhibition of CB1 and/or CB2 receptors using the pharmacological CB receptor antagonists rimonabant and SR144528 in the presence of sub-chronic MPTP treatment was done to determine which receptor type was responsible for the resistance to MPTP induced DA depletion. The dosages of antagonists administered were chosen based on previous studies which used these CB antagonists to effectively block CB induced effects (Diana et al., 1998; Giuffrida et al., 1999; Ferrer et al., 2007; Melis et al., 2007; Paldyova et al., 2007; Russo et al., 2007). However, CB1 or CB2 receptor blockade alone or in combination did not alter sub-chronic MPTP induced DA depletion. The implications of these findings is that a lack of CB1 and CB2 receptors may not be the underlying reason for attenuation of DA depletion in the striatum. Instead, other possible reasons for these findings are differential ability of MPP+ to inhibit the activity of Complex I, a reduction in conversion of MPTP to MPP+, or epigenetic alterations in CB1/CB2 KO mice inducing a neuroprotective mechanism.

The first possibility was addressed by measuring Complex I activity using an *in vitro* assay system (Janssen et al., 2007), in striatal homogenates of WT and CB1/CB2 KO mice treated with a single injection of MPTP 4 or 8 h prior to decapitation. If Complex I activity were initially reduced in CB1/CB2 KO mice this could explain the resistance to MPTP induced DA depletion, because MPP+ would not be able to induce as

a great a reduction in enzyme activity. However, Complex I activity was similar in saline treated WT and CB1/CB2 KO mice ruling out this possibility. Inhibition of Complex I activity by MPP+ could not be detected 4 and 8 h following MPTP treatment, possibly due to limited sensitivity of the assay system. Therefore, this assay system could not be used to evaluate if there was differential inhibition of Complex I by MPP+ in CB1/CB2 KO mice.

Differential susceptibility to MPTP could be due to diminished conversion of MPTP to MPP+ in the striatum of CB1/CB2 KO mice. MPP+ concentrations in the striatum of WT and CB1/CB2 KO mice were determined at several time points following MPTP administration to test for this possibility. Indeed, CB1/CB2 KO mice had lower concentrations of MPP+ within the striatum which could explain the resistance to MPTP. However, the reduction in MPP+ concentration in CB1/CB2 KO mice is significant but quite small suggesting that the dramatic recovery from acute MPTP injection or resistance to sub-chronic MPTP induced DA depletion in the striatum is likely due to another underlying mechanism.

One possible explanation for the CB1/CB2 KO mice resistance to MPTP treatment is an upregulation in the opioid system. Opioids like ECB can also increase NSDA neuronal activity (Alper et al., 1980; Melis et al., 2000). The levels of mRNA for opioid peptide precursors and activity of opioid receptors within the striatum are increased in CB1 KO mice (Steiner et al., 1999; Uriguen et al., 2005; Gerald et al., 2006), suggesting that an upregulation in opioid system activity could be a viable mechanism which explains the resistance seen in CB1/CB2 KO mice. Opioid system activity is enhanced in animal models of PD and in PD patients (Samadi et al., 2006), similar to the

ECB system. Opioids such as enkephalin and dynorphin, are neuropeptides which can be released by GABAergic striatonigral or striatopallidal medium spiny neurons projecting from the striatum, and can inhibit GABA release (Steiner and Gerfen, 1998), also similar to the effects of ECB. These findings therefore make it plausible that CB1/CB2 KO mice have an enhancement of opioid system activity leading to resistance to MPTP.

The content of various proteins associated with microglial activation (p67Phox), PD (alpha-synuclein and parkin), and crosstalk between D2 and CB receptors in the striatum (DARPP-32) was evaluated following an acute MPTP injection. Lack of a change in p67Phox protein content is not surprising since NSDA axonal terminals are likely not lost this early after MPTP, but rather are depleted of DA (Reinhard et al., 1987) (Liu et al., 1992; Behrouz et al., 2007). Surprisingly CB1/CB2 KO mice had higher basal levels of alpha-synuclein which were decreased following MPTP treatment, whereas alpha-synuclein was unchanged in WT mice. No relationship between ECB and alpha-synuclein has been established, and higher basal levels of alpha-synuclein could be a spurious finding especially since levels of this protein between WT and CB1/CB2 KO MPTP treated mice are not different. In agreement levels of other PD-related proteins including parkin and DARPP-32 which were not different between WT or CB1/CB2 KO mice.

The potential effects of MPTP treatment on MLDA axon terminal integrity and/or activity in CB1/CB2 KO mice was evaluated in both the acute and sub-chronic MPTP models. MLDA neurons are more resistant to MPTP treatment compared to NSDA neurons, which is also seen in PD with MLDA neurons less affected than NSDA neurons

(Uhl et al., 1985; Sundstrom et al., 1990; Behrouz et al., 2007). Interestingly, CB1/CB2 KO mice are resistant to acute MPTP induced DA depletion in the nucleus accumbens, which was accompanied by an attenuated reduction in DOPAC concentrations. These findings are similar to those seen in the striatum with acute MPTP treatment indicating that dopaminergic neurons in CB1/CB2 KO mice appear to more readily recover from the MPTP insult.

In the sub-chronic MPTP model sparing of MLDA axon terminals is more apparent as DA concentrations are not changed in WT or CB1/CB2 KO mice. Although DOPAC concentrations were reduced in CB1/CB2 KO mice in the nucleus accumbens, the DOPAC/DA ratio was not altered with MPTP treatment in either WT or CB1/CB2 KO mice indicating that MLDA neuronal activity was unaffected by MPTP treatment 3 days following conclusion of MPTP treatment. CB antagonist administration concurrent with sub-chronic MPTP treatment also failed to induce a loss in DA concentrations except in the presence of MPTP and SR144528, although the activity of MLDA neurons was not affected by the either CB antagonists or MPTP as indicated by the DOPAC/DA ratio. These results would support previous finding that MLDA neurons are more resistant to MPTP induced DA depletion than NSDA neurons (Sundstrom et al., 1990).

The effects of acute and sub-chronic treatment of MPTP on TIDA neurons were also evaluated in WT and CB1/CB2 KO mice. Acute MPTP treatment typically induces a transient loss in median eminence DA concentrations with recovery occurring after a few hours (Behrouz et al., 2007), whereas sub-chronic MPTP treatment fails to induce a long term loss in DA concentrations (Behrouz et al., 2007). In agreement, in the present study acute MPTP treatment of WT mice caused a transient decrease in median eminence

DA concentrations with recovery by 8 h, but not in CB1/CB2 KO mice. However a decrease in DOPAC concentrations and the DOPAC/DA ratio in WT and CB1/CB2 KO mice indicated that TIDA neurons were still affected by MPTP, but were able to maintain normal DA concentrations in the median eminence.

Sub-chronic MPTP treatment as expected did not effect the TIDA neuron integrity or activity. However, CB1/CB2 KO mice had significantly higher median eminence DA concentrations than WT mice, which was likely the reason DA concentrations in MPTP treated mice were lower. A lack of any change in the DOPAC/DA ratio with MPTP treatment in WT or CB1/CB2 KO mice is consistent with the conclusion that higher DA concentrations in saline treated mice was likely a spurious result. These findings would be further supported by CB antagonist treatment lacking an effect on DA concentrations or the activity of TIDA neurons with MPTP treatment.

Serotoninergic neuronal activity was evaluated following acute MPTP treatment in the striatum and nucleus accumbens. 5HT neurons are typically only affected long term when exposed to very high dosing regimens of MPTP (Hallman et al., 1985; Date et al., 1990; Rousselet et al., 2003). Interestingly, 5HT concentrations were significantly increased in CB1/CB2 KO mice following MPTP injection in the nucleus accumbens (but not the striatum), which was not accompanied by a change in 5HIAA concentrations. However, a significant decrease in the activity of serotoninergic neurons terminating in both the striatum and nucleus accumbens of CB1/CB2 KO mice suggests that CB receptors may contribute to resistance of serotoninergic neurons to MPTP reduction of activity.

In conclusion, the resistance to MPTP induced DA depletion in the striatum of CB1/CB2 KO mice in the sub-chronic model and recovery in the acute model suggested that CB1 and/or CB2 receptors may contribute to the MPTP induced loss of NSDA axon terminals. However, inhibition of these respective receptors individually or simultaneously failed to pharmacologically recapitulate the resistance to MPTP seen in CB1/CB2 KO mice. It is possible that CB1/CB2 KO mice have reduced Complex I activity or conversion of MPTP to MPP+, but differential Complex I activity was not responsible for the resistance and reduced MPP+ production from MPTP is not likely to be the primary mechanism for resistance since CB1/CB2 KO had only slightly less MPP+ within the striatum following MPTP administration compared to WT mice. The possibility exists that an enhancement in the opioid system in CB1/CB2 KO mice could be a potential mechanism responsible for resistance to MPTP treatment, since CB1 KO mice have increased opioid receptor activity and mRNA for opioid precursor peptides (Steiner et al., 1999; Uriguen et al., 2005; Gerald et al., 2006).

Interestingly, CB1/CB2 KO mice were also resistant to the acute effects of MPTP on MLDA and TIDA neurons, and serotoninergic neurons have reduced activity in the face of this same MPTP treatment paradigm. These results suggest that MPTP does affect several populations of neurons, but that lasting effects on these populations is relatively limited to NSDA neurons.

Chapter 7: Lipopolysaccharide Activation of Microglia as an Inflammatory Model of PD in Wildtype and CB1/CB2 Receptor KO Mice

A. Introduction

Lipopolysaccharide (LPS) can be used as a selective inflammatory model of PD because of its inability to directly induce the death of NSDA neurons like other neurotoxin models (Qin et al., 2004). LPS activates microglia by binding the Toll Like Receptor-4 (TLR-4) that frees the transcription factor nuclear factor-κB (NFκB) from a cytoplasmic binding protein. NFκB translocates to the nucleus inducing the production of free radical species and transcription of pro-inflammatory cytokines (Doyle and O'Neill, 2006).

The LPS induced production of free radical species can be attributed to NFκB activation of the enzyme NADPH oxidase which produces the ROS superoxide (Doyle and O'Neill, 2006). Superoxide is a relatively unstable ROS incapable of crossing the cellular membrane, but other ROS such as hydrogen peroxide and hydroxyl radical can be formed from NADPH oxidase derived superoxide (Sumimoto et al., 2005). These secondary ROS produced from superoxide have been implicated in a number of processes including microglial proliferation, pro-inflammatory cytokine release, and induction of iNOS leading to the production of nitric oxide (Pawate et al., 2004; Jekabsone et al., 2006; Mander et al., 2006).

The pro-inflammatory cytokines induced by LPS directly, or indirectly through superoxide production, include TNF-α and IL-1β. TNF-α can induce activation and recruitment of other microglial cells to the site of inflammation (Block and Hong, 2005).

TNF-α can also act in an autocrine manner on receptors on the cell from which it was released inducing further activation of NFκB which contributes to the process of microgliosis (Kariko et al., 2004; Doyle and O'Neill, 2006). The superoxide induced production of reactive nitrogen species such as nitric oxide in the presence of superoxide can lead to the formation of peroxynitrite. Nitric oxide and peroxynitrite both are capable of inhibiting the mitochondrial respiratory chain (Ebadi and Sharma, 2003). Peroxynitrite has been implicated in NSDA neuronal death (Tieu et al., 2003), suggesting that NADPH oxidase is a key enzyme involved in microglial derived NSDA neuronal death induced by LPS and making LPS an ideal method to study inflammation induced loss of NSDA neurons.

Several methods of administration of LPS *in vivo* have been used to induce inflammation within the substantia nigra including direct stereotaxic injection into the substantia nigra (intra-nigral), striatum, or peripheral injection of LPS into the peritoneal cavity. Intra-nigral administration of LPS is ideal in that it induces a relatively localized inflammation in the ventral midbrain that contains the highest percentage of microglial cells in the brain (Kim et al., 2000). LPS delivered into the substantia nigra induces an increase in the number of amoeboid activated microglia, pro-inflammatory cytokines, and iNOS protein that leads within days to a decrease in the number of NSDA neuronal cell bodies within the substantia nigra and DA concentrations in the striatum (Castano et al., 1998; Gao et al., 2002b; Iravani et al., 2002; Arimoto and Bing, 2003; Zhou et al., 2005). The percentage of NSDA neuronal cell body loss or extent of DA depletion from axon terminals varies by length of time following injection, dosage of LPS, and whether it is an acute injection or a chronic infusion of LPS (Castano et al., 1998; Liu et al., 2000b;

Gao et al., 2002b; Arai et al., 2004; Qin et al., 2004; Iravani et al., 2005). The intra-nigral LPS induced loss of NSDA neurons appears to be rather selective since serotoninergic neuronal terminals in the striatum appear to be only minimally affected or not affected at all (Castano et al., 1998, 2002; Hsieh et al., 2002). The increased vulnerability of NSDA neurons to LPS likely results from the reduced anti-oxidant ability of these neurons (Fitzmaurice et al., 2003).

The advantage of intra-nigral injection of LPS is that the LPS stimulates microglia within the cell body region of NSDA neurons in addition to increasing the number of microglial cells within this region. However, LPS injection into the striatum can also induce a severe loss of NSDA neuronal terminals and cell bodies which is accompanied by an increase in iNOS in the striatum and activation of microglia in the striatum and substantia nigra (Zhang et al., 2006b; Hunter et al., 2007).

Unlike stereotaxic injection into the substantia nigra or striatum, peripheral administration of LPS induces a widespread inflammatory reaction throughout the brain. The reaction is likely initiated by cytokine stimulation from outside the blood brain barrier, as LPS does not cross the blood brain barrier except at extremely high concentrations (Singh and Jiang, 2004; Qin et al., 2007). Peripheral LPS treatment induces an increase in TNF-α, IL-6, and iNOS mRNA and/or protein within hours following injection (Pitossi et al., 1997; Singh and Jiang, 2004; Cunningham et al., 2005; Qin et al., 2007). However, rapid induction of inflammation within the brain following peripheral LPS treatment does not induce a significant decrease in the number of TH cells until approximately 7 months following a single injection (Qin et al., 2007). This finding does not rule out the possibility that acute inflammation will not affect dopaminergic

neuronal function because acute LPS treatment increases the activity of dopaminergic neurons and TH, decreases DA in the striatum, increases the DA/DOPAC ratio in the medial basal hypothalamus, and increases DA release into the anterior pituitary (Dunn, 1992; Cho et al., 1999; De Laurentiis et al., 2002). This fact makes the peripheral LPS model an alternative method to study the affects of acute inflammatory reactions on dopaminergic neurons.

An anti-inflammatory role of CB receptors has been suggested on the basis of the observation that LPS activation of microglial cells and pro-inflammatory cytokine and free radical species production is reduced following activation of these receptors (Franklin and Stella, 2003; Walter et al., 2003; Carrier et al., 2004; Ehrhart et al., 2005; Eljaschewitsch et al., 2006; Fernandez-Lopez et al., 2006). However, increases in ECB concentrations following inhibition of metabolism or blockade of reuptake increases peripheral LPS induced plasma TNF-α concentrations more than LPS alone which was reversed in the presence of a CB1 or a CB2 antagonist (Roche et al., 2008), suggesting that ECB may also be pro-inflammatory.

CB1 and CB2 receptors are both expressed by microglial cells in the brain, although CB2 receptors have been implicated in most of the beneficial effects of CB (Begg et al., 2005; Ehrhart et al., 2005). CB2 receptors are also upregulated in activated microglial cells following LPS treatment *in vitro* and *in vivo* under neuropathological states such as multiple sclerosis, hypoxic stroke, Alzheimer's disease, and amyotrophic lateral sclerosis (Benito et al., 2003; Maresz et al., 2005; Mukhopadhyay et al., 2006; Yiangou et al., 2006; Ashton et al., 2007), and are involved in microglial migration. A

lack of CB receptors may or may not be beneficial for dopaminergic neurons in the face of acute inflammation based on this information.

Hypothesis #1: Injection of LPS into the substantia nigra of mice will activate microglia and induce a loss of NSDA neuronal cell bodies and axon terminals.

This hypothesis was tested by examining:

1) The concentrations of DA and DOPAC on each side of the striatum and the DOPAC/DA ratio to evaluate the integrity of NSDA axon terminals and the activity of NSDA neurons following LPS treatment.

2) The number of TH immunoreactive cells and the protein content of TH within the substantia nigra unilaterally to determine if LPS induced a loss of NSDA cell bodies.

3) Microglial NADPH oxidase activation by determining the protein content of membrane bound p67Phox in the unilateral substantia nigra of mice injected with LPS.

Hypothesis #2: Acute peripheral LPS treatment of WT and CB1/CB2 KO mice will alter dopaminergic neuronal integrity or neuronal activity.

This hypothesis was tested by determining:

1) The concentrations of DA in the striatum, nucleus accumbens, and median eminence to evaluate the integrity of NSDA, MLDA, and TIDA neuronal terminals following LPS treatment.

2) The ratio of the concentrations of DOPAC to DA in the striatum, nucleus accumbens, and median eminence to examine the activity of NSDA, MLDA, and TIDA neurons.

B. Materials and Methods

Male C57BL/6 mice (Jackson Labs) were used for the intra-nigral LPS study and as WT controls for CB1/CB2 KO mice for the peripheral LPS study. Male CB1/CB2 KO mice were obtained from a breeding colony at MSU for the peripheral LPS experiment. Intra-nigral administration of PBS vehicle or LPS (2.5, 5, or 10 ug per mouse) was done using a stereotaxic apparatus as described (Chapter 2, Section B, Drugs). Briefly, mice were sedated with 50 mg/kg Ketamine/2.5 mg/kg Xylazine, anesthetized with isoflurane, and positioned in a stereotaxic apparatus. The stereotaxic coordinates at Bregma were determined and either PBS or LPS was stereotaxically injected into the left substantia nigra at +1.3 mm (lateral/medial plane), -3.0 mm (anterior/posterior plane), -4.7 mm (dorsal/ventral plane) with regard to Bregma (Franklin and Paxinos, 1996). LPS was obtained from escherichia coli O111:B4 (Catalog #: L3012-10 mg, Batch #: 067K4139, Sigma Aldrich). Mice were killed either by decapitation for neurochemistry and Western blot analysis, or perfused with 4% paraformaldehyde for immunohistochemistry analysis of TH immunoreactive cells 14 days following surgery as described (Chapter 2, Section C, Brain Tissue Preparation).

Neurochemical analysis of DA and DOPAC and Western blot analysis of TH and p67Phox protein content was done as described (Chapter 2, Section D, Assay of Amines, Amine Metabolites, and Apocynin in Brain Tissue and Section G, Western Blot Analysis). The brains from mice perfused for immunohistochemical analysis of TH immunoreactive cells in the substantia nigra were sectioned, stained for TH, and cell numbers counted using an unbiased stereology method as described (Chapter 2, Section H, Immunohistochemistry and Stereology Cell Counts).

LPS obtained from escherichia coli O111:B4 (Catalog # L3012-5 mg, Batch #: 047K4089, Sigma-Aldrich) was administered to WT and CB1/CB2 KO mice for the peripheral LPS experiment. Mice received either 0.9% NaCl vehicle or LPS 5 mg/kg body weight administered in a 0.5 mg/mL LPS solution via i.p. injection 1 h prior to decapitation. Brains were removed following decapitation, sectioned, and prepared for HPLC-EC analysis of DA and DOPAC in the striatum, nucleus accumbens, and median eminence as described (Chapter 2, Section D, Assay of Amines, Amine Metabolites, and Apocynin in Brain Tissue).

C. Results

Lack of an Effect with Intra-nigral LPS Treatment

Mice were stereotaxically injected with either PBS vehicle or LPS (2.5, 5, or 10 ug in a volume of 0.6 uL) unilaterally into the left substantia nigra and killed 14 days following injection of PBS or LPS. DA concentrations were measured in the striatum of the ipsilateral and contralateral side to the injection as an index of NSDA neuronal terminal integrity. As shown in Figure 7-1(Panel A), DA concentrations were not significantly different between the ipsilateral and contralateral sides in mice injected with PBS or LPS (2.5, 5, or 10 ug), indicating a lack of LPS induced axon terminal loss of NSDA neurons with either PBS or LPS treatment.

The DOPAC concentrations and the DOPAC/DA ratio were measured unilaterally in the striatum of PBS and LPS treated mice to determine if stereotaxic injection of PBS or LPS altered the activity of NSDA neurons. Injection of PBS unilaterally into the substantia nigra did not alter DOPAC concentrations or the DOPAC/DA ratio compared to the contralateral side. Similarly LPS (2.5, 5, or 10 ug) injection did not alter DOPAC concentrations or the DOPAC/DA ratio compared to the contralateral side indicating that LPS did not alter the activity of NSDA neurons (Figure 7-1; Panels B and C).

NSDA neuronal cell body integrity was evaluated since LPS injection into the substantia nigra may be more apt initially to induce a loss in cell bodies versus axon terminals since the cell bodies of NSDA neurons were located at the site of LPS injection. TH immunoreactive neurons within the substantia nigra were counted using the unbiased stereology optical fractionater method and revealed a lack of any change in the number of

NSDA neuronal cell bodies within the unilateral injected substantia nigra in the presence or absence of PBS or LPS treatment (Figure 7-2).

NSDA neuronal cell body integrity was also evaluated by examining TH protein content in the ipsilateral and contralateral substantia nigra of PBS and LPS treated mice. TH protein content within the substantia nigra was not changed with PBS or LPS injection (Figure 7-3).

The protein content of the NADPH oxidase cytosolic subunit p67Phox was measured in the substantia nigra to determine if LPS induced an increase in p67Phox protein content in the cytosolic fraction as a consequence of microglial activation. Surprisingly, the protein content of p67Phox was significantly increased on the ipsilateral side of the substantia nigra of PBS treated mice. In contrast, p67Phox was not altered in the ipsilateral side of the substantia nigra of LPS treated mice (Figure 7-4), suggesting a lack of microglial activation with LPS intra-nigral administration.

A.

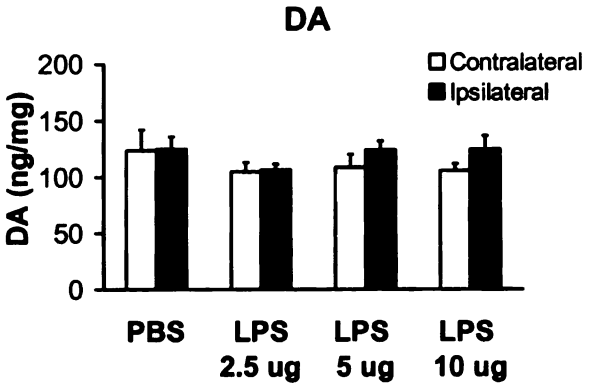

B.

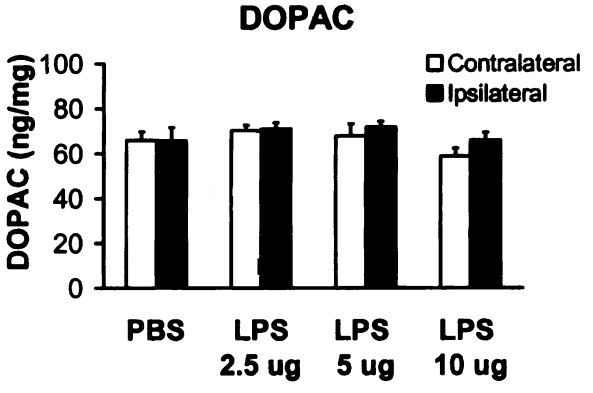

C.

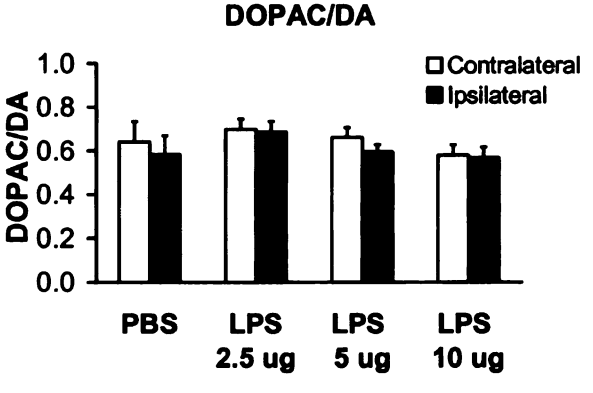

Figure 7-1. Ipsilateral and contralateral concentrations of DA and DOPAC and the DOPAC/DA ratio in the striatum of mice injected unilaterally with PBS or LPS into the substantia nigra. Mice were stereotaxically injected with either PBS vehicle or LPS 2.5, 5, or 10 ug in a volume of 0.6 uL into the left substantia nigra and decapitated 14 days following PBS or LPS administration. Concentrations of DA (Panel A) and DOPAC (Panel B), and the DOPAC/DA ratio (Panel C) in the contralateral and ipsilateral striatum, n=10. Columns represent means and bars one SEM.

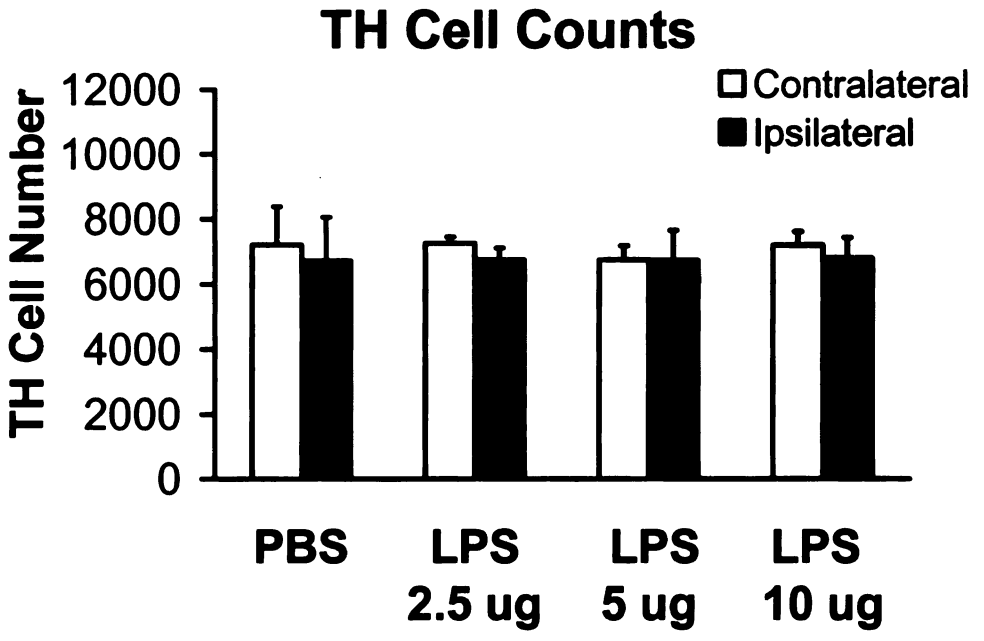

Figure 7-2. TH cell numbers in the contralateral and ipsilateral substantia nigra of mice injected unilaterally with either PBS or LPS into the substantia nigra. Mice were stereotaxically injected with either PBS vehicle or LPS 2.5, 5, or 10 ug in a volume of 0.6 uL into the left substantia nigra and perfused 14 days following PBS or LPS administration. The number of TH cells within each side of the substantia nigra were counted using an unbiased stereology method, n=3-4. Columns represent means and bars one SEM.

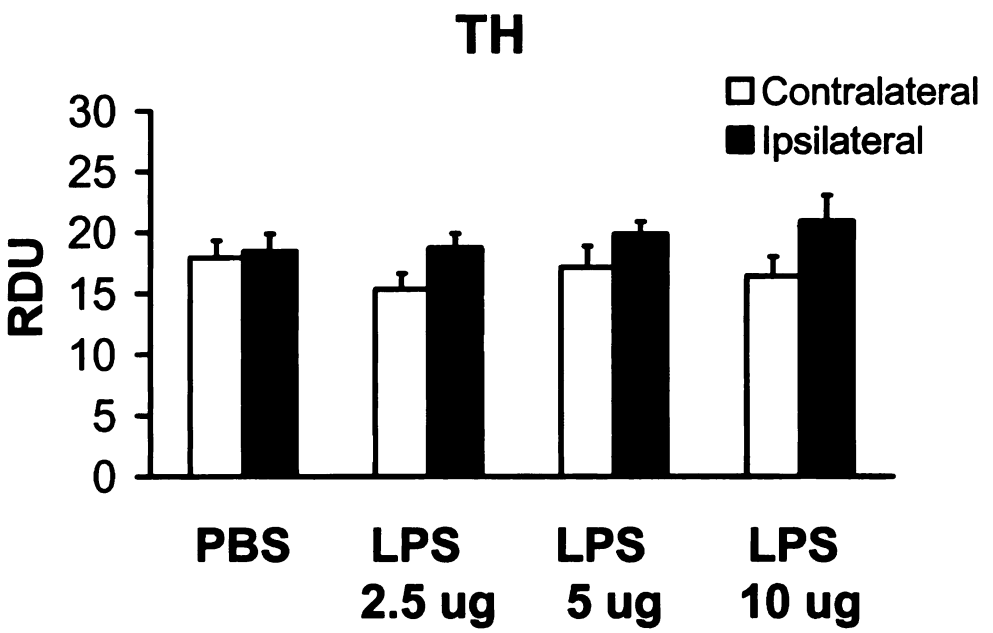

Figure 7-3. TH protein content in the contralateral and ipsilateral substantia nigra of mice injected with either PBS or LPS. Mice were stereotaxically injected with either PBS vehicle or LPS 2.5, 5, or 10 ug in a volume of 0.6 uL into the left substantia nigra and decapitated 14 days later. TH protein content was normalized to GAPDH and multiplied by a factor of 100 and expressed as RDU, n=10. Columns represent means and bars one SEM.

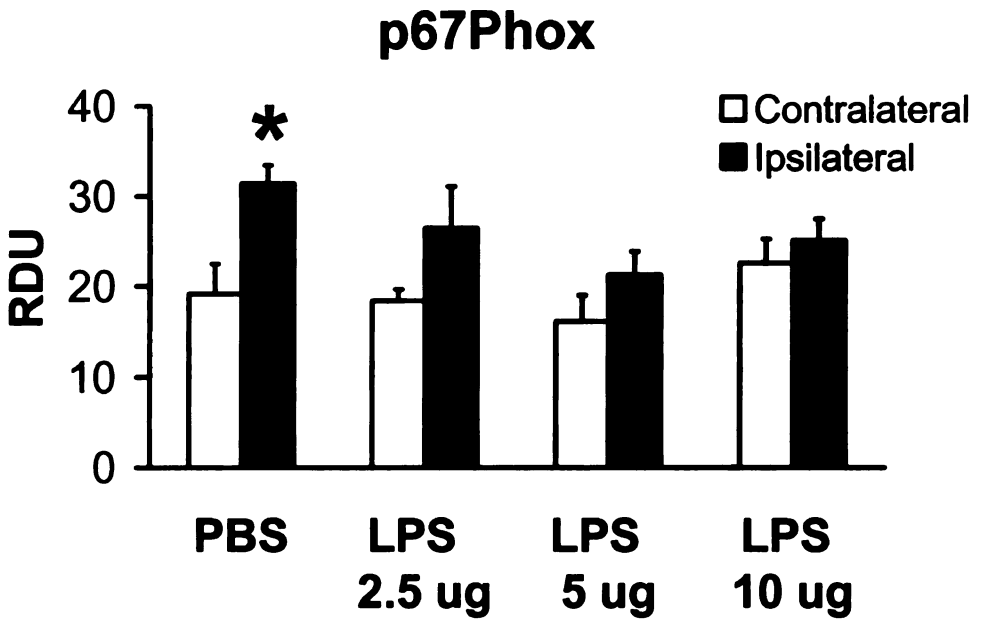

Figure 7-4. Cytosolic p67Phox protein content in the contralateral and ipsilateral substantia nigra of mice injected with either PBS or LPS. Mice were stereotaxically injected with either PBS vehicle or LPS 2.5, 5, or 10 ug in a volume of 0.6 uL into the left substantia nigra and decapitated 14 days later. p67Phox protein content was normalized to GAPDH and multiplied by a factor of 1,000 and expressed as RDU, n=9-10. Columns represent means and bars one SEM. *Values for ipsilateral substantia nigra which were significantly different from the contralateral side within a treatment group, $p \leq 0.05$.

The Effects of Peripheral LPS Administration

Peripheral i.p. administration of LPS induces an acute inflammatory reaction within the brain in 1 h, as demonstrated by an elevated cytokine profile (Qin et al., 2007). CB reduce inflammation in brain tissue *in vitro* via a CB2 receptor mediated mechanism (Ehrhart et al., 2005). The potential effects that an acute peripheral injection of LPS (5 mg/kg, i.p.) could have on dopaminergic integrity and activity was therefore examined in WT and CB1/CB2 KO mice 1 h following LPS administration. Dopaminergic neuronal populations evaluated included NSDA, MLDA, and TIDA neurons.

DA concentrations in the striatum were measured in WT and CB1/CB2 KO mice injected with either saline vehicle or LPS. WT and CB1/CB2 KO mice treated with saline vehicle had similar DA concentrations in the striatum as shown in Figure 7-5 (Panel A), and these values were not changed following LPS treatment. CB1/CB2 KO mice treated with LPS had slightly less DA than WT mice treated with LPS. These results indicate that acute LPS treatment does not alter NSDA axonal integrity in WT or CB1/CB2 KO mice.

The activity of NSDA neurons was examined by determining DOPAC concentrations and the DOPAC/DA ratio in the striatum of WT and CB1/CB2 KO mice treated peripherally with saline vehicle or LPS. DOPAC concentrations in the striatum of WT and CB1/CB2 KO mice treated with LPS did not change (Figure 7-5; Panel B). The DOPAC/DA ratio was slightly higher in the striatum of CB1/CB2 KO mice treated with saline or LPS compared to the respective treated WT group (Figure 7-5; Panel C). LPS treatment did not alter the DOPAC/DA ratio in either WT or CB1/CB2 KO mice.

DA and DOPAC concentrations were also measured in the nucleus accumbens of WT and CB1/CB2 KO mice to evaluate MLDA axon terminal integrity and activity. DA and DOPAC concentrations were not changed with acute LPS injection within either WT or CB1/CB2 KO mice (Figure 7-6; Panels A & B). CB1/CB2 KO mice did have elevated concentrations of both DA and DOPAC in the nucleus accumbens in the presence or absence of LPS compared to WT mice. The DOPAC/DA ratio was similar between WT and CB1/CB2 KO mice treated with saline, but was significantly increased in the nucleus accumbens of WT (but not CB1/CB2 KO) mice treated with LPS (Figure 7-6; Panel C).

TIDA neuronal integrity and activity were also examined in WT and CB1/CB2 following acute LPS injection. DA and DOPAC concentrations in the median eminence were not different in saline treated WT and CB1/CB2 KO mice (Figure 7-7; Panels A & B). The DOPAC/DA ratio in the median eminence was also similar in WT and CB1/CB2 KO mice treated with saline, but was significantly increased by LPS in both WT and CB1/CB2 KO mice (Figure 7-7; Panel C).

A.

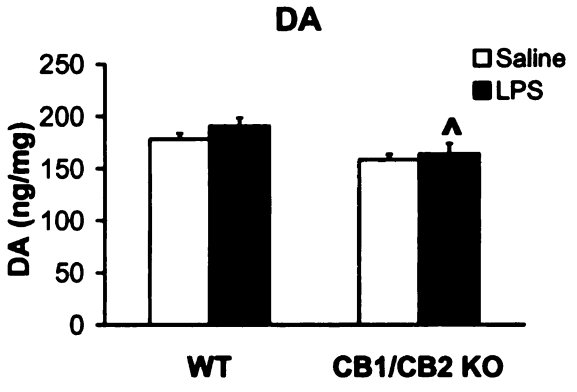

B.

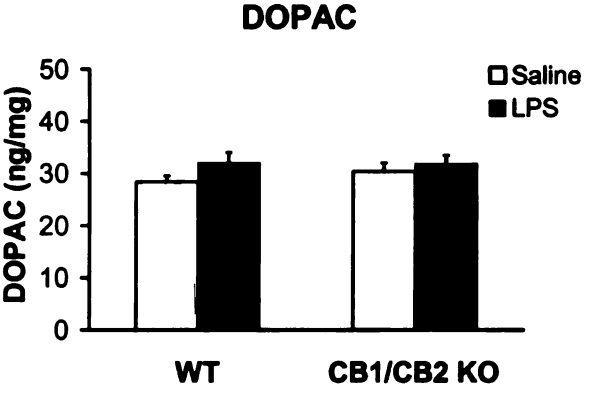

C.

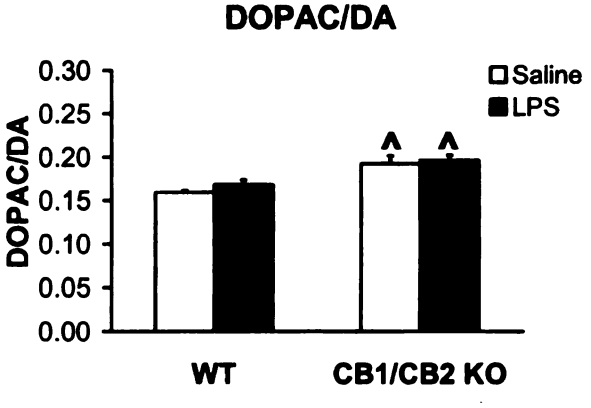

Figure 7-5. Concentrations of DA, DOPAC, and the DOPAC/DA ratio in the striatum of WT and CB1/CB2 KO mice following peripheral LPS administration. WT and CB1/CB2 KO mice were treated with either saline or LPS (5 mg/kg, i.p.) 1 h prior to decapitation. Concentrations of DA (Panel A) and DOPAC (Panel B), and the DOPAC/DA ratio (Panel C) in the striatum, n=8-9. Columns represent means and bars one SEM. ^Significant difference between WT and CB1/CB2 KO mice within a treatment group, $p \leq 0.05$.

A.

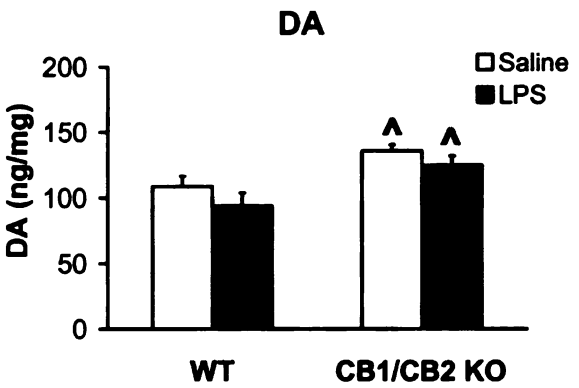

B.

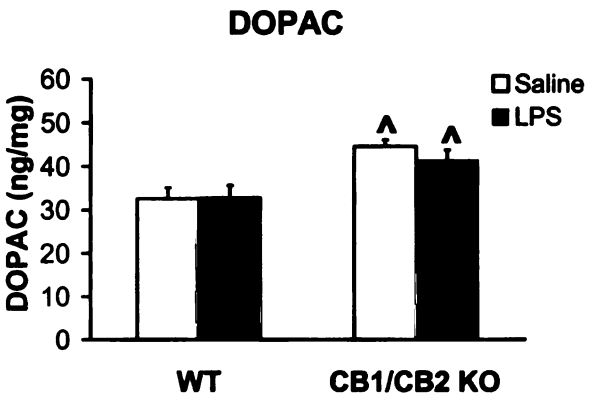

C.

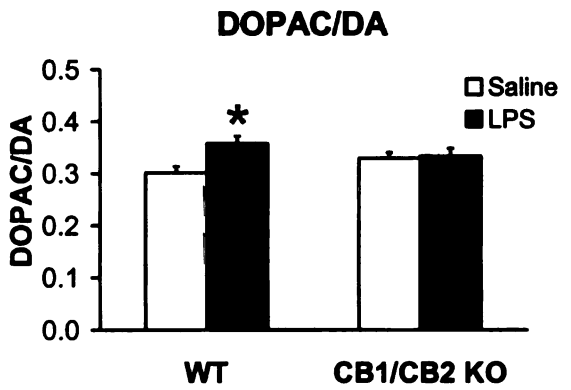

Figure 7-6. Concentrations of DA, DOPAC, and the DOPAC/DA ratio in the nucleus accumbens of WT and CB1/CB2 KO mice following peripheral LPS administration. WT and CB1/CB2 KO mice were treated with either saline or LPS (5 mg/kg, i.p.) 1 h prior to decapitation. Concentrations of DA (Panel A), DOPAC (Panel B), and the DOPAC/DA ratio (Panel C) in the nucleus accumbens, n=8-9. Columns represent means and bars one SEM. ^Significant difference between WT and CB1/CB2 KO mice within a treatment group. *Significant difference between saline and LPS treated mice, $p \leq 0.05$.

A.

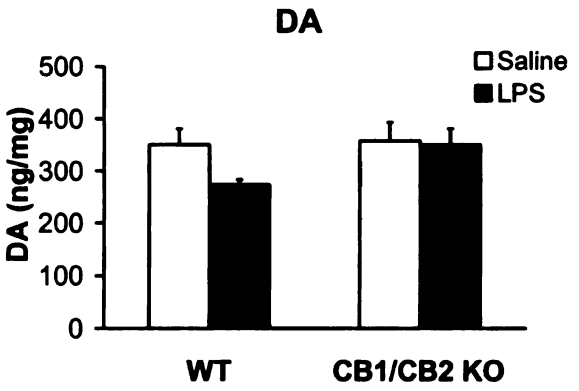

B.

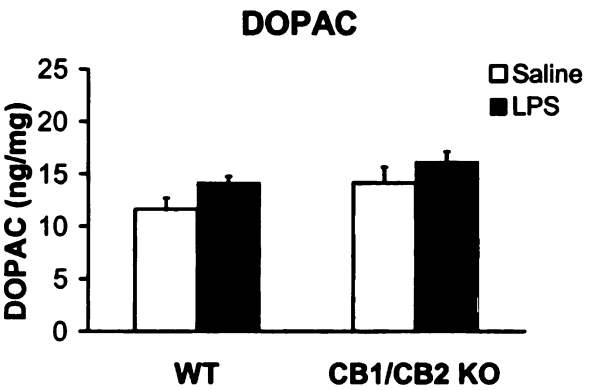

C.

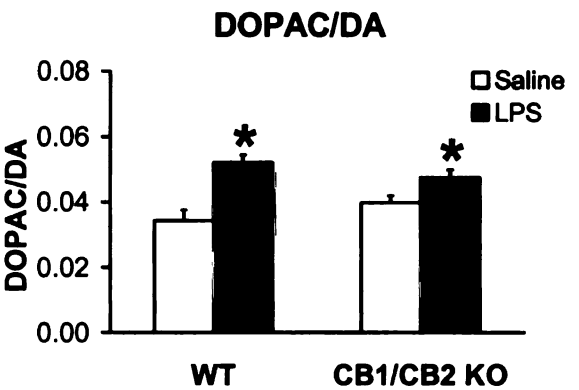

Figure 7-7. Concentrations of DA, DOPAC, and the DOPAC/DA ratio in the median eminence of WT and CB1/CB2 KO mice following peripheral LPS administration. WT and CB1/CB2 KO mice were treated with either saline or LPS (5 mg/kg, i.p.) 1 h prior to decapitation. Concentrations of DA (Panel A) and DOPAC (Panel B), and the DOPAC/DA ratio (Panel C) in the median eminence, n=7-10. Columns represent means and bars one SEM. *Significant difference between saline and LPS treated mice, $p \leq 0.05$.

D. Discussion

Intra-nigral administration of LPS has been used to study inflammatory mediated death of NSDA neurons and typically induces microglial activation and subsequent microglial mediated cell death of NSDA neurons (Castano et al., 1998; Gao et al., 2002b; Iravani et al., 2002; Arimoto and Bing, 2003; Zhou et al., 2005). The purpose of establishing this model was to use it to study potential neuroprotective anti-inflammatory drugs, thus avoiding the direct neurotoxicity properties that other PD models have. Results from this study where LPS (2.5, 5, or 10 ug) was unilaterally injected into the substantia nigra demonstrated a lack of NSDA neuronal cell body or terminal loss with LPS treatment. NSDA neuronal terminal integrity was not altered as reflected by DA concentrations in the striatum. NSDA neuronal cell body integrity was evaluated by determining the number of TH immunoreactive cells and total protein content of TH by Western blotting within the substantia nigra of the ipsilateral and contralateral sides to PBS vehicle or LPS administration. LPS treatment did not induce a loss of NSDA neuronal cell bodies or TH protein content within the substantia nigra of the ipsilateral side. The content of p67Phox was also measured unilaterally in the substantia nigra and was not altered with LPS treatment compared to the contralateral side of the substantia nigra. This finding suggests that the LPS likely did not induce activation of microglial cells when injected directly into the ipsilateral substantia nigra. However, the cytosolic p67Phox protein content was significantly increased with PBS administration on the ipsilateral side of the substantia nigra. This result was likely spurious given a lack of an increase in p67Phox on the ipsilateral side of LPS injected mice.

Failure of intra-nigral LPS administration to induce microglial activation and subsequent loss of NSDA neurons was unexpected. Studies showing that an acute intra-nigral LPS injection induces the loss of NSDA neurons demonstrate a loss in TH immunoreactive cells within the substantia nigra by 7 days following administration (Kim et al., 2000; Hsieh et al., 2002; Arai et al., 2004), and mice used in this study were killed 14 days following PBS or LPS administration. This would suggest that by 14 days LPS should have induced a significant lesion of NSDA neurons. However, the ability of LPS to induce inflammation can vary depending on the type of bacteria it was obtained from and the number of endotoxin units within each mg of LPS.

The structure of LPS consists of three parts; a lipid A region which attaches to the membrane of the bacteria, a core region linking the lipid A region to the third region, the O-specific chain which is highly diverse (Woltmann et al., 1998; Wiese et al., 1999; Caroff and Karibian, 2003). The biological activity of LPS is initiated by its lipid A region with the shape of the region effecting the ability of the LPS to induce an inflammatory reaction (Wiese et al., 1999). LPS possessing a conical shaped lipid A region such as that obtained from escherichia coli used in these studies induces an inflammatory reaction that is much greater than LPS having a cylindrical shape (Wiese et al., 1999). Each batch of LPS also has a fixed number of endotoxin units/weight of LPS, in which the higher the number of endotoxin units the greater the inflammatory reaction should be. Although, the LPS injected into the substantia nigra and peripherally in these studies were derived from separate batches of the same strain of escherichia coli, each had approximately 3 million endotoxin units/mg of LPS each, as determined by Sigma-Aldrich. Almost all studies published in the literature fail to report the number of

endotoxin units per/weight of LPS thus making it difficult to determine the correct dosage required to induce inflammation when using a batch of LPS that is different than what others have used.

LPS was administered peripherally as an alternative to intra-nigral LPS administration with the knowledge that peripheral LPS treatment at the 1 h time point induces a maximal increase in TNF-α concentrations within the brain compared to later time points (Qin et al., 2007). The activity of dopaminergic neurons within the brain is reported to be increased following acute peripheral LPS treatment (Dunn, 1992; De Laurentiis et al., 2002), suggesting that acute inflammation can effect the function of dopaminergic neurons. The ECB system is involved in the inflammatory reaction within the brain as CB can increase or decrease the inflammatory response of microglial cells (Ehrhart et al., 2005; Marchalant et al., 2007b; Marchalant et al., 2007a; Roche et al., 2008). Treatment of WT and CB1/CB2 KO mice with a peripheral LPS injection did not affect dopaminergic neuronal integrity but had differential effects on the NSDA, MLDA, and TIDA neuronal activity.

A localized inflammatory reaction by direct intra-nigral injection of LPS typically induces a significant inflammatory reaction and acute death of NSDA neurons versus peripheral induced inflammation where a loss of NSDA neurons is not seen until months later (Castano et al., 1998; Gao et al., 2002b; Iravani et al., 2002; Arimoto and Bing, 2003; Zhou et al., 2005). Peripheral LPS treatment induces a slight decrease in DA concentrations in the striatum at 6 and 24 h following LPS administration (Cho et al., 1999). The activity of NSDA neurons as indicated by the DOPAC/DA ratio was not altered with LPS treatment in WT or CB1/CB2 KO mice though suggesting that if

peripheral LPS treatment does affect dopaminergic activity it may do so at a later time point than at 1 h.

MLDA neuronal DA release and neuronal activity increases following peripheral LPS treatment (Borowski et al., 1998; Lacosta et al., 1999) which corresponds to an increase in the DOPAC/DA ratio in the nucleus accumbens of WT mice treated with LPS in this study. In contrast to WT mice, CB1/CB2 KO mice did not have an increase in MLDA neuronal activity suggesting that a lack of CB receptors reduces inflammatory mediated effects on these neurons. Since ECB have primarily been noted for anti-inflammatory effects on microglial cells this finding would contradict others, but CB can also increase plasma concentrations of TNF-α which is believed to be the primary mechanism by which peripheral LPS administration treatment induces brain inflammation (Ehrhart et al., 2005; Qin et al., 2007; Roche et al., 2008). An increase in TNF-α concentrations that is reversed in the presence of CB1 or CB2 antagonists would instead support the findings that, CB1/CB2 KO mice do not have an increase in MLDA neuronal activity with LPS treatment.

LPS induced inflammation induces a significant increase in the activity of TIDA neurons as indicated by an increase in the DOPAC/DA ratio in the median eminence (Lacosta et al., 1999; De Laurentiis et al., 2002). The release of the hormone prolactin is reduced following LPS treatment and may be due to an increase in TIDA neuronal activity since TIDA neurons inhibit the release of prolactin (De Laurentiis et al., 2002; Hollis et al., 2005). TIDA neuronal activity significantly increased with LPS in WT and CB1/CB2 KO mice, which is in agreement with previous findings (De Laurentiis et al., 2002). TIDA axon terminals reside outside of the blood brain barrier. Therefore, it is

possible that a peripheral inflammatory reaction may increase the activity of these neurons, whereas inflammatory mediators must cross the blood brain barrier in order to change the activity of NSDA neurons that completely reside within the brain.

In summary the lack of a loss in NSDA neuronal cells with intra-nigral LPS was surprising as intra-nigral LPS administration is reported to induce a loss of NSDA neuronal cell bodies and terminals over time. It is possible though that either the LPS used in this study did not successfully activate microglial cells or that the number of endotoxin units injected was to low to induce inflammation mediated loss of NSDA neurons. The use of the peripheral LPS model instead facilitated the investigation as to if acute inflammation affected dopaminergic neuronal function in the presence or absence of CB1 or CB2 receptors. CB1/CB2 KO mice indeed had either no change in activity with LPS treatment (MLDA neurons) in contrast to WT mice, or an increase in TIDA neuronal activity like WT mice with LPS peripheral administration. These results suggest that CB receptors may play a role in acute inflammation effects on dopaminergic neuronal activity.

Chapter 8: Concluding Remarks

PD is a debilitating neurodegenerative disease associated with the progressive loss of NSDA neurons. The progressive nature of DA neuronal loss allows remaining NSDA neurons to compensate for the loss of others, and explains the delayed diagnoses of PD which occurs generally when approximately 50-60% of NSDA neurons and 80% of DA has been depleted. PD is likely due to multiple causes of NSDA neuronal loss which include, but are not limited to; exposure to environmental toxins, mitochondrial dysfunction, oxidative stress, protein misfolding and aggregation, and inflammatory related damage to NSDA neurons.

The location of NSDA neurons makes these neurons especially vulnerable to oxidative stress and inflammation. These neurons are susceptible to increased endogenous oxidative stress due to oxidation of cytosolic DA to form DA quinones that bind and damage cellular proteins. NSDA neurons also contain iron which reacts with hydrogen peroxide to form ROS hydroxyl radicals which are highly reactive. When NSDA neurons die due to increased oxidative stress the cellular debris activates microglial cells within the SNpc. The ventral midbrain containing the SNpc has the highest number of microglia compared to other brain regions likely making this region more prone to an intense inflammatory reaction following loss of NSDA neurons. Once initiated, the inflammatory reaction can be self-amplifying leading to microgliosis. Microglial activation persists within the SNpc in PD patients and several animal models of the disease long after neurotoxin or inflammatory insult.

The challenge of developing neuroprotective therapies for PD has mainly focused on treatments that could either slow or halt the loss of remaining unlesioned NSDA

neurons. These targets include reducing oxidative stress and inflammation by inhibiting the production of free radical species and pro-inflammatory cytokines which continually induce the production of one another. Alternatively potential treatments to regenerate or replace NSDA neurons have been attempted to restore function of the NSDA neurons.

The purpose of this dissertation was to identify one or more potential neuroprotective treatments for PD using neurotoxic and inflammatory models of the disease to test pharmacologic agents or explore the effects of the genetic knockout of CB1 and CB2 receptors. Although the effects of MPTP and LPS on other neuronal populations in the presence or absence of these various neuroprotective drugs were also examined they were not the primary focus of this dissertation and thus will not be discussed in this chapter.

The use of MPTP and LPS under differing administration paradigms was aimed at evaluating potential neuroprotective effects that may be observed depending on the cause of PD. Acute MPTP treatment was used to examine the effects of rapid DA depletion and is ideal to evaluate NSDA neuronal activity in response to a neurotoxic insult. The repeated acute MPTP model was used to evaluate the effects of induction of microglial activation in response to necrotic loss of NSDA neurons. The sub-chronic and chronic MPTP administration paradigms were aimed at examining neuroprotective potential in a long term repetitive lesioning of NSDA neurons and microglial activation.

The intra-nigral LPS model was used to study a localized inflammatory mediated death of NSDA neurons, although failure of inflammation to be observed in this model prevented it from being used in subsequent neuroprotection studies. The peripheral LPS model was used to study the acute effects of inflammation on NSDA neurons, rather than

loss of NSDA neurons since mice were killed within 1 h following administration of LPS. The differences in these models and treatment paradigms demonstrates their utility to study mechanisms of NSDA neuronal degeneration or activity, but also reveals that none of these models can replicate the exact pathology that occurs with PD in humans.

The first objective of this dissertation investigated the potential induction of neurogenesis of adult neural stem cells by increasing cGMP in the brain resulting from sildenafil inhibition of phosphodiesterase-5 (PDE5). Three different sildenafil administration paradigms were employed to determine if sildenafil was neuroprotective in the chronic MPTP model. The chronic MPTP model was ideal for this study because it consists of a long term repeated exposure of the neurotoxin, which was extended by concurrent administration with probenecid.

Neuroprotection was examined by determining if there was a potential recovery in NSDA neuronal cell body or axon terminal loss with sildenafil treatment in the presence of MPTP, and if this was due to the migration and formation of new NSDA neurons from adult progenitor stem cells. Previous studies in a rodent stroke model strongly suggested that sildenafil would be neuroprotective, since it resulted in partial neurologic recovery. However, since sildenafil failed to cause generation of new NSDA neurons it was concluded that this compound was not neuroprotective in this MPTP model. However, one key finding resulting from these studies is that sildenafil did not induce the loss of NSDA neurons itself in the presence of either saline or MPTP treatment. This finding suggests that patients with PD can safely take sildenafil as a treatment for erectile dysfunction (ED). The greater incidence of ED in patients with PD makes this finding especially important.

The second objective of this dissertation investigated the NADPH oxidase enzyme inhibitor apocynin as a potential neuroprotective agent in the repeated acute and sub-chronic MPTP inflammatory models of PD. The contribution of microglial NADPH oxidase to MPTP induced loss of NSDA neurons following the initial toxic insult is clear as loss of NSDA neurons is attenuated in mice lacking the crucial gp91Phox subunit of the enzyme. Apocynin appeared initially to be an ideal agent to reduce the loss of NSDA neurons, but the short half-life of this drug made it hard to establish the frequency and dosage required to maintain continual inhibition of NADPH oxidase. The choice to use two different MPTP treatment paradigms was an attempt to first observe a potential neuroprotective effect in a model that has a slightly more modest loss of NSDA neurons and likely less microglial activation, although NSDA axon terminal loss was not attenuated in this model with apocynin. The repeated acute model was employed to induce not only a more severe and rapid loss of NSDA neurons but also a greater activation of microglial cells and NADPH oxidase. However, even in the repeated acute MPTP model NSDA neuronal loss or NADPH oxidase activation was not reduced by apocynin. These results demonstrated the challenges of working with a drug that has a short half-life and that has a suspected active metabolite diapocynin which has only minimally been studied.

The role of the ECB system and CB1 and CB2 receptors were studied as a final objective of this dissertation. Initially, NSDA neuronal integrity, activity, and regulation were investigated to determine if CB1/CB2 KO mice were different compared to WT mice. Results indicated that CB1/CB2 KO mice were similar to their WT counterparts and were deemed ideal to study how the lack of CB receptors may be beneficial or

detrimental in acute or sub-chronic MPTP DA depletion and or loss of NSDA neurons. It was hypothesized that CB1/CB2 receptor KO mice would be more prone to MPTP induced DA depletion in the striatum, since the ECB appears to be upregulated in animal models of PD, likely leading to enhancement of dopamine release.

Results from these studies instead led to the rejection of the proposed hypothesis as CB1/CB2 KO receptors were partially resistant to MPTP induced DA depletion in the striatum of the sub-chronic model, and recovered from DA depletion in the acute model. Surprisingly, attenuation in DA depletion was not accompanied by less of a reduction in TH protein in the striatum, suggesting that CB1/CB2 KO mice had a similar loss of NSDA neuronal terminals. This finding contradicts resistance to DA depletion but lack of an increase in NSDA activity in CB1/CB2 KO mice suggested that lack of CB receptors led to less depletion of vesicular DA explaining the differential results between DA and TH loss in the striatum. The ability of CB agonists to increase firing of NSDA neurons and release of DA would therefore support these results.

The implications of these findings is that CB1 and/or CB2 receptor inhibition could potentially be used to reduce the compensatory activity of remaining NSDA neurons, thereby attenuating the progressive loss of these neurons. However, either individual or simultaneous inhibition of CB1 and CB2 receptors failed to replicate findings of resistance to DA depletion in the sub-chronic MPTP model observed in the striatum of CB1/CB2 KO mice. Based on these results it was hypothesized that either CB1/CB2 KO mice had differences in Complex I activity or MPP+ inhibition of the Complex, reduced conversion of MPTP to MPP+, or a genetic compensation due to a lack of CB1 and CB2 receptors which conferred the resistance to DA depletion.

Measurement of Complex I activity revealed CB1/CB2 KO mice had typical activity of the complex, but CB1/CB2 KO mice did have less MPP+ in the striatum at 1, 2, and 4 h following an acute injection of MPTP. This would suggest that CB1/CB2 KO mice had reduced metabolism of MPTP to MPP+, but the decrease in MPP+ concentrations in the striatum compared to WT mice was so small that it is highly unlikely that this was the major reason why CB1/CB2 KO mice were partially resistant to MPTP. Thus, future studies to determine the reason for the resistance observed in CB1/CB2 KO mice would need to focus on genetic differences in the CB1/CB2 KO mice. Investigation into the opioid system involved in the regulation of NSDA neurons is one potential target to focus on as CB1 KO mice have higher mRNA levels of opioid peptide precursors.

The role of CB in inflammation within the brain has mainly been noted to be anti-inflammatory in nature. This was investigated in these studies using the acute peripheral LPS model in WT and CB1/CB2 KO mice to determine the acute effects of inflammation on NSDA neurons. NSDA neuronal activity was not affected in WT or CB1/CB2 KO mice with LPS, suggesting that lack of CB1 and CB2 receptors at least with an acute inflammatory reaction is not detrimental to these neurons.

As the work of this dissertation has demonstrated the search and investigation for potential neuroprotective treatments for PD will be an ongoing and challenging one. Although sildenafil, did not lead to the generation of new NSDA neurons it can not be ruled out that other PDE inhibitors may be neuroprotective, since the levels of other PDE may be higher in the brain then PDE5 and thus contribute to a greater increase in cGMP to induce neurogenesis.

The over arching conclusion for apocynin as a potential neuroprotective drug is that the pharmacokinetics of the drug made it hard to determine the ideal time points, frequency and methods of administration. Apocynin or another NADPH oxidase inhibitor may still be determined to be neuroprotective in the future if the pharmacokinetics of the drug is better known. Additionally, the use of another PD model that is solely inflammatory mediated may have been more apt to reveal a neuroprotective effect of apocynin, as opposed to a MPTP model which induces indirect microglial activation in response to the loss of NSDA neurons.

Interestingly, mice lacking CB1 and CB2 receptors were partially resistant to MPTP induced DA depletion in the striatum, that is likely due to reduced compensatory activity of intact NSDA neurons. Increased activation of NSDA neurons following neurotoxin lesioning contributes to the progressive loss of these remaining neurons, so if a CB antagonist could be given to slow or prevent the loss of remaining neurons this would be a potential neuroprotective drug. However, failure of either CB1 or CB2 receptor antagonists to prevent the loss of DA with sub-chronic MPTP treatment argued against this hypothesis. Differential inhibition of Complex I was not the primary mechanism for the resistance observed in CB1/CB2 KO, suggesting that a developmental compensation in CB1/CB2 KO mice due to the absence of functional CB receptors may be responsible for this resistance. Future experiments would need to explore the integrity and activity of other systems that are involved in regulation of NSDA neurons in the CB1/CB2 KO mice. The opioid system which is also involved in regulating NSDA neurons would be the first ideal target to investigate this hypothesis since CB1 KO mice appear to have increased opioid peptide precursor mRNA.

In summary the objectives of this dissertation to identify one or more potential neuroprotective treatments for PD proved challenging. Although sildenafil and apocynin were not neuroprotective some conclusions were still made from these studies. However, most interesting were the resistance of CB1/CB2 KO mice to MPTP treatment, these studies demonstrated that even if CB receptors are not the primary reason for this resistance further characterization of the these mice may still identify this reason.

References

Abramov AY, Jacobson J, Wientjes F, Hothersall J, Canevari L, Duchen MR (2005) Expression and modulation of an NADPH oxidase in mammalian astrocytes. J Neurosci 25:9176-9184.

Alper RH, Demarest KT, Moore KE (1980) Morphine differentially alters synthesis and turnover of dopamine in central neuronal systems. J Neural Transm 48:157-165.

Amadesi S, Cottrell GS, Divino L, Chapman K, Grady EF, Bautista F, Karanjia R, Barajas-Lopez C, Vanner S, Vergnolle N, Bunnett NW (2006) Protease-activated receptor 2 sensitizes TRPV1 by protein kinase Cepsilon- and A-dependent mechanisms in rats and mice. J Physiol 575:555-571.

Andersson M, Usiello A, Borgkvist A, Pozzi L, Dominguez C, Fienberg AA, Svenningsson P, Fredholm BB, Borrelli E, Greengard P, Fisone G (2005) Cannabinoid action depends on phosphorylation of dopamine- and cAMP-regulated phosphoprotein of 32 kDa at the protein kinase A site in striatal projection neurons. J Neurosci 25:8432-8438.

Andoh T, Lee SY, Chiueh CC (2000) Preconditioning regulation of bcl-2 and p66shc by human NOS1 enhances tolerance to oxidative stress. Faseb J 14:2144-2146.

Andoh T, Chock PB, Chiueh CC (2002) The roles of thioredoxin in protection against oxidative stress-induced apoptosis in SH-SY5Y cells. J Biol Chem 277:9655-9660.

Andoh T, Chiueh CC, Chock PB (2003) Cyclic GMP-dependent protein kinase regulates the expression of thioredoxin and thioredoxin peroxidase-1 during hormesis in response to oxidative stress-induced apoptosis. J Biol Chem 278:885-890.

Arai H, Furuya T, Yasuda T, Miura M, Mizuno Y, Mochizuki H (2004) Neurotoxic effects of lipopolysaccharide on nigral dopaminergic neurons are mediated by microglial activation, interleukin-1beta, and expression of caspase-11 in mice. J Biol Chem 279:51647-51653.

Ariano MA, Stromski CJ, Smyk-Randall EM, Sibley DR (1992) D2 dopamine receptor localization on striatonigral neurons. Neurosci Lett 144:215-220.

Arimoto T, Bing G (2003) Up-regulation of inducible nitric oxide synthase in the substantia nigra by lipopolysaccharide causes microglial activation and neurodegeneration. Neurobiol Dis 12:35-45.

Asanuma M, Miyazaki I, Diaz-Corrales FJ, Ogawa N (2004) Quinone formation as dopaminergic neuron-specific oxidative stress in the pathogenesis of sporadic

Parkinson's disease and neurotoxin-induced parkinsonism. Acta Med Okayama 58:221-233.

Ashton JC, Rahman RM, Nair SM, Sutherland BA, Glass M, Appleton I (2007) Cerebral hypoxia-ischemia and middle cerebral artery occlusion induce expression of the cannabinoid CB2 receptor in the brain. Neurosci Lett 412:114-117.

Babior BM (1999) NADPH oxidase: an update. Blood 93:1464-1476.

Bambico FR, Katz N, Debonnel G, Gobbi G (2007) Cannabinoids elicit antidepressant-like behavior and activate serotonergic neurons through the medial prefrontal cortex. J Neurosci 27:11700-11711.

Bannon MJ, Michaud RL, Roth RH (1981) Mesocortical dopamine neurons. Lack of autoreceptors modulating dopamine synthesis. Mol Pharmacol 19:270-275.

Barbieri SS, Cavalca V, Eligini S, Brambilla M, Caiani A, Tremoli E, Colli S (2004) Apocynin prevents cyclooxygenase 2 expression in human monocytes through NADPH oxidase and glutathione redox-dependent mechanisms. Free Radic Biol Med 37:156-165.

Barc S, Page G, Barrier L, Huguet F, Fauconneau B (2002) Progressive alteration of neuronal dopamine transporter activity in a rat injured by an intranigral injection of MPP+. Brain Res 941:72-81.

Barcia C, Sanchez Bahillo A, Fernandez-Villalba E, Bautista V, Poza YPM, Fernandez-Barreiro A, Hirsch EC, Herrero MT (2004) Evidence of active microglia in substantia nigra pars compacta of parkinsonian monkeys 1 year after MPTP exposure. Glia 46:402-409.

Basavarajappa BS (2007) Critical enzymes involved in endocannabinoid metabolism. Protein Pept Lett 14:237-246.

Basu A, Krady JK, Levison SW (2004) Interleukin-1: a master regulator of neuroinflammation. J Neurosci Res 78:151-156.

Begg M, Pacher P, Batkai S, Osei-Hyiaman D, Offertaler L, Mo FM, Liu J, Kunos G (2005) Evidence for novel cannabinoid receptors. Pharmacol Ther 106:133-145.

Behrouz B, Drolet RE, Sayed ZA, Lookingland KJ, Goudreau JL (2007) Unique responses to mitochondrial complex I inhibition in tuberoinfundibular dopamine neurons may impart resistance to toxic insult. Neuroscience 147:592-598.

Benarroch E (2007) Endocannabinoids in basal ganglia circuits: implications for Parkinson disease. Neurology 69:306-309.

Benito C, Nunez E, Tolon RM, Carrier EJ, Rabano A, Hillard CJ, Romero J (2003) Cannabinoid CB2 receptors and fatty acid amide hydrolase are selectively overexpressed in neuritic plaque-associated glia in Alzheimer's disease brains. J Neurosci 23:11136-11141.

Berry SA, Gudelsky GA (1991) Effect of D2 dopamine agonists on tuberoinfundibular dopamine neurons. Neuropharmacology 30:961-965.

Best AR, Regehr WG (2008) Serotonin evokes endocannabinoid release and retrogradely suppresses excitatory synapses. J Neurosci 28:6508-6515.

Betarbet R, Sherer TB, MacKenzie G, Garcia-Osuna M, Panov AV, Greenamyre JT (2000) Chronic systemic pesticide exposure reproduces features of Parkinson's disease. Nat Neurosci 3:1301-1306.

Bianca VD, Dusi S, Bianchini E, Dal Pra I, Rossi F (1999) beta-amyloid activates the O-2 forming NADPH oxidase in microglia, monocytes, and neutrophils. A possible inflammatory mechanism of neuronal damage in Alzheimer's disease. J Biol Chem 274:15493-15499.

Bisogno T, Melck D, De Petrocellis L, Di Marzo V (1999) Phosphatidic acid as the biosynthetic precursor of the endocannabinoid 2-arachidonoylglycerol in intact mouse neuroblastoma cells stimulated with ionomycin. J Neurochem 72:2113-2119.

Bjorklund A, Hokfelt, T, ed (1984a) Classical Transmitters in the CNS, Part I. Amsterdam: Elsevier.

Bjorklund A, Hokfelt, T, Kuhar, M.J., ed (1984b) Classical Neurotransmitters and the Transmitter Receptors in the CNS, Part II. Amsterdam: Elsevier.

Blankman JL, Simon GM, Cravatt BF (2007) A comprehensive profile of brain enzymes that hydrolyze the endocannabinoid 2-arachidonoylglycerol. Chem Biol 14:1347-1356.

Block ML, Hong JS (2005) Microglia and inflammation-mediated neurodegeneration: multiple triggers with a common mechanism. Prog Neurobiol 76:77-98.

Bobrovskaya L, Gilligan C, Bolster EK, Flaherty JJ, Dickson PW, Dunkley PR (2007) Sustained phosphorylation of tyrosine hydroxylase at serine 40: a novel mechanism for maintenance of catecholamine synthesis. J Neurochem 100:479-489.

Boismenu D, Mamer O, Ste-Marie L, Vachon L, Montgomery J (1996) In vivo hydroxylation of the neurotoxin, 1-methyl-4-phenylpyridinium, and the effect of

monoamine oxidase inhibitors: electrospray-MS analysis of intra-striatal microdialysates. J Mass Spectrom 31:1101-1108.

Borgundvaag B, George SR (1985) Dopamine inhibition of anterior pituitary adenylate cyclase is mediated through the high-affinity state of the D2 receptor. Life Sci 37:379-386.

Borlongan CV, Stahl CE, Cameron DF, Saporta S, Freeman TB, Cahill DW, Sanberg PR (1996) CNS immunological modulation of neural graft rejection and survival. Neurol Res 18:297-304.

Borowski T, Kokkinidis L, Merali Z, Anisman H (1998) Lipopolysaccharide, central in vivo biogenic amine variations, and anhedonia. Neuroreport 9:3797-3802.

Bove J, Prou D, Perier C, Przedborski S (2005) Toxin-induced models of Parkinson's disease. NeuroRx 2:484-494.

Bozzi Y, Borrelli E (2006) Dopamine in neurotoxicity and neuroprotection: what do D2 receptors have to do with it? Trends Neurosci 29:167-174.

Brotchie JM (2003) CB1 cannabinoid receptor signalling in Parkinson's disease. Curr Opin Pharmacol 3:54-61.

Buckley NE, McCoy KL, Mezey E, Bonner T, Zimmer A, Felder CC, Glass M, Zimmer A (2000) Immunomodulation by cannabinoids is absent in mice deficient for the cannabinoid CB(2) receptor. Eur J Pharmacol 396:141-149.

Bunzow JR, Van Tol HH, Grandy DK, Albert P, Salon J, Christie M, Machida CA, Neve KA, Civelli O (1988) Cloning and expression of a rat D2 dopamine receptor cDNA. Nature 336:783-787.

Burns RS, Chiueh CC, Markey SP, Ebert MH, Jacobowitz DM, Kopin IJ (1983) A primate model of parkinsonism: selective destruction of dopaminergic neurons in the pars compacta of the substantia nigra by N-methyl-4-phenyl-1,2,3,6-tetrahydropyridine. Proc Natl Acad Sci U S A 80:4546-4550.

Cadogan AK, Alexander SP, Boyd EA, Kendall DA (1997) Influence of cannabinoids on electrically evoked dopamine release and cyclic AMP generation in the rat striatum. J Neurochem 69:1131-1137.

Camus A, Javoy-Agid F, Dubois A, Scatton B (1986) Autoradiographic localization and quantification of dopamine D2 receptors in normal human brain with [3H]N-n-propylnorapomorphine. Brain Res 375:135-149.

Caroff M, Karibian D (2003) Structure of bacterial lipopolysaccharides. Carbohydr Res 338:2431-2447.

Carrier EJ, Kearn CS, Barkmeier AJ, Breese NM, Yang W, Nithipatikom K, Pfister SL, Campbell WB, Hillard CJ (2004) Cultured rat microglial cells synthesize the endocannabinoid 2-arachidonylglycerol, which increases proliferation via a CB2 receptor-dependent mechanism. Mol Pharmacol 65:999-1007.

Castano A, Herrera AJ, Cano J, Machado A (1998) Lipopolysaccharide intranigral injection induces inflammatory reaction and damage in nigrostriatal dopaminergic system. J Neurochem 70:1584-1592.

Castano A, Herrera AJ, Cano J, Machado A (2002) The degenerative effect of a single intranigral injection of LPS on the dopaminergic system is prevented by dexamethasone, and not mimicked by rh-TNF-alpha, IL-1beta and IFN-gamma. J Neurochem 81:150-157.

Cerrito F, Raiteri M (1979) Serotonin release is modulated by presynaptic autoreceptors. Eur J Pharmacol 57:427-430.

Chan CS, Guzman JN, Ilijic E, Mercer JN, Rick C, Tkatch T, Meredith GE, Surmeier DJ (2007) 'Rejuvenation' protects neurons in mouse models of Parkinson's disease. Nature 447:1081-1086.

Cheer JF, Wassum KM, Heien ML, Phillips PE, Wightman RM (2004) Cannabinoids enhance subsecond dopamine release in the nucleus accumbens of awake rats. J Neurosci 24:4393-4400.

Cheer JF, Wassum KM, Sombers LA, Heien ML, Ariansen JL, Aragona BJ, Phillips PE, Wightman RM (2007) Phasic dopamine release evoked by abused substances requires cannabinoid receptor activation. J Neurosci 27:791-795.

Chen LW, Wei LC, Liu HL, Duan L, Ju G, Chan YS (2000) Retinal dopaminergic neurons (A17) expressing neuromedin K receptor (NK(3)): a double immunocytochemical study in the rat. Brain Res 885:122-127.

Cho L, Tsunoda M, Sharma RP (1999) Effects of endotoxin and tumor necrosis factor alpha on regional brain neurotransmitters in mice. Nat Toxins 7:187-195.

Chun HS, Son JJ, Son JH (2000) Identification of potential compounds promoting BDNF production in nigral dopaminergic neurons: clinical implication in Parkinson's disease. Neuroreport 11:511-514.

Ciani E, Virgili M, Contestabile A (2002) Akt pathway mediates a cGMP-dependent survival role of nitric oxide in cerebellar granule neurones. J Neurochem 81:218-228.

Corbin JD, Francis SH (1999) Cyclic GMP phosphodiesterase-5: target of sildenafil. J Biol Chem 274:13729-13732.

Cravatt BF, Giang DK, Mayfield SP, Boger DL, Lerner RA, Gilula NB (1996) Molecular characterization of an enzyme that degrades neuromodulatory fatty-acid amides. Nature 384:83-87.

Cunningham C, Wilcockson DC, Campion S, Lunnon K, Perry VH (2005) Central and systemic endotoxin challenges exacerbate the local inflammatory response and increase neuronal death during chronic neurodegeneration. J Neurosci 25:9275-9284.

Darmani NA, Janoyan JJ, Kumar N, Crim JL (2003) Behaviorally active doses of the CB1 receptor antagonist SR 141716A increase brain serotonin and dopamine levels and turnover. Pharmacol Biochem Behav 75:777-787.

Date I, Felten DL, Felten SY (1990) Long-term effect of MPTP in the mouse brain in relation to aging: neurochemical and immunocytochemical analysis. Brain Res 519:266-276.

Dauer W, Przedborski S (2003) Parkinson's disease: mechanisms and models. Neuron 39:889-909.

De Laurentiis A, Pisera D, Caruso C, Candolfi M, Mohn C, Rettori V, Seilicovich A (2002) Lipopolysaccharide- and tumor necrosis factor-alpha-induced changes in prolactin secretion and dopaminergic activity in the hypothalamic-pituitary axis. Neuroimmunomodulation 10:30-39.

DeLong MR, Wichmann T (2007) Circuits and circuit disorders of the basal ganglia. Arch Neurol 64:20-24.

Demarest KT, Moore KE (1979) Comparison of dopamine synthesis regulation in the terminals of nigrostriatal, mesolimbic, tuberoinfundibular and tuberohypophyseal neurons. J Neural Transm 46:263-277.

Demarest KT, Lawson-Wendling KL, Moore KE (1983) d-Amphetamine and gamma-butyrolactone alteration of dopamine synthesis in the terminals of nigrostriatal and mesolimbic neurons. Possible role of various autoreceptor sensitivities. Biochem Pharmacol 32:691-697.

Demuth DG, Molleman A (2006) Cannabinoid signalling. Life Sci 78:549-563.

Devane WA, Hanus L, Breuer A, Pertwee RG, Stevenson LA, Griffin G, Gibson D, Mandelbaum A, Etinger A, Mechoulam R (1992) Isolation and structure of a brain constituent that binds to the cannabinoid receptor. Science 258:1946-1949.

Di Marzo V, Fontana A, Cadas H, Schinelli S, Cimino G, Schwartz JC, Piomelli D (1994) Formation and inactivation of endogenous cannabinoid anandamide in central neurons. Nature 372:686-691.

Diana M, Melis M, Gessa GL (1998) Increase in meso-prefrontal dopaminergic activity after stimulation of CB1 receptors by cannabinoids. Eur J Neurosci 10:2825-2830.

Diana MA, Marty A (2004) Endocannabinoid-mediated short-term synaptic plasticity: depolarization-induced suppression of inhibition (DSI) and depolarization-induced suppression of excitation (DSE). Br J Pharmacol 142:9-19.

Dinh TP, Carpenter D, Leslie FM, Freund TF, Katona I, Sensi SL, Kathuria S, Piomelli D (2002) Brain monoglyceride lipase participating in endocannabinoid inactivation. Proc Natl Acad Sci U S A 99:10819-10824.

Doyle SL, O'Neill LA (2006) Toll-like receptors: from the discovery of NFkappaB to new insights into transcriptional regulations in innate immunity. Biochem Pharmacol 72:1102-1113.

Drechsel DA, Patel M (2008) Role of reactive oxygen species in the neurotoxicity of environmental agents implicated in Parkinson's disease. Free Radic Biol Med 44:1873-1886.

Drolet RE, Behrouz B, Lookingland KJ, Goudreau JL (2004) Mice lacking alpha-synuclein have an attenuated loss of striatal dopamine following prolonged chronic MPTP administration. Neurotoxicology 25:761-769.

Dubois A, Savasta M, Curet O, Scatton B (1986) Autoradiographic distribution of the D1 agonist [3H]SKF 38393, in the rat brain and spinal cord. Comparison with the distribution of D2 dopamine receptors. Neuroscience 19:125-137.

Dunkley PR, Bobrovskaya L, Graham ME, von Nagy-Felsobuki EI, Dickson PW (2004) Tyrosine hydroxylase phosphorylation: regulation and consequences. J Neurochem 91:1025-1043.

Dunn AJ (1992) Endotoxin-induced activation of cerebral catecholamine and serotonin metabolism: comparison with interleukin-1. J Pharmacol Exp Ther 261:964-969.

Eaton MJ, Lookingland KJ, Moore KE (1994) Effects of the selective dopaminergic D2 agonist quinelorane on the activity of dopaminergic and noradrenergic neurons projecting to the diencephalon of the rat. J Pharmacol Exp Ther 268:645-652.

Eaton MJ, Tian Y, Lookingland KJ, Moore KE (1992) Comparison of the effects of remoxipride and raclopride on nigrostriatal and mesolimbic dopaminergic neuronal activity and on the secretion of prolactin and alpha-melanocyte-stimulating hormone. Neuropsychopharmacology 7:205-211.

Ebadi M, Sharma SK (2003) Peroxynitrite and mitochondrial dysfunction in the pathogenesis of Parkinson's disease. Antioxid Redox Signal 5:319-335.

Egertova M, Cravatt BF, Elphick MR (2003) Comparative analysis of fatty acid amide hydrolase and cb(1) cannabinoid receptor expression in the mouse brain: evidence of a widespread role for fatty acid amide hydrolase in regulation of endocannabinoid signaling. Neuroscience 119:481-496.

Ehrhart J, Obregon D, Mori T, Hou H, Sun N, Bai Y, Klein T, Fernandez F, Tan J, Shytle RD (2005) Stimulation of cannabinoid receptor 2 (CB2) suppresses microglial activation. J Neuroinflammation 2:29.

Eljaschewitsch E, Witting A, Mawrin C, Lee T, Schmidt PM, Wolf S, Hoertnagl H, Raine CS, Schneider-Stock R, Nitsch R, Ullrich O (2006) The endocannabinoid anandamide protects neurons during CNS inflammation by induction of MKP-1 in microglial cells. Neuron 49:67-79.

Fahn S (2003) Description of Parkinson's disease as a clinical syndrome. Ann N Y Acad Sci 991:1-14.

Fallon JH, Moore RY (1978) Catecholamine innervation of the basal forebrain. IV. Topography of the dopamine projection to the basal forebrain and neostriatum. J Comp Neurol 180:545-580.

Felter HW, Lloyd JU (1898) King's American Dispensatory. In.

Fernandez-Lopez D, Martinez-Orgado J, Nunez E, Romero J, Lorenzo P, Moro MA, Lizasoain I (2006) Characterization of the neuroprotective effect of the cannabinoid agonist WIN-55212 in an in vitro model of hypoxic-ischemic brain damage in newborn rats. Pediatr Res 60:169-173.

Ferrer B, Gorriti MA, Palomino A, Gornemann I, de Diego Y, Bermudez-Silva FJ, Bilbao A, Fernandez-Espejo E, Moratalla R, Navarro M, Rodriguez de Fonseca F (2007) Cannabinoid CB1 receptor antagonism markedly increases dopamine receptor-mediated stereotypies. Eur J Pharmacol 559:180-183.

Fink KB, Gothert M (2007) 5-HT receptor regulation of neurotransmitter release. Pharmacol Rev 59:360-417.

Fitzmaurice PS, Ang L, Guttman M, Rajput AH, Furukawa Y, Kish SJ (2003) Nigral glutathione deficiency is not specific for idiopathic Parkinson's disease. Mov Disord 18:969-976.

Fitzpatrick PF (2003) Mechanism of aromatic amino acid hydroxylation. Biochemistry 42:14083-14091.

Foreman MM, Fuller RW, Hynes MD, Gidda JS, Nichols CL, Schaus JM, Kornfeld EC, Clemens JA (1989) Preclinical studies on quinelorane, a potent and highly selective D2-dopaminergic agonist. J Pharmacol Exp Ther 250:227-235.

Franklin A, Stella N (2003) Arachidonylcyclopropylamide increases microglial cell migration through cannabinoid CB2 and abnormal-cannabidiol-sensitive receptors. Eur J Pharmacol 474:195-198.

Franklin K, Paxinos G (1996) The Mouse Brain in Stereotaxic Coordinates San Diego: Academic Press.

French ED, Dillon K, Wu X (1997) Cannabinoids excite dopamine neurons in the ventral tegmentum and substantia nigra. Neuroreport 8:649-652.

Gainetdinov RR, Fumagalli F, Jones SR, Caron MG (1997) Dopamine transporter is required for in vivo MPTP neurotoxicity: evidence from mice lacking the transporter. J Neurochem 69:1322-1325.

Galvin JE (2006) Interaction of alpha-synuclein and dopamine metabolites in the pathogenesis of Parkinson's disease: a case for the selective vulnerability of the substantia nigra. Acta Neuropathol 112:115-126.

Gao HM, Hong JS, Zhang W, Liu B (2002a) Distinct role for microglia in rotenone-induced degeneration of dopaminergic neurons. J Neurosci 22:782-790.

Gao HM, Liu B, Zhang W, Hong JS (2003) Critical role of microglial NADPH oxidase-derived free radicals in the in vitro MPTP model of Parkinson's disease. Faseb J 17:1954-1956.

Gao HM, Jiang J, Wilson B, Zhang W, Hong JS, Liu B (2002b) Microglial activation-mediated delayed and progressive degeneration of rat nigral dopaminergic neurons: relevance to Parkinson's disease. J Neurochem 81:1285-1297.

Gaoni YaM, R. (1964) Isolation, Structure, and Partial Synthesis of an Active Constituent of Hashish. J Am Chem Soc 86:1646-1647.

Gerald TM, Ward GR, Howlett AC, Franklin SO (2006) CB1 knockout mice display significant changes in striatal opioid peptide and D4 dopamine receptor gene expression. Brain Res 1093:20-24.

Gerdeman G, Lovinger DM (2001) CB1 cannabinoid receptor inhibits synaptic release of glutamate in rat dorsolateral striatum. J Neurophysiol 85:468-471.

Gessa GL, Melis M, Muntoni AL, Diana M (1998) Cannabinoids activate mesolimbic dopamine neurons by an action on cannabinoid CB1 receptors. Eur J Pharmacol 341:39-44.

Giang DK, Cravatt BF (1997) Molecular characterization of human and mouse fatty acid amide hydrolases. Proc Natl Acad Sci U S A 94:2238-2242.

Giasson BI, Duda JE, Murray IV, Chen Q, Souza JM, Hurtig HI, Ischiropoulos H, Trojanowski JQ, Lee VM (2000) Oxidative damage linked to neurodegeneration by selective alpha-synuclein nitration in synucleinopathy lesions. Science 290:985-989.

Giuffrida A, Parsons LH, Kerr TM, Rodriguez de Fonseca F, Navarro M, Piomelli D (1999) Dopamine activation of endogenous cannabinoid signaling in dorsal striatum. Nat Neurosci 2:358-363.

Gong JP, Onaivi ES, Ishiguro H, Liu QR, Tagliaferro PA, Brusco A, Uhl GR (2006) Cannabinoid CB2 receptors: immunohistochemical localization in rat brain. Brain Res 1071:10-23.

Gonzalez S, Scorticati C, Garcia-Arencibia M, de Miguel R, Ramos JA, Fernandez-Ruiz J (2006) Effects of rimonabant, a selective cannabinoid CB1 receptor antagonist, in a rat model of Parkinson's disease. Brain Res 1073-1074:209-219.

Gorell JM, Johnson CC, Rybicki BA, Peterson EL, Richardson RJ (1998) The risk of Parkinson's disease with exposure to pesticides, farming, well water, and rural living. Neurology 50:1346-1350.

Greenamyre JT, Sherer TB, Betarbet R, Panov AV (2001) Complex I and Parkinson's disease. IUBMB Life 52:135-141.

Groemping Y, Rittinger K (2005) Activation and assembly of the NADPH oxidase: a structural perspective. Biochem J 386:401-416.

Gubellini P, Picconi B, Bari M, Battista N, Calabresi P, Centonze D, Bernardi G, Finazzi-Agro A, Maccarrone M (2002) Experimental parkinsonism alters endocannabinoid degradation: implications for striatal glutamatergic transmission. J Neurosci 22:6900-6907.

Gudelsky GA, Nash JF (1996) Carrier-mediated release of serotonin by 3,4-methylenedioxymethamphetamine: implications for serotonin-dopamine interactions. J Neurochem 66:243-249.

Gueudet C, Santucci V, Rinaldi-Carmona M, Soubrie P, Le Fur G (1995) The CB1 cannabinoid receptor antagonist SR 141716A affects A9 dopamine neuronal activity in the rat. Neuroreport 6:1421-1425.

Guillemin I, Becker M, Ociepka K, Friauf E, Nothwang HG (2005) A subcellular prefractionation protocol for minute amounts of mammalian cell cultures and tissue. Proteomics 5:35-45.

Gundersen HJ, Jensen EB (1987) The efficiency of systematic sampling in stereology and its prediction. J Microsc 147:229-263.

Ha KS, Kim KM, Kwon YG, Bai SK, Nam WD, Yoo YM, Kim PK, Chung HT, Billiar TR, Kim YM (2003) Nitric oxide prevents 6-hydroxydopamine-induced apoptosis in PC12 cells through cGMP-dependent PI3 kinase/Akt activation. Faseb J 17:1036-1047.

Hald A, Lotharius J (2005) Oxidative stress and inflammation in Parkinson's disease: is there a causal link? Exp Neurol 193:279-290.

Hallman H, Lange J, Olson L, Stromberg I, Jonsson G (1985) Neurochemical and histochemical characterization of neurotoxic effects of 1-methyl-4-phenyl-1,2,3,6-tetrahydropyridine on brain catecholamine neurones in the mouse. J Neurochem 44:117-127.

Hanisch UK (2002) Microglia as a source and target of cytokines. Glia 40:140-155.

Hanus L, Abu-Lafi S, Fride E, Breuer A, Vogel Z, Shalev DE, Kustanovich I, Mechoulam R (2001) 2-arachidonyl glyceryl ether, an endogenous agonist of the cannabinoid CB1 receptor. Proc Natl Acad Sci U S A 98:3662-3665.

Harraz MM, Marden JJ, Zhou W, Zhang Y, Williams A, Sharov VS, Nelson K, Luo M, Paulson H, Schoneich C, Engelhardt JF (2008) SOD1 mutations disrupt redox-sensitive Rac regulation of NADPH oxidase in a familial ALS model. J Clin Invest 118:659-670.

Heikkila RE, Cohen G (1973) 6-Hydroxydopamine: evidence for superoxide radical as an oxidative intermediate. Science 181:456-457.

Heikkila RE, Hess A, Duvoisin RC (1984) Dopaminergic neurotoxicity of 1-methyl-4-phenyl-1,2,5,6-tetrahydropyridine in mice. Science 224:1451-1453.

Herkenham M, Lynn AB, de Costa BR, Richfield EK (1991a) Neuronal localization of cannabinoid receptors in the basal ganglia of the rat. Brain Res 547:267-274.

Herkenham M, Lynn AB, Johnson MR, Melvin LS, de Costa BR, Rice KC (1991b) Characterization and localization of cannabinoid receptors in rat brain: a quantitative in vitro autoradiographic study. J Neurosci 11:563-583.

Herkenham M, Lynn AB, Little MD, Johnson MR, Melvin LS, de Costa BR, Rice KC (1990) Cannabinoid receptor localization in brain. Proc Natl Acad Sci U S A 87:1932-1936.

Hida T, Hasegawa Y, Arai R (1999) Histochemical study of dopamine-degrading monoamine oxidase activity in dopaminergic neurons of rat brain. Brain Res 842:491-495.

Hohmann AG, Herkenham M (2000) Localization of cannabinoid CB(1) receptor mRNA in neuronal subpopulations of rat striatum: a double-label in situ hybridization study. Synapse 37:71-80.

Hollis JH, Lightman SL, Lowry CA (2005) Lipopolysaccharide has selective actions on sub-populations of catecholaminergic neurons involved in activation of the hypothalamic-pituitary-adrenal axis and inhibition of prolactin secretion. J Endocrinol 184:393-406.

Houchi H, Babovic D, Pierrefiche O, Ledent C, Daoust M, Naassila M (2005) CB1 receptor knockout mice display reduced ethanol-induced conditioned place preference and increased striatal dopamine D2 receptors. Neuropsychopharmacology 30:339-349.

Hsieh PF, Chia LG, Ni DR, Cheng LJ, Ho YP, Tzeng SF, Chang MH, Hong JS (2002) Behavior, neurochemistry and histology after intranigral lipopolysaccharide injection. Neuroreport 13:277-280.

Hungund BL, Szakall I, Adam A, Basavarajappa BS, Vadasz C (2003) Cannabinoid CB1 receptor knockout mice exhibit markedly reduced voluntary alcohol consumption and lack alcohol-induced dopamine release in the nucleus accumbens. J Neurochem 84:698-704.

Hunter RL, Dragicevic N, Seifert K, Choi DY, Liu M, Kim HC, Cass WA, Sullivan PG, Bing G (2007) Inflammation induces mitochondrial dysfunction and dopaminergic neurodegeneration in the nigrostriatal system. J Neurochem 100:1375-1386.

Hussain IF, Brady CM, Swinn MJ, Mathias CJ, Fowler CJ (2001) Treatment of erectile dysfunction with sildenafil citrate (Viagra) in parkinsonism due to Parkinson's disease or multiple system atrophy with observations on orthostatic hypotension. J Neurol Neurosurg Psychiatry 71:371-374.

Imamura K, Hishikawa N, Sawada M, Nagatsu T, Yoshida M, Hashizume Y (2003) Distribution of major histocompatibility complex class II-positive microglia and cytokine profile of Parkinson's disease brains. Acta Neuropathol (Berl) 106:518-526.

Iravani MM, Kashefi K, Mander P, Rose S, Jenner P (2002) Involvement of inducible nitric oxide synthase in inflammation-induced dopaminergic neurodegeneration. Neuroscience 110:49-58.

Iravani MM, Leung CC, Sadeghian M, Haddon CO, Rose S, Jenner P (2005) The acute and the long-term effects of nigral lipopolysaccharide administration on dopaminergic dysfunction and glial cell activation. Eur J Neurosci 22:317-330.

Jackson-Lewis V, Jakowec M, Burke RE, Przedborski S (1995) Time course and morphology of dopaminergic neuronal death caused by the neurotoxin 1-methyl-4-phenyl-1,2,3,6-tetrahydropyridine. Neurodegeneration 4:257-269.

Jakowec MW, Nixon K, Hogg E, McNeill T, Petzinger GM (2004) Tyrosine hydroxylase and dopamine transporter expression following 1-methyl-4-phenyl-1,2,3,6-tetrahydropyridine-induced neurodegeneration of the mouse nigrostriatal pathway. J Neurosci Res 76:539-550.

Janssen AJ, Trijbels FJ, Sengers RC, Smeitink JA, van den Heuvel LP, Wintjes LT, Stoltenborg-Hogenkamp BJ, Rodenburg RJ (2007) Spectrophotometric assay for complex I of the respiratory chain in tissue samples and cultured fibroblasts. Clin Chem 53:729-734.

Jarai Z, Wagner JA, Varga K, Lake KD, Compton DR, Martin BR, Zimmer AM, Bonner TI, Buckley NE, Mezey E, Razdan RK, Zimmer A, Kunos G (1999) Cannabinoid-induced mesenteric vasodilation through an endothelial site distinct from CB1 or CB2 receptors. Proc Natl Acad Sci U S A 96:14136-14141.

Javitch JA, D'Amato RJ, Strittmatter SM, Snyder SH (1985) Parkinsonism-inducing neurotoxin, N-methyl-4-phenyl-1,2,3,6 -tetrahydropyridine: uptake of the metabolite N-methyl-4-phenylpyridine by dopamine neurons explains selective toxicity. Proc Natl Acad Sci U S A 82:2173-2177.

Jekabsone A, Mander PK, Tickler A, Sharpe M, Brown GC (2006) Fibrillar beta-amyloid peptide Abeta1-40 activates microglial proliferation via stimulating TNF-alpha release and H2O2 derived from NADPH oxidase: a cell culture study. J Neuroinflammation 3:24.

Jonsson G, Sachs C (1975) Actions of 6-hydroxydopamine quinones on catecholamine neurons. J Neurochem 25:509-516.

Julian MD, Martin AB, Cuellar B, Rodriguez De Fonseca F, Navarro M, Moratalla R, Garcia-Segura LM (2003) Neuroanatomical relationship between type 1 cannabinoid receptors and dopaminergic systems in the rat basal ganglia. Neuroscience 119:309-318.

Kariko K, Weissman D, Welsh FA (2004) Inhibition of toll-like receptor and cytokine signaling--a unifying theme in ischemic tolerance. J Cereb Blood Flow Metab 24:1288-1304.

Kim K, Moore DH, Makriyannis A, Abood ME (2006) AM1241, a cannabinoid CB2 receptor selective compound, delays disease progression in a mouse model of amyotrophic lateral sclerosis. Eur J Pharmacol 542:100-105.

Kim WG, Mohney RP, Wilson B, Jeohn GH, Liu B, Hong JS (2000) Regional difference in susceptibility to lipopolysaccharide-induced neurotoxicity in the rat brain: role of microglia. J Neurosci 20:6309-6316.

Klaidman LK, Adams JD, Jr., Leung AC, Kim SS, Cadenas E (1993) Redox cycling of MPP+: evidence for a new mechanism involving hydride transfer with xanthine oxidase, aldehyde dehydrogenase, and lipoamide dehydrogenase. Free Radic Biol Med 15:169-179.

Klees RF, De Marco PC, Salasznyk RM, Ahuja D, Hogg M, Antoniotti S, Kamath L, Dordick JS, Plopper GE (2006) Apocynin derivatives interrupt intracellular signaling resulting in decreased migration in breast cancer cells. J Biomed Biotechnol 2006:87246.

Kotera J, Fujishige K, Omori K (2000) Immunohistochemical localization of cGMP-binding cGMP-specific phosphodiesterase (PDE5) in rat tissues. J Histochem Cytochem 48:685-693.

Kreitzer AC, Regehr WG (2001) Retrograde inhibition of presynaptic calcium influx by endogenous cannabinoids at excitatory synapses onto Purkinje cells. Neuron 29:717-727.

Kulkarni SK, Patil CS (2004) Phosphodiesterase 5 enzyme and its inhibitors: update on pharmacological and therapeutical aspects. Methods Find Exp Clin Pharmacol 26:789-799.

Lacosta S, Merali Z, Anisman H (1999) Behavioral and neurochemical consequences of lipopolysaccharide in mice: anxiogenic-like effects. Brain Res 818:291-303.

Langston JW, Ballard P, Tetrud JW, Irwin I (1983) Chronic Parkinsonism in humans due to a product of meperidine-analog synthesis. Science 219:979-980.

Langston JW, Forno LS, Tetrud J, Reeves AG, Kaplan JA, Karluk D (1999) Evidence of active nerve cell degeneration in the substantia nigra of humans years after 1-methyl-4-phenyl-1,2,3,6-tetrahydropyridine exposure. Ann Neurol 46:598-605.

Lastres-Becker I, Cebeira M, de Ceballos ML, Zeng BY, Jenner P, Ramos JA, Fernandez-Ruiz JJ (2001) Increased cannabinoid CB1 receptor binding and activation of GTP-binding proteins in the basal ganglia of patients with Parkinson's syndrome and of MPTP-treated marmosets. Eur J Neurosci 14:1827-1832.

Lau YS, Meredith GE (2003) From drugs of abuse to parkinsonism. The MPTP mouse model of Parkinson's disease. Methods Mol Med 79:103-116.

Lau YS, Trobough KL, Crampton JM, Wilson JA (1990) Effects of probenecid on striatal dopamine depletion in acute and long-term 1-methyl-4-phenyl-1,2,3,6-tetrahydropyridine (MPTP)-treated mice. Gen Pharmacol 21:181-187.

Lee CS, Song EH, Park SY, Han ES (2003) Combined effect of dopamine and MPP+ on membrane permeability in mitochondria and cell viability in PC12 cells. Neurochem Int 43:147-154.

Lee XP, Kumazawa T, Fujishiro M, Hasegawa C, Arinobu T, Seno H, Ishii A, Sato K (2004) Determination of paraquat and diquat in human body fluids by high-performance liquid chromatography/tandem mass spectrometry. J Mass Spectrom 39:1147-1152.

Legros H, Dingeval MG, Janin F, Costentin J, Bonnet JJ (2004) Toxicity of a treatment associating dopamine and disulfiram for catecholaminergic neuroblastoma SH-SY5Y cells: relationships with 3,4-dihydroxyphenylacetaldehyde formation. Neurotoxicology 25:365-375.

Lehnardt S, Massillon L, Follett P, Jensen FE, Ratan R, Rosenberg PA, Volpe JJ, Vartanian T (2003) Activation of innate immunity in the CNS triggers neurodegeneration through a Toll-like receptor 4-dependent pathway. Proc Natl Acad Sci U S A 100:8514-8519.

Leng Y, Chase TN, Bennett MC (2001) Muscarinic receptor stimulation induces translocation of an alpha-synuclein oligomer from plasma membrane to a light vesicle fraction in cytoplasm. J Biol Chem 276:28212-28218.

Li L, Watts SW, Banes AK, Galligan JJ, Fink GD, Chen AF (2003) NADPH oxidase-derived superoxide augments endothelin-1-induced venoconstriction in mineralocorticoid hypertension. Hypertension 42:316-321.

Liberatore GT, Jackson-Lewis V, Vukosavic S, Mandir AS, Vila M, McAuliffe WG, Dawson VL, Dawson TM, Przedborski S (1999) Inducible nitric oxide synthase stimulates dopaminergic neurodegeneration in the MPTP model of Parkinson disease. Nat Med 5:1403-1409.

Liu B (2006) Modulation of microglial pro-inflammatory and neurotoxic activity for the treatment of Parkinson's disease. Aaps J 8:E606-621.

Liu B, Du L, Hong JS (2000a) Naloxone protects rat dopaminergic neurons against inflammatory damage through inhibition of microglia activation and superoxide generation. J Pharmacol Exp Ther 293:607-617.

Liu B, Jiang JW, Wilson BC, Du L, Yang SN, Wang JY, Wu GC, Cao XD, Hong JS (2000b) Systemic infusion of naloxone reduces degeneration of rat substantia nigral dopaminergic neurons induced by intranigral injection of lipopolysaccharide. J Pharmacol Exp Ther 295:125-132.

Liu P, Bilkey DK, Darlington CL, Smith PF (2003) Cannabinoid CB1 receptor protein expression in the rat hippocampus and entorhinal, perirhinal, postrhinal and temporal cortices: regional variations and age-related changes. Brain Res 979:235-239.

Liu Y, Roghani A, Edwards RH (1992) Gene transfer of a reserpine-sensitive mechanism of resistance to N-methyl-4-phenylpyridinium. Proc Natl Acad Sci U S A 89:9074-9078.

Lomnitski L, Foley JE, Grossman S, Shaul VB, Maronpot RR, Moomaw CR, Carbonatto M, Nyska A (2000) Effects of apocynin and natural antioxidant from spinach on inducible nitric oxide synthase and cyclooxygenase-2 induction in lipopolysaccharide-induced hepatic injury in rat. Pharmacol Toxicol 87:18-25.

Lookingland KJ, Jarry HD, Moore KE (1987a) The metabolism of dopamine in the median eminence reflects the activity of tuberoinfundibular neurons. Brain Res 419:303-310.

Lookingland KJ, Gunnet JW, Moore KE (1987b) Electrical stimulation of the arcuate nucleus increases the metabolism of dopamine in terminals of tuberoinfundibular neurons in the median eminence. Brain Res 436:161-164.

Lookingland KJaM, K (2005) Functional Neuroanatomy of Hypothalamic Dopaminergic Neuroendocrine Systems. In: Handbook of Chemical Neuroanatomy, 1 Edition (Dunnett S. B. BM, Bjorklund A, Hokfelt T, ed): Elsevier.

Loughney K, Hill TR, Florio VA, Uher L, Rosman GJ, Wolda SL, Jones BA, Howard ML, McAllister-Lucas LM, Sonnenburg WK, Francis SH, Corbin JD, Beavo JA, Ferguson K (1998) Isolation and characterization of cDNAs encoding PDE5A, a human cGMP-binding, cGMP-specific 3',5'-cyclic nucleotide phosphodiesterase. Gene 216:139-147.

Lowry OH, Rosebrough NJ, Farr AL, Randall RJ (1951) Protein measurement with the Folin phenol reagent. J Biol Chem 193:265-275.

Mackie K (2008) Signaling via CNS cannabinoid receptors. Mol Cell Endocrinol.

Magerkurth C, Schnitzer R, Braune S (2005) Symptoms of autonomic failure in Parkinson's disease: prevalence and impact on daily life. Clin Auton Res 15:76-82.

Mander PK, Jekabsone A, Brown GC (2006) Microglia proliferation is regulated by hydrogen peroxide from NADPH oxidase. J Immunol 176:1046-1052.

Marcellino D, Carriba P, Filip M, Borgkvist A, Frankowska M, Bellido I, Tanganelli S, Muller CE, Fisone G, Lluis C, Agnati LF, Franco R, Fuxe K (2008) Antagonistic cannabinoid CB(1)/dopamine D(2) receptor interactions in striatal CB(1)/D(2) heteromers. A combined neurochemical and behavioral analysis. Neuropharmacology 54:815-823.

Marchalant Y, Rosi S, Wenk GL (2007a) Anti-inflammatory property of the cannabinoid agonist WIN-55212-2 in a rodent model of chronic brain inflammation. Neuroscience 144:1516-1522.

Marchalant Y, Cerbai F, Brothers HM, Wenk GL (2007b) Cannabinoid receptor stimulation is anti-inflammatory and improves memory in old rats. Neurobiol Aging.

Maresz K, Carrier EJ, Ponomarev ED, Hillard CJ, Dittel BN (2005) Modulation of the cannabinoid CB2 receptor in microglial cells in response to inflammatory stimuli. J Neurochem 95:437-445.

Maresz K, Pryce G, Ponomarev ED, Marsicano G, Croxford JL, Shriver LP, Ledent C, Cheng X, Carrier EJ, Mann MK, Giovannoni G, Pertwee RG, Yamamura T, Buckley NE, Hillard CJ, Lutz B, Baker D, Dittel BN (2007) Direct suppression of CNS autoimmune inflammation via the cannabinoid receptor CB1 on neurons and CB2 on autoreactive T cells. Nat Med 13:492-497.

Markey SP, Johannessen JN, Chiueh CC, Burns RS, Herkenham MA (1984) Intraneuronal generation of a pyridinium metabolite may cause drug-induced parkinsonism. Nature 311:464-467.

Martin AB, Fernandez-Espejo E, Ferrer B, Gorriti MA, Bilbao A, Navarro M, Rodriguez de Fonseca F, Moratalla R (2007) Expression and Function of CB(1) Receptor in the Rat Striatum: Localization and Effects on D(1) and D(2) Dopamine Receptor-Mediated Motor Behaviors. Neuropsychopharmacology.

Matyas F, Yanovsky Y, Mackie K, Kelsch W, Misgeld U, Freund TF (2006) Subcellular localization of type 1 cannabinoid receptors in the rat basal ganglia. Neuroscience 137:337-361.

Matyas F, Urban GM, Watanabe M, Mackie K, Zimmer A, Freund TF, Katona I (2008) Identification of the sites of 2-arachidonoylglycerol synthesis and action imply retrograde endocannabinoid signaling at both GABAergic and glutamatergic synapses in the ventral tegmental area. Neuropharmacology 54:95-107.

McGeer PL, Itagaki S, Boyes BE, McGeer EG (1988) Reactive microglia are positive for HLA-DR in the substantia nigra of Parkinson's and Alzheimer's disease brains. Neurology 38:1285-1291.

Mechoulam R, Ben-Shabat S, Hanus L, Ligumsky M, Kaminski NE, Schatz AR, Gopher A, Almog S, Martin BR, Compton DR, et al. (1995) Identification of an endogenous 2-monoglyceride, present in canine gut, that binds to cannabinoid receptors. Biochem Pharmacol 50:83-90.

Melis M, Gessa GL, Diana M (2000) Different mechanisms for dopaminergic excitation induced by opiates and cannabinoids in the rat midbrain. Prog Neuropsychopharmacol Biol Psychiatry 24:993-1006.

Melis M, Pistis M, Perra S, Muntoni AL, Pillolla G, Gessa GL (2004a) Endocannabinoids mediate presynaptic inhibition of glutamatergic transmission in rat ventral tegmental area dopamine neurons through activation of CB1 receptors. J Neurosci 24:53-62.

Melis M, Perra S, Muntoni AL, Pillolla G, Lutz B, Marsicano G, Di Marzo V, Gessa GL, Pistis M (2004b) Prefrontal cortex stimulation induces 2-arachidonoyl-glycerol-mediated suppression of excitation in dopamine neurons. J Neurosci 24:10707-10715.

Melis T, Succu S, Sanna F, Boi A, Argiolas A, Melis MR (2007) The cannabinoid antagonist SR 141716A (Rimonabant) reduces the increase of extra-cellular dopamine release in the rat nucleus accumbens induced by a novel high palatable food. Neurosci Lett 419:231-235.

Meredith GE, Totterdell S, Petroske E, Santa Cruz K, Callison RC, Jr., Lau YS (2002) Lysosomal malfunction accompanies alpha-synuclein aggregation in a progressive mouse model of Parkinson's disease. Brain Res 956:156-165.

Meschler JP, Howlett AC (2001) Signal transduction interactions between CB1 cannabinoid and dopamine receptors in the rat and monkey striatum. Neuropharmacology 40:918-926.

Michelakis E, Tymchak W, Archer S (2000) Sildenafil: from the bench to the bedside. Cmaj 163:1171-1175.

Missale C, Nash SR, Robinson SW, Jaber M, Caron MG (1998) Dopamine receptors: from structure to function. Physiol Rev 78:189-225.

Moerman DE (1998) Native American Ethnobotany. Portland: Timber Press, Inc.

Molina-Holgado F, Amaro A, Gonzalez MI, Alvarez FJ, Leret ML (1996) Effect of maternal delta 9-tetrahydrocannabinol on developing serotonergic system. Eur J Pharmacol 316:39-42.

Molina-Holgado F, Alvarez FJ, Gonzalez I, Antonio MT, Leret ML (1997) Maternal exposure to delta 9-tetrahydrocannabinol (delta 9-THC) alters indolamine levels and turnover in adult male and female rat brain regions. Brain Res Bull 43:173-178.

Moore KE (1987) Interactions between prolactin and dopaminergic neurons. Biol Reprod 36:47-58.

Moore KE, Wuerthele SM (1979) Regulation of nigrostriatal and tuberoinfundibular-hypophyseal dopaminergic neurons. Prog Neurobiol 13:325-359.

Moore RY, Halaris AE, Jones BE (1978) Serotonin neurons of the midbrain raphe: ascending projections. J Comp Neurol 180:417-438.

Moranta D, Esteban S, Garcia-Sevilla JA (2004) Differential effects of acute cannabinoid drug treatment, mediated by CB1 receptors, on the in vivo activity of tyrosine and tryptophan hydroxylase in the rat brain. Naunyn Schmiedebergs Arch Pharmacol 369:516-524.

Morera-Herreras T, Ruiz-Ortega JA, Gomez-Urquijo S, Ugedo L (2008) Involvement of subthalamic nucleus in the stimulatory effect of Delta(9)-tetrahydrocannabinol on dopaminergic neurons. Neuroscience 151:817-823.

Muijsers RB, van Den Worm E, Folkerts G, Beukelman CJ, Koster AS, Postma DS, Nijkamp FP (2000) Apocynin inhibits peroxynitrite formation by murine macrophages. Br J Pharmacol 130:932-936.

Mukhopadhyay S, Das S, Williams EA, Moore D, Jones JD, Zahm DS, Ndengele MM, Lechner AJ, Howlett AC (2006) Lipopolysaccharide and cyclic AMP regulation of CB(2) cannabinoid receptor levels in rat brain and mouse RAW 264.7 macrophages. J Neuroimmunol 181:82-92.

Muller AA, Reiter SA, Heider KG, Wagner H (1999) Plant-derived acetophenones with antiasthmatic and anti-inflammatory properties: inhibitory effects on chemotaxis, right angle light scatter and actin polymerization of polymorphonuclear granulocytes. Planta Med 65:590-594.

Murrin LC, Roth RH (1987) Nigrostriatal dopamine neurons: modulation of impulse-induced activation of tyrosine hydroxylation by dopamine autoreceptors. Neuropharmacology 26:591-595.

Nakamizo T, Kawamata J, Yoshida K, Kawai Y, Kanki R, Sawada H, Kihara T, Yamashita H, Shibasaki H, Akaike A, Shimohama S (2003) Phosphodiesterase inhibitors are neuroprotective to cultured spinal motor neurons. J Neurosci Res 71:485-495.

Nakazi M, Bauer U, Nickel T, Kathmann M, Schlicker E (2000) Inhibition of serotonin release in the mouse brain via presynaptic cannabinoid CB1 receptors. Naunyn Schmiedebergs Arch Pharmacol 361:19-24.

Narushima M, Hashimoto K, Kano M (2006) Endocannabinoid-mediated short-term suppression of excitatory synaptic transmission to medium spiny neurons in the striatum. Neurosci Res 54:159-164.

Novikova L, Garris BL, Garris DR, Lau YS (2006) Early signs of neuronal apoptosis in the substantia nigra pars compacta of the progressive neurodegenerative mouse 1-methyl-4-phenyl-1,2,3,6-tetrahydropyridine/probenecid model of Parkinson's disease. Neuroscience 140:67-76.

Nowycky MC, Roth RH (1979) Chronic gamma-butyrolactone (GBL) treatment: a potential model of dopamine hypoactivity. Naunyn Schmiedebergs Arch Pharmacol 309:247-254.

Nunez E, Benito C, Tolon RM, Hillard CJ, Griffin WS, Romero J (2008) Glial expression of cannabinoid CB(2) receptors and fatty acid amide hydrolase are beta amyloid-linked events in Down's syndrome. Neuroscience 151:104-110.

Ogren SO, Hall H, Kohler C, Magnusson O, Sjostrand SE (1986) The selective dopamine D2 receptor antagonist raclopride discriminates between dopamine-mediated motor functions. Psychopharmacology (Berl) 90:287-294.

Onaivi ES, Ishiguro H, Gong JP, Patel S, Perchuk A, Meozzi PA, Myers L, Mora Z, Tagliaferro P, Gardner E, Brusco A, Akinshola BE, Liu QR, Hope B, Iwasaki S, Arinami T, Teasenfitz L, Uhl GR (2006) Discovery of the presence and functional expression of cannabinoid CB2 receptors in brain. Ann N Y Acad Sci 1074:514-536.

Onali P, Olianas MC, Gessa GL (1985) Characterization of dopamine receptors mediating inhibition of adenylate cyclase activity in rat striatum. Mol Pharmacol 28:138-145.

Ouchi Y, Yoshikawa E, Sekine Y, Futatsubashi M, Kanno T, Ogusu T, Torizuka T (2005) Microglial activation and dopamine terminal loss in early Parkinson's disease. Ann Neurol 57:168-175.

Pagano PJ, Ito Y, Tornheim K, Gallop PM, Tauber AI, Cohen RA (1995) An NADPH oxidase superoxide-generating system in the rabbit aorta. Am J Physiol 268:H2274-2280.

Paldyova E, Bereczki E, Santha M, Wenger T, Borsodi A, Benyhe S (2007) Noladin ether, a putative endocannabinoid, inhibits mu-opioid receptor activation via CB2 cannabinoid receptors. Neurochem Int.

Palkovits M, Brownstein M (1983) Microdissection of Brain Areas by the Punch Technique In: Brain Microdissection Techniques (Cuello A, ed). New York: Wiley-Interscience.

Papatsoris AG, Deliveliotis C, Singer C, Papapetropoulos S (2006) Erectile dysfunction in Parkinson's disease. Urology 67:447-451.

Pappas SS, Behrouz B, Janis KL, Goudreau JL, Lookingland KJ (2008) Lack of D2 receptor mediated regulation of dopamine synthesis in A(11) diencephalospinal neurons in male and female mice. Brain Res 1214:1-10.

Paris D, Town T, Mullan M (2000) Novel strategies for opposing murine microglial activation. Neurosci Lett 278:5-8.

Paris D, Town T, Parker TA, Tan J, Humphrey J, Crawford F, Mullan M (1999) Inhibition of Alzheimer's beta-amyloid induced vasoactivity and proinflammatory response in microglia by a cGMP-dependent mechanism. Exp Neurol 157:211-221.

Pawate S, Shen Q, Fan F, Bhat NR (2004) Redox regulation of glial inflammatory response to lipopolysaccharide and interferongamma. J Neurosci Res 77:540-551.

Petroske E, Meredith GE, Callen S, Totterdell S, Lau YS (2001) Mouse model of Parkinsonism: a comparison between subacute MPTP and chronic MPTP/probenecid treatment. Neuroscience 106:589-601.

Petrucelli L, O'Farrell C, Lockhart PJ, Baptista M, Kehoe K, Vink L, Choi P, Wolozin B, Farrer M, Hardy J, Cookson MR (2002) Parkin protects against the toxicity associated with mutant alpha-synuclein: proteasome dysfunction selectively affects catecholaminergic neurons. Neuron 36:1007-1019.

Pickel VM, Chan J, Kearn CS, Mackie K (2006) Targeting dopamine D2 and cannabinoid-1 (CB1) receptors in rat nucleus accumbens. J Comp Neurol 495:299-313.

Pistis M, Ferraro L, Pira L, Flore G, Tanganelli S, Gessa GL, Devoto P (2002) Delta(9)-tetrahydrocannabinol decreases extracellular GABA and increases extracellular

glutamate and dopamine levels in the rat prefrontal cortex: an in vivo microdialysis study. Brain Res 948:155-158.

Pitossi F, del Rey A, Kabiersch A, Besedovsky H (1997) Induction of cytokine transcripts in the central nervous system and pituitary following peripheral administration of endotoxin to mice. J Neurosci Res 48:287-298.

Porter AC, Sauer JM, Knierman MD, Becker GW, Berna MJ, Bao J, Nomikos GG, Carter P, Bymaster FP, Leese AB, Felder CC (2002) Characterization of a novel endocannabinoid, virodhamine, with antagonist activity at the CB1 receptor. J Pharmacol Exp Ther 301:1020-1024.

Price DA, Owens WA, Gould GG, Frazer A, Roberts JL, Daws LC, Giuffrida A (2007) CB1-independent inhibition of dopamine transporter activity by cannabinoids in mouse dorsal striatum. J Neurochem 101:389-396.

Price DAK, W Roberts, J L Guiffrida, A (2007) Neuroprotective Effects of Cannabinoids in a Mouse Model of Parkinson's Disease. In: Society for Neuroscience. San Diego, CA.

Priyadarshi A, Khuder SA, Schaub EA, Priyadarshi SS (2001) Environmental risk factors and Parkinson's disease: a metaanalysis. Environ Res 86:122-127.

Przedborski S, Levivier M, Jiang H, Ferreira M, Jackson-Lewis V, Donaldson D, Togasaki DM (1995) Dose-dependent lesions of the dopaminergic nigrostriatal pathway induced by intrastriatal injection of 6-hydroxydopamine. Neuroscience 67:631-647.

Przedborski S, Jackson-Lewis V, Naini AB, Jakowec M, Petzinger G, Miller R, Akram M (2001) The parkinsonian toxin 1-methyl-4-phenyl-1,2,3,6-tetrahydropyridine (MPTP): a technical review of its utility and safety. J Neurochem 76:1265-1274.

Purisai MG, McCormack AL, Cumine S, Li J, Isla MZ, Di Monte DA (2007) Microglial activation as a priming event leading to paraquat-induced dopaminergic cell degeneration. Neurobiol Dis 25:392-400.

Qin L, Liu Y, Wang T, Wei SJ, Block ML, Wilson B, Liu B, Hong JS (2004) NADPH oxidase mediates lipopolysaccharide-induced neurotoxicity and proinflammatory gene expression in activated microglia. J Biol Chem 279:1415-1421.

Qin L, Li G, Qian X, Liu Y, Wu X, Liu B, Hong JS, Block ML (2005) Interactive role of the toll-like receptor 4 and reactive oxygen species in LPS-induced microglia activation. Glia 52:78-84.

Qin L, Wu X, Block ML, Liu Y, Breese GR, Hong JS, Knapp DJ, Crews FT (2007) Systemic LPS causes chronic neuroinflammation and progressive neurodegeneration. Glia 55:453-462.

Ramirez BG, Blazquez C, Gomez del Pulgar T, Guzman M, de Ceballos ML (2005) Prevention of Alzheimer's disease pathology by cannabinoids: neuroprotection mediated by blockade of microglial activation. J Neurosci 25:1904-1913.

Ravina BM, Fagan SC, Hart RG, Hovinga CA, Murphy DD, Dawson TM, Marler JR (2003) Neuroprotective agents for clinical trials in Parkinson's disease: A systematic assessment. Neurology 60:1234-1240.

Reinhard JF, Jr., Diliberto EJ, Jr., Viveros OH, Daniels AJ (1987) Subcellular compartmentalization of 1-methyl-4-phenylpyridinium with catecholamines in adrenal medullary chromaffin vesicles may explain the lack of toxicity to adrenal chromaffin cells. Proc Natl Acad Sci U S A 84:8160-8164.

Rey P, Lopez-Real A, Sanchez-Iglesias S, Munoz A, Soto-Otero R, Labandeira-Garcia JL (2006) Angiotensin type-1-receptor antagonists reduce 6-hydroxydopamine toxicity for dopaminergic neurons. Neurobiol Aging.

Riegel AC, Lupica CR (2004) Independent presynaptic and postsynaptic mechanisms regulate endocannabinoid signaling at multiple synapses in the ventral tegmental area. J Neurosci 24:11070-11078.

Robbe D, Kopf M, Remaury A, Bockaert J, Manzoni OJ (2002) Endogenous cannabinoids mediate long-term synaptic depression in the nucleus accumbens. Proc Natl Acad Sci U S A 99:8384-8388.

Roche M, Kelly JP, O'Driscoll M, Finn DP (2008) Augmentation of endogenous cannabinoid tone modulates lipopolysaccharide-induced alterations in circulating cytokine levels in rats. Immunology.

Rock RB, Gekker G, Hu S, Sheng WS, Cheeran M, Lokensgard JR, Peterson PK (2004) Role of microglia in central nervous system infections. Clin Microbiol Rev 17:942-964, table of contents.

Rodriguez-Pallares J, Parga JA, Munoz A, Rey P, Guerra MJ, Labandeira-Garcia JL (2007) Mechanism of 6-hydroxydopamine neurotoxicity: the role of NADPH oxidase and microglial activation in 6-hydroxydopamine-induced degeneration of dopaminergic neurons. J Neurochem 103:145-156.

Rodriguez de Fonseca F, Del Arco I, Bermudez-Silva FJ, Bilbao A, Cippitelli A, Navarro M (2005) The endocannabinoid system: physiology and pharmacology. Alcohol Alcohol 40:2-14.

Romero J, Berrendero F, Perez-Rosado A, Manzanares J, Rojo A, Fernandez-Ruiz JJ, de Yebenes JG, Ramos JA (2000) Unilateral 6-hydroxydopamine lesions of nigrostriatal dopaminergic neurons increased CB1 receptor mRNA levels in the caudate-putamen. Life Sci 66:485-494.

Roth RH (1984) CNS dopamine autoreceptors: distribution, pharmacology, and function. Ann N Y Acad Sci 430:27-53.

Rousselet E, Joubert C, Callebert J, Parain K, Tremblay L, Orieux G, Launay JM, Cohen-Salmon C, Hirsch EC (2003) Behavioral changes are not directly related to striatal monoamine levels, number of nigral neurons, or dose of parkinsonian toxin MPTP in mice. Neurobiol Dis 14:218-228.

Roy A, Fung YK, Liu X, Pahan K (2006) Up-regulation of microglial CD11b expression by nitric oxide. J Biol Chem 281:14971-14980.

Russo R, Loverme J, La Rana G, Compton TR, Parrott J, Duranti A, Tontini A, Mor M, Tarzia G, Calignano A, Piomelli D (2007) The fatty acid amide hydrolase inhibitor URB597 (cyclohexylcarbamic acid 3'-carbamoylbiphenyl-3-yl ester) reduces neuropathic pain after oral administration in mice. J Pharmacol Exp Ther 322:236-242.

Samadi P, Bedard PJ, Rouillard C (2006) Opioids and motor complications in Parkinson's disease. Trends Pharmacol Sci 27:512-517.

Sano K, Mishima K, Koushi E, Orito K, Egashira N, Irie K, Takasaki K, Katsurabayashi S, Iwasaki K, Uchida N, Egawa T, Kitamura Y, Nishimura R, Fujiwara M (2008) Delta 9-tetrahydrocannabinol-induced catalepsy-like immobilization is mediated by decreased 5-HT neurotransmission in the nucleus accumbens due to the action of glutamate-containing neurons. Neuroscience 151:320-328.

Savasta M, Dubois A, Scatton B (1986) Autoradiographic localization of D1 dopamine receptors in the rat brain with [3H]SCH 23390. Brain Res 375:291-301.

Schmidt N, Ferger B (2001) Neurochemical findings in the MPTP model of Parkinson's disease. J Neural Transm 108:1263-1282.

Schmitz C, Hof PR (2005) Design-based stereology in neuroscience. Neuroscience 130:813-831.

Scorticati C, Mohn C, De Laurentiis A, Vissio P, Fernandez Solari J, Seilicovich A, McCann SM, Rettori V (2003) The effect of anandamide on prolactin secretion is modulated by estrogen. Proc Natl Acad Sci U S A 100:2134-2139.

Sealfon SC, Olanow CW (2000) Dopamine receptors: from structure to behavior. Trends Neurosci 23:S34-40.

Sellix MT, Freeman ME (2003) Circadian rhythms of neuroendocrine dopaminergic neuronal activity in ovariectomized rats. Neuroendocrinology 77:59-70.

Serrano F, Kolluri NS, Wientjes FB, Card JP, Klann E (2003) NADPH oxidase immunoreactivity in the mouse brain. Brain Res 988:193-198.

Sesack SR, Aoki C, Pickel VM (1994) Ultrastructural localization of D2 receptor-like immunoreactivity in midbrain dopamine neurons and their striatal targets. J Neurosci 14:88-106.

Sherer TB, Betarbet R, Kim JH, Greenamyre JT (2003) Selective microglial activation in the rat rotenone model of Parkinson's disease. Neurosci Lett 341:87-90.

Sherman MY, Goldberg AL (2001) Cellular defenses against unfolded proteins: a cell biologist thinks about neurodegenerative diseases. Neuron 29:15-32.

Shimizu-Albergine M, Rybalkin SD, Rybalkina IG, Feil R, Wolfsgruber W, Hofmann F, Beavo JA (2003) Individual cerebellar Purkinje cells express different cGMP phosphodiesterases (PDEs): in vivo phosphorylation of cGMP-specific PDE (PDE5) as an indicator of cGMP-dependent protein kinase (PKG) activation. J Neurosci 23:6452-6459.

Shimoji M, Zhang L, Mandir AS, Dawson VL, Dawson TM (2005) Absence of inclusion body formation in the MPTP mouse model of Parkinson's disease. Brain Res Mol Brain Res 134:103-108.

Singh AK, Jiang Y (2004) How does peripheral lipopolysaccharide induce gene expression in the brain of rats? Toxicology 201:197-207.

Sokoloff P, Giros B, Martres MP, Bouthenet ML, Schwartz JC (1990) Molecular cloning and characterization of a novel dopamine receptor (D3) as a target for neuroleptics. Nature 347:146-151.

Soria G, Mendizabal V, Tourino C, Robledo P, Ledent C, Parmentier M, Maldonado R, Valverde O (2005) Lack of CB1 cannabinoid receptor impairs cocaine self-administration. Neuropsychopharmacology 30:1670-1680.

Souilhac J, Poncelet M, Rinaldi-Carmona M, Le Fur G, Soubrie P (1995) Intrastriatal injection of cannabinoid receptor agonists induced turning behavior in mice. Pharmacol Biochem Behav 51:3-7.

Squire Lea, ed (2003) Fundamental Neuroscience, 2nd Edition. Amsterdam: Academic Press.

Steffens M, Feuerstein TJ (2004) Receptor-independent depression of DA and 5-HT uptake by cannabinoids in rat neocortex--involvement of Na(+)/K(+)-ATPase. Neurochem Int 44:529-538.

Steiner H, Gerfen CR (1998) Role of dynorphin and enkephalin in the regulation of striatal output pathways and behavior. Exp Brain Res 123:60-76.

Steiner H, Bonner TI, Zimmer AM, Kitai ST, Zimmer A (1999) Altered gene expression in striatal projection neurons in CB1 cannabinoid receptor knockout mice. Proc Natl Acad Sci U S A 96:5786-5790.

Stolk J, Hiltermann TJ, Dijkman JH, Verhoeven AJ (1994) Characteristics of the inhibition of NADPH oxidase activation in neutrophils by apocynin, a methoxy-substituted catechol. Am J Respir Cell Mol Biol 11:95-102.

Storch A, Ludolph AC, Schwarz J (2004) Dopamine transporter: involvement in selective dopaminergic neurotoxicity and degeneration. J Neural Transm 111:1267-1286.

Sumimoto H, Miyano K, Takeya R (2005) Molecular composition and regulation of the Nox family NAD(P)H oxidases. Biochem Biophys Res Commun 338:677-686.

Sunahara RK, Guan HC, O'Dowd BF, Seeman P, Laurier LG, Ng G, George SR, Torchia J, Van Tol HH, Niznik HB (1991) Cloning of the gene for a human dopamine D5 receptor with higher affinity for dopamine than D1. Nature 350:614-619.

Sundstrom E, Fredriksson A, Archer T (1990) Chronic neurochemical and behavioral changes in MPTP-lesioned C57BL/6 mice: a model for Parkinson's disease. Brain Res 528:181-188.

Sundstrom E, Stromberg I, Tsutsumi T, Olson L, Jonsson G (1987) Studies on the effect of 1-methyl-4-phenyl-1,2,3,6-tetrahydropyridine (MPTP) on central catecholamine neurons in C57BL/6 mice. Comparison with three other strains of mice. Brain Res 405:26-38.

Svizenska I, Dubovy P, Sulcova A (2008) Cannabinoid receptors 1 and 2 (CB1 and CB2), their distribution, ligands and functional involvement in nervous system structures - A short review. Pharmacol Biochem Behav.

Takamidoh H, Naoi M, Nagatsu T (1987) Inhibition of type A monoamine oxidase by 1-methyl-4-phenylpyridine. Neurosci Lett 73:293-297.

Tanaka Y, Engelender S, Igarashi S, Rao RK, Wanner T, Tanzi RE, Sawa A, V LD, Dawson TM, Ross CA (2001) Inducible expression of mutant alpha-synuclein decreases proteasome activity and increases sensitivity to mitochondria-dependent apoptosis. Hum Mol Genet 10:919-926.

Tang LL, Ye K, Yang XF, Zheng JS (2007) Apocynin attenuates cerebral infarction after transient focal ischaemia in rats. J Int Med Res 35:517-522.

Tang XN, Cairns B, Cairns N, Yenari MA (2008) Apocynin improves outcome in experimental stroke with a narrow dose range. Neuroscience 154:556-562.

Thiemann G, Fletcher BC, Ledent C, Molleman A, Hasenohrl RU (2007) The genetic versus pharmacological invalidation of the cannabinoid CB(1) receptor results in differential effects on 'non-associative' memory and forebrain monoamine concentrations in mice. Neurobiol Learn Mem 88:416-423.

Thomas EA, Cravatt BF, Danielson PE, Gilula NB, Sutcliffe JG (1997) Fatty acid amide hydrolase, the degradative enzyme for anandamide and oleamide, has selective distribution in neurons within the rat central nervous system. J Neurosci Res 50:1047-1052.

Tian Y, Eaton MJ, Manzanares J, Lookingland KJ, Moore KE (1992) Characterization of opioid receptor-mediated regulation of incertohypothalamic dopamine neurons: lack of evidence for a role of 5-hydroxytryptaminergic neurons in mediating the stimulatory effects of morphine. Brain Res 591:116-121.

Tieu K, Ischiropoulos H, Przedborski S (2003) Nitric oxide and reactive oxygen species in Parkinson's disease. IUBMB Life 55:329-335.

Tillerson JL, Caudle WM, Reveron ME, Miller GW (2002) Detection of behavioral impairments correlated to neurochemical deficits in mice treated with moderate doses of 1-methyl-4-phenyl-1,2,3,6-tetrahydropyridine. Exp Neurol 178:80-90.

Tipton KF, Singer TP (1993) Advances in our understanding of the mechanisms of the neurotoxicity of MPTP and related compounds. J Neurochem 61:1191-1206.

Tretter L, Sipos I, Adam-Vizi V (2004) Initiation of neuronal damage by complex I deficiency and oxidative stress in Parkinson's disease. Neurochem Res 29:569-577.

Tzavara ET, Davis RJ, Perry KW, Li X, Salhoff C, Bymaster FP, Witkin JM, Nomikos GG (2003) The CB1 receptor antagonist SR141716A selectively increases monoaminergic neurotransmission in the medial prefrontal cortex: implications for therapeutic actions. Br J Pharmacol 138:544-553.

Uhl GR, Hedreen JC, Price DL (1985) Parkinson's disease: loss of neurons from the ventral tegmental area contralateral to therapeutic surgical lesions. Neurology 35:1215-1218.

Uriguen L, Berrendero F, Ledent C, Maldonado R, Manzanares J (2005) Kappa- and delta-opioid receptor functional activities are increased in the caudate putamen of cannabinoid CB1 receptor knockout mice. Eur J Neurosci 22:2106-2110.

Van den Worm E, Beukelman CJ, Van den Berg AJ, Kroes BH, Labadie RP, Van Dijk H (2001) Effects of methoxylation of apocynin and analogs on the inhibition of reactive oxygen species production by stimulated human neutrophils. Eur J Pharmacol 433:225-230.

van der Stelt M, Fox SH, Hill M, Crossman AR, Petrosino S, Di Marzo V, Brotchie JM (2005) A role for endocannabinoids in the generation of parkinsonism and levodopa-induced dyskinesia in MPTP-lesioned non-human primate models of Parkinson's disease. Faseb J 19:1140-1142.

Van Sickle MD, Duncan M, Kingsley PJ, Mouihate A, Urbani P, Mackie K, Stella N, Makriyannis A, Piomelli D, Davison JS, Marnett LJ, Di Marzo V, Pittman QJ, Patel KD, Sharkey KA (2005) Identification and functional characterization of brainstem cannabinoid CB2 receptors. Science 310:329-332.

Van Staveren WC, Steinbusch HW, Markerink-Van Ittersum M, Repaske DR, Goy MF, Kotera J, Omori K, Beavo JA, De Vente J (2003) mRNA expression patterns of the cGMP-hydrolyzing phosphodiesterases types 2, 5, and 9 during development of the rat brain. J Comp Neurol 467:566-580.

Van Tol HH, Bunzow JR, Guan HC, Sunahara RK, Seeman P, Niznik HB, Civelli O (1991) Cloning of the gene for a human dopamine D4 receptor with high affinity for the antipsychotic clozapine. Nature 350:610-614.

Vilhardt F (2005) Microglia: phagocyte and glia cell. Int J Biochem Cell Biol 37:17-21.

Vyas I, Heikkila RE, Nicklas WJ (1986) Studies on the neurotoxicity of 1-methyl-4-phenyl-1,2,3,6-tetrahydropyridine: inhibition of NAD-linked substrate oxidation by its metabolite, 1-methyl-4-phenylpyridinium. J Neurochem 46:1501-1507.

Waksman Y, Olson JM, Carlisle SJ, Cabral GA (1999) The central cannabinoid receptor (CB1) mediates inhibition of nitric oxide production by rat microglial cells. J Pharmacol Exp Ther 288:1357-1366.

Walker DK, Ackland MJ, James GC, Muirhead GJ, Rance DJ, Wastall P, Wright PA (1999) Pharmacokinetics and metabolism of sildenafil in mouse, rat, rabbit, dog and man. Xenobiotica 29:297-310.

Walter L, Franklin A, Witting A, Wade C, Xie Y, Kunos G, Mackie K, Stella N (2003) Nonpsychotropic cannabinoid receptors regulate microglial cell migration. J Neurosci 23:1398-1405.

Walters JR, Roth RH (1976) Dopaminergic neurons: an in vivo system for measuring drug interactions with presynaptic receptors. Naunyn Schmiedebergs Arch Pharmacol 296:5-14.

Wang L, Gang Zhang Z, Lan Zhang R, Chopp M (2005) Activation of the PI3-K/Akt pathway mediates cGMP enhanced-neurogenesis in the adult progenitor cells derived from the subventricular zone. J Cereb Blood Flow Metab 25:1150-1158.

Wang Q, Tompkins KD, Simonyi A, Korthuis RJ, Sun AY, Sun GY (2006) Apocynin protects against global cerebral ischemia-reperfusion-induced oxidative stress and injury in the gerbil hippocampus. Brain Res 1090:182-189.

Wiese A, Brandenburg K, Ulmer AJ, Seydel U, Muller-Loennies S (1999) The dual role of lipopolysaccharide as effector and target molecule. Biol Chem 380:767-784.

Wilson RI, Nicoll RA (2001) Endogenous cannabinoids mediate retrograde signalling at hippocampal synapses. Nature 410:588-592.

Wilson RI, Kunos G, Nicoll RA (2001) Presynaptic specificity of endocannabinoid signaling in the hippocampus. Neuron 31:453-462.

Winklhofer KF (2007) The parkin protein as a therapeutic target in Parkinson's disease. Expert Opin Ther Targets 11:1543-1552.

Wirtz-Brugger F, Giovanni A (2000) Guanosine 3',5'-cyclic monophosphate mediated inhibition of cell death induced by nerve growth factor withdrawal and beta-amyloid: protective effects of propentofylline. Neuroscience 99:737-750.

Wittmann G, Deli L, Kallo I, Hrabovszky E, Watanabe M, Liposits Z, Fekete C (2007) Distribution of type 1 cannabinoid receptor (CB1)-immunoreactive axons in the mouse hypothalamus. J Comp Neurol 503:270-279.

Woltmann A, Hamann L, Ulmer AJ, Gerdes J, Bruch HP, Rietschel ET (1998) Molecular mechanisms of sepsis. Langenbecks Arch Surg 383:2-10.

Wu DC, Teismann P, Tieu K, Vila M, Jackson-Lewis V, Ischiropoulos H, Przedborski S (2003) NADPH oxidase mediates oxidative stress in the 1-methyl-4-phenyl-1,2,3,6-tetrahydropyridine model of Parkinson's disease. Proc Natl Acad Sci U S A 100:6145-6150.

Wu DC, Jackson-Lewis V, Vila M, Tieu K, Teismann P, Vadseth C, Choi DK, Ischiropoulos H, Przedborski S (2002) Blockade of microglial activation is neuroprotective in the 1-methyl-4-phenyl-1,2,3,6-tetrahydropyridine mouse model of Parkinson disease. J Neurosci 22:1763-1771.

Wurtman RJ, Fernstrom JD (1975) Control of brain monoamine synthesis by diet and plasma amino acids. Am J Clin Nutr 28:638-647.

Wykes V, Bellamy TC, Garthwaite J (2002) Kinetics of nitric oxide-cyclic GMP signalling in CNS cells and its possible regulation by cyclic GMP. J Neurochem 83:37-47.

Ximenes VF, Kanegae MP, Rissato SR, Galhiane MS (2007) The oxidation of apocynin catalyzed by myeloperoxidase: Proposal for NADPH oxidase inhibition. Arch Biochem Biophys 457:134-141.

Yang L, Matthews RT, Schulz JB, Klockgether T, Liao AW, Martinou JC, Penney JB, Jr., Hyman BT, Beal MF (1998) 1-Methyl-4-phenyl-1,2,3,6-tetrahydropyride neurotoxicity is attenuated in mice overexpressing Bcl-2. J Neurosci 18:8145-8152.

Yiangou Y, Facer P, Durrenberger P, Chessell IP, Naylor A, Bountra C, Banati RR, Anand P (2006) COX-2, CB2 and P2X7-immunoreactivities are increased in activated microglial cells/macrophages of multiple sclerosis and amyotrophic lateral sclerosis spinal cord. BMC Neurol 6:12.

Yung KK, Bolam JP, Smith AD, Hersch SM, Ciliax BJ, Levey AI (1995) Immunocytochemical localization of D1 and D2 dopamine receptors in the basal ganglia of the rat: light and electron microscopy. Neuroscience 65:709-730.

Zangen A, Nakash R, Overstreet DH, Yadid G (2001) Association between depressive behavior and absence of serotonin-dopamine interaction in the nucleus accumbens. Psychopharmacology (Berl) 155:434-439.

Zesiewicz TA, Helal M, Hauser RA (2000) Sildenafil citrate (Viagra) for the treatment of erectile dysfunction in men with Parkinson's disease. Mov Disord 15:305-308.

Zhan G, Serrano F, Fenik P, Hsu R, Kong L, Pratico D, Klann E, Veasey SC (2005) NADPH oxidase mediates hypersomnolence and brain oxidative injury in a murine model of sleep apnea. Am J Respir Crit Care Med 172:921-929.

Zhang L, Zhang RL, Wang Y, Zhang C, Zhang ZG, Meng H, Chopp M (2005) Functional recovery in aged and young rats after embolic stroke: treatment with a phosphodiesterase type 5 inhibitor. Stroke 36:847-852.

Zhang R, Wang Y, Zhang L, Zhang Z, Tsang W, Lu M, Zhang L, Chopp M (2002) Sildenafil (Viagra) induces neurogenesis and promotes functional recovery after stroke in rats. Stroke 33:2675-2680.

Zhang RL, Zhang Z, Zhang L, Wang Y, Zhang C, Chopp M (2006a) Delayed treatment with sildenafil enhances neurogenesis and improves functional recovery in aged rats after focal cerebral ischemia. J Neurosci Res 83:1213-1219.

Zhang W, Shin EJ, Wang T, Lee PH, Pang H, Wie MB, Kim WK, Kim SJ, Huang WH, Wang Y, Zhang W, Hong JS, Kim HC (2006b) 3-Hydroxymorphinan, a metabolite of dextromethorphan, protects nigrostriatal pathway against MPTP-elicited damage both in vivo and in vitro. Faseb J 20:2496-2511.

Zhou HF, Liu XY, Niu DB, Li FQ, He QH, Wang XM (2005) Triptolide protects dopaminergic neurons from inflammation-mediated damage induced by lipopolysaccharide intranigral injection. Neurobiol Dis 18:441-449.

Zhou J, Struthers AD, Lyles GA (1999) Differential effects of some cell signalling inhibitors upon nitric oxide synthase expression and nuclear factor-kappaB activation induced by lipopolysaccharide in rat aortic smooth muscle cells. Pharmacol Res 39:363-373.

Zhu JH, Horbinski C, Guo F, Watkins S, Uchiyama Y, Chu CT (2007) Regulation of autophagy by extracellular signal-regulated protein kinases during 1-methyl-4-phenylpyridinium-induced cell death. Am J Pathol 170:75-86.

Zimmer A, Zimmer AM, Hohmann AG, Herkenham M, Bonner TI (1999) Increased mortality, hypoactivity, and hypoalgesia in cannabinoid CB1 receptor knockout mice. Proc Natl Acad Sci U S A 96:5780-5785.